SEMMELWEIS EGYETEM

DOKTORI ISKOLA

Ph.D. értekezések

3367.

HORVÁTH CSENGE

Magatartástudományok
című program

Programvezető: Dr. Kovács József, egyetemi tanár

Témavezető: Dr. Bódizs Róbert, egyetemi tanár

Power-law parametrization of the sleep electroencephalography spectra: a new framework for modelling sleep-wake regulation

PhD thesis

Csenge G. Horváth

Semmelweis University Doctoral School
Division of mental health

Supervisor: Róbert Bódizs, Ph.D.

Official reviewers: Gábor Csukly, MD, Ph.D
Attila Tóth, Ph.D

Head of the Complex Examination Committee:
Zsolt Unoka, MD, Ph.D

Members of the Complex Examination Committee:
Pálma Benedek, MD, Ph.D
Ildikó Nagyné Baji, MD, Ph.D
Gergely Vadai, Ph.D

Budapest
2025

Table of Contents

List of Abbreviations 5

1. Introduction 6

1.1. Definition, measurement and composition of sleep 6

1.2. Sleep regulation 8

1.2.1. Neurobiological basis of sleep-wake regulation 8

1.2.1.1. Sleep-wake switch 9

1.2.1.2. Slow waves and sleep spindles: major constituents of NREM sleep 9

1.2.2. Two process model of sleep regulation 10

1.2.2.1. Homeostatic process 11

1.2.2.2. Circadian process 11

1.3. Experimental setups for investigating human sleep-wake dynamics by EEG 12

1.3.1. Setups for measuring homeostasis 12

1.3.1.1. Homeostatic characteristic of the NREM sleep EEG spectrum beyond SWA 13

1.3.2. Setups for measuring time of day effects 14

1.3.2.1. Circadian characteristic of sleep spindles 15

1.4. Individual differences of the sleep EEG in terms of age, sex and intelligence 16

1.5. Spectral analysis of the sleep EEG 16

1.4.1. Spectral parametrization 17

2. Objectives 20

3. Methods 21

3.1. Study 1 and Study 2 21

3.1.1. Sample 21

3.1.3. Polysomnography 22

3.1.4. Power spectral analysis 22

3.1.6. Spectrum parametrization 23

3.1.7. Statistical analyses 23
3.1.7.1. Study 1 23
3.1.7.2. Study 2 24
3.1.7.3. Goodness of Fit assessment 25
3.2. Study 3 25
3.2.1. Sample 25
3.2.2. Study design 26
3.2.3. Sleep electroencephalography 27
3.2.3. EEG spectral analyses 27
3.2.3.2. Spectrum parametrization 27
3.2.4. Munich Chronotype Questionnaire, Sleepiness scales 28
3.2.6. Statistical analyses 28
4. Results 31
4.1. Study 1 31
4.1.1. Spectral peaks of the 9–18 Hz frequency range 31
4.1.2. Effects of age on spectral peaks and slope 33
4.1.3. Sex differences in spectral peaks and intercept 34
4.1.4. Associations of IQ with spindle peak amplitude 35
4.1.5. Interrelationship between spectral slope and intercept 36
4.2. Study 2 36
4.2.1. Overnight dynamics of the spindle peak frequency 37
4.2.2. Anterior-posterior changes in spindle peak frequency 38
4.2.3. Overnight dynamics of spectral slope, spindle peak amplitude and SWA ... 39
4.3.4. Spectral slope and SWA: relationship and interindividual variability 41
4.3. Study 3 43
4.3.1. Effect of sleep deprivation on spectral slope dynamics 44

4.3.2. Effect of sleep deprivation on SWA 47
4.3.3. Effect of sleep deprivation on spindle peak frequency 48
5. Discussion 52
5.1. Largest peak in the 9–18 Hz range reflects spindle activity 52
5.2. NREM sleep EEG spectral parameters reflect known individual differences 53
5.3. Overnight dynamics of spectral parameters correspond to sleep regulation 56
5.4. Sleep deprivation has a substantial impact on spectral parameters 59
5.5. Advantages of spectral parameters over the gold-standard indicators 61
5.6. Outlook: Fractal and Oscillatory Adjustment Model (FOAM) 62
6. Conclusions 64
7. Summary 65
8. References 66
9. Bibliography of the candidate's publications 84
9.1. Publications constituting the present thesis 84
9.2. Other publications by the candidate 84
10. Acknowledgements 86

List of Abbreviations

AASM	American Academy of Sleep Medicine
ARAS	Ascending Reticular Activating System
BDI	Beck Depression Inventory
BS	Baseline Sleep
CFT	Culture Fair Test
DDA	Descriptive Data Analysis
ECG	Electrocardiography
EEG	Electroencephalography
EMG	Electromyography
EOG	Electrooculography
FFT	Fast Fourier Transform
GABA	gamma-aminobutyric acid
GLM	General Linear Model
IQ	Intelligence Quotient
KL	Kullback–Leibler divergence
lnSWA	natural logarithm of SWA
MCTQ	Munich Chronotype Questionnaire
MnPn	Median Preoptic Nucleus
MSFsc	oversleep-adjusted sleep middle
N2	NREM sleep Stage 2
N3	NREM sleep Stage 3
NREM	Non-Rapid Eye Movement
NSSF	Nadir of Sleep Spindle Frequency
PPG	Photoplethysmography
PSD	Power Spectral Density
PSQI	Pittsburgh Sleep Quality Index
RS	Recovery Sleep
SWA	Slow Wave Activity
TRN	Thalamic Reticular Nucleus
VLPO	Ventrolateral Preoptic Nuclues

1. Introduction

1.1. Definition, measurement and composition of sleep

According to Hendricks et al. (2000), sleep can be defined as a state characterized by a lack of voluntary movements, reversibility, spontaneous occurrence that follows a circadian rhythm, species-specific posture, elevated arousal threshold, homeostatic control influenced by the circadian rhythm, state-dependent neural changes and recognisability as a stable characteristic of the species. However, besides those phenomenological ones, sleep of birds and mammalians can also be characterized by marked polysomnography-measured electrophysiological activity changes.

The first precise physiological characterization of sleep became possible following Hans Berger's invention of human electroencephalography (EEG) in 1924 (H. Berger, 1929). Today, polysomnography (PSG) is the gold-standard method for measuring sleep. A polysomnography recording typically includes, in addition to EEG channels, electrooculography (EOG) and electromyography (EMG) derivations, which measures the electrical activity of the scalp, eyes, and muscles, respectively. EEG electrodes simultaneously capture signals from numerous neurons, reflecting the aggregate electrical activity within a given region. When this population-level neuronal activity is synchronized (i.e., several neurons firing together), their combined electrical signals summate, producing prominent, well-defined waveforms in the EEG recording. A detectable EEG signal requires approximately 10,000–50,000 neurons to be active synchronously (Murakami & Okada, 2006). Conversely, when neuronal activity is more random, the resulting electrical signal is desynchronized, producing low-amplitude waveforms characterized by seemingly irregular patterns. After researchers recognized that specific waveforms recur cyclically during the sleep period, they were able to characterize the different phases and stages of sleep.

The first evidence that not only sleep-wake variation but also sleep itself is cyclical, came when Aserinsky and Kleitman (1953) described recurrent episodes of fast, abrupt and binocularly symmetrical eye movements during whole night sleep records of adult subjects. They reported 1-sec-long large potentials in the EOG channel, and a low-amplitude, irregular EEG signal which they observed to recur 3–4 times in a lengthier sleep episode. Thereafter, sleep was divided into two phases: the so-called rapid eye movement (REM) sleep, and non-rapid eye movement (NREM) sleep. The typical signal

characteristics of the latter—such as slow waves, sleep spindles, and K-complexes (Loomis et al., 1938)—were recognised earlier but were considered as general features of sleep. This study revealed that sleep has a more complex composition. Later, by revising the work of Dement and Kleitman (1957a), based on the consensus of the era's renowned sleep researchers, Rechtschaffen and Kales (1968) described the scoring rules for different sleep stages. Altogether, 4 stages of NREM sleep and stage REM was reported. Nowadays, epochs containing a moderate or large amount of slow waves are no longer separated, thus, the division of NREM sleep has been reduced to three stages. The universally accepted rules are periodically reviewed by the American Academy of Sleep Medicine (AASM) and published in the latest guidelines every few years. However, the fundamental criteria have not changed substantially since 1968. The most important characteristics of the different stages are summarized below.

PSG activity indicates wakefulness (W) if more than 50% of the staging epoch (20 or 30 sec) contains alpha rhythm (~8–13 Hz) and/or eye blinks, eye movements (either rapid eye movements accompanied by high chin muscle tone, or slow, reading eye movements); NREM 1 (N1) is characterized by low-amplitude EEG activity in the 4–7 Hz range, less than 50% of alpha activity, and/or the occurrence of vertex sharp waves. Chin EMG amplitude is variable, lower than wake, and slow-rolling eye movements may be observed; A NREM stage 2 (N2) epoch should contain at least one K-complex (a sharp, high-voltage, diphasic EEG waveform with at least 0.5 sec duration) unassociated with arousals, and/or at least one sleep spindle (a train of separate sinusoidal EEG waves with 11–16 Hz frequency, lasting at least 0.5 sec). Chin EMG amplitude is variable, lower than in wakefulness, eye movement is not noticed; NREM stage 3 (N3), otherwise known as slow wave sleep (SWS), is scored when more than 20% of the epoch is dominated by frontally located EEG waves of 0.5–2 Hz frequency and a peak-to-peak amplitude exceeding 75 μV. Chin EMG amplitude is variable, lower than in N2, sometimes resembles that of REM sleep, furthermore, eye movements are not observed; REM is characterized by mixed-frequency activity with low amplitude. No spindles or K-complexes, instead, sawtooth waves (2–6 Hz triangular waves) can be observed. EOG reveal sharply-peaked, rapid eye movements, chin EMG amplitude is low, especially during the eye movements (Berry et al., 2018; Lázár et al., 2022).

During a whole-night sleep, NREM and REM phases alternate. That is sleep has an ultradian (less than 24 hours) rhythmicity with a cycle length approximately 90 minutes (Aserinsky & Kleitman, 1953; Dement & Kleitman, 1957a). An average sleep period contains around 4–6 full sleep cycles (NREM-REM alternations), and interestingly, the alternation of sleep stages is strictly regular. However, the signal characteristics of the successive sleep cycles are not stable over time. In later sections I will discuss that some of these overnight changes are known to be linked to sleep regulatory processes.

1.2. Sleep regulation

1.2.1. Neurobiological basis of sleep-wake regulation

The first brain region linked to sleep-wake regulation was the hypothalamus, after Von Economo discovered that patients with anterior hypothalamus lesions suffered from insomnia, whereas lesions in the posterior hypothalamus led to sopor (hypersomnolence) (Economo, 1930). Second major discovery was related to the midbrain. Arousal-like activity was found as a result of electrical stimulation of the reticular formation in anesthetized cats (Moruzzi & Magoun, 1949). Based on that, along with previous findings regarding the inability of afferent stimuli to initiate arousal from somnolence, lethargy, or coma caused by damage to the upper brainstem while the primary sensory pathways to the cortex remain unaffected, the ascending reticular activating system was described (Moruzzi & Magoun, 1949). Finally, early studies have shown that pons plays an essential role in REM sleep, as lesions in the caudal pons disrupt muscle atonia while preserving fast EEG activity, whereas, the transections at the rostral pons maintained atonia and abolished fast EEG patterns (Jouvet, 1962; Siegel et al., 1984).

All the aforementioned early findings served as a first step in the discovery of the main sleep-wake promoting systems in the brain. Now we understand that the interaction of several excitatory and inhibitory neurotransmitters supports the ability to wake up and fall asleep. The waking process is promoted by acetylcholine, norepinephrine, dopamine, serotonin, histamine, and orexin (also known as hypocretin) in brain regions such as the midbrain, pons and the posterior hypothalamus (Muza, 2018). Meanwhile, the arousal system is suppressed by neurotransmitters such as gamma-aminobutyric acid (GABA) and galanin, and the key brain regions involved in the initiation of the sleep process are

the anterior hypothalamus, particularly the preoptic area and nearby forebrain structures (NREM sleep) (Muza, 2018). REM sleep generation relies on the activity of the pons and adjacent midbrain regions, where neurotransmitters like acetylcholine, glutamate, and glycine play a significant role (Muza, 2018).

1.2.1.1. Sleep-wake switch

As mentioned above, early studies revealed that the preoptic area contains sleep promoting neurons primarily associated with SWS. Later studies demonstrated that mainly the inhibitory GABAergic neurons of the median preoptic nucleus (MnPn) and of the ventrolateral preoptic nucleus (VLPO) are involved, both having a role in initiating and sustaining sleep (Luppi & Fort, 2019).

The flip-flop model, proposed by Saper et al. (2001, 2010), suggests that the wake-sleep transition operates as a flip-flop switch mechanism, similar to that in electronics. This model describes a dynamically opposing interaction between VLPO and the arousal-promoting system, where neurons on each side inhibit those on the other. Specifically, before and during sleep, GABAergic neurons in the VLPO suppress wake-promoting neurons including orexinergic, monoaminergic and cholinergic populations. Conversely, when wakefulness is required, these populations inhibit the sleep-active neurons of the VLPO. Just like in electronics, the model proposes that by strongly inhibiting each other, the two sides of the flip-flop circuit create a bistable feedback loop that stabilizes two distinct firing patterns, while preventing any intermediate state (Saper et al., 2001, 2010). As a result, the "seesaw" tilts from one side to the other. However, later research identified additional structures involved in sleep and wakefulness including parafacial zone, reticular thalamic nucleus and nucleus accumbens which role needs further investigation (Luppi & Fort, 2019).

1.2.1.2. Slow waves and sleep spindles: major constituents of NREM sleep

While the flip-flop model provides a compelling concept for transitions between sleep and wakefulness, the mechanisms assumed to underlie deep sleep are also important to consider when discussing neurobiological basis of sleep regulation.

As will be discussed in later sections, the depth and intensity of sleep are most strongly linked to SWS. Slow oscillations (<1 Hz) originate from the cortex and reflect up- and-down state alternations, which refers to synchronized membrane depolarization and hyperpolarization, respectively (Ishii et al., 2024). Layer V of the cortex (pyramidal

cells) plays a primary role in up-state initiation. Subcortical input may trigger the onset of the down-state, whereas the thalamus plays a key role in generating the slow oscillations in conjunction with the cerebral cortex (Ishii et al., 2024). Furthermore, it has been shown that slow waves "travel" from the anterior to the posterior regions (Murphy et al., 2009) and can also appear locally (Vyazovskiy et al., 2011).

Sleep spindles are well recognisable signal patterns observed in stage N2 and N3 sleep, characterized by sinusoidal oscillations with frequencies ranging from 11 to 16 Hz with duration of at least 0.5 sec, and typically, with highest amplitudes in the central regions according to the AASM (Berry et al., 2018). Spindle bursts represent a typical oscillatory pattern in the human NREM sleep EEG, appearing as prominent spectral peaks in the power spectra (Bódizs et al., 2024) and associated with equivalent neural activity in the thalamus. Indeed, pioneering experiments on cats, ferrets and rodents revealed that the thalamic reticular nucleus (TRN) is a key generator of sleep spindles through its reciprocal interactions with thalamocortical cells (Fernandez & Lüthi, 2020). TRN is a GABAergic cell layer surrounding the thalamus, projecting inhibitory signals to all thalamic nuclei. During NREM sleep, TRN neurons fire in a burst mode triggered by hyperpolarization, which helps initiate and phase-lock thalamocortical spindle activity (Fernandez & Lüthi, 2020). Based on frequency, two types of spindle can be distinguished: slow (~12 Hz) and fast (~14 Hz) spindles, which also differ in their topographical distribution as slow spindles are predominantly frontal, while fast spindles are more centro-parietally located (Fernandez & Lüthi, 2020). Spindles also exhibit marked inter-individual differences (see Section 1.4.), show intraindividual stability and are largely heritable (De Gennaro et al., 2008; Finelli et al., 2001; Gennaro et al., 2005). In conjunction with the latter property, spindles are thought to mirror the strength and plasticity of thalamocortical circuits that contribute to unique cognitive functioning (Fernandez & Lüthi, 2020).

1.2.2. Two process model of sleep regulation

Alexander Borbély's original model (1982) assumes sleep regulation is governed by two separate processes: a homeostatic, sleep-history-dependent mechanism and a circadian rhythm. While sleep depth is primarily defined by the former process, the propensity of sleep results from the combined influence of both mechanisms. The model represents process S with an exponential function which is increasing during wakefulness

and decreasing as sleep progresses. Process C was postulated as a sine function, fitted to the 24-hours day. The sum of the two functions is defined as sleep propensity, and their intersection represents the time of awakening in the model (Borbély, 2022).

1.2.2.1. Homeostatic process

Homeostatic S process, which represents sleep pressure/debt, builds up during wakefulness and depletes during sleep, fluctuating within a range that is typically aligned with the day-night cycle by the circadian pacemaker (Borbély et al., 2016). When S reaches the lower boundary of this range, it triggers wakefulness, while approaching the upper boundary signals the need for sleep (Borbély, 1982; Borbély et al., 2016). In the original model sleep homeostat was entirely based on SWS (stage N3), and especially on slow wave activity (SWA, the EEG activity in the 0.75–4.5 Hz frequency range) as it appears to best reflect the classical concept of homeostasis by maintaining the balance within the sleep-wake cycle. The author supported this assumption with studies showing that SWS is deeper (more un-respondent to external stimuli than other stages)(Goodenough et al., 1965; Loomis et al., 1937; Williams et al., 1964), increases following sleep deprivation (R. J. Berger & Oswald, 1962; Borbély et al., 1981; J. M. Moses et al., 1975; Webb & Agnew, 1971) and decreases as a result of longer prior sleep episodes or daytime sleep (Feinberg et al., 1980; Karacan et al., 1970). However, spectral analyses have made it possible to examine the whole-night variation in sleep EEG frequency composition, which is more dynamic than sleep macrostructure, and revealed that SWA increases as a result of sleep deprivation, as well as decreases throughout the sleep episode as sleep debt is diminished (Borbély, 1982; Borbély et al., 1981). These findings align with the idea that when sleep debt due to wakefulness accumulates, SWA during the sleep episode compensates to restore equilibrium, and vice versa. Therefore, S process was illustrated with SWA in the original model, and became the gold-standard measure of sleep homeostasis in later research.

1.2.2.2. Circadian process

The rotation of the Earth around the Sun and its own axis creates predictable environmental changes, prompting organisms to develop biological clocks early in evolution to better adapt, leading to a complex network of central and peripheral timekeepers in mammals (Deboer, 2020). The recognition of those biological clocks is based on the crucial finding that, even in the absence of external signals, organisms still

maintain their daily patterns, although the cycle length may slightly deviate from the 24-hour. Thus, there is an entrainment (synchronization) between the inner and environmental (day-night) rhythms, which occurs with the help of the so-called zeitgebers (time-cues) (Roenneberg & Foster, 1997). The most important time cue is light, which modulates the activity of the suprachiasmatic nucleus in the hypothalamus ("the master clock": central regulator of all peripheral timekeepers) through the retinohypothalamic tract (Deboer, 2020). The two process model takes into account that sleep is influenced by the circadian oscillator, which is independent of sleep-wake history and mostly plays a role in the timing of the sleep episode (Borbély, 1982).

However, the circadian C process was only postulated in the original model, and was not described by any PSG variables. Instead, extensive research was cited, demonstrating that sleep propensity depends not only on sleep-wake history, but also on the time of day. The author discussed the development of sleepiness, and sleep duration throughout the day—both of which follow a circadian rhythm (Akerstedt & Gillberg, 1981; J. Moses et al., 1978; Murray et al., 1958; Patrick & Gilbert, 1896)—, to support the above hypothesis. In addition to sleep propensity, Borbély (1982) highlights that some macro-structural properties of REM sleep have also been shown to exhibit a circadian rhythmicity (Endo et al., 1981; Webb & Agnew, 1967) and to be associated with markers of the circadian rhythm, such as core body temperature (Czeisler, Weitzman, et al., 1980; Czeisler, Zimmerman, et al., 1980; J. Moses et al., 1978). He suggests that while NREM (SWS) represents sleep homeostasis, REM sleep reflects the level of process C (Borbély, 1982).

1.3. Experimental setups for investigating human sleep-wake dynamics by EEG

1.3.1. Setups for measuring homeostasis

Sleep deprivation is the most important constituent of the methodology in analysing sleep-wake dependent processes. Already in the very first sleep deprivation experiment in humans (Patrick & Gilbert, 1896) which was carried out almost 130 years ago—30 years before the first human EEG recording (H. Berger, 1929)—researchers concluded that "owing to the greater 'depth' of sleep after the sleep fast, the anabolism accompanying restoration was more rapid", and "that the subjects, in other words, although apparently awake and, indeed, as wide awake as they could be kept, were

nevertheless at times partially asleep" (Patrick & Gilbert, 1896, p. 479), based on their finding that the duration of recovery sleep was disproportionately short relative to the preceding 90 hours of wakefulness. Many of the above quoted ideas have now become clearly defined and well-measurable pieces of evidence such as the deeper sleep in recovery sleep, micro sleeps as a result of sleep restriction (Bougard et al., 2018), local sleep (Krueger et al., 2019) and hallucinations during wakefulness after a prolonged sleep deprivation period (Waters et al., 2018). Thus, this early paper serves as a remarkable example of how much can be observed about sleep simply by depriving it. Once the EEG methodology became available and the main components of sleep were defined, researchers applied various deprivation protocols to test which component is influenced by the preceding sleep-wake history. The above-described study design applied 90-hour-long acute total sleep deprivation; however, nowadays, sleep deprivation lasting more than 48 hours is considered unethical. Therefore, later studies usually applied ~24–40 hours of wakefulness, depending on whether phase delay was also investigated. Other commonly used paradigms include one-time partial-, and chronic partial sleep restrictions, both of which aim to simulate everyday life situations (e.g. waking up early for work). Sleep can also be selectively deprived for different sleep stages. For example, in a SWS deprivation experiment, the EEG signal is monitored online and when SWS occurs, it is disturbed by stimuli (often acoustic stimuli) without causing awakening. Selective deprivation of REM sleep in humans often induced by awakening when entering the stage. It should be noted that paradigms using extensive sleep (the inverse of deprivation) are also useful for examining the influence of sleep-wake history on sleep. For this purpose, various types of nap studies (early morning, afternoon, or early evening naps) and constant bedrest paradigms are usually applied.

1.3.1.1. Homeostatic characteristic of the NREM sleep EEG spectrum beyond SWA

SWA became the gold-standard of sleep homeostasis, as it reliably and strikingly reacted with a rebound to all types of deprivation/extension protocols. SWA increases after total deprivation, and the extent of this increase depends on the length of preceding waking period. As a result of selectively depriving SWS in the first half of the night, SWA levels are elevated after the deprivation is discontinued. Partial sleep deprivation causes an SWA increment during the following morning nap; furthermore, chronic partial deprivation results in a minor elevation of SWA in recovery sleeps. Finally, extensive

sleep results in decreased SWA in the following habitual episode (review of the different protocols and studies can be seen in Achermann & Borbély, 2017; Borbély & Achermann, 1992). However, several of these studies also examined higher frequency EEG activities and found that, in addition to SWA, other frequency bands, sometimes up to lower beta range (20 Hz) could also change as a result of sleep progression or deprivation. The direction of these changes varies across the spectrum. Finelli et al. (2001) found that NREM sleep EEG power increases in the 0.75–10.5 Hz range but decreases in the 12–12.25 Hz and 13.25–25 Hz ranges as a result of sleep deprivation. Similarly, earlier research reported a significant increase in 15–16 Hz activity across sleep cycles and decrease due to sleep deprivation (Borbély et al., 1981). Another study found and increase in power density in the 13.25–14 Hz range during baseline sleep, with the opposite pattern observed following sleep deprivation (Dijk et al., 1990). Not to mention the reported negative correlation between the overnight variation of the power in 20–28 Hz and 0.3–3 Hz (Uchida et al., 1992). These findings raise the possibility that SWA is a necessary but not sufficient component for modelling sleep homeostasis.

1.3.2. Setups for measuring time of day effects

As it was introduced above (Section 1.2.2.2.), the internal circadian rhythm is synchronized with the environmental rhythm. However, in our world—at least since the introduction of artificial light usage—the social "clock" has also become a factor influencing the entrainment between environmental and inner time (Roenneberg et al., 2019). Therefore, examining internal circadian rhythm independent of the environment is difficult and requires strict resource-intensive protocols. The main goal of such protocols is to exclude all potential zeitgebers, including both social and natural light factors, that is, anything that could provide information about the time of day. Two well-established paradigms are the constant routine and forced desynchrony. The former when applied to humans, not only involves the removal of cyclic environmental cues but also eliminates periodic behaviour influences such as eating or the sleep-wake cycle. Thus, an optimal constant routine should last at least 24 hours and include constant ambient light, a stable room temperature, minimum physical activity while maintaining a consistent posture, and evenly distributed food intake across day and night (J. F. Duffy & Dijk, 2002). The forced desynchrony protocol has similar aims, namely the elimination of the synchronization between the internal and environmental rhythms, while controlling for

undesired effects of sleep deprivation. In contrast to total sleep deprivation in constant routine, this protocol involves artificially created days with schedules shorter or longer than the natural 24-hour sleep-wake cycle. The most common schedule is 28-hour days, with one third of each day (~9.33-hours) dedicated to sleep (Carskadon et al., 1999; Dijk et al., 1992, 1999; J. F. Duffy et al., 1998). This schedule typically lasts several weeks (usually 20–40 days), allowing both wake and sleep periods to occur in different phases of the circadian rhythm. As a result, internal rhythms (such as core body temperature or melatonin) become desynchronized from the sleep-wake cycle, causing them to oscillate at their own intrinsic period.

In human circadian research, core body temperature and melatonin are the primary indicators of rhythmic activity. However, the implementation of these measurements can be costly or inconvenient, therefore, metrics derived directly from EEG recordings would offer a significant advantage in assessing the circadian component of sleep regulation in both sleep medicine and research (Bódizs et al., 2022). Studies using the above described protocols revealed that beside REM sleep propensity, several aspects of sleep spindles modulated by circadian rhythm (Aeschbach et al., 1997; Knoblauch et al., 2005; Purcell et al., 2017; Wei et al., 1999).

1.3.2.1. Circadian characteristic of sleep spindles

As mentioned above, studies using the forced desynchrony protocol have found substantial circadian variation in spindles. For instance, one study observed that spindle activity follows an opposite circadian rhythm to the melatonin rhythm, furthermore, slow spindle activity is highest and fast spindle activity is lowest when sleep occurred during the phase of melatonin secretion (Dijk et al., 1997). Spindle frequency was also associated with the phase of melatonin, being lowest at the acrophase of melatonin secretion (Knoblauch et al., 2005). Additionally, spindle frequency was found to follow a similar pattern to the core body temperature rhythm, specifically, spindle frequency was lowest and highest during the same phases as body temperature (Wei et al., 1999). Furthermore, daytime recovery sleep following 25 hours of wakefulness was characterized by increased sleep spindle frequency compared to baseline nocturnal sleep (Rosinvil et al., 2015). In our recent studies, we could strengthen these findings as we observed higher frequency spindles during nap sleep compared to night sleep records, as well as a sleep-middle

deceleration of spindles, reflecting a U-shaped overnight dynamic of spindle frequency (Bódizs et al., 2022; G. Horváth & Bódizs, 2024).

1.4. Individual differences of the sleep EEG in terms of age, sex and intelligence

A previous study demonstrated that advancing age is linked to a reduction in NREM sleep SWA, alongside a concurrent increase in higher-frequency EEG power in healthy adults (Carrier et al., 2001). Additionally, age has been associated with a decline in sleep spindle activity and a shift toward higher intra-spindle oscillation frequencies with age (Nicolas et al., 2001; Principe & Smith, 1982; Purcell et al., 2017).

Several studies have reported sex differences across multiple EEG frequency bands, with females exhibiting greater spectral power than males, independently of sleep stage or frequency range, suggesting a generally higher EEG amplitude in women (Carrier et al., 2001; Dijk, Beersma, & Bloem, 1989). Moreover, women tend to show higher spindle density, power (Carrier et al., 2001; Crowley et al., 2002; Dijk, Beersma, & Bloem, 1989; Ujma et al., 2014), as well as higher spindle frequency than men (Ujma et al., 2014).

Sleep spindle activity has also been reported to correlate positively with measures of intellectual ability (Bódizs et al., 2005; Schabus et al., 2006), suggesting a potential link between spindle dynamics and cognitive performance. Interestingly, this association has been shown to exhibit sexual dimorphism, with significant correlations between spindle amplitude and intelligence in women, but not in men (Ujma et al., 2014, 2017); however, this finding has not been consistently supported in more recent studies (Pesonen et al., 2019; Ujma, 2021).

In sum, spectral features of sleep EEG reliably reflect individual traits like age, sex, and intelligence. However, analytical variability can lead to inconsistent findings, making standardisable spectral methods essential.

1.5. Spectral analysis of the sleep EEG

The objective method of assessing sleep became even more reliable when researchers found out that the EEG signal can be decomposed into its frequency components with Fourier transformation. The moduli of the resulting complex coefficients represent wave amplitudes across frequencies, forming the amplitude spectrum, whereas their squared values define the power spectrum, which reflects signal

power distribution over frequencies. As EEG is a discrete time-domain signal sampled at a specific frequency, resulting in n data points, it can be transformed into frequency domain using the discrete Fourier Transform, producing n complex numbers that span the range from negative to positive Nyquist frequency (which latter is the half of the sampling rate). Computational demand of the discrete Fourier Transform is optimized via Fast Fourier Transform (FFT), which requires the data points to be a power of 2 (2^n, where n is a positive integer). The transformation assumes that the data are stationary. However, as sleep EEG does not meet this assumption, Welch's method is commonly used. In this method, the power spectral density (PSD) is estimated by dividing the signal into short, overlapping (usually 50%) segments (that can be considered stationary). A windowing function is then applied to minimize edge artefacts, the FFT is estimated to each segment, and the resulting spectra are averaged (Cox & Fell, 2020).

Commonly used EEG spectral power measures are band-limited based on standard frequency ranges, and are often represented as integrals over specific segments of the spectrum or calculated bin-by-bin, indicating the amplitude of narrow frequency band (e.g. 1 Hz wide) (Bódizs et al., 2024). Analysing pre-defined frequency bands carries the risk of biases, as EEG data can be examined various ways depending on the specific electrophysiological phenomenon is being studied (Bódizs et al., 2021). Furthermore, the analysis specifications are not always clearly stated, making comparisons between studies challenging, as these studies may use PSD or power, raw or log-transformed values, which are either summed, averaged or integrated (Cox & Fell, 2020). Thus, an overall characterization of the power spectra my serve as a more objective tool for analysing sleep EEG.

1.4.1. Spectral parametrization

Previous research has consistently shown that neurophysiological signals consist of rhythmic oscillatory activities and an aperiodic component. The scalp EEG spectrum follows a power-law distribution (Pereda et al., 1998; Pritchard, 1992) which implies a linear relationship between the logarithms of amplitude and frequency (Feinberg et al., 1984). The 1/f pattern represents the aperiodic aspect of the signal, stemming from the inherent scale-free nature of power-law functions. Essentially, this suggests that no specific frequency dominates the signal; instead, the slope of the spectrum (without the spectral peaks) reveals the overall frequency distribution within the time series (G.

Horváth et al., 2022), providing the constant ratio between lower and higher frequency power (Bódizs et al., 2021, 2024). As EEG spectra can be accurately described by a power law function, band power measures are inherently redundant, reflecting the same statistical pattern across different frequency ranges (Bódizs et al., 2024). However, oscillatory activity also occurs in particular frequency ranges of the power spectrum, making it essential to properly separate these two components for a precise characterization of sleep EEG. We suggest that the Fourier spectrum can be accurately represented by the following function, which considers both aperiodic part and peaks of the spectrum (Figure 1):

$$P(f) = Cf^{\alpha}P_{Peak}(f)$$

Here, P represents power as a function of frequency (f), P_{peak} denotes the peak power at frequency f (equalling 1 in the absence of peak and greater otherwise), the constant C is the intercept reflecting the frequency-independent EEG amplitude, and α is the spectral exponent (negative value). We can obtain the slope of the spectrum by applying a double logarithmic scaling to the above, resulting in the exponent becoming the spectral slope:

$$\ln P(f) = \ln C + \alpha * \ln f + \ln P_{Peak}(f)$$

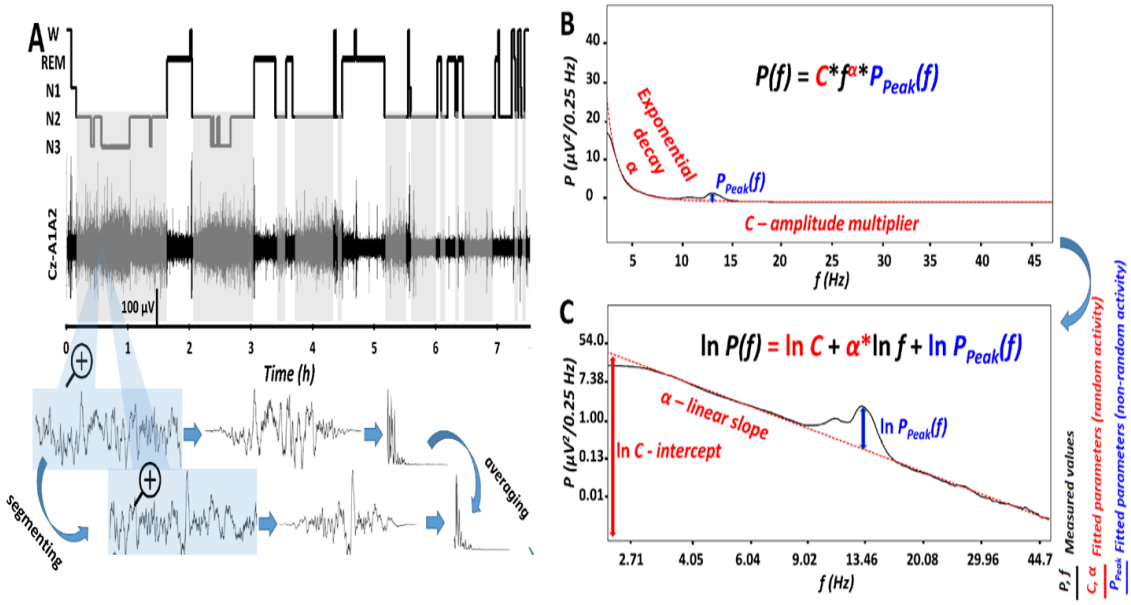

Figure 1. The parametrization of non-rapid eye movement (NREM) sleep electroencephalogram (EEG) spectra. A. Hypnogram and workflow of spectral EEG analysis illustrated using a representative recording from a young male participant. Grey-shaded areas indicate NREM sleep. Blue-shaded EEG segments depict magnified

4-second epochs (with 2-second overlap) that were Hann-windowed prior to power spectral analysis using mixed-radix Fast Fourier Transformation (FFT). B. Mean spectral power (P) described by a frequency (f)-dependent exponential decay (α), a frequency-independent amplitude multiplier (C) and a peak power multiplier at specific frequencies [$P_{Peak}(f)$]. C. The natural logarithm of spectral power (P) is a linear function of the natural logarithm of frequency (f), yields a linear slope α (identical to α in panel B) and an intercept (the natural logarithm of the amplitude multiplier C in panel B). This linear function is further summed with the natural logarithm of the peak power multiplier [$P_{Peak}(f)$, the same function as in panel B]. Figure is adapted from Bódizs et al. (2021).

Previous studies on the aperiodic characteristics of EEG suggest that spectral slope is a function of age (Feinberg et al., 1984; Tan et al., 2001; Voytek et al., 2015), as well as of arousal level, as it can successfully discriminate between sleep and wake states, or different levels of consciousness (Colombo et al., 2019; Lendner et al., 2020; Waschke et al., 2021; Zhang et al., 2023). Furthermore, spectral slope has been shown to become progressively steeper with the deepening of sleep, with the flattest slope observed in wakefulness (Favaro et al., 2023; Freeman et al., 2006; Miskovic et al., 2019; Pereda et al., 1998; Schneider et al., 2022) and was reported as one of the most reliable metric of sleep stage categorization (Krakovská & Mezeiová, 2011). It can also differentiate between sleep cycles (Rosenblum et al., 2023), and between brain states of restful and active wakefulness (Höhn et al., 2024). Therefore, based on these result, one can assume that the spectral slope is a reliable marker of the homeostatic process of sleep regulation. It is likely more standardisable than the gold-standard (as reported values vary within a much narrower range compared to SWA) while still capturing interindividual differences (such as age), and accounts for the entire frequency composition of the spectrum. This may be crucial for modelling sleep homeostasis, as not only SWA changes in response to sleep pressure (see Section 1.3.1.1.).

On the other hand, since spectral peaks represent oscillatory activity at particular frequencies (Gao, 2016), the most prominent peak of the 9–18 Hz range (broad sigma range) can be considered spindle activity if its characteristics (e.g. spatial distribution frequency, sex and age differences) align with the results obtained regarding sleep spindles (see Section 1.3.2.1. and 1.4.). As spindle frequency has been shown to reflect circadian variation in several studies (Section 1.3.2.1.), obtaining the spectral peak frequency in the spindle band using spectral parametrization procedures, would greatly simplify the investigation of the circadian process of sleep regulation.

2. Objectives

The examination of the two key processes underlying sleep regulation (sleep homeostasis, circadian rhythm) by PSG remains unresolved. While no validated EEG marker exits for the circadian process, sleep homeostasis is typically indicated by SWA of NREM sleep EEG. However, a major criticism of the latter is that quantitative EEG indicators are redundant and cannot be standardized, making intra-individual comparisons challenging and preventing the establishment of normative values for optimal sleep. Therefore, the overall objective of my PhD research was to characterize the NREM sleep EEG Fourier spectrum by considering its power-law scaling properties, with a primary focus on how the derived non-redundant parameters can be captured within the context of sleep regulatory processes.

To achieve these objectives, the presented studies set out to accomplish the following:

In the first study, we aimed to demonstrate that the parametrization procedure effectively reduces the typically analysed 191 spectral measures to just 4 (spectral slope, intercept, amplitude and frequency of the largest peak in the spindle frequency range), which reliably capture the known age-, sex-, and intelligence-related associations of the sleep EEG.

The second study examined the overnight dynamics of those 4 parameters, focusing on the first four consecutive sleep cycles of habitual PSG recordings. The aim was to investigate whether separating the aperiodic and periodic components of the NREM spectra could serve as reliable indicators of known overnight sleep cycle dynamics associated with sleep regulatory processes. The main research question was whether spectral slope associates with SWA and more standardizable than the gold-standard, as well as whether spindle peak frequency evolves in a U-shaped curve during the night.

Finally, Study 3 aimed to validate the role of spectral parametrization in examining sleep regulatory processes using a 35-hour home sleep deprivation protocol with chronotype-dependent baseline sleep (BS) onsets. The main objective was to assess spectral slope and peak frequency by challenging the homeostatic process (sleep deprivation) and slightly advancing sleep onset, with the aim of unravelling the circadian rhythm (reschedule of recovery sleep (RS) by advancing it with ~ 4.5 hours).

3. Methods

3.1. Study 1 and Study 2

For the first two studies, overlapping database and the same spectrum parametrization techniques were used, but different analytical approaches were applied to address our research questions. In the following sections, methods of Study 1 and Study 2 will be described together, with clear indications where the applied procedures differed. The aims and research settings of the studies are presented in Table 1.

3.1.1. Sample

The sample was drawn from the Budapest-Munich database (Bódizs et al., 2017) for both studies. This database includes N = 251 healthy participants (122 females) with an age between 4 and 69 years (mean: 25.13). In Study 2, the entire database was utilized (G. Horváth et al., 2022); however, in Study 1, data from children under the age of 17 were excluded, resulting in a dataset of N=175 participants (81 females, mean age: 29.23, min. age: 17 years) (Bódizs et al., 2021). Intelligence Quotient (IQ) scores were assessed for N =149 participants (68 females, mean age: 29.23 years) with additional recruitment through Mensa Germany and Mensa Hungary to increase the representation of highly intelligent individuals (IQ score estimation is described in Bódizs et al. (2021)).

Semi-structured interviews with experienced psychiatrists or psychologists confirmed that all participants were in good health, had no history of neurological or psychiatric disorders, and were free of any current drug effects, except for contraceptive use in females. The majority of the sample were non-smokers (only six men and two women self-identified as light-to-moderate smokers). Maximum allowed caffeine intake was defined as up to two cups of coffee before noon (moderate consumption), while alcohol was strictly prohibited. The research protocols were verified by the Ethics Committees of Semmelweis University (Budapest, Hungary) or the Medical Faculty of the Ludwig Maximilians University (Munich, Germany) (146/2010). All experiments were conducted in accordance with the principles outlined in the Declaration of Helsinki. All participants (or in case of minors, their parents/guardians) provided written informed consent to participate in the study.

3.1.3. Polysomnography

The procedures for detailed data recording of the different studies in the Budapest-Munich database can be found in Bódizs et al. (2017). The polysomnography data were recorded over two successive nights, with EEG electrodes placed based on the international 10-20 system at Fp1, Fp2, F3, F4, Fz, F7, F8, C3, C4, Cz, P3, P4, T3, T4, T5, T6, O1, and O2, re-referenced to mathematically linked mastoids. Besides EEG channels, EMG, EOG and electrocardiography (ECG) were also registered. Sampling frequency was either 249 Hz, 250 Hz or 1024 Hz depending on the site of data collection. However, the impedances for the electrodes were kept below 8 kΩ in all cases of the database. All PSG records were scored manually, in accordance with the standard criteria of sleep-wake states (Civan et al., 1992). Sleep scoring was followed by a 4-second based manual artefact removal. Only the second night of the sleep records were analysed in both studies to avoid first-night effect. In Study 1, analyses were conducted across all recording sites for NREM (N2 and N3) sleep of the entire sleep episode. In contrast, Study 2 focused only on parasagittal electrode sites (Fp1, Fp2, F3, F4, C3, C4, P3, P4, O1, O2) and analysed NREM episodes (N2 and N3) separately in consecutive sleep cycles. Sleep architecture was divided into sleep cycles according to the criteria proposed by Aeschbach & Borbély (1993).

3.1.4. Power spectral analysis

First, NREM (N2 + N3) power spectra were computed from 0 to Nyquist frequency (in μV^2/0.25 Hz) after artefact-free 4-second epochs (with 2-second overlap) were Hann-windowed and processed using a mixed-radix fast Fourier transform. This was performed on the entire sleep period in Study 1, whereas in Study 2, it was applied separately to successive sleep cycles. Subsequently, EEG-location specific power spectral densities from all 4-second windows were averaged for the entire night (Study 1) or within the successive sleep cycles (Study 2). SWA in Study 2 was quantified as the sum of power values from each frequency bin (power spectral density) in the 0.75–4.5 Hz frequency range of the EEG signal. Analysis was performed using data from the left frontal electrode site (F3), with results averaged over N2 and N3 stages during complete sleep cycles.

3.1.6. Spectrum parametrization

The parametrization of the power spectra in both studies was conducted with the parametrization procedure proposed in Study 1 (Bódizs et al., 2021). Main steps of the method are the following:

1. Piecewise cubic Hermite interpolation of the log–log scale of NREM (N2 and N3) sleep EEG spectra to equidistant, 0.0052 Hz bins (the smallest frequency step).
2. Estimation of spectral slope by fitting a linear function to the spectrum, excluding frequency bins below 2 Hz and between 6–18 Hz, to prevent fitting bias caused by non-random oscillatory activity in those frequency ranges.
3. Detection of spectral peaks in the 9–18 Hz frequency range, known as broad sigma range. Peak detection was defined as searching for local maxima and minima in mathematical terms within the sigma range. Therefore, we utilized the first and second derivatives to identify critical points and distinguish between maxima and minima, respectively. A spectral peak was recognised and validated when the first derivative was 0 and the second derivative was negative.

3.1.7. Statistical analyses

TIBCO Statistica 13 software was used for statistical analyses. Parametric tests were performed for normally distributed data, while non-parametric tests were applied for non-Gaussian distributions. Normality was assessed using the Shapiro-Wilk test in all cases. In cases of significant effects or interactions Unequal N HSD post hoc test was conducted for further evaluation.

3.1.7.1. Study 1

Correlational analyses (Pearson product-moment-, Spearman's rank correlation) and between-group comparisons (independent samples t-test, Mann-Whitney U test) were applied to assess the associations of age and IQ with the different spectral parameters, as well as to examine sex-related differences in these parameters. To control for Type-I errors arising from multiple electrodes and hypotheses, we applied a modified version of the Descriptive Data Analyses (DDA) protocol (Abt, 1987) specifically adapted for neurophysiological data (Abt, 1990; F. H. Duffy et al., 1990). Taking into account the intercorrelations among different electrodes, DDA relies on the identification of Rüger's areas (Rüger, 1978), which are clusters of spatially adjacent results that are descriptively

significant ($p<0.05$). A Rüger area is significant, when either at least one-third of the descriptively significant results meet a threshold of $p = 0.017$ (0.05/3) or at least half reach $p = 0.025$ (0.05/2). In the present study both criteria were applied concurrently.

Anterior-posterior changes in peak frequency were tested by the following analysis. As a first step, parasagittal regions were created by averaging peak frequencies in frontopolar (Fp1, Fp2), frontal (F3, F4, Fz), central (C3, C4, Cz), parietal (P3, P4, Pz), as well as occipital (O1, O2) derivations. Thereafter, the differences in spectral peak frequencies of all adjacent antero-posterior regions were calculated. That is, we subtracted the mean of the frontopolar region from the mean of the frontal region, the frontal from the central et cetera. The outputs represent shifts in peak frequency along the antero-posterior axis, with positive values indicating anterior-to-posterior increases. Successive frequency changes were summed per subject, which was then averaged across the sample. The maxima were also identified and localized individually, yielding a sample mean of maximal shift and its topographical distribution.

3.1.7.2. Study 2

The sample was divided into 4 age groups as in our earlier study (Bódizs et al., 2017): children (4–9 years, N=31, 15 females), teenagers (10–19 years, N = 36, 18 females), young adults (20–39 years, N = 150, 75 females), and middle-aged adults (40–69 years, N = 34, 14 females).

General linear models were conducted with age groups and sex as between-subject factors; sleep cycles, brain regions and hemisphere as within-subject factors. Here we considered the secondary interactions of the factors with significant main effects.

In correlational analyses, the log-transformed SWA (lnSWA) was utilized ensuring compliance with the assumptions of parametric statistical tests. However, since classical SWA is typically reported in most research articles, the results of the general linear model are presented here using both type of SWA values.

With respect to the spectral peak frequencies, their antero-posterior distribution was also tested. On one hand, we performed the descriptive analysis of the dominant frequency shift by relying on the procedure implemented in Study 1 (Bódizs et al., 2021), but separately for each sleep cycles. On the other hand, these frequency shifts were analysed using an adaptation of the Kullback–Leibler (KL) distance measure (Kullback & Leibler, 1951), a statistical tool to quantify differences between two distributions.

Precise description of these analyses can be seen in (G. Horváth et al., 2022). The goal was to assess whether region-specific variations in peak frequencies follow a uniform antero-posterior distribution, implying an equal likelihood of changes in the antero-posterior direction across all adjacent parasagittal regions (null hypothesis: continuous antero-posterior frequency shifts), or if the changes are discontinuous, suggesting a distinction between slow and fast sleep spindles, potentially driven by non-continuous antero-posterior shifts.

3.1.7.3. Goodness of Fit assessment

The goodness of fit between the linear model and the equidistant log-log spectral data was assessed using Pearson product-moment correlations. These correlations were then Fisher Z-transformed, averaged, and back-transformed following the recommendations of Silver & Dunlap (1987). Finally, the mean r-value was squared to determine the shared variance. The standard deviation (SD) was calculated from the Fisher Z-transformed dataset and subsequently back-transformed.

3.2. Study 3

3.2.1. Sample

Healthy young adults, free of neurological and psychiatric disease, as well as any acute or chronic illnesses based on self-reports took part in the experiment (G. Horváth & Bódizs, 2025). The recruitment process combined convenience and snowball samplings utilizing personal contacts and social media outreach. Due to the strict exclusion criteria, out of more than 300 applicants, overall N=46 subjects participated in the examination. Inclusion criteria were based on questionnaires and were the following: Hungarian version of the Pittsburgh Sleep Quality Index (PSQI) (Takács et al., 2016) score below 5, Beck Depression Inventory (BDI) score below 13 (Beck et al., 1961), no alarm clock usage on free days, daytime work schedule, a Munich Chronotype Questionnaire (MCTQ) chronotype score (MSFsc) within the mean +/-3 SD range of young Hungarian subjects reported in (Haraszti et al., 2014), and age between 18 and 40 years.

Ultimately, the final, analysable sample comprised N = 38 participants (age range: 18–39 years, mean age= 24.9, 19 females). The reduction in sample size was due to low-quality EEG recordings or complete data loss.

3.2.2. Study design

After pre-screening, applicants who met the requirements were invited to the laboratory and received detailed information on the use of the mobile EEG device and completed cognitive tests. EEG-recorded sleep was performed at the home of the participants with the mobile EEG headband. During the BS measurement, participants were free to choose their bedtime, allowing them to follow their own sleep preferences. The use of an alarm clock was not permitted on either morning of the headband-EEG-recorded sleep sessions (BS and RS). Upon awakening from BS, the sleep deprivation phase began, requiring participants to remain awake for the next 35 hours. During this period, alcohol intake was forbidden, whereas stimulant use restricted to caffeine, which could be consumed in the form of coffee in amounts consistent with the participant's usual daily intake. However, total caffeine consumption was limited to a maximum equivalent of three espresso shots over this 35-hour period. Participants were free to choose their activities during the sleep deprivation. However, they were required to maintain continuous contact with the experimenter–providing at least one hourly report on their well–being and current activity via mobile phone messages–and to complete sleepiness scale questionnaires at designated time points (0, 12, 24 and 35 hours after sleep deprivation onset). Additionally, experimenters visited participants in their homes at the 24^{th} and 34^{th} hour of the course of prolonged wakefulness to conduct cognitive task recordings, assess their well-being, and ensure adherence to the study protocol in person. Compliance was monitored by verifying the availability of all hourly text messages and completed questionnaires at each designated time point. Before RS, the experimenter assisted participants to put on the EEG headband and instructed them to turn off the lights and go to bed. Upon waking, participants completed the sleepiness scales one last time, concluding their participation in the experiment. The present study focuses on the analyses of selected questionnaires (MCTQ, sleepiness scale) and the sleep EEG data.

National Public Health Centre Institutional Committee of Science and Research Ethics approved the research protocols (48594-7/2020/EÜIG), and the experiment was implemented in accordance with the Declaration of Helsinki. Every participant signed an informed consent about their attendance in the study.

3.2.3. Sleep electroencephalography

Sleep data was obtained by Hypnodyne corp. Zmax EEG headband. The device records two EEG derivations at F7-Fpz and F8-Fpz with sampling rate of 256 Hz, photoplethysmography (PPG), accelerometry, skin temperature, light- and acoustic noise intensity. EEG channels were re-referenced to their common average. Sleep staging was manually performed based on the consensual criteria for different states (Berry et al., 2018), using 20-second epochs. Similar scoring schemas could be applied as for PSG data, as the aforementioned measurements offer nearly identical information content as the originally recommended derivations, such as EMG (can be substituted by head movement measure and muscle artefacts) or ECG (can be replaced by the PPG). After scoring, hypnograms were divided into consecutive NREM-REM periods (sleep cycles) according to the modified criteria of Feinberg & Floyd (1979) which takes into account the possible absence of stage REM in the first sleep cycle (Jenni & Carskadon, 2004).

3.2.3. EEG spectral analyses

Manual artefact removal was followed by a power spectral density (PSD) analysis based on the Welch method: EEG signal was segmented into 4-second epochs with an overlap of 50%, after which a Hann window function was applied, and Fast Fourier Transform (FFT) was computed for every NREM (N2 + N3) period in each sleep cycle. Finally, the resulting spectra were averaged across all 4-second epoch within each sleep cycles. SWA was determined by summing the PSD values within the 0.75–4.5 Hz range of EEG activity from the averaged N2 and N3 episodes across complete sleep cycles.

3.2.3.2. Spectrum parametrization

In contrast to Study 1 and Study 2, the parametrization of the power spectra was performed by the fitting oscillations and one over f (FOOOF) method, developed by Donoghue, Dominguez, et al. (2020). This procedure aims to separate aperiodic from the periodic components of the spectrum by first estimating and removing an approximated 1/f-like background trend using a linear function, resulting in a flattened spectrum that highlights spectral peaks. After identifying and fitting oscillatory peaks, the aperiodic component is re-fitted. The combined version of the periodic and refitted aperiodic component can be used for further analyses.

Fitting range was set to 2–48 Hz frequency range, with a bandwidth of accepted peaks of 0.7–3 Hz, and with a peak threshold of 1, as this setting were used in (Schneider et al., 2022) to avoid over- or under fitting.

In this study (Study 3), only two spectral parameters, namely, slope and spindle peak frequency were analysed as they were hypothesized to be most closely linked to the examined sleep regulatory processes. Spindle frequency was defined as follows: the first three largest peaks were obtained and ranked by amplitude. The peak within the 9–16 Hz (broad spindle) frequency range with the highest amplitude among the three was retained and its frequency was analysed (which parameter is referred to as peak frequency in the remaining part of my thesis). If all three fell outside the spindle range, the spectrum considered to lack a spindle peak (thus peak frequency) for that specific spectrum.

3.2.4. Munich Chronotype Questionnaire, Sleepiness scales

The MCTQ gathers information on habitual bedtimes, wake-up times, sleep latency and sleep inertia for work- and free days separately. Chronotype (denoted as MSFsc) is determined as the middle point of the sleep period on free days corrected for oversleeping. In the present study, MSFsc was used both as a continuous predictor and for the categorization of chronotypes. Participants whose MSFsc values fell outside the ± 1 SD range of the mean reported for young Hungarian individuals (Haraszti et al., 2014) were classified as morning or evening types, while those within ± 1 SD range were categorized as intermediate types.

Subjects completed two different sleepiness scales six times during the experiment (see study design for specific time points). A Likert scale with the following instruction: “Please indicate your sleepiness level on a scale from 1 to 10 where 1 means ‘not sleepy at all’ while 10 refers to ‘very sleepy’.”. This approach was found to be more sensitive to measure daytime dysfunction than other scales in a former study (Riegel et al., 2013). Furthermore, the Stanford Sleepiness Scale was applied (Hoddes et al., 1973). This questionnaire comprises seven statements describing different levels of sleepiness, from which participants select the one that best reflects their actual state.

3.2.6. Statistical analyses

Data examination was carried out using TIBCO Statistica software in multiple settings to examine the overnight dynamics of spectral slope and spindle peak frequency

during baseline (BS) and recovery sleep (RS), as well as the differences in these parameters between the two nights. On the one hand, in order to maximize statistical power, we aimed to maintain the highest feasible sample size as a consequence, lower number of sleep cycles (first 4) remained available for analyses. On the other hand, we aimed to analyse the overnight dynamics of the aforementioned parameters across the entire night. To achieve this, subjects were categorized based on the number of sleep cycles they had (separately for the two nights), and the nocturnal variations of these variables were examined within each group. Although the group sizes were small in these analyses, this approach allowed for the assessment of the entire night for each participant who had complete recordings. Since the cycle effect was expected to be substantial, we deemed a group analysable if it had a minimum sample size of N = 7. As a result, BS groups with 3 and 7 sleep cycles, as well as RS groups with 6 and 10 cycles had to be excluded, as they comprised no more than 3 participants. Lastly, we compared specific cycles (those at the beginning, middle, and end of the sleep periods), as well as the BS vs RS cycle numbers in which the minimum and maximum values of the parameters occurred on the respective nights.

Dependent samples t-tests were used for comparing two variables or conditions, repeated measures ANOVA for analyses involving more than two variables or time points, and General Linear Models when multiple factors were included. When the sample size was less than 10 (in the cycle group-wise analyses) or if any of the variables had non-Gaussian distribution, non-parametric alternatives of the aforementioned tests were applied. Normality was tested using Shapiro-Wilk W test for all variables. The number of sleep cycles in both conditions, the sleep cycle during which participants reached their peak frequency minimum in BS, BS cycle 4 slope values, RS cycle 7 slope values, cycle numbers in which the minimum and maximum slope values occurred, and both sleepiness scales at all time-points were characterized by a non-Gaussian distribution. In case of multiple comparisons, Bonferroni correction was applied. We reported mean (m) and standard deviation (SD) for normally distributed data, while median (Mdn) and interquartile range (IQR=[lower bound, upper bound]) are provided for non-normally distributed data.

Table 1. Overview of the samples, aims, and methods of the three studies.

	Participants			**Aims**	**Methods**				
	Sample size	*Age range (years)*	*Exclusion criteria*	*Hypothesis to be tested*	*Analysed Sleep stage*	*Analysed EEG channels*	*Sampling rate*	*Spectrum parametrization method*	*Additional metrics*
Study 1	175 (81 females)	17–69	Diseases Neurological/ psychiatric disorders Current drug effect	To derive physiologically meaningful metrics by parametrizing the sleep EEG spectrum	Whole night average of N2 & N3	Fp1, Fp2, F3, F4, Fz, F7, F8, C3, C4, Cz, P3, P4, T3, T4, T5, T6, O1, O2	249 / 250 / 1024 Hz	(Bódizs et al., 2021)	IQ score
Study 2	251 (122 females)	4–69	Diseases Neurological/ psychiatric disorders Current drug effect	To capture known overnight dynamics associated with sleep regulation using metrics derived from spectral parametrization of the EEG signal in successive sleep cycles	Average of N2 & N3 by sleep cycles (first 4 cycles)	Fp1, Fp2, F3, F4, C3, C4, P3, P4, O1, O2	249 / 250 / 1024 Hz	(Bódizs et al., 2021)	SWA at F3 recording location
Study 3	38	18–39	Diseases Neurological/ psychiatric disorders Current drug effect PSQI>5 BDI>13 Alarm clock on usage on free days, Daytime work schedule, Extreme chronotype	To validate spectral parametrization as a novel approach to measuring sleep regulatory processes using a 35-hour sleep deprivation protocol	Average of N2 & N3 by sleep cycles	F7-Fpz, F8-Fpz	256 Hz	(Donoghue, Haller, et al., 2020)	SWA, MSFsc, sleepiness

4. Results

4.1. Study 1

As a first step, we tested whether the linear model of our parametrization procedure has a good fit on the data (see section 3.1.7.3. Goodness of Fit assessment). The linear model applied to the [2–6]∪[18–48] Hz frequencies exhibited goodness of fit values spanning from 0.8955 to 0.9997, across individuals and EEG recording sites. The squared Pearson correlation coefficient between the fitted linear model and the spectral data was found to be R^2=0.9952 (SD=0.1578).

Spectral slope sample mean of 175 healthy participants, measured across up to 18 common EEG derivations, ranged from -2.73 (SD=0.22) to -2.33 (SD=0.22), whereas the mean of intercepts (lnC) varied between 5.67 (SD=0.69) and 3.74 (SD=0.73). These values corresponded to the means of the frontocentral (Fz) and left temporal (T5) regions, respectively.

4.1.1. Spectral peaks of the 9–18 Hz frequency range

Spectral peaks within the 9–18 Hz range were identified using a combination of first- and second-derivative analyses, which mathematically pinpoint local maxima. The detected peaks were ranked based on their whitened amplitude, with the influence of coloured noise—characterized by the spectral slope (α) and intercept (C)—being removed prior to ranking. The presence of at least one peak was observed in 81.16% to 100% of participants, varying by EEG recording site. The largest peak (with the highest whitened amplitude) in this frequency range aligned with the general topographical-frequency distribution characteristic of sleep spindles. Specifically, spectral peaks in anterior regions appeared at lower frequencies compared to those in posterior areas (see example in Figure 2). The total increase in the frequency of the largest peak along the antero-posterior cortical axis was 1.99 Hz in average across subjects. However, this frequency shift was not gradual; instead, more than 83% (1.67 Hz) of the total increase occurred as a discrete jump, primarily localized to specific cortical transitions: frontal-to-central (54.77% of subjects), frontopolar-to-frontal (36.94%), central-to-parietal (6.36%), and parietal-to-occipital (1.91%). Peak frequencies identified rostral to the highest antero-posterior frequency transition are hypothesized to correspond to slow sleep spindles,

occurring in 100% of frontopolar, 63.05% of frontal, 8.28% of central, 1.91% of parietal, and 0% of occipital recording sites. In contrast, caudal spectral peaks are presumed to represent fast sleep spindles observed in 0%, 36.95%, 91.72%, 98.09%, and 100% of frontopolar, frontal, central, parietal, and occipital regions, respectively.

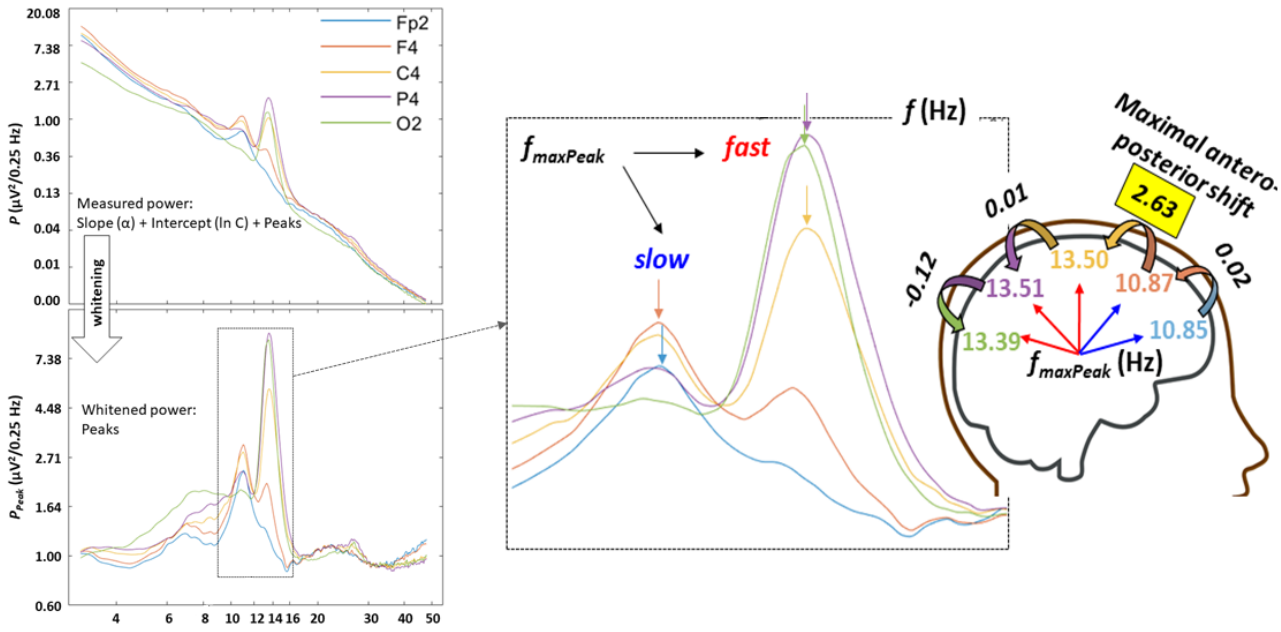

Figure 2. Examples for spectral peaks over the antero-posterior cortical axis in one of the subjects. Top left panel: periodograms plotted in the double natural logarithmic plane displaying a combination of linear trends and spectral peaks. Bottom left panel: whitened powers obtained by subtracting the fitted linear components: ln P – (ln C + α ln f). Note the uniform baseline power (~1) and the spectral peaks. Right panel: enlarged spectral peaks in the spindle frequency range, characterized by lower frequency maxima in the anterior as compared to the posterior recording locations (see colour-coded arrows); maximal antero-posterior shifts in peak frequency emerged between the frontal and central recording sites, demarcating slow-anterior and fast-posterior sleep spindle-related spectral peaks. Figure adapted from Bódizs et al., (2021).

Second largest spectral peaks, with approximately half the amplitude of the primary ones, were identified in a subset of participants and EEG derivations (6.29–50.64%). However, in most cases, these secondary peaks were about 1.5 Hz slower than the reported slow sleep spindle frequencies (Ujma et al., 2014) (Figure 3). This suggests that these peaks likely reflected alpha activity (~10 Hz) rather than genuine slow or fast sleep spindles. In other words, while the method applied in this study proved robust for reliably detection of the dominant spectral peak associated with sleep spindling at each recording site, it lacked the sensitivity to accurately capture non-dominant spindle peaks—namely, fast spindles in anterior regions and slow spindles in posterior regions.

Thus, throughout the rest of this study and in Study 2, we focused on the frequency and amplitude of the largest (maximal in amplitude) peak of the spectra, regarded as the spindle peak and referred to as peak frequency/amplitude.

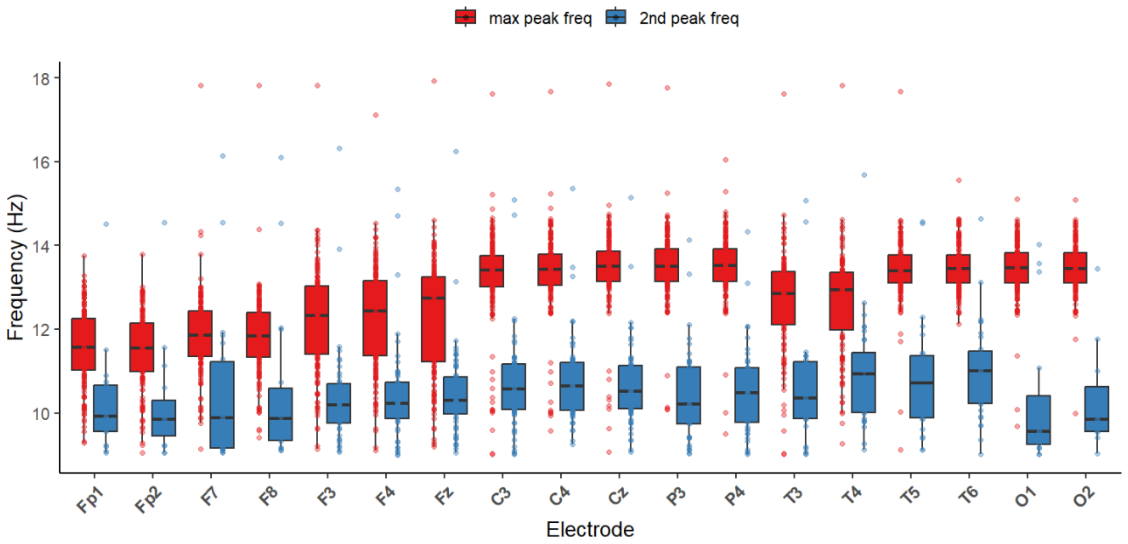

Figure 3. Boxplots of spectral peak frequencies at different electrode sites. Note that the widest interquartile range of peak frequencies, covering both slow and fast sleep spindles, was found in the prefrontal region (F3, F4, Fz), suggesting a mix of spindle types at these locations. In contrast, narrower ranges in anterior and posterior areas reflect predominantly slow and fast spindles, respectively. Figure was created based on the supplementary materials of Bódizs et al. (2021).

4.1.2. Effects of age on spectral peaks and slope

Age positively associated with spectral slope at all, and negatively with peak amplitudes and peak frequencies at 10 and 8 EEG derivations, respectively. All those areas can be considered significant according to the DDA (Table 2).

As we hypothesized age-related increase in peak frequency, we tested whether changes in slow and fast spindle sizes underlie our contradictory finding. Specifically, if the dominant peak shifts from fast to slow spindle frequency more frequently in the frontal regions of older individuals. To investigate this, we compared the ages of a group with the largest antero-posterior frequency shift from the frontal to frontopolar region, and a group with the shift occurring from the central to the frontal area. Mann-Whitney U-test indicated significantly higher age in the central to frontal shift group ($U = -2.41$, $\eta^2 = 0.713$, $p = 0.015$), that is age-related reduction in frequency may reflect a decline in the occurrence of fast sleep spindles in the frontal region among older adults.

Table 2. Spearman rank correlations(ρ) indicating the associations of age with spectral slopes (a), peak amplitudes (b) and frequencies (c) of NREM sleep EEG. a, Spearman rank correlations between age and spectral exponents (α) of NREM sleep EEG. Note the significance of correlations at the descriptive level of significance (p < .05), as well as at both of the new critical p levels corresponding to p < .025 and p < .017. The minimum criteria of a significant Rüger's area is 10 out of 18 (a), 5 out of 9 (b) and 5 out of 8 (c) descriptive significances to meet the p < .025 and 7 out of 18 descriptive significances to meet the p < .017 criteria. Table is sourced from supplementary materials of Bódizs et al. (2021).

Recording location	a, slope (α)			b, peak amplitude ($P_{Peak}(f_{maxPeak})$)			c, peak frequency ($f_{maxPeak}$)		
	ρ	p	N	ρ	p	N	ρ	p	N
Fp1	.38	***<.001***	163	-.107	.193	150	-.22	***.006***	150
Fp2	.39	***<.001***	171	-.035	.669	155	-.21	***.007***	155
F3	.39	***<.001***	174	-.184	***.018***	166	-.27	***<.001***	166
F4	.42	***<.001***	173	-.17	*.029*	165	-.25	***.001***	165
Fz	.44	***<.001***	156	-.288	***<.001***	151	-.37	***<.001***	151
F7	.36	***<.001***	153	-.105	.223	137	-.29	***.001***	137
F8	.38	***<.001***	154	-.002	.978	141	-.21	***.010***	141
C3	.38	***<.001***	174	-.328	***<.001***	172	-.05	.46	172
C4	.39	***<.001***	175	-.32	***<.001***	172	-.04	.586	172
Cz	.35	***<.001***	156	-.409	***<.001***	155	-.06	.44	155
P3	.34	***<.001***	175	-.23	***.002***	175	.10	.16	175
P4	.37	***<.001***	175	-.227	***.003***	174	.08	.253	174
T3	.39	***<.001***	154	-.141	.116	125	-.14	.119	125
T4	.39	***<.001***	156	-.125	.154	131	-.30	***.001***	131
T5	.33	***<.001***	154	-.176	*.030*	152	.01	.861	152
T6	.37	***<.001***	155	-.213	***.009***	151	-.00	.988	151
O1	.29	***<.001***	175	-.127	.097	173	.10	.179	173
O2	.33	***<.001***	174	-.132	.085	172	.11	.152	172

4.1.3. Sex differences in spectral peaks and intercept

Women had higher intercepts, and faster peak frequencies ($p<0.05$, except for T3 and T4 locations; Figure 4) than man, and the two sex groups did not differ in terms of the whitened spindle peak amplitude at any derivations ($p>0.05$). All the significant areas can be considered significant according to the DDA (results of the Mann–Whitney U-tests and t-tests can be seen in Supplementary Table 4 in Bódizs et al., (2021)).

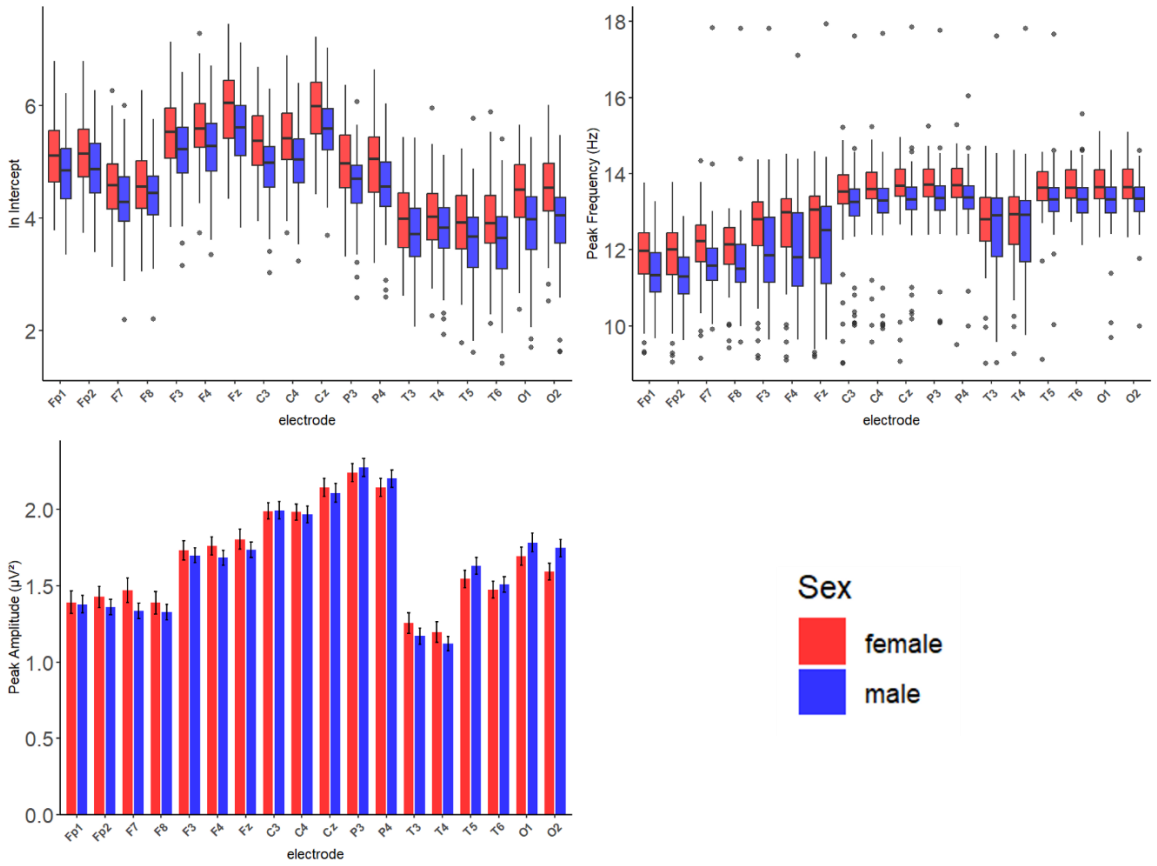

Figure 4. Sex differences in intercept, peak frequency and peak amplitude across different recording locations. The upper panels display boxplots showing the median and interquartile range, while the bottom panel shows peak amplitude as means with 95% confidence intervals. Figure was created based on the supplementary materials of Bódizs et al. (2021).

4.1.4. Associations of IQ with spindle peak amplitude

Significant relationships between peak amplitudes and IQ were revealed in women according to the results of Pearson correlation (Figure 5), at the following recording sites: C3 (N=67, r=0.33, p=0.007), C4 (N=66, r=0.34, p=0.005), Cz (N=55, r=0.34, p=0.010), P3 (N=68, r=0.26, p=0.031), P4 (N=68, r=0.28, p=0.020), and T3 (N=45, r=0.32, p=0.031). Correlations remained significant in the centroparietal-left temporal region after adjusting for multiple comparisons with DDA. Specifically, 4 out of 6 correlations remained significant at $\alpha = 0.025$ (0.05/2) and 3 out of 6 at $\alpha = 0.0167$ (0.05/3). No significant associations were found in men.

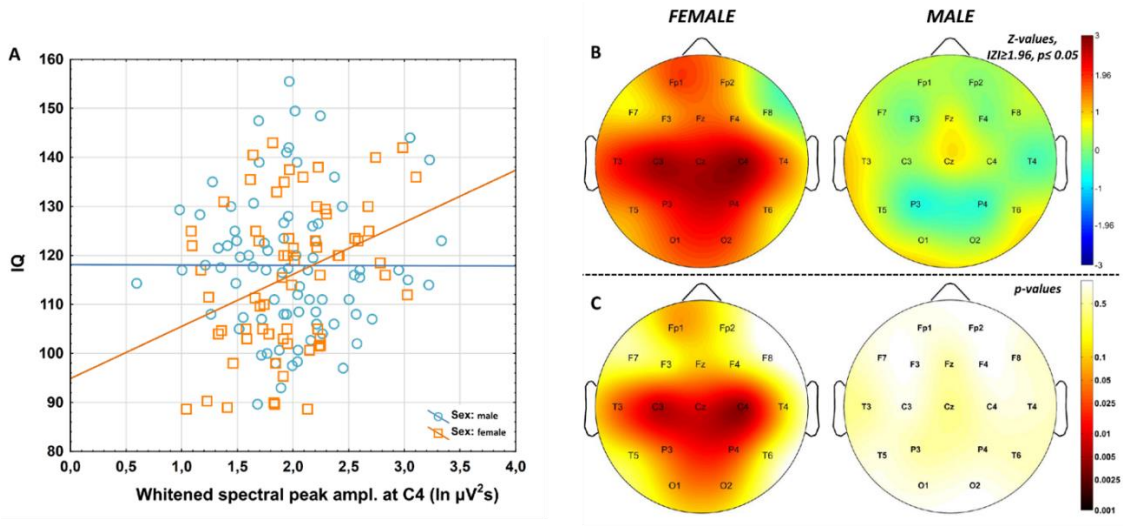

Figure 5. Correlations between NREM sleep EEG spindle frequency whitened spectral peak amplitudes and IQ in females and males. A. Categorized scatterplot representing the correlation between whitened spectral peak amplitude of the NREM sleep EEG spindle frequency range (recording site: F4) and IQ in women and men. B. Pearson r-values were transformed to Z-values and represented on topographical maps. C. Significance probability maps of the correlations presented in B. Figure is sourced from Bódizs et al. (2021).

4.1.5. Interrelationship between spectral slope and intercept

Although there were sex differences regarding intercepts, but no sex difference revealed in terms of spectral slopes, the two measurements strongly and negatively correlated in the sample. Steeper spectral slopes reflected higher intercepts (that is higher EEG amplitudes, Pearson's r ranged between -0.85–(-0.76), $p<0.001$ across electrode locations). Thus, from this point onward, the present thesis focuses on the spindle peak characteristics (amplitude and frequency) and spectral slope.

4.2. Study 2

In the second study, the overnight dynamics of the different parameters of the parametrized power spectra were tested by dividing sleep into sleep cycles. The average number of sleep cycles in the sample was m=4.25, with two participants having only two, nine having three, 165 having four, and 75 participants having five full sleep cycles. The fifth sleep cycle was excluded from the statistical analyses to prevent a substantial reduction in sample size. Since the effect of hemisphere (left vs. right) did not reach significance in either model ($p > 0.05$), it was not investigated further.

Although in Study 1 we found that the goodness of fit for our parametrization procedure was around 0.8–0.9, we re-evaluate it here, as the sample size was increased by including additional subjects, and the fitting procedure was conducted separately for the consecutive sleep cycles rather than for the entire sleep period. The applied linear model showed a strong fit [2–6]∪[18–48] Hz spectral data in all cycles. Specifically, the goodness of fit ranged from 0.9195 to 0.9998 in cycle 1, 0.9002 to 0.9998 in cycle 2, 0.8938 to 0.9998 in cycle 3, and 0.7686 to 0.9997 in cycle 4, across subjects and EEG recording locations. The squared Fisher Z-transformed Pearson correlations between the fitted linear model and the spectral data, after averaging and back-transformation, resulted in $R^2 = 0.9844$ (SD = 0.42).

4.2.1. Overnight dynamics of the spindle peak frequency

GLM revealed significant main effects of age, sex, sleep cycles and region (Table 4) indicating slower spindle frequencies in children, in adult males, in sleep cycles closer to the beginning of the sleep period, and in more anterior regions, respectively. Across the first 4 sleep cycles a U-shape-like trend can be observed in peak frequency variation in all except the middle-aged group (Figure 6). However, peak frequency of the first three cycles did not differ statistically from each other and the peak frequency of the fourth cycle was significantly higher than that of the earlier cycles. Post-hoc test of the significant cycle × age group interaction ($F(9,543)=2.38$, $p=0.012$) supported the aforementioned effect in both teenagers and young adults, as their peak frequencies in the 4^{th} sleep cycle was higher than in the preceding ones (Figure 6). Electrode location also impacted the effect of sleep cycles on peak frequency (cycle × region: $F(12,2172)=5.34$, $p<0.001$), indicating lower peak frequencies in the frontopolar regions during the second and third sleep cycles compared to the first and fourth (means and post-hoc test results can be seen in Table 2 of G. Horváth et al. (2022)). This effect also tended to emerge in the parietal and occipital regions; however, the overnight dynamics of the peak frequencies in the frontal and central areas were not U-shaped. Interaction of age group × region was significant ($F(12,724)=9.51$, $p<0.0001$), indicating lower peak frequencies for children in the central, parietal, and occipital electrode locations compared to the other age groups, and higher frontopolar and frontal peak frequencies for teenagers compared to middle-aged adults (Figure 6).

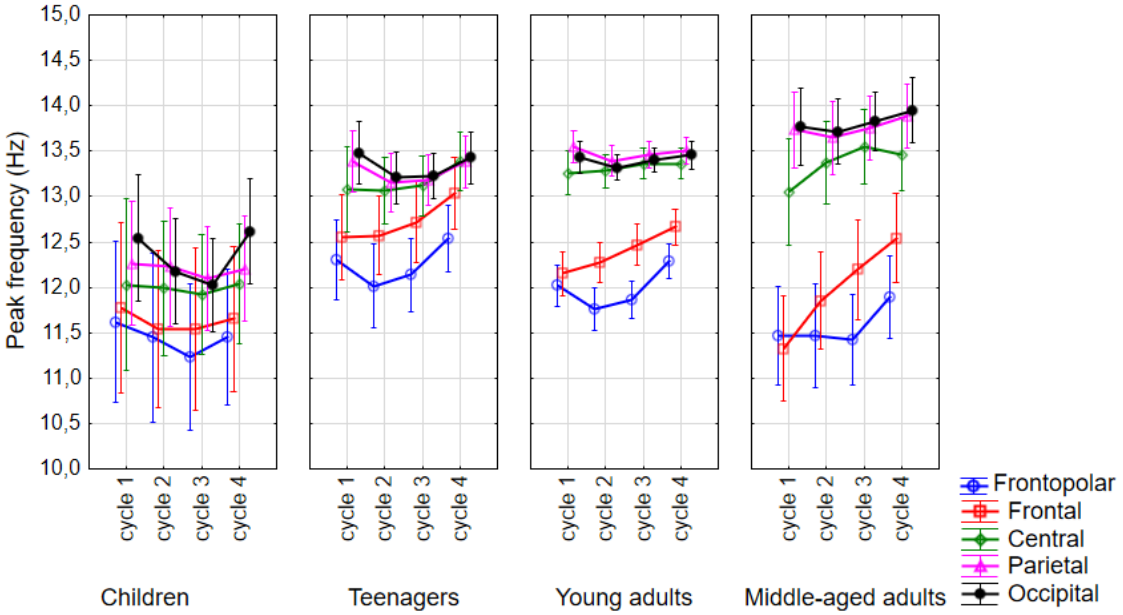

Figure 6. Cycle dynamics of the frequencies of the largest peaks in the spindle range. Dots are group mean values, whereas vertical bars denote 95% confidence intervals (G. Horváth et al., 2022).

4.2.2. Anterior-posterior changes in spindle peak frequency

Spindle frequency was also varied along the anterior-posterior axis in all cycles (Figure 6). More specifically, it increased by 1.53 Hz in the first, 1.59 Hz in the second, 1.5 Hz in the third and 1.14 Hz in the fourth sleep cycle, from the frontopolar to the occipital regions. Location of the maximal frequency transitions were estimated by sleep cycles and tested using a modified KL distance measure incorporating surrogate control analyses (Kullback & Leibler, 1951). The measured frequency transitions significantly diverged from the uniform distribution (KL distance Z-values were 64.69 for cycle 1, 84.26 for cycle 2, 80.97 for cycle 3, and 61.77 for cycle 4), suggesting substantial discontinuities in the anterior-posterior variations of the maximal peak frequencies. However, there was a dominant location of the largest frequency shift in every sleep cycles according to the descriptive statistics. Specifically, the maximal frequency transition occurred from the central to frontal region during the first two and the fourth sleep cycle for the majority of the sample (54.2%, 50.6%, and 40.6%, respectively). During the third cycle, the dominant location of the frequency transition was from the frontal to the frontopolar region, as 45% of the sample had their largest shift there (Table 3).

Table 3. Percentage distribution of the location of maximal frequency shifts in the sample. Numbers mean percent of the occurrence of the maximum frequency shift in a given area. Table is from the supplementary materials of G. Horváth et al., (2022).

	1. cycle (%)	2. cycle (%)	3. cycle (%)	4. cycle (%)
Frontal-Frontopolar	17.53	31.47	45.02	38.25
Central-Frontal	54.18	50.60	41.83	40.64
Parietal-Central	15.54	5.98	4.78	8.76
Occipital-Parietal	3.98	4.38	2.79	4.78

4.2.3. Overnight dynamics of spectral slope, spindle peak amplitude and SWA

Significant main effects of GLMs indicated that earlier cycles and younger age predicts steeper spectral slopes, higher SWA/lnSWA, and lower maximal sigma peak amplitudes (see statistics in Table 4). Additionally, more anterior brain region suggests steeper slope and lower peak amplitudes as well (effect of brain region was not analysed for SWA as data was only available from the left frontal derivation for that metric). Effect of sex was not significant any of the aforementioned models. However, several of the statistically meaningful main effects interacted significantly.

Table 4. Main effects of the General Linear Models conducted on different spectral parameters using sleep cycles, age groups, brain regions, sex and hemisphere as within subject factors. The main effect of hemisphere was not significant for any of the variables, thus is not included here. Table was created from the results published in (G. Horváth et al., 2022).

	Sleep cycles	Age groups	Brain region	Sex	children	teenagers	y. adults	m.a. adults
	F (p-value)				Group sizes			
Slope	**210.78 (<0.001)**	**17.05 (<0.001)**	**211.14 (<0.001)**	0 (0.97)	30	36	142	32
Peak amplitude	**78.45 (<0.001)**	**11.93 (<0.001)**	**56.94 (<0.001)**	1.81 (0.28)	9	33	125	22
Peak frequency	**11.65 (<0.001)**	**10.34 (<0.001)**	**150.1 (<0.001)**	**4.1 (0.044)**	9	33	125	22
SWA	**524.88 (<0.001)**	**162.36 (<0.001)**	-	0.7 (0.38)	30	36	142	32
lnSWA	**858.84 (<0.001)**	**58.68 (<0.001)**	-	3.05 (0.08)	30	36	142	32

The interactions in the slope GLM indicated increased overnight variation in the children's spectral slope compared to that of the adults (cycle × age groups: $F(9,696) = 15$, $p < 0.0001$), an absence of notable regional differences in children (region × age groups: $F(12,928) = 3.66$, $p < 0.0001$), and regional differences in the overnight variation of the slope (cycle × region: $F(12,2784) = 51.92$, $p < 0.0001$). The post-hoc test showed significantly higher slope values (flatter slope) in each subsequent sleep cycle compared to the preceding one in the young adult group, while children and teenagers only demonstrated this significant flattening of slope during the first three sleep cycles. A trend toward a further flattening was observed in the fourth cycle (see group means and post-hoc test results in G. Horváth et al. (2022), Table 2). The middle-aged group showed smaller increment in slope values (flattening of the spectral slope) throughout the sleep period, leading to non-significant differences between consecutive sleep cycles (Figure 7/a). Regional differences were significant across all cycles (Figure 7/b).

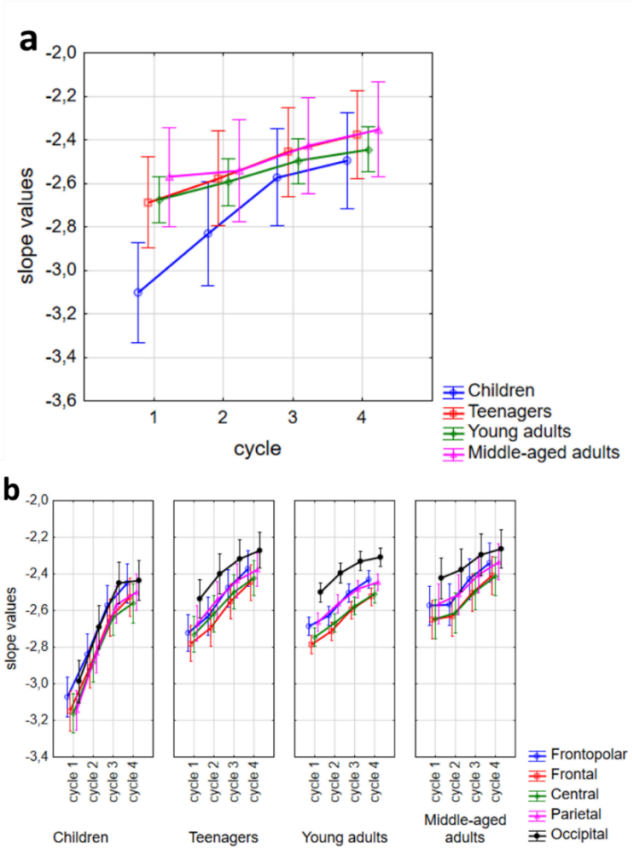

Figure 7. NREM sleep EEG spectral slopes as functions of sleep cycles, age and recording location. a. Interaction between cycle x age group in spectral slope values. b. Interaction of sleep cycle, region and age group in spectral slope values. Group means are shown as dots with vertical bars representing 95% confidence intervals. Figure is adapted from (G. Horváth et al., 2022).

GLM interactions regarding the amplitude of the maximal peak in the sigma range indicated reduced overnight rise in sigma peak amplitude of the middle-aged (cycle × age group: $F(9) = 3.65$, $p < 0.001$), lower peak amplitudes in the centro-posterior regions of children (region × age group: $F(12) = 8.67$, $p < 0.001$), as well as faster overnight amplitude increment in the posterior region (cycle × region: $F(12) = 16.64$, $p < 0.001$). The increase of sigma peak amplitude across the four sleep cycles was significant in the young adult group according to the post-hoc analyses of cycle × age group interaction (Table 2 in G. Horváth et al. (2022)).

Interaction of cycle × age group in the SWA/lnSWA GLMs was also significant (SWA: $F(9,696) = 153.85$, $p < 0.001$; lnSWA: $F(9,696) = 5.42$, $p < 0.001$). Furthermore, according to the post-hoc tests, lnSWA values significantly decreased across all four sleep cycles in all age groups. In contrast, the decrement of the classical SWA values was evident only during the first 3 cycle in the children and young adult groups ($p<0.001$), during the first two sleep cycles in the teenager group ($p<0.001$), and no significant difference were found between sleep cycles in the middle-aged participants ($p>0.05$) (Figure 8).

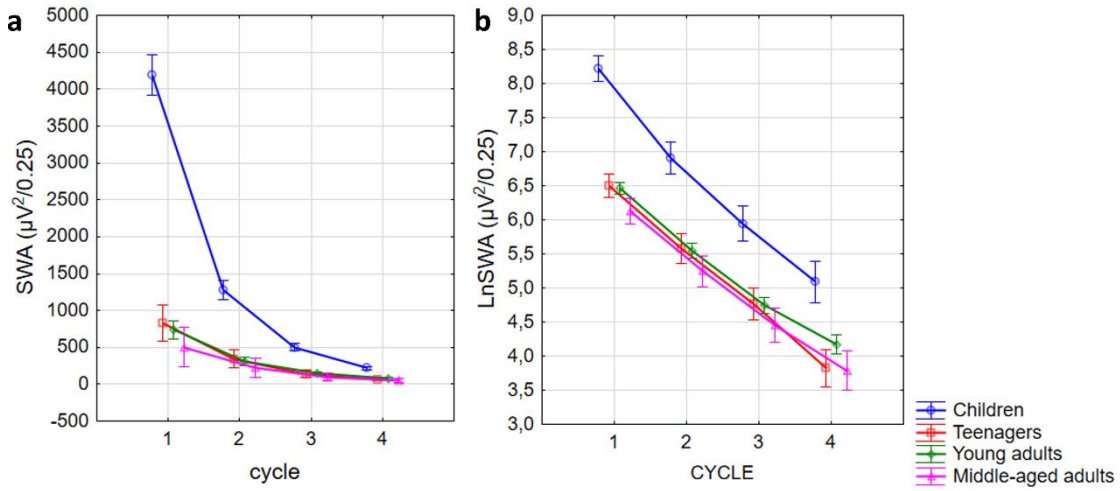

Figure 8. Cycle-by-cycle dynamics of slow wave activity. a. Cycle dynamics of slow wave activity in different age groups. b. Cycle dynamics of the natural logarithm of SWA in different age groups. Note that the decline in lnSWA is follows a nearly linear pattern.(G. Horváth et al., 2022)

4.3.4. Spectral slope and SWA: relationship and interindividual variability

Pearson correlation (focusing on the left frontal EEG derivation) revealed a significant negative, moderate-to-strong associations between lnSWA and spectral slope

in all sleep cycles (Cycle 1: N = 251 r = − 0.73, p < 0.001; Cycle 2: N = 251 r = − 0.61, p < 0.001; Cycle 3: N = 249 r = − 0.56, p < 0.001; Cycle 4: N = 240 r = − 0.56, p < 0.001).

To check the interindividual differences in both metrics, the number of outliers was visualized (Figure 9) and coefficients of variation were estimated (Table 5).

Table 5. Descriptive statistics and Coefficients of Variation of NREM sleep EEG lnSWA and spectral slopes (left frontal recording location: F3) (G. Horváth et al., 2022).

	cycle	Valid N	Mean	Minimum	Maximum	Std.Dev.	**Coef.Var.**
ln SWA + 4	1	251	10.65	8.98	13.12	0.81	**7.64**
	2	251	9.68	7.63	12.05	0.81	**8.38**
	3	249	8.85	6.15	11.32	0.84	**9.46**
	4	240	8.18	1.77	10.18	0.91	**11.11**
slope + 4	1	251	6.82	6.06	7.52	0.25	**3.72**
	2	251	6.72	6.08	7.41	0.23	**3.38**
	3	249	6.58	5.99	7.08	0.21	**3.16**
	4	240	6.50	5.70	7.05	0.21	**3.30**

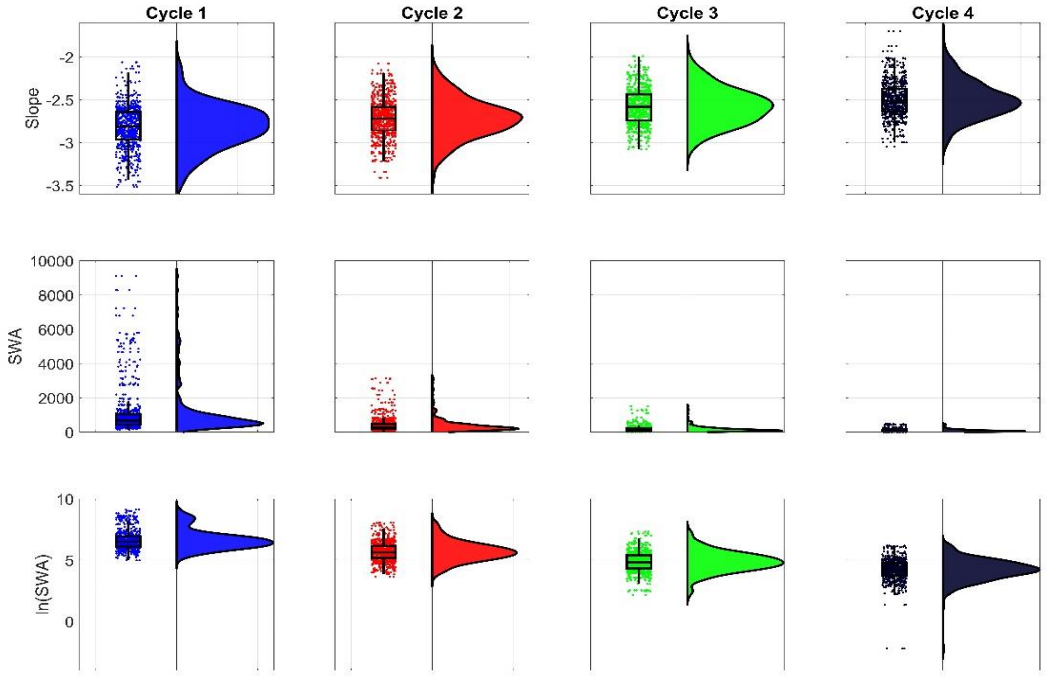

Figure 9. Raincloud plot of NREM sleep EEG spectral slopes, SWA, and lnSWA in the first four sleep cycles. Note the skewness and/or bimodality of the distributions, as well as the increased number of outliers of SWA and lnSWA compared to slope values (G. Horváth et al., 2022).

For comparability, rescaling to a common absolute null point of the two measurements (slope and lnSWA) was a necessary step before calculating the coefficient of variation (which is a relative standard deviation). Both variables were shifted by 4 as

neither of them was lower than -4. The coefficients of variation were calculated on the scale-shifted variables and was approximately 2-to-3 times as high for lnSWA as for the spectral slopes in all four cycles (see Table 5).

4.3. Study 3

Due to technical issues, such as electrode problems, unexpected shutdown of the device or poor-quality data, three BS and seven RS recordings were incomplete. These data were excluded from analyses that assume the total length of the nights (e.g. overnight dynamics, minimum/maximum assessment, circadian phase examination), but were involved in cycle-based (sample means) evaluations of differences between BS and RS.

The actual length of the sleep deprivation period can be calculated for participants with complete BS recordings by subtracting the end of the last sleep epoch in BS from the time of sleep onset in RS. Median length of this period was Mdn=35.79 hours (~35 h. and 47 min; min-max range: 34.9–37.3) in the sample. Analyses of complete recordings revealed that the mean sleep duration was m_{BS}=7.9 (min-max: 5.8–10.7) hours in BS and m_{RS}=12.2 (min-max: 9.7–14.74) hours in RS, while the sample median of the number of sleep cycles increased from Mdn_{BS}=5 (min-max:3–7) to Mdn_{RS}=8 (min-max: 6–10).

Self-reported oversleeping adjusted sleep midpoint (MCTQ MSFsc) was at 04:34 (SD=1:16) hh:mm in average and the sample can be divided into 7 early-, 15 intermediate-, and 16 evening type (5, 6, 8 females respectively) participants. BS onset strongly and positively correlated with MSFsc (self-reported chronotype metric; $p<0.0001$, $r=0.61$) which assumes that subjects gone to bed according to their own circadian timing (or preferences) in the BS condition. However, the correlation between RS onset and MSFsc was not significant ($r=0.3$, $p=0.07$; Figure 10/A) which was expected due to the RS phase advancement introduced in our experimental intervention. Sleepiness (measured by both scales) increased significantly reaching its highest level between the 12^{th} and 24^{th} hour ($t_{likert}(37)=-9.78$, $t_{SSS}(37)=-9.82$, $p<0.0001$) during the sleep deprivation period, and then decreased significantly from the 35^{th} hour to RS wake ($t_{likert}(37)=6.81$, $t_{SSS}(37)=6.2$, $p<0.0001$; Figure 10/B).

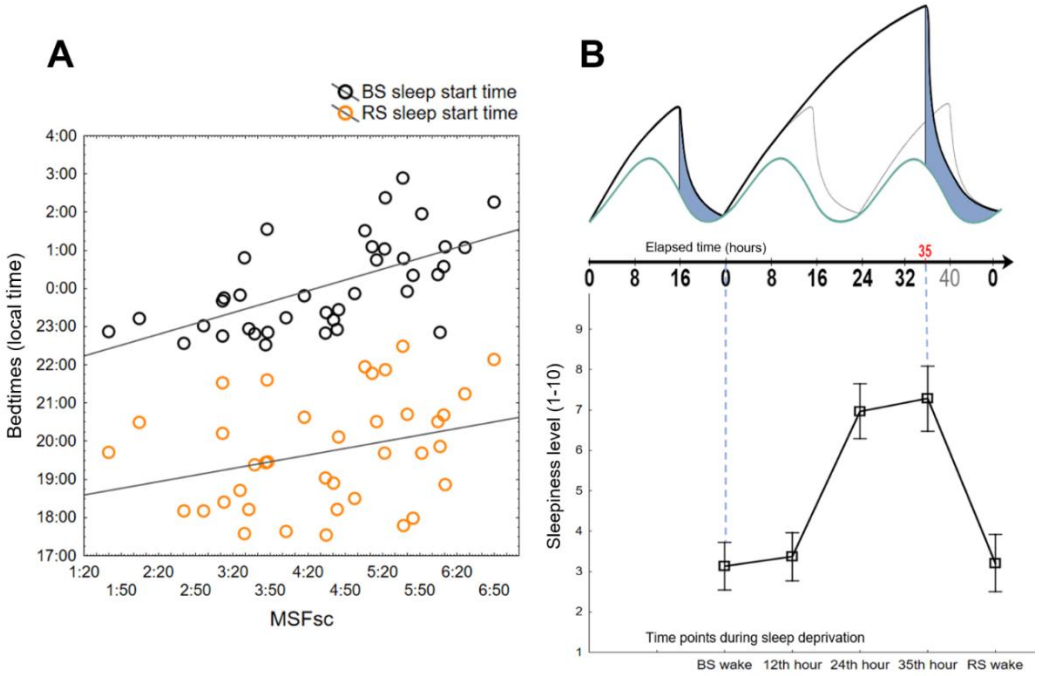

Figure 10. Subjective chronotype and sleepiness along with the expected sleep pressure and circadian time according to the two-process model of sleep regulation. A) Correlation between the MCTQ chronotype indicator (MSFsc) and actual bedtimes of BS and RS. B) Schematic representation of the expected behaviour of the two sleep regulatory processes (top) and the actual development of sleepiness according to the Likert scale (bottom) during the experiment. On the top, blue area indicates the approximate time duration of the sleep periods, while the black and light-grey lines demonstrate the homeostatic sleep pressure due to the intervention, and under normal circumstances without sleep deprivation, respectively (note the heightened sleep pressure due to the extended wakefulness). On the bottom, the graph displays the sample means with 95% confidence intervals of sleepiness levels at different time points during the wakefulness (G. Horváth & Bódizs, 2025).

4.3.1. Effect of sleep deprivation on spectral slope dynamics

General linear model with sleep condition (RS, BS) and sleep cycle serving as within-subject factors revealed that spectral slope flattens during the first 4 cycles of sleep ($F=65.94$, $p<0.0001$) and it is significantly steeper in RS compared to BS ($F=98.25$, $p<0.0001$; Table 6). Additionally, the factors (condition × cycle) interact significantly ($F=2.95$, $p=0.037$, Figure 11). Sample-level differences in spectral slope values between successive sleep cycles (Figure 11) were tested using Unequal N HSD post-hoc tests, which indicated significantly steeper slope in C2 than in C3 (BS & RS: $p<0.001$), and in C3 than in C4 (BS: $p=0.02$, RS: $p<0.001$), but not in C1 compared to C2 (BS: $p=1.0$, RS: $p=0.83$, see descriptive statistics in Table 6).

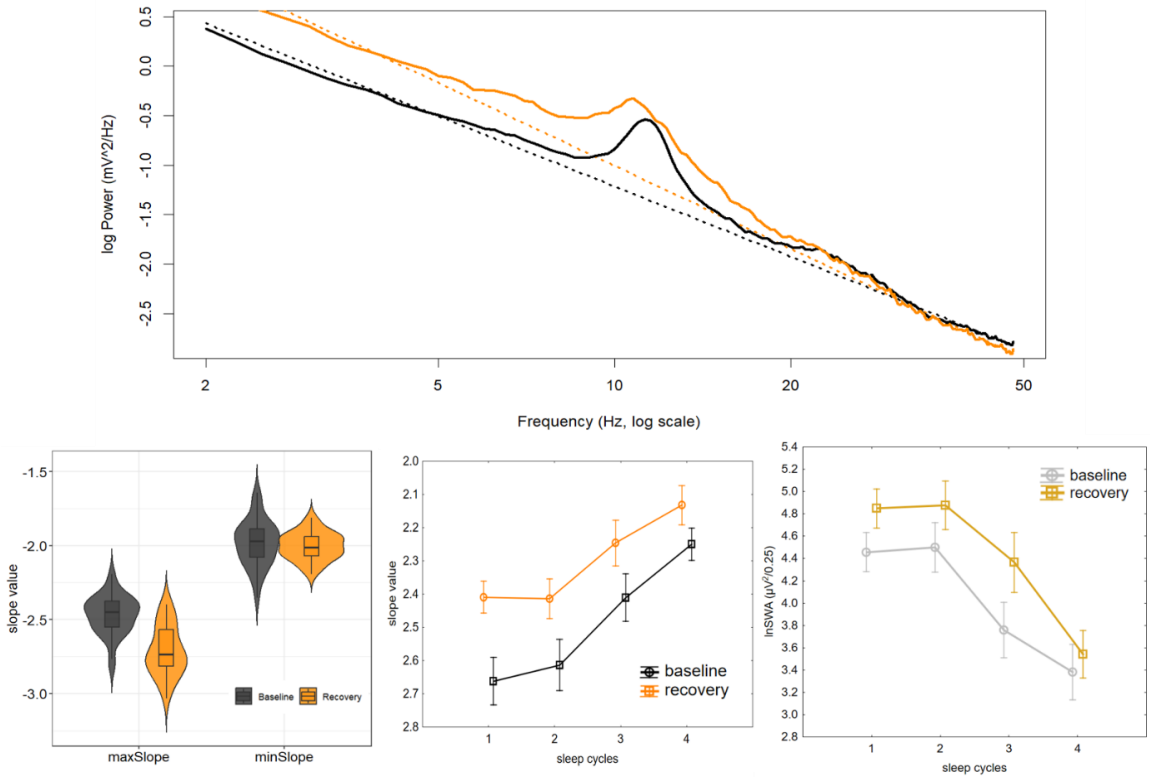

Figure 11. Spectral slopes of the NREM sleep EEG during the first four sleep cycles of the baseline and the recovery nights. Upper panel shows the spectrum of the first cycle of sleep for BS (black) and RS (orange), as well as the fitted aperiodic components with dashed lines in a 24-year-old male participant. Violin plots (left side of the lower panel) depict the distribution of the maximal and minimal slope values, whereas inner boxplots show the difference between sleep conditions: while maximum slope values got larger due to the sleep deprivation, slope minima returned to approximately the same level in the two conditions. Middle and right panels show the sample means and 95% confidence interval of slope values and lnSWA, respectively, in the first 4 cycle of sleep in BS and RS. At the beginning of the sleep RS as compared to BS Spectral slopes and lnSWA are steeper and larger, respectively (Figure adapted from (G. Horváth & Bódizs, 2025).

Table 6. Sample means and standard deviations of slope values in the first four sleep cycles (G. Horváth & Bódizs, 2025)

	baseline sleep (BS)			recovery sleep (RS)		
cycle	N	Mean	SD	N	Mean	SD
1	36	-2.402602	0.126357	38	-2.625733	0.214957
2	36	-2.388576	0.170833	36	-2.615997	0.199933
3	37	-2.218177	0.205926	34	-2.410661	0.189354
4	36	-2.100263	0.179556	33	-2.247819	0.129501

The overnight dynamics in NREM sleep EEG spectral slopes were further analysed within the context of the whole record approach in both the group- and cycle-specific manner.

The effect of sleep cycle remained significant even when the whole-night sleep including all cycles was considered, as demonstrated by the Friedman ANOVA analyses of the cycle count-based groups (Table 7, Figure 13). The Wilcoxon matched-pairs test was conducted to test the difference of successive sleep cycles (e.g. cycle 1 vs. cycle 2, cycle 2 vs. cycle 3, …, cycle 6 vs. cycle 7). To adjust for multiple comparisons, Bonferroni correction was applied, setting the significance thresholds at $p < 0.0125$, $p < 0.01$, $p < 0.008$, $p < 0.007$, $p < 0.00625$, and $p < 0.00555$ for 4, 5, 6, 7, 8, and 9 comparisons, respectively. None of the consecutive slope values of BS cycles remained significant after correction in any of the cycle count-based groups. However, in RS, spectral slope remained significantly steeper in C2 compared to C3 in the 9-cycle group ($Z=2.8$, $p=0.0051$).

Table 7. Overnight cycle effect of slope, peak frequency and lnSWA in the separate cycle count-based groups. Friedman ANOVA revealed significant or marginally significant cycle effect in all groups except with regards peak frequency in the BSC4 group (G. Horváth & Bódizs, 2025)

Groups defined by maximum cycle count	Sample size	Slope		Peak frequency		lnSWA	
	N (N for Pfreq)	$\chi2$	p	$\chi2$	p	$\chi2$	p
BSC4	7 (6)	7.3	0.06	1.8	0.61	14.7	0.002
BSC5	12 (10)	33.33	<0.0001	13.5	0.009	24.87	<0.001
BSC6	11	37.13	<0.0001	23.94	0.0002	37.96	<0.0001
ReSC7	8 (7)	41.3	<0.0001	11.51	0.07	42.5	<0.0001
ReSC8	8 (7)	47.54	<0.0001	22.86	0.002	42.5	<0.0001
ReSC9	10	60.27	<0.0001	34.24	<0.0001	61.1	<0.0001

To evaluate the hypothesis that the largest difference in spectral slope will be at the beginning of the sleep periods, we compared the values of the first and last sleep cycles between BS and RS (BS C1 vs. RS C1, BS C_{last} vs. RS C_{last}). The results turned out as expected, with RS C1 spectral slope being significantly steeper than BS C1 (BS: $m=2.4$, $SD=0.1$; RS: $m=2.63$, $SD=0.2$, $t(35)=-6.6$, $p<0.0001$), while no significant difference was detected between the slope values of the last sleep cycles in the two conditions (BS: $m=2.06$, $SD=0.15$; RS: $m=2.08$, $SD=0.14$; $t(29)=-0.5$, $p=0.62$). Furthermore, we identified the sleep cycle (ordinal position within the sleep period) in which maximum and minimum spectral slope values occurred, as we hypothesized that

slope is the steepest at the beginning-, and the flattest at the end of the sleep periods. Finally, a comparison of these metrics between sleep conditions was conducted to support the assumption that BS vs. RS difference in the maxima will exceed the divergence observed in the minimum values. Results revealed that for 16 participants the steepest slope value occurred in the first sleep cycle; for 17 subjects the slope was the steepest in the 2nd sleep cycle; and for 2, steepest value appeared in the 3rd sleep cycle, during their BS. In RS, slope was the steepest in first sleep cycle for 18 subjects and in the second for 13. Complete recordings were unavailable for the remaining participants. There was no statistical difference between BS and RS in which sleep cycle the steepest slope value fell ($Z=0.2$, $p=0.23$, BS: Mdn=2 (2nd cycle), IQR=[1,2]; RS: Mdn=1(1st cycle), IQR=[1,2]). Individual maxima of the absolute slope values in RS exceeded the respective assessments in BS, indicating significantly steeper slopes in the former condition ($t(29)=-9.5$, $p<0.0001$). In contrast, the minima were statistically similar between the two sleep conditions ($t(29)=-1.2$, $p=0.24$, Figure 11). Additionally, flattest slope values not necessarily occurred in the last cycle of the sleep periods (BS: $Z=4.2$, $p<0.0001$, cycle index of C_{last}: Mdn=5, IQR=[5, 6], cycle index of C_{min}: Mdn=4.5, IQR=[3, 5]; RS: $Z=3.9$, $p<0.0001$, cycle index of C_{last}: Mdn=8, IQR=[7, 9], cycle index of C_{min}: Mdn=7, IQR=[6, 8]).

4.3.2. Effect of sleep deprivation on SWA

Effect of condition and sleep cycles were tested with General Linear Model for the first 4 sleep cycles of BS and RS. Significant main effects but non-significant interaction were found (BS/RS: $F(1,32)=22.23$, $p<0.001$, cycle: $F(3,96)=80.1$, $p<0.001$; condition × cycle: $F(3,96)=2.17$, $p=0.096$; Figure 12). The pattern of differences of lnSWA values in consecutive sleep cycles was similar to the one revealed for the spectral slopes. The difference was significant in both sleep conditions between C2 and C3 (BS & RS: $p<0.001$), furthermore, between C3 and C4 (BS: $p=0.05$, RS: $p=0.002$) and non-significant between C1 and C2 (BS & RS: $p<0.001$) when the whole sample was analysed. Additionally, cycle effect remained significant when the full-night recordings in the cycle-count based groups were evaluated (Table 7). However, Bonferroni-adjusted results of the Wilcoxon matched-pairs test did not show significant difference in lnSWA values between consecutive cycles in any of the cycle count-based groups, except for the RS 9-cycle group and BS 6-cycle group. In these groups the differences between C3 vs. C4

(Z=2.8, p=0.0051), and C2 vs. C3 (Z=2.67, p=0.0076) remained significant even after the correction, respectively. Ultimately, as expected, lnSWA was markedly higher in the first cycle of RS (m=4.8, SD=0.51) compared to that in the first cycle of BS (m=4.5, SD=0.5) (t(37)=-3.6, p<0.001), and converged to similar levels by the end of the sleep episodes in both conditions (BS C_{last}:m=3.1, SD=0.6, vs. RS C_{last}: m=2.9, SD=0.5; t(29)=1.13, p=0.27, m=2.9, SD=0.5, see Figure 12).

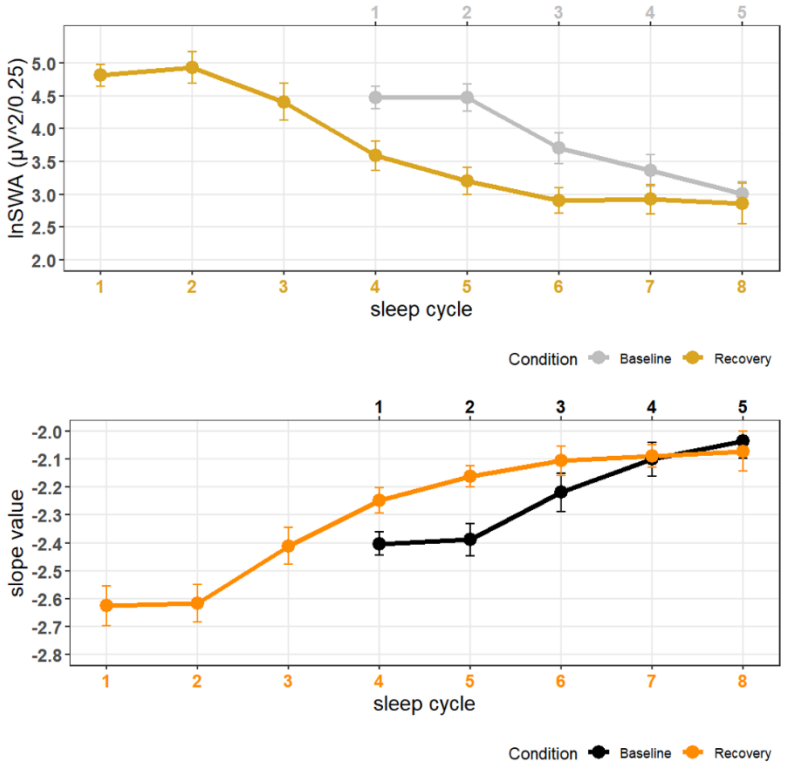

Figure 12. NREM sleep EEG SWA and spectral slope values in successive sleep cycles. Sample means and 95% confidence intervals are displayed in accordance with the phase advanced RS as compared to regularly timed BS (phase shift: approximately 3 sleep cycles). Figure adapted from G. Horváth & Bódizs, (2025).

4.3.3. Effect of sleep deprivation on spindle peak frequency

Sample-level test of peak frequency in the first 4 sleep cycles was conducted using General Linear Model with sleep condition and cycle as within subject factors. Only sleep cycle had a significant main effect on peak frequency values (BS/RS: F(1,27)=3.13, p=0.1, cycle: F(3,81)=3.27, p=0.025), while the effect of condition and condition × cycle interaction was not significant.

A separate analysis of the cycle count-based groups, along with a sample-level examination of specific sleep cycles (first/middle/last), provided deeper insight into the

overnight dynamics of both sleep periods, as well as into the similarities/differences of the peak frequency values between BS and RS.

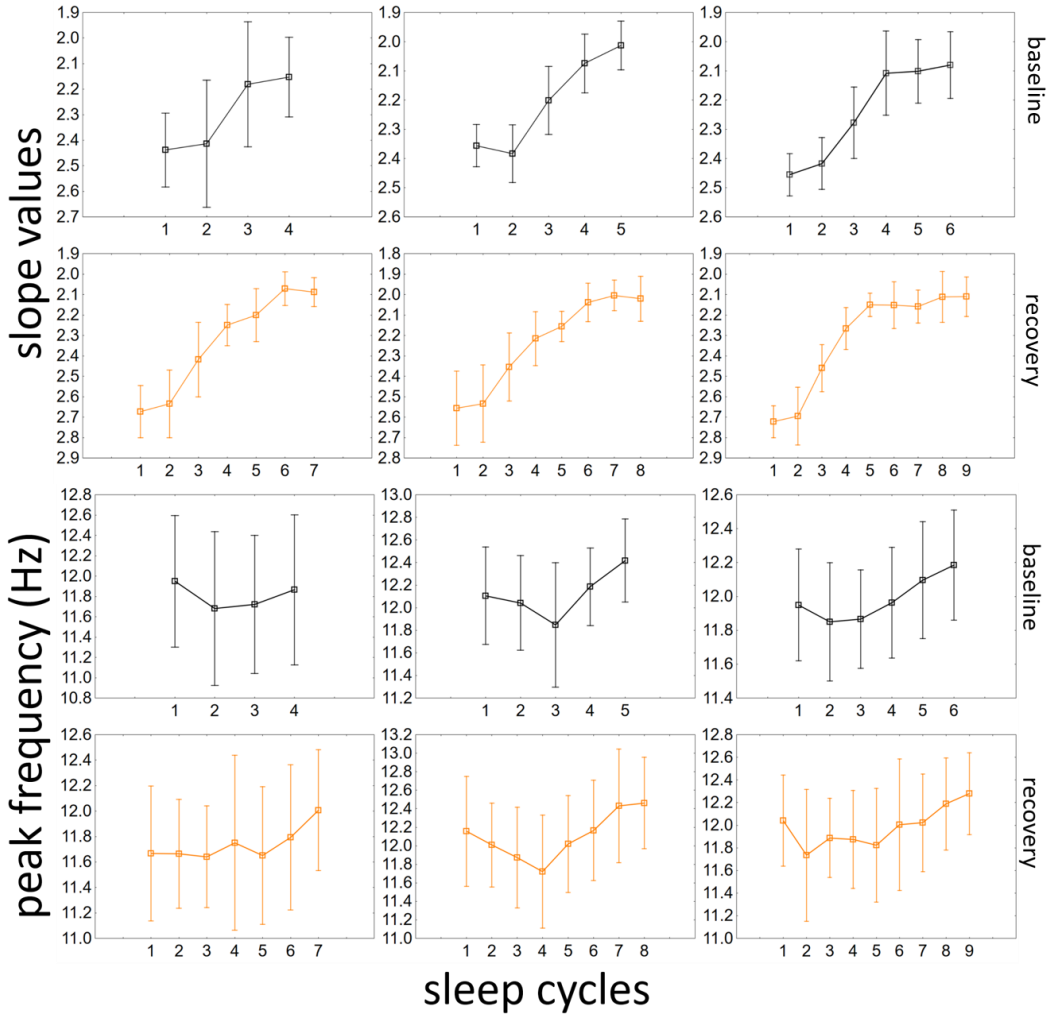

Figure 13. Overnight dynamics of slope values and peak frequencies in the different cycle count-based groups. Means (open squares) and 95% confidence intervals (vertical lines) can be seen in successive sleep cycles. NREM sleep EEG spectral slopes get flatter during the night, while peak frequency follows a decreasing trend then starts to increase toward the end of the night. Figure adapted from (G. Horváth & Bódizs, 2025).

There was a significant effect of sleep cycle on peak frequency in all cycle count-based groups except the 4-cycle group in BS and the 7-cycle group in RS (Table 7, descriptive statistics can be seen in Table 3 of G. Horváth & Bódizs (2025)). Dependent samples t-tests were used to check whether peak frequency is decreased to the middle of the sleep period. Accounting for multiple comparisons the significance threshold was set at $p<0.025$ due to Bonferroni correction for comparisons between the first and middle, as well as the middle and last sleep cycle (2 comparisons). The mean of the middle two cycles was taken as the middle peak frequency value when the maximum cycle count was

even. Results showed that the peak frequency was significantly decelerated in the middle of the sleep period compared to the end of the nights (**BS**: C_{middle} [m=11.85, SD=0.7] vs. C_{last} [m=12.25, SD=0.7]: t(34)=-3.8, p<0.001; **RS**: C_{middle} [m=11.8, SD=0.66] vs. C_{last} [m=12.31, SD=0.6]: t(30)=-5.3, p<0.0001), however, difference between sleep middle peak frequency and peak frequency in the first cycle was only a tendency (**BS**: C_{first} [m=12.03, SD=0.6] vs. C_{middle} : t(32)=1.86, p=0.07; **RS**: C_{first} [m=11.93, SD=0.7] vs. C_{middle} : t(28)=1.04, p=0.31). Indeed, peak frequency values of the last sleep cycles was significantly heightened compared to the peak frequency values in the first sleep cycle in both sleep conditions (**BS**: t(33)=-3.8, p<0.001; **RS**: t(28)=-4.2, p<0.001, Figure 13).

Consistent with our hypothesis, peak frequency did not differ between the two sleep conditions, neither in the last nor in the first cycle of the sleep periods (C_{last}: t(29)=0.12, p=0.91, C_{first}: t(32)=0.89, p=0.38). To further test our assumption about the circadian phase, we estimated the timing of peak frequency minimum during sleep, defining it as the midpoint of the sleep cycle containing the slowest peak frequency value (marked as NSSF).

As a first step, we examined to what extent the self-reported chronotype (both predefined chronotype groups and continuous MSFsc variable) was reflected in NSSF during the different sleep conditions. Although One-Way ANOVA revealed a significant difference between the three chronotype groups in BS (F(2)=3.81, p=0.03, m_{early}=2:18, SD=2:34, m_{interm}=3:04, SD=2:15, m_{late}=4:45, SD=1:44 hh:mm), NSSF did not differ among the groups in RS (F(2)=1.08, p=0.4, m_{early}=23:07, SD=1:14, m_{interm}=00:59, SD=2:08, m_{late}=0:56, SD=3:17 hh:mm; Figure 14). Correlational analyses between MSFsc and NSSF yielded similar results, as although RS NSSF and MSFsc did not correlated significantly (r=0.2, p=0.28), the positive association between BS NSSF and MSFsc was substantial (r=0.56, p<0.0001).

Secondly, we tested whether minimum peak frequency occurred around the same time of day during both BS and RS, thus we compared NSSF between the conditions. Contrary to our hypothesis, NSSF fell earlier in RS than in BS (t(28)=5.7, p<0.0001, BS: m=03:44, SD=2:14 hh:mm; RS: m=00:40, SD=2:34 hh:mm). Based on the observation that NSSF typically takes place near the midpoint of sleep under normal conditions, we aimed to investigate whether earlier RS NSSF could be explained by its stronger connection to the midpoint of the sleep period rather than its alignment with the time of

day. Thus, to further examine the aforementioned difference, we estimated the midpoint (time) of the sleep periods for all individuals in both nights and compared those to the NSSFs.

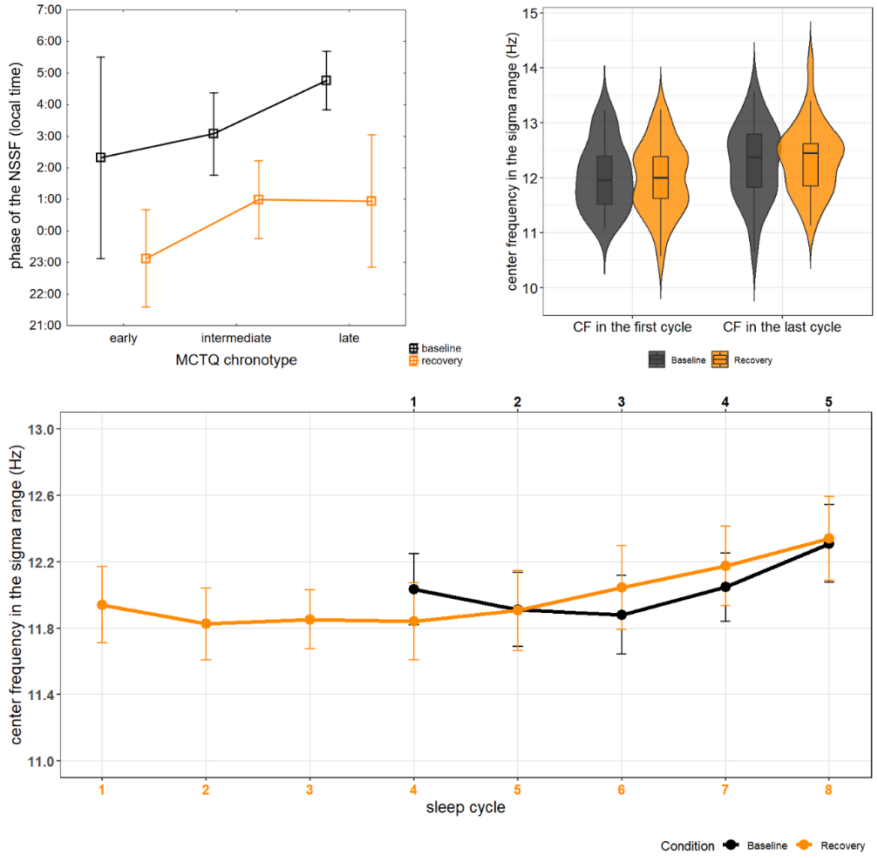

Figure 14. Difference in the phase of the peak frequency minima (NSSF) in RS and BS between MCTQ chronotype groups, and in peak frequency values between sleep conditions. Subjectively measured chronotype is well reflected in the time of BS NSSF, but not in RS NSSF, additionally, NSSF times differ between sleep conditions (upper left panel). Distribution, and medians of peak frequency in the first and last cycles of the sleep episodes are not different (violin/boxplot on the right). Lower panel represents the sample means and 95% confidence intervals of peak frequency in successive sleep cycles in both conditions and displays the shifted sleep period which was advanced by approximately 3 sleep cycles (G. Horváth & Bódizs, 2025).

Similar means and strong associations were revealed between BS NSSF and BS Midsleep ($Z=0.97$, $p=0.33$, Mdn_{NSSF}=04:07, $Mdn_{Midsleep}$=03:47 hh:mm; Spearman $R=0.64$, $p<0.0001$), but significantly different means and nominally lower correlations were revealed for the relationship between RS NSSF and RS Midsleep ($t(30)=3.2$, $p=0.003$, Mdn_{NSSF}=00:11, $Mdn_{Midsleep}$=01:46 hh:mm; $r=0.41$, $p=0.02$).

5. Discussion

The present thesis focused on the parameters characterizing the NREM sleep EEG Fourier spectrum by considering its power-law scaling properties and their usefulness in describing the fundamental sleep regulatory processes proposed by Alexander Borbély (Borbély, 1982). By separating periodic and aperiodic components of the NREM Fourier spectrum, it can be characterized by merely four parameters, namely the spectral slope, intercept, peak amplitude and peak frequency (Bódizs et al., 2021). We demonstrated that the most prominent peak of the 9–18 frequency range in the NREM sleep EEG spectrum is exhibiting equivalent properties in frequency and topographical distribution to one of the most recognizable characteristics of the NREM EEG signal: sleep spindles. We showed that the aforementioned spectral parameters capture known individual differences in NREM sleep EEG related to age-, sex-, intelligence, as well as known changes throughout sleep related to the homeostatic and circadian processes. These findings established our main question regarding whether these regulatory processes are reliably indexed by the sleep EEG. We revealed that the aperiodic part of the spectrum (spectral slope and intercept) changes in line with the changes in sleep pressure and its gold-standard measure, SWA. Specifically, spectral slope flattens as sleep diminishes in depth throughout the night and becomes steeper as a result of sleep deprivation. Furthermore, unlike spectral slope, intercept is affected by sex, however, this measure is far from being independent of the slope value. Our examinations of the periodic component (the largest spectral peak in the spindle range) revealed that peak amplitude increased during the night and with age, and this was accompanied by a U-shaped curve-like peak frequency dynamics in the frontopolar regions for all age groups, except older adults. This spindle deceleration in the middle of the sleep period was observed in habitual sleep, but the timing of peak frequency minimum was advanced as a result of the 35-hour sleep deprivation.

5.1. Largest peak in the 9–18 Hz range reflects spindle activity

In Study 1, one of the aims was to support our assumption, as the peaks of the NREM spectrum in the 9–18 Hz rage correspond to sleep spindles. As introduced earlier, these EEG waveforms can be categorized to fast and slow types based on their dominant frequency and topographical distribution. The boundary for distinguishing between the two types is usually defined as 12.5 Hz. Fast spindles, typically found in centroparietal

regions, oscillate at around 14 Hz, whereas, slow spindles are predominant in the frontal areas, oscillating at approximately 12 Hz (Cox et al., 2017; Gibbs & Gibbs, 1951). We found that frequencies of the largest peaks were higher in the centroparietal than in the frontal areas where the average frequency ranged between 11.55 and 13.50 Hz across electrode locations (Figure 3). We hypothesized that the frequency difference of peak frequencies between locations reflects the presence of the two spindle types on the scalp, as the observed frequency increase was not gradual along the anterior-posterior axis. Since more than 83% of the frequency increase occurred as a single shift, we considered the spatial location of this maximal anterior-posterior frequency change as a threshold for distinguishing slow and fast spindles in each participant. Following this definition, based on our findings when considering the entire NREM sleep period, 100% of the frontopolar and 63.5% of the frontal spindles can be classified as slow spindles. Additionally, 91.72%, 98.09%, and 100% of the identified peak frequencies correspond to fast spindle frequencies in the central, parietal and occipital regions. We complemented these findings in Study 2, where we analysed frequency shifts across successive sleep cycles separately, and found that, in the majority of the sample, the maximal frequency transition occurred from the central to the frontal region in the 1st, 2nd and 4th sleep cycles. While these observations are in line with the aforementioned literature regarding the topographical distribution of fast and slow spindles (Gibbs & Gibbs, 1951), they will be discussed further in later sections.

However, the average frequency of the second largest peak was approximately 1.5 Hz lower than the detected slow spindle frequencies reported in a previous study using the same database (Ujma et al., 2014). It is possible that the detected secondary peaks mostly corresponded to alpha activity rather than sleep spindles. Thus, in overall, we concluded that the parametrization procedure used was capable of the detecting and distinguishing dominant spindles at all recording sites, but it could not reliably identify non-dominant spindle activity across electrodes.

5.2. NREM sleep EEG spectral parameters reflect known individual differences

When introducing new parameters, it is important to test whether they are physiologically (psychologically, etc., depending on the field) meaningful. This can be achieved by assessing how well the metric reflects known or hypothesized individual differences. Although studies before 2020 addressed the significance and utility of

spectral parametrization of sleep or resting state EEG (Colombo et al., 2019; Donoghue, Haller, et al., 2020; Dumermuth et al., 1977; Feinberg et al., 1984; He et al., 2010; Lendner et al., 2020; Miller et al., 2009; Miskovic et al., 2019; Pereda et al., 1998; Pritchard, 1992; Voytek et al., 2015; Wen & Liu, 2016), particularly in terms of spectral slope, none specifically focused on individual differences—except for Feinberg et al. (1984) and Voytek et al. (2015), who found age-related changes in the slope metric. Thus, in Study 1 and partly in Study 2, we examined well-known effects from the literature in relation to the spectral parameters, based on variable availability in our database.

Age-related changes in the sleep EEG are a long-studied area of research in the field. Physiological aging parallels significant changes in sleep duration, architecture, as well as the quality and quantity of the different oscillations (Campos-Beltrán & Marshall, 2021; Mander et al., 2017). In terms of the parametrized power spectrum we found that NREM sleep EEG spectral slope flattened, whereas the amplitude and frequency of the dominant spectral peak decreased with increasing age. As spectral slope reflects a constant ratio of activity between low and high frequencies, our finding of a flatter spectral slope in older participants aligns with earlier studies observing an increased or unchanged activity in higher frequencies (Carrier et al., 2001; Schwarz et al., 2017; Sprecher et al., 2016), beyond the most commonly reported age-related SWA and spindle activity reduction (Carrier et al., 2011; De Gennaro & Ferrara, 2003; Martin et al., 2013; Taillard et al., 2021). Furthermore, effects of age on the overnight slope and SWA dynamics found in Study 2 were also in line with the literature which describes shallower SWA dissipation throughout the night in older subjects (Dijk, Beersma, & van den Hoofdakker, 1989; Landolt et al., 1996), as we found a smaller amount of slope flattening and less SWA decrease during the night in the middle-aged as compared to other age groups. As regarding peak amplitude in the spindle range, its decrement with increasing age in Study 1 (where no data from children was included) and the attenuated overnight increase in middle-aged subjects found in Study 2 were consistent with the reported decline in spindle activity during adulthood (Principe & Smith, 1982; Purcell et al., 2017). However, age-related decrease in peak frequency of the frontal and right temporal areas (Table 2) contrasted with our presumptions. Indeed, aging was associated with increasing spindle frequency during adulthood in most (Crowley et al., 2002; Principe & Smith, 1982), but not all (Purcell et al., 2017) reports. As we discussed earlier (Bódizs et al.,

2021), our controversial results could be due to the decrease in the occurrence of fast spindles in the frontal regions with aging. This assumption is supported by the finding that participants with the largest shift from fast to slow spindles between the central and frontal regions were older than those in whom this shift occurred from the frontal to the frontopolar area. Additionally, in Study 2, we observed lower peak frequencies in children compared to other age groups, which is a known association between spindle frequency and age (Purcell et al., 2017). We also found a dampened overnight dynamics in spectral peak frequencies in middle-aged individuals, with no significant differences between consecutive sleep cycles, whereas a U-shaped dynamics tended to appear in teenagers and young adults (Figure 6).

Sex differences in EEG power was reported for most frequency bands in several studies indicating higher power for females as compared to males (Armitage, 1995; Dijk, Beersma, & Bloem, 1989; Eggert et al., 2021; Mongrain et al., 2005). These results indicate that higher EEG power in females is independent of frequency suggesting that non-neural factors such as skull thickness, likely play a role in this effect (Dijk, Beersma, & Bloem, 1989). Although a recent systematic review considers sex effect to be moderate or of low certainty (Chapman et al., 2025), our results revealed similar differences regarding the intercept—which was proposed as a measure of the overall frequency-independent amplitude (Bódizs et al., 2021)—as it was significantly higher in females than in males. However, we also found no sexual dimorphism in the whitened peak amplitude when the aperiodic component (intercept and slope) was removed from the spectrum. Finally, we could replicate the findings of a previous report from our laboratory including an overlapping sample with Study 1 in the present thesis. In this, Ujma et al., (2014) found significantly higher spindle frequency in females using a validated spindle detection method. In Study 1, we also found higher peak frequency in females, suggesting that analysing the frequency of the largest peak in the 9–18 Hz range results in similar outcomes to those of direct spindle analysis performed on the time-domain signals.

Intelligence correlated significantly with spindle density, amplitude, and power in the spindle range in some studies (see meta-analysis in Ujma et al., 2020). Here, we could replicate previous report using overlapping database revealing a sex effect of IQ and spindle amplitude correlations (Ujma et al., 2014) as we found a significant correlation between IQ and peak amplitudes in females, but not in males.

Overall, it can be stated that decomposing the power spectrum into only slope, intercept, and peak properties offers a comprehensive approach to define and understand individual variations in sleep, as key characteristics of NREM sleep EEG can be effectively summarised using the aforementioned metrics (at least in terms of their relationship with age, sex and IQ).

5.3. Overnight dynamics of spectral parameters correspond to sleep regulation

After the authors of early studies recognized that sleep duration is a secondary metric in describing sleep quality—as it does not increase substantially even after drastic sleep restriction (Gulevich et al., 1966; Patrick & Gilbert, 1896)—, the observation of sleep depth/intensity came into the spotlight. Several studies found that SWA is largely associated with sleep intensity as it changes in coherence with sleep-wake history (Borbély et al., 1981; Dement & Kleitman, 1957b; Karacan et al., 1970; Webb & Agnew, 1971) thus, its overnight dynamic served as a cornerstone in the visualization and modelling of the homeostatic process of sleep regulation (Borbély, 1982). In Study 2 we showed, that besides SWA, the slope of the Fourier spectrum follows the same behaviour as "expected" from a putative sleep intensity metric during the first four sleep cycles of the night (~first 6 hours of sleep). First of all, it flattened from cycle to cycle at all derivations, thus was the steepest after sleep onset (in the first sleep cycle). Secondly, the decrement of spectral slope steepness during the first 3 cycles was only non-significant for the middle-aged group, which is similar to the reported observations for SWA dynamics of older participants, the latter hypothesized to be related to decreased sleep efficiency in the elderly (Landolt et al., 1996). However, one of the interesting results of our study was that between cycles 3 and 4, the decrement was not significant for any group except young adults, neither in terms of SWA nor regarding spectral slope. An early study revealed similar results for SWA dynamics (Borbély et al., 1981). This diminishing decay rate of sleep intensity toward the end of the night fits well within the concept of the "exponentially shaped" homeostatic process. Indeed, in a later work, Dijk et al. (1990) reported a significant reduction in SWA during the first 3 sleep cycles of habitual sleep and the first 5 cycles of recovery sleep following 36 hours of wakefulness, but after then SWA nearly stabilized at a constant level. In Study 3, where we applied a 35-hour sleep deprivation protocol, we found significant slope flattening and lnSWA reduction from the second to the fourth sleep cycles when the first four cycles of the

whole sample were analysed. The steepest slopes were observed at the onset of sleep, while the lowest appeared toward the end of the night, however, contrary to our expectations, steepest slopes were not confined solely to the first sleep cycle. One possible explanation for the absence of a significant difference between the first and second NREM periods in spectral slope values is the "first-use effect" of the headband EEG device in BS. Another explanation could be that the headband-derived EEG data has its own limitations in signal quality, which is reflected in these results. However, this does not undermine the validity of using slope as a homeostatic marker, as the gold-standard SWA showed similar patterns in this particular dataset and the slope metric reliably reproduced other expected effects. For example, when the sample was divided according to the number of cycles participants had during their sleep periods, the same tendencies were found on both nights regarding both metrics (slope and lnSWA) in all cycle count-based groups. All cycle effects were significant, although the significant post hoc test results regarding the comparisons of successive sleep cycles did not survive Bonferroni correction. However, it should be noted that the first published report relying on a highly similar experimental procedure (Dijk et al., 1990) did not apply any corrections for multiple comparisons. Finally, in Study 2, spectral slope varied between recording locations. Specifically, slope was steeper in the frontal-central locations than in the occipital regions, in all sleep cycles. This spatial distribution is also in line with the known frontal predominance of slow waves (Werth, Achermann, & Borbély, 1997).

Peak amplitude increased in successive sleep cycles which result parallels studies finding that spindle activity increases during the night in the higher spindle band (<12.5 Hz) and shows an opposite pattern to SWA (Aeschbach & Borbély, 1993; Dijk et al., 1993; Fernandez & Lüthi, 2020; Uchida et al., 1991, 1994). However, it does not aligns with a published inverse trend of slow spindle activity (Werth, Achermann, Dijk, et al., 1997).

Spindle frequency was associated with markers of the circadian rhythm, such as melatonin and core body temperature, as well as with the time of day by authors of early research reports (Aeschbach et al., 1997; Knoblauch et al., 2005; Wei et al., 1999). Our initial attempt to examine the assumed circadian modulation of sleep spindle frequency targeted the issue of nocturnal and daytime variation of this metric. In this pioneering study (Bódizs et al., 2022) we found that sleep spindle frequency (detected by the IAM

method (Bódizs et al., 2009)) decreased by ~0.1 Hz toward the middle of the sleep period in the sample and this decrement was larger for younger participants. Furthermore, spindle frequency was higher in afternoon nap than in nocturnal sleep. Thus, in Study 2 we assumed that peak frequency would follow similar trends during the first 4 sleep cycles. We found that the U-shaped curve dynamic was significant only in the frontopolar region. As mentioned above, an early study found that the power of slow spindles decrease, while the power of fast spindles increase in consecutive NREM periods (Werth, Achermann, Dijk, et al., 1997), furthermore, that the current source density in frontal and parietal regions follows a decreasing and increasing trend, respectively, across successive sleep cycles (Alfonsi et al., 2019). Thus, the lack of significance in central and frontal regions might be due to time-varying dominance in discrete frequencies (slow vs. fast) during the night (especially in the middle cycles) over these areas. Furthemore, around the central regions, the largest peak may vary across subjects, corresponding to either slow or fast spindles, leading to a mixture of both types contributing to the sample mean. Indeed, a study found substantial interindividual topographical difference of slow and fast spindles, but with a reliable stability across nights (Cox et al., 2017). That reasoning is partly supported by our findings regarding the location of the maximal frequency shifts in the sample. We found dominant central-to-frontal shift in the first two cycles, and largest shift from frontal to frontopolar region in the third cycle. In the fourth cycle the shift predominantly occurred in the central to frontal region (~40% of the sample), however, as the sleep cycles progressed, the difference between the most and second most dominant locations of the shifts gradually diminished (see Table 3). While the first cycle showed a clear central-to-frontal predominance, the 4th cycle exhibited a more balanced distribution between central-to-frontal and frontal-to-frontopolar shifts. Again, we suggest that the cycle-by-cycle dynamics of peak frequencies are influenced by both the assumed circadian dynamics and the sleep duration-dependent reorganization of fast and slow spindles, except the frontopolar region, which seems to be characterized by an unchanged dominance in slow spindles. In Study 3, we had the chance to reveal the overnight dynamics of peak frequency both during a habitual, chronotype-adjusted sleep (BS), and in a slightly advanced (~4–5 hours) sleep schedule after 35 hours of wakefulness (RS). Awakenings from both nights were spontaneous; thus, we could observe the true build-up of peak frequency during the sleep periods. We found that cycle

effect was not significant when analysing the first four cycles of the whole sample. However, when considering complete recordings, the cycle effect reached significance in most cycle count-based groups. The fact that the majority of the sample had more than four sleep cycles even in BS (the median was 5) appeared to be a logical explanation for this phenomenon as we expected a peak frequency decrease toward mid-sleep in BS and the corresponding local time in RS. Accordingly, we carried out comparisons between the peak frequencies of the middle and the first/last sleep cycles. Peak frequency was significantly higher in the last than in the middle sleep cycles, however, only a trend emerged regarding the difference between the first and middle sleep cycles. Furthermore, the last peak frequencies were higher than the first ones. Due to the fact that our analysis covered sleep periods of longer duration than usually reported in the literature, it is reasonable to assume that spindle frequency peaks around the first half of the biological day. This hypothesis is partially corroborated by findings showing that daytime sleep spindle frequency is higher than sleep spindle frequency of a night time sleep (Knoblauch et al., 2003, 2005; Rosinvil et al., 2015; Wei et al., 1999). However, as we can only measure sleep spindle frequencies in the frontal region (common average reference of F7Fpz and F8Fpz derivations) in Study 3, the above explanation of the changing predominance of slow and fast spindles during the night may also be applicable here.

5.4. Sleep deprivation has a substantial impact on spectral parameters

Sleep deprivation is the most effective method for experimentally challenging the sleep homeostat, whereas the displacement of sleep has been shown to induce time-of-day variations in certain aspects of sleep (Akerstedt & Gillberg, 1981). Therefore, using this kind of paradigms to examine the homeostatic and circadian aspects of the spectral parameters of human EEG appears to be an effective approach for providing direct evidence and drawing conclusions on their role in sleep regulatory processes.

Our assumption on the sleep homeostasis indexing role of the spectral slope did not rely solely on our findings regarding its similar dynamics to those of the SWA (e.g. with age, during sleep, etc.), instead, on studies showing differences of this metric across- (Lendner et al., 2020), and within brain states (Höhn et al., 2024), sleep cycles (Rosenblum et al., 2023), and between sleep stages (Schneider et al., 2022). We found an overall effect of sleep deprivation, with a steeper slope (& higher lnSWA) in the first four cycles, with a more pronounced steepest slope (& higher lnSWA) in RS than in BS,

furthermore, with nearly identical flattest slopes (& lnSWA values) between the two conditions. This latter finding is important within the context of homeostasis, as it suggests that spectral slope returns to a nearly steady state after the "sleep hunger" of the organism was satisfied, furthermore, as discussed above, the same can be observed regarding SWA (Aeschbach et al., 1997; Dijk et al., 1990).

Contrary to our hypotheses, we found that in addition to spectral slope, sleep deprivation also affected the peak frequency. Although peak frequency was similar in the first and last cycles of BS and RS, which is in line with our expectations, we had assumed that the first 4 cycles would differ between the conditions, as bedtime was advanced, and sleep duration was longer for all subjects in RS. That is, we expected higher frequencies to persist until the habitual bedtime of the participants in RS. However, this hypothesis was not supported, as the peak frequency began to decrease already in the second cycle in both nights. Furthermore, we observed a substantial deviation in the phase of the assumed (and previously evidenced (Bódizs et al., 2022; G. Horváth & Bódizs, 2024)) circadian phase-indicator, NSSF in RS as compared to BS. We assumed that NSSF would develop around the same local time in both sleep conditions, but it was advanced in RS when compared to BS. Moreover, in contrast to BS, RS NSSF did not reflect subjective chronotype and did not occur around the middle of the night. We concluded that a logical explanation of these discrepancies may lie in the severity of the intervention, which implies the immediate need for a strong homeostatic process-based compensatory mechanism while overshadowing or even resetting some of the core components of the circadian clock. Indeed, nowadays works focusing on clock gene expression suggest that the two processes of sleep regulation are not as independent as originally proposed by Borbély (1982) (Franken & Dijk, 2024). This is supported by findings indicating that the circadian rhythmicity of sleep can change naturally (Crosley-Lyons et al., 2025), as well as by data on circadian rhythm markers. For example, phase-advancing effect of morning bright light was indicating in terms of diminished Dim Light Melatonin Onset (DLMO) after acute partial sleep deprivation (Burgess, 2010). Furthermore, one night of sleep deprivation has been linked to delayed melatonin peak and suppressed BMAL1 gene expression (Ackermann et al., 2013) while the phase-shifting effects of darkness has also been demonstrated in former studies (Buxton et al., 2000; Santhi et al., 2005). In the present study, participants were not only severely sleep deprived, but darkness was also

artificially advanced in RS due to earlier bedtimes. Based on the aforementioned literature both factors could contribute to an advanced circadian phase. Additionally, a study which found that electrical activity of the SCN (the circadian "master clock") is a function of the vigilance state, with NREM sleep lowering its activity (Deboer et al., 2003). This suggests that sleep pressure during an advanced sleep onset can influence sleep EEG spectral peak frequency, even if it is primarily regulated by a circadian mechanism orchestrated by the SCN. Since the evolution of peak frequency in BS aligned with our expectations, we believe that the phase advancement in RS was rather a limitation for time-of-day analyses of peak frequency.

5.5. Advantages of spectral parameters over the gold-standard indicators

The primary aim of the studies presented in my thesis was to identify EEG-derived metrics that are non-redundant, relatively easy to implement, and last but not least standardisable—potentially serving as a reference values for distinguishing between health and disease. Spectral slope appears to roughly meet these expectations, which is its main advantage over the gold-standard measures of sleep homeostasis, SWA. Although homeostasis was originally modelled using SWA itself, one of its biggest drawbacks is its high individual specificity, making it difficult to establish universal reference points for healthy sleep (Gander et al., 2010; Hertenstein et al., 2018; Tucker et al., 2007). While SWA is effective in predicting its own future fluctuations when considering the sleep-wake history of the organism, it is not well suited for comparing recordings across individuals (Bódizs et al., 2024). In contrast, spectral slope follows a normal distribution, and as shown in Study 2, exhibits lower interindividual variability even when compared to the log-normalized value of SWA. It should be noted that while slope is less individual-specific, it still preserves essential differences, such as those related to age or regional distribution. This suggests that slope could be a useful metric for differentiating between healthy and unhealthy sleep, whereas SWA could be superior in predicting within-subject changes according to sleep-wake history.

Although PSG is the gold-standard method for assessing sleep, there is no widely-accepted EEG-derived metric for measuring the circadian component of sleep regulation. Several non-PSG-based methods exist to estimate circadian phase, including objective but invasive approaches such as melatonin or core body temperature assessment, as well as non-invasive techniques of temperature measurement and actigraphy-based of sleep-

wake cycle assessment. However, these objective methods are often time-consuming and costly, requiring complex study protocols, such as the DLMO measurements, or multi-day recordings. A metric derived directly from PSG data could significantly simplify circadian rhythm assessment in both sleep medicine and research (Bódizs et al., 2022; G. Horváth & Bódizs, 2024).

5.6. Outlook: Fractal and Oscillatory Adjustment Model (FOAM)

A recent work by Bódizs et al. (2024)—heavily relying on the results discussed in the present thesis—proposed a new model of sleep regulation considering that periodic and aperiodic part of the sleep EEG spectrum are two intertwined components conveying equally important information content.

In this review, we suggested that a steeper spectral slope reflects a statistical trend in which increased membrane hyperpolarization in neural network tends to be followed by even greater hyperpolarization, while increased depolarization similarly leads to further depolarization (Bódizs et al., 2024). This pattern reflects the bistability of neural networks. We based this assumption on studies which found spectrum of rat and human LFP recordings with alternating up and down states/phases of sustained, rapid firing and periods of quiescence resulted in spectral exponent around -2 (Baranauskas et al., 2012; Milstein et al., 2009), suggesting that bistability alone may give rise to Brownian-type power spectra (i.e. red noise: relative lower frequency predominance). Additionally, spectral slope may also be influenced by the E:I ratio of the nervous system, as differences in post-spike decay rates between excitatory and inhibitory neurons result in different LFP spectral slopes, with steeper slopes indicating stronger inhibition (Gao et al., 2017). Findings on the relationship between spectral slope and neurochemical sleep regulatory factors further support its role in homeostasis (Bódizs et al., 2024). That is, spectral slope, beyond its widely discussed associations with various aspects of the homeostatic process in the present thesis (regarding age, topography, overnight dynamics, sleep history, etc.), can also be linked to neurophysiological mechanisms previously identified as essential for sleep regulation (network bistability, E:I balance, neurotransmitter release) (Bódizs et al., 2024).

FOAM proposes oscillatory spindle frequency as an index of the circadian rhythm (Bódizs et al., 2024). In the three studies of the present thesis, an indirect measure of this metric was introduced and analysed in detail—specifically, the frequency of the largest

peak in the spindle range. As the relevant literature has been thoroughly reviewed in earlier sections, it will not be reiterated here.

In addition to the sleep regulatory processes introduced and measured in the present thesis, this model also considers the ultradian component of sleep regulation. According to FOAM, the ultradian regulation of sleep (NREM-REM variation) can be modelled by abrupt shifts in peak frequency (Bódizs et al., 2024). The role of shifts in peak frequency is supported by early findings, based on binwise examination of the power spectra during state transitions showing that variation in the predominance of different frequency band values determines the architecture of sleep cycles (Aeschbach & Borbély, 1993; Merica & Fortune, 1997). Furthermore, recent evidence shows that, after parametrizing the power spectra, the frequency of the largest peak differs between sleep stages. Maximal peaks tend to appear in the spindle range during N2 and N3, whereas wakefulness and REM sleep are dominated by non-spindle spectral peaks, in the theta, alpha, or beta frequency bands (Schneider et al., 2022). However, ultradian rhythmicity can also be modelled by the time series of fractal spectral slopes (Bódizs et al., 2024), which have been shown to decrease and increase cyclically over the course of the night, in parallel with the progression of sleep cycles. This observation has been proposed in one study as a potential new definition of sleep cycles (Rosenblum et al., 2023).

The most important advantage of the FOAM compared to the two process model is its assumption that the derived metrics indexing the sleep regulatory processes could be somnologically meaningful (Bódizs et al., 2024). Although spectral parametrization is a relatively new approach, there are some examples which support this assumption. For instance, it seems that spectral slope can reliably discriminate participants with major depressive disorder (Rosenblum et al., 2022), insomnia (Andrillon et al., 2020; Bódizs et al., 2024), NREM parasomnia (Pani et al., 2021) from the control groups. Besides, increased spindle frequency has been reported in both Williams syndrome (Bódizs et al., 2012) and post-traumatic stress disorder (Denis et al., 2021) compared to controls, conditions previously linked to circadian dysregulation.

Thus, based on the literature, the combination of oscillatory and aperiodic activity can be proposed as reliable, mathematically precise and somnologically meaningful markers of EEG dynamics, as their joint analysis provides comprehensive view of its most important changes.

6. Conclusions

According to our results, the following conclusions can be drawn:

1. A proper distinction between the periodic and aperiodic components of the sleep EEG Fourier spectrum results in four physiologically and behaviourally meaningful metrics that efficiently characterize the known age-, sex- and IQ-correlates of the sleep EEG.
2. The largest peaks in the 9–18 Hz frequency range, as detected by our parametrization procedure in Study 1 and 2, effectively mirror spindles as they replicate topographical, sex-, age- and cognitive ability-related properties of sleep spindles.
3. The overnight dynamics of spectral slope are similar to those of the gold-standard sleep homeostasis indicator, SWA. Furthermore, this measure has lower interindividual variability, suggesting its potential as an easily conceptualized reference value in future research and medical works.
4. The overnight dynamics of peak frequency in the spindle range follow a U-shaped curve during habitual sleep, which has been associated with circadian modulation in other studies.
5. Sleep deprivation evidently induces changes in spectral slope, leading to spectral steepening due to heightened sleep pressure. However, it also affects peak frequency and advances the time of its minimum in RS, which may indicate the entanglement of the two regulatory processes.

In sum, our results strongly support spectral slope as a reliable marker of sleep homeostasis, while promising about peak frequency. However, latter requires further research involving the direct manipulation of the circadian cycle to gain deeper insights.

7. Summary

Two process model is one of the most extensively used framework characterizing the regulation of sleep-wake states which lacks standardisable, non-redundant EEG markers. In my thesis, I aim to demonstrate, that by proper separation of the aperiodic and periodic part of the NREM sleep EEG Fourier spectrum, we obtain physiologically interpretable markers effectively reflecting known individual differences in sleep EEG and could serve as reliable indicators for homeostatic and circadian processes of sleep.

In Study 1, we demonstrated that spontaneous human brain activity measured by EEG during NREM sleep—in addition to rhythmic oscillations in specific frequency bands—, exhibits aperiodic, scale-free properties that follow a power-law scaling of the Fourier spectra. We derived four metrics using our parametrization procedures: spectral slope, the intercept, peak amplitude, and peak frequency in the spindle range. We showed that these measures, are sufficient to capture known age-, sex-, and IQ-related changes in the sleep EEG.

In Study 2, we analysed the first four NREM periods of sleep from 251 healthy human subjects (aged 4–69 years). We observed a flattening of spectral slopes, decrease in intercept, increase in spectral peak amplitude, and a U-shaped dynamic of peak frequencies in frontopolar regions. While the spectral slope reflected known age- and sex-related effects, the variability in its steepness was lower than that of SWA. Our findings suggest that combining scale-free and oscillatory measures of sleep EEG could offer composite indicators of sleep dynamics with minimal redundancy, potentially providing new insights into sleep regulation.

Finally, in Study 3, we validated the sleep homeostasis-related assumption regarding the spectral slope using a 35-hour sleep deprivation study. Spectral slope steepening effectively reflected changes in sleep depth due to sleep deprivation. Peak frequency during BS showed the expected overnight dynamics, with mid-sleep minima. BS timing of these minima significantly correlated with self-reported chronotype. However, sleep deprivation advanced the timing of the peak frequency minima in RS and reduced its correlation with chronotype.

Overall, our study highlights the spectral slope of sleep EEG as a marker of wake-sleep homeostasis and encourages further research on EEG-derived indicators of the circadian rhythm, particularly their interaction with the homeostatic process.

8. References

Abt, K. (1987). Descriptive data analysis: A concept between confirmatory and exploratory data analysis. *Methods of Information in Medicine*, *26*(2), 77–88. https://doi.org/10.1055/s-0038-1635488

Abt, K. (1990). Statistical aspects of neurophysiologic topography. *Journal of Clinical Neurophysiology*, *7*(4), 519–534. https://doi.org/10.1097/00004691-199010000-00007

Achermann, P., & Borbély, A. A. (2017). Sleep homeostasis and models of sleep regulation. In M. H. Kryger, T. Roth, & W. C. Dement (Eds.), *Principles and Practice of Sleep Medicine* (6th ed., pp. 377–387). Elsevier.

Ackermann, K., Plomp, R., Lao, O., Middleton, B., Revell, V. L., Skene, D. J., & Kayser, M. (2013). Effect of sleep deprivation on rhythms of clock gene expression and melatonin in humans. *Chronobiology International*, *30*(7), 901–909. https://doi.org/10.3109/07420528.2013.784773

Aeschbach, D., & Borbély, A. A. (1993). All-night dynamics of the human sleep EEG. *Journal of Sleep Research*, *2*(2), 70–81. https://doi.org/10.1111/j.1365-2869.1993.tb00065.x

Aeschbach, D., Dijk, D. J., & Borbély, A. A. (1997). Dynamics of EEG spindle frequency activity during extended sleep in humans: Relationship to slow-wave activity and time of day. *Brain Research*, *748*(1–2), 131–136. https://doi.org/10.1016/S0006-8993(96)01275-9

Akerstedt, T., & Gillberg, M. (1981). The circadian variation of experimentally displaced sleep. *Sleep*, *4*(2), 159–169. https://doi.org/10.1093/sleep/4.2.159

Alfonsi, V., D'Atri, A., Gorgoni, M., Scarpelli, S., Mangiaruga, A., Ferrara, M., & De Gennaro, L. (2019). Spatiotemporal dynamics of sleep spindle sources across NREM sleep cycles. *Frontiers in Neuroscience*, *13*(JUL). https://doi.org/10.3389/fnins.2019.00727

Andrillon, T., Solelhac, G., Bouchequet, P., Romano, F., Le Brun, M. P., Brigham, M., Chennaoui, M., & Léger, D. (2020). Revisiting the value of polysomnographic data in insomnia: more than meets the eye. *Sleep Medicine*, *66*, 184–200. https://doi.org/10.1016/j.sleep.2019.12.002

Armitage, R. (1995). The distribution of EEG frequencies in REM and NREM sleep

stages in healthy young adults. *Sleep*, *18*(5), 334–341. https://doi.org/10.1093/sleep/18.5.334

Aserinsky, E., & Kleitman, N. (1953). Regularly occurring periods of eye motility, and concomitant phenomena, during sleep. *Science*, *118*(3062), 273–274. https://doi.org/10.1126/science.118.3062.273

Baranauskas, G., Maggiolini, E., Vato, A., Angotzi, G., Bonfanti, A., Zambra, G., Spinelli, A., & Fadiga, L. (2012). Origins of 1/f 2 scaling in the power spectrum of intracortical local field potential. *Journal of Neurophysiology*, *107*(3), 984–994. https://doi.org/10.1152/jn.00470.2011

Beck, A. T., Ward, C. H., Mendelson, M., Mock, J., & Erbaugh, J. (1961). An Inventory for Measuring Depression. *Archives of General Psychiatry*, *4*(6), 561–571. https://doi.org/10.1001/archpsyc.1961.01710120031004

Berger, H. (1929). Über das Elektrenkephalogramm des Menschen. *Archiv Für Psychiatrie Und Nervenkrankheiten*, *87*(1), 527–570. https://doi.org/10.1007/BF01797193

Berger, R. J., & Oswald, I. (1962). Effects of sleep deprivation on behaviour, subsequent sleep, and dreaming. *The Journal of Mental Science*, *108*, 457–465. https://doi.org/10.1192/bjp.108.455.457

Berry, R. B., Albertario, C. L., Harding, S. M., Lloyd, R. M., Plante, D. T., Quan, S. F., Troester, M. M., Vaughn, B. V, & for the American Academy of Sleep Medicine. (2018). *The AASM Manual for the Scoring of Sleep and Associated Events: Rules, Terminology and Technical Specifications. Version 2.5.* American Academy of Sleep Medicine.

Bódizs, R., Gombos, F., & Kovács, I. (2012). Sleep EEG fingerprints reveal accelerated thalamocortical oscillatory dynamics in Williams syndrome. *Research in Developmental Disabilities*, *33*(1), 153–164. https://doi.org/10.1016/j.ridd.2011.09.004

Bódizs, R., Gombos, F., Ujma, P. P., Szakadát, S., Sándor, P., Simor, P., Pótári, A., Konrad, B. N., Genzel, L., Steiger, A., Dresler, M., & Kovács, I. (2017). The hemispheric lateralization of sleep spindles in humans. *Sleep Spindles & Cortical Up States, 1*(1), 42–54. https://doi.org/10.1556/2053.01.2017.002

Bódizs, R., Horváth, C. G., Szalárdy, O., Ujma, P. P., Simor, P., Gombos, F., Kovács, I.,

Genzel, L., & Dresler, M. (2022). Sleep-spindle frequency: Overnight dynamics, afternoon nap effects, and possible circadian modulation. *Journal of Sleep Research*, *31*(3), 1–13. https://doi.org/10.1111/jsr.13514

Bódizs, R., Kis, T., Lázár, A. S., Havrán, L., Rigó, P., Clemens, Z., & Halász, P. (2005). Prediction of general mental ability based on neural oscillation measures of sleep. *Journal of Sleep Research*, *14*(3), 285–292. https://doi.org/10.1111/j.1365-2869.2005.00472.x

Bódizs, R., Körmendi, J., Rigó, P., & Lázár, A. S. (2009). The individual adjustment method of sleep spindle analysis: Methodological improvements and roots in the fingerprint paradigm. *Journal of Neuroscience Methods*, *178*(1), 205–213. https://doi.org/10.1016/j.jneumeth.2008.11.006

Bódizs, R., Schneider, B., Ujma, P. P., Horváth, C. G., Dresler, M., & Rosenblum, Y. (2024). Fundamentals of sleep regulation: Model and benchmark values for fractal and oscillatory neurodynamics. In *Progress in Neurobiology* (Vol. 234). https://doi.org/10.1016/j.pneurobio.2024.102589

Bódizs, R., Szalárdy, O., Horváth, C., Ujma, P. P., Gombos, F., Simor, P., Pótári, A., Zeising, M., Steiger, A., & Dresler, M. (2021). A set of composite, non-redundant EEG measures of NREM sleep based on the power law scaling of the Fourier spectrum. *Scientific Reports*, *11*(1), 2041. https://doi.org/10.1038/s41598-021-81230-7

Borbély, A. A. (1982). A two process model of sleep regulation. *Human Neurobiology*, *1*(3), 195–204.

Borbély, A. A. (2022). The two-process model of sleep regulation: Beginnings and outlook†. In *Journal of Sleep Research* (Vol. 31, Issue 4). https://doi.org/10.1111/jsr.13598

Borbély, A. A., & Achermann, P. (1992). Concepts and models of sleep regulation: an overview. *Journal of Sleep Research*, *1*(2), 63–79. https://doi.org/10.1111/j.1365-2869.1992.tb00013.x

Borbély, A. A., Baumann, F., Brandeis, D., Strauch, I., & Lehmann, D. (1981). Sleep deprivation: Effect on sleep stages and EEG power density in man. *Electroencephalography and Clinical Neurophysiology*, *51*(5), 483–493. https://doi.org/10.1016/0013-4694(81)90225-X

Borbély, A. A., Daan, S., Wirz-Justice, A., & Deboer, T. (2016). The two-process model of sleep regulation: A reappraisal. *Journal of Sleep Research*, *25*(2), 131–143. https://doi.org/10.1111/jsr.12371

Bougard, C., Gomez-Merino, D., Rabat, A., Arnal, P., Van Beers, P., Guillard, M., Léger, D., Sauvet, F., & Chennaoui, M. (2018). Daytime microsleeps during 7 days of sleep restriction followed by 13 days of sleep recovery in healthy young adults. *Consciousness and Cognition*, *61*, 1–12. https://doi.org/10.1016/j.concog.2018.03.008

Burgess, H. J. (2010). Partial sleep deprivation reduces phase advances to light in humans. *Journal of Biological Rhythms*, *25*(6), 460–468. https://doi.org/10.1177/0748730410385544

Buxton, O. M., L'Hermite-Balériaux, M., Turek, F. W., & Van Cauter, E. (2000). Daytime naps in darkness phase shift the human circadian rhythms of melatonin and thyrotropin secretion. *American Journal of Physiology - Regulatory Integrative and Comparative Physiology*, *278*(2). https://doi.org/10.1152/ajpregu.2000.278.2.r373

Campos-Beltrán, D., & Marshall, L. (2021). Changes in sleep EEG with aging in humans and rodents. In *Pflugers Archiv European Journal of Physiology* (Vol. 473, Issue 5, pp. 841–851). https://doi.org/10.1007/s00424-021-02545-y

Carrier, J., Land, S., Buysse, D. J., Kupfer, D. J., & Monk, T. H. (2001). The effects of age and gender on sleep EEG power spectral density in the middle years of life (ages 20-60 years old). *Psychophysiology*, *38*(2), 232–242. https://doi.org/10.1017/S0048577201991838

Carrier, J., Viens, I., Poirier, G., Robillard, R., Lafortune, M., Vandewalle, G., Martin, N., Barakat, M., Paquet, J., & Filipini, D. (2011). Sleep slow wave changes during the middle years of life. *European Journal of Neuroscience*, *33*(4), 758–766. https://doi.org/10.1111/j.1460-9568.2010.07543.x

Carskadon, M. A., Labyak, S. E., Acebo, C., & Seifer, R. (1999). Intrinsic circadian period of adolescent humans measured in conditions of forced desynchrony. *Neuroscience Letters*, *260*(2), 129–132. https://doi.org/10.1016/S0304-3940(98)00971-9

Chapman, R., Najima, S., Tylinski Sant'Ana, T., Lee, C. C. K., Filice, F., Babineau, J., & Mollayeva, T. (2025). Sex differences in electrical activity of the brain during

sleep: a systematic review of electroencephalographic findings across the human lifespan. *BioMedical Engineering OnLine*, *24*(1), 33. https://doi.org/10.1186/s12938-025-01354-z

Civan, M. M., Peterson-Yantorno, K., Coca-Prados, M., & E.Yantorno, R. (1992). Regulatory volume decrease by cultured non-pigmented ciliary epithelial cells. In *Experimental Eye Research* (Version 2., Vol. 54, Issue 2). American Academy of Sleep Medicine. https://doi.org/10.1016/S0014-4835(05)80207-6

Colombo, M. A., Napolitani, M., Boly, M., Gosseries, O., Casarotto, S., Rosanova, M., Brichant, J. F., Boveroux, P., Rex, S., Laureys, S., Massimini, M., Chieregato, A., & Sarasso, S. (2019). The spectral exponent of the resting EEG indexes the presence of consciousness during unresponsiveness induced by propofol, xenon, and ketamine. *NeuroImage*, *189*, 631–644. https://doi.org/10.1016/j.neuroimage.2019.01.024

Cox, R., & Fell, J. (2020). Analyzing human sleep EEG: A methodological primer with code implementation. *Sleep Medicine Reviews*, *54*, 101353. https://doi.org/10.1016/j.smrv.2020.101353

Cox, R., Schapiro, A. C., Manoach, D. S., & Stickgold, R. (2017). Individual differences in frequency and topography of slow and fast sleep spindles. *Frontiers in Human Neuroscience*, *11*. https://doi.org/10.3389/fnhum.2017.00433

Crosley-Lyons, R., Li, J., Wang, W. L., Wang, S. D., Huh, J., Bae, D., Intille, S. S., & Dunton, G. F. (2025). Exploring person-centred sleep and rest–activity cycle dynamics over 6 months. *Journal of Sleep Research*. https://doi.org/10.1111/jsr.14471

Crowley, K., Trinder, J., Kim, Y., Carrington, M., & Colrain, I. M. (2002). The effects of normal aging on sleep spindle and K-complex production. *Clinical Neurophysiology*, *113*(10), 1615–1622. https://doi.org/10.1016/S1388-2457(02)00237-7

Czeisler, C. A., Weitzman, E. D., Moore-Ede, M. C., Zimmerman, J. C., & Knauer, R. S. (1980). Human sleep: Its duration and organization depend on its circadian phase. *Science*, *210*(4475), 1264–1267. https://doi.org/10.1126/science.7434029

Czeisler, C. A., Zimmerman, J. C., Ronda, J. M., Moore-Ede, M. C., & Weitzman, E. D. (1980). Timing of REM sleep is coupled to the circadian rhythm of body temperature

in man. *Sleep*, *2*(3), 329–346. https://doi.org/10.1093/sleep/2.3.329

De Gennaro, L., & Ferrara, M. (2003). Sleep spindles: An overview. In *Sleep Medicine Reviews* (Vol. 7, Issue 5, pp. 423–440). https://doi.org/10.1053/smrv.2002.0252

De Gennaro, L., Marzano, C., Fratello, F., Moroni, F., Pellicciari, M. C., Ferlazzo, F., Costa, S., Couyoumdjian, A., Curcio, G., Sforza, E., Malafosse, A., Finelli, L. A., Pasqualetti, P., Ferrara, M., Bertini, M., & Rossini, P. M. (2008). The electroencephalographic fingerprint of sleep is genetically determined: A twin study. *Annals of Neurology*, *64*(4), 455–460. https://doi.org/10.1002/ana.21434

Deboer, T. (2020). Circadian regulation of sleep in mammals. In *Current Opinion in Physiology* (Vol. 15, pp. 89–95). https://doi.org/10.1016/j.cophys.2019.12.015

Deboer, T., Vansteensel, M. J., Détári, L., & Meijer, J. H. (2003). Sleep states alter activity of suprachiasmatic nucleus neurons. *Nature Neuroscience*, *6*(10), 1086–1090. https://doi.org/10.1038/nn1122

Dement, W., & Kleitman, N. (1957a). Cyclic variations in EEG during sleep and their relation to eye movements, body motility, and dreaming. *Electroencephalography and Clinical Neurophysiology*, *9*(4), 673–690. https://doi.org/10.1016/0013-4694(57)90088-3

Dement, W., & Kleitman, N. (1957b). The relation of eye movements during sleep to dream activity: An objective method for the study of dreaming. *Journal of Experimental Psychology*, *53*(5), 339–346. https://doi.org/10.1037/h0048189

Denis, D., Bottary, R., Cunningham, T. J., Zeng, S., Daffre, C., Oliver, K. L., Moore, K., Gazecki, S., Kram Mendelsohn, A., Martinez, U., Gannon, K., Lasko, N. B., & Pace-Schott, E. F. (2021). Sleep Power Spectral Density and Spindles in PTSD and Their Relationship to Symptom Severity. *Frontiers in Psychiatry*, *12*. https://doi.org/10.3389/fpsyt.2021.766647

Dijk, D. J., Beersma, D. G. M., & Bloem, G. M. (1989). Sex differences in the sleep EEG of young adults: Visual scoring and spectral analysis. *Sleep*, *12*(6), 500–507. https://doi.org/10.1093/sleep/12.6.500

Dijk, D. J., Beersma, D. G. M., & van den Hoofdakker, R. H. (1989). All night spectral analysis of EEG sleep in young adult and middle-aged male subjects. *Neurobiology of Aging*, *10*(6), 677–682. https://doi.org/10.1016/0197-4580(89)90004-3

Dijk, D. J., Brunner, D. P., & Borbély, A. A. (1990). Time course of EEG power density

during long sleep in humans. *American Journal of Physiology-Regulatory, Integrative and Comparative Physiology*, *258*(3), R650–R661. https://doi.org/10.1152/ajpregu.1990.258.3.r650

Dijk, D. J., Duffy, J. F., & Czeisler, C. A. (1992). Circadian and sleep/wake dependent aspects of subjective alertness and cognitive performance. *Journal of Sleep Research*, *1*(2). https://doi.org/10.1111/j.1365-2869.1992.tb00021.x

Dijk, D. J., Duffy, J. F., Kiel, E., Shanahan, T. L., & Czeisler, C. A. (1999). Ageing and the circadian and homeostatic regulation of human sleep during forced desynchrony of rest, melatonin and temperature rhythms. *Journal of Physiology*, *516*(2), 611–627. https://doi.org/10.1111/j.1469-7793.1999.0611v.x

Dijk, D. J., Hayes, B., & Czeisler, C. A. (1993). Dynamics of electroencephalographic sleep spindles and slow wave activity in men: effect of sleep deprivation. *Brain Research*, *626*(1–2), 190–199. https://doi.org/10.1016/0006-8993(93)90579-C

Dijk, D. J., Shanahan, T. L., Duffy, J. F., Ronda, J. M., & Czeisler, C. A. (1997). Variation of electroencephalographic activity during non-rapid eye movement and rapid eye movement sleep with phase of circadian melatonin rhythm in humans. *Journal of Physiology*, *505*(3), 851–858. https://doi.org/10.1111/j.1469-7793.1997.851ba.x

Donoghue, T., Dominguez, J., & Voytek, B. (2020). Electrophysiological frequency band ratio measures conflate periodic and aperiodic neural activity. *ENeuro*, *7*(6), ENEURO.0192-20.2020. https://doi.org/10.1523/ENEURO.0192-20.2020

Donoghue, T., Haller, M., Peterson, E. J., Varma, P., Sebastian, P., Gao, R., Noto, T., Lara, A. H., Wallis, J. D., Knight, R. T., Shestyuk, A., & Voytek, B. (2020). Parameterizing neural power spectra into periodic and aperiodic components. *Nature Neuroscience*, *23*(12), 1655–1665. https://doi.org/10.1038/s41593-020-00744-x

Duffy, F. H., Jones, K., Bartels, P., Albert, M., McAnulty, G. B., & Als, H. (1990). Quantified Neurophysiology with mapping: Statistical inference, Exploratory and Confirmatory data analysis. *Brain Topography*, *3*(1), 3–12. https://doi.org/10.1007/BF01128856

Duffy, J. F., & Dijk, D. J. (2002). Getting through to circadian oscillators: Why use constant routines? In *Journal of Biological Rhythms* (Vol. 17, Issue 1, pp. 4–13). https://doi.org/10.1177/074873002129002294

Duffy, J. F., Dijk, D. J., Klerman, E. B., & Czeisler, C. A. (1998). Later endogenous

circadian temperature nadir relative to an earlier wake time in older people. *American Journal of Physiology - Regulatory Integrative and Comparative Physiology*, *275*(5 44-5). https://doi.org/10.1152/ajpregu.1998.275.5.r1478

Dumermuth, G., Gasser, T., Germann, P., Hecker, A., Herdan, M., & Lange, B. (1977). Studies on EEG activities in the beta band. *European Neurology*, *16*(1–6), 197–202. https://doi.org/10.1159/000114900

Economo, C. V. (1930). Sleep as a problem of localization. *Journal of Nervous and Mental Disease*, *71*(3), 249–259. https://doi.org/10.1097/00005053-193003000-00001

Eggert, T., Dorn, H., & Danker-Hopfe, H. (2021). Nocturnal brain activity differs with age and sex: Comparisons of sleep eeg power spectra between young and elderly men, and between 60–80-year-old men and women. *Nature and Science of Sleep*, *13*, 1611–1630. https://doi.org/10.2147/NSS.S327221

Endo, S., Kobayashi, T., Yamamoto, T., Fukuda, H., Sasaki, M., & Ohta, T. (1981). Persistence of the circadian rhythm of REM sleep: A variety of experimental manipulations of the sleep-wake cycle. *Sleep*, *4*(3), 319–328. https://doi.org/10.1093/sleep/4.3.319

Favaro, J., Colombo, M. A., Mikulan, E., Sartori, S., Nosadini, M., Pelizza, M. F., Rosanova, M., Sarasso, S., Massimini, M., & Toldo, I. (2023). The maturation of aperiodic EEG activity across development reveals a progressive differentiation of wakefulness from sleep. *NeuroImage*, *277*, 120264. https://doi.org/10.1016/j.neuroimage.2023.120264

Feinberg, I., Fein, G., & Floyd, T. . (1980). EEG patterns during and following extended sleep in young adults. *Electroencephalography and Clinical Neurophysiology*, *50*(5–6), 467–476. https://doi.org/10.1016/0013-4694(80)90013-9

Feinberg, I., & Floyd, T. C. (1979). Systematic Trends Across the Night in Human Sleep Cycles. *Psychophysiology*, *16*(3), 283–291. https://doi.org/10.1111/j.1469-8986.1979.tb02991.x

Feinberg, I., March, J. D., Floyd, T. C., Fein, G., & Aminoff, M. J. (1984). Log amplitude is a linear function of log frequency in NREM sleep EEG of young and elderly normal subjects. *Electroencephalography and Clinical Neurophysiology*, *58*(2), 158–160. https://doi.org/10.1016/0013-4694(84)90029-4

Fernandez, L. M. J., & Lüthi, A. (2020). Sleep spindles: Mechanisms and functions. *Physiological Reviews*, *100*(2), 805–868. https://doi.org/10.1152/physrev.00042.2018

Finelli, L. A., Ackermann, P., & Borbély, A. A. (2001). Individual "fingerprints" in human sleep EEG topography. *Neuropsychopharmacology*, *25*(5), S57–S62. https://doi.org/10.1016/S0893-133X(01)00320-7

Franken, P., & Dijk, D. J. (2024). Sleep and circadian rhythmicity as entangled processes serving homeostasis. In *Nature Reviews Neuroscience* (Vol. 25, Issue 1, pp. 43–59). https://doi.org/10.1038/s41583-023-00764-z

Freeman, W. J., Holmes, M. D., West, G. A., & Vanhatalo, S. (2006). Fine spatiotemporal structure of phase in human intracranial EEG. *Clinical Neurophysiology*, *117*(6), 1228–1243. https://doi.org/10.1016/j.clinph.2006.03.012

G. Horváth, C., & Bódizs, R. (2024). Association of actigraphy-derived circadian phase indicators with the nadir of spindle frequency. *Biological Rhythm Research*, *55*(1), 16–29. https://doi.org/10.1080/09291016.2023.2283656

G. Horváth, C., & Bódizs, R. (2025). Effect of sleep deprivation on fractal and oscillatory spectral measures of the sleep EEG: A window on basic regulatory processes. *NeuroImage*, *314*. https://doi.org/10.1016/j.neuroimage.2025.121260

G. Horváth, C., Szalárdy, O., Ujma, P. P., Simor, P., Gombos, F., Kovács, I., Dresler, M., Bódizs, R., Horváth, C. G., Szalárdy, O., Ujma, P. P., Simor, P., Gombos, F., Kovács, I., Dresler, M., & Bódizs, R. (2022). Overnight dynamics in scale-free and oscillatory spectral parameters of NREM sleep EEG. *Scientific Reports*, *12*(1), 18409. https://doi.org/10.1038/s41598-022-23033-y

Gander, P., Signal, L., Van Dongen, H. P. A., Muller, D., & Van Den Berg, M. (2010). Stable inter-individual differences in slow-wave sleep during nocturnal sleep and naps. *Sleep and Biological Rhythms*, *8*(4), 239–244. https://doi.org/10.1111/j.1479-8425.2010.00454.x

Gao, R. (2016). Interpreting the electrophysiological power spectrum. *Journal of Neurophysiology*, *115*(2), 628–630. https://doi.org/10.1152/jn.00722.2015

Gao, R., Peterson, E. J., & Voytek, B. (2017). Inferring synaptic excitation/inhibition balance from field potentials. *NeuroImage*, *158*, 70–78. https://doi.org/10.1016/j.neuroimage.2017.06.078

Gennaro, L. De, Ferrara, M., Vecchio, F., Curcio, G., & Bertini, M. (2005). An electroencephalographic fingerprint of human sleep. *NeuroImage*, *26*(1), 114–122. https://doi.org/10.1016/j.neuroimage.2005.01.020

Gibbs, F. A., & Gibbs, E. L. (1951). *Atlas of Electroencephalography*. Addison-Wesley Press.

Goodenough, D. R., Lewis, H. B., Shapiro, A., Jaret, L., & Sleser, I. (1965). Dream reporting following abrupt and gradual awakenings from different types of sleep. *Journal of Personality and Social Psychology*, *2*(2), 170–179. https://doi.org/10.1037/h0022424

Gulevich, G., Dement, W., & Johnson, L. (1966). Psychiatric and EEG Observations on a Case of Prolonged (264 Hours) Wakefulness. *Archives of General Psychiatry*, *15*(1), 29–35. https://doi.org/10.1001/archpsyc.1966.01730130031005

Haraszti, R. Á., Ella, K., Gyöngyösi, N., Roenneberg, T., & Káldi, K. (2014). Social jetlag negatively correlates with academic performance in undergraduates. *Chronobiology International*, *31*(5). https://doi.org/10.3109/07420528.2013.879164

He, B. J., Zempel, J. M., Snyder, A. Z., & Raichle, M. E. (2010). The temporal structures and functional significance of scale-free brain activity. *Neuron*, *66*(3), 353–369. https://doi.org/10.1016/j.neuron.2010.04.020

Hendricks, J. C., Sehgal, A., & Pack, A. I. (2000). The need for a simple animal model to understand sleep. In *Progress in Neurobiology* (Vol. 61, Issue 4, pp. 339–351). https://doi.org/10.1016/S0301-0082(99)00048-9

Hertenstein, E., Gabryelska, A., Spiegelhalder, K., Nissen, C., Johann, A. F., Umarova, R., Riemann, D., Baglioni, C., & Feige, B. (2018). Reference data for polysomnography-measured and subjective sleep in healthy adults. *Journal of Clinical Sleep Medicine*, *14*(4), 523–532. https://doi.org/10.5664/jcsm.7036

Hoddes, E., Zarcone, V., Smythe, H., Phillips, R., & Dement, W. C. (1973). Quantification of Sleepiness: A New Approach. *Psychophysiology*, *10*(4), 431–436. https://doi.org/10.1111/j.1469-8986.1973.tb00801.x

Höhn, C., Hahn, M. A., Lendner, J. D., & Hoedlmoser, K. (2024). Spectral Slope and Lempel-Ziv complexity as robust markers of brain states during sleep and wakefulness. *Eneuro*, ENEURO.0259-23.2024. https://doi.org/10.1523/eneuro.0259-23.2024

Ishii, T., Taweesedt, P. T., Chick, C. F., O'Hara, R., & Kawai, M. (2024). From macro to micro: slow-wave sleep and its pivotal health implications. *Frontiers in Sleep, 3*. https://doi.org/10.3389/frsle.2024.1322995

Jenni, O. G., & Carskadon, M. A. (2004). Spectral analysis of the sleep electroencephalogram during adolescence. *Sleep, 27*(4), 774–783. https://doi.org/10.1093/sleep/27.4.774

Jouvet, M. (1962). Research on the neural structures and responsible mechanisms in different phases of physiological sleep. *Archives Italiennes de Biologie*, *100*, 125–206.

Karacan, I., Finley, W. W., Williams, R. L., & Hursch, C. J. (1970). Changes in stage 1-REM and stage 4 sleep during naps. *Biological Psychiatry*, *2*(3), 261–265.

Knoblauch, V., Martens, W. L. J., Wirz-Justice, A., & Cajochen, C. (2003). Human sleep spindle characteristics after sleep deprivation. *Clinical Neurophysiology*, *114*(12), 2258–2267. https://doi.org/10.1016/S1388-2457(03)00238-4

Knoblauch, V., Münch, M., Blatter, K., Martens, W. L. J., Schröder, C., Schnitzler, C., Wirz-Justice, A., & Cajochen, C. (2005). Age-related changes in the circadian modulation of sleep-spindle frequency during nap sleep. In *Sleep* (Vol. 28, Issue 9). https://doi.org/10.1093/sleep/28.9.1093

Krakovská, A., & Mezeiová, K. (2011). Automatic sleep scoring: A search for an optimal combination of measures. *Artificial Intelligence in Medicine*, *53*(1), 25–33. https://doi.org/10.1016/j.artmed.2011.06.004

Krueger, J. M., Nguyen, J. T., Dykstra-Aiello, C. J., & Taishi, P. (2019). Local sleep. In *Sleep Medicine Reviews* 43, (pp. 14–21). https://doi.org/10.1016/j.smrv.2018.10.001

Kullback, S., & Leibler, R. A. (1951). On Information and Sufficiency. *The Annals of Mathematical Statistics*, *22*(1), 79–86. https://doi.org/10.1214/aoms/1177729694

Landolt, H. P., Dijk, D. J., Achermann, P., & Borbély, A. A. (1996). Effect of age on the sleep EEG: Slow-wave activity and spindle frequency activity in young and middle-aged men. *Brain Research*, *738*(2), 205–212. https://doi.org/10.1016/S0006-8993(96)00770-6

Lázár, A. S., Lázár, Z. I., & Bódizs, R. (2022). Frequency Characteristics of Sleep. In G. Philip, M. Matthew, & B. Edward (Eds.), *The Oxford Handbook of EEG Frequency* (pp. 401-C17.P221). Oxford University Press.

https://doi.org/10.1093/oxfordhb/9780192898340.013.17

Lendner, J. D., Helfrich, R. F., Mander, B. A., Romundstad, L., Lin, J. J., Walker, M. P., Larsson, P. G., & Knight, R. T. (2020). An electrophysiological marker of arousal level in humans. *ELife*, *9*, 1–29. https://doi.org/10.7554/eLife.55092

Loomis, A. L., Harvey, E. N., & Hobart, G. A. (1937). Cerebral states during sleep, as studied by human brain potentials. *Journal of Experimental Psychology*, *21*(2), 127–144. https://doi.org/10.1037/h0057431

Loomis, A. L., Harvey, E. N., & Hobart, G. A. (1938). Distribution of Disturbance-Patterns in the Human Electroencephalogram, With Special Reference To Sleep. *Journal of Neurophysiology*, *1*(5), 413–430. https://doi.org/10.1152/jn.1938.1.5.413

Luppi, P. H., & Fort, P. (2019). Neuroanatomical and Neurochemical Bases of Vigilance States. In *Handbook of Experimental Pharmacology* (Vol. 253, pp. 35–58). https://doi.org/10.1007/164_2017_84

Mander, B. A., Winer, J. R., & Walker, M. P. (2017). Sleep and Human Aging. In *Neuron* (Vol. 94, Issue 1, pp. 19–36). https://doi.org/10.1016/j.neuron.2017.02.004

Martin, N., Lafortune, M., Godbout, J., Barakat, M., Robillard, R., Poirier, G., Bastien, C., & Carrier, J. (2013). Topography of age-related changes in sleep spindles. *Neurobiology of Aging*, *34*(2), 468–476. https://doi.org/10.1016/j.neurobiolaging.2012.05.020

Merica, H., & Fortune, R. D. (1997). A neuronal transition probability model for the evolution of power in the sigma and delta frequency bands of sleep EEG. *Physiology and Behavior*, *62*(3), 585–589. https://doi.org/10.1016/S0031-9384(97)00165-0

Miller, K. J., Sorensen, L. B., Ojemann, J. G., & Den Nijs, M. (2009). Power-law scaling in the brain surface electric potential. *PLoS Computational Biology*, *5*(12), e1000609. https://doi.org/10.1371/journal.pcbi.1000609

Milstein, J., Mormann, F., Fried, I., & Koch, C. (2009). Neuronal shot noise and brownian 1/f2 behavior in the local field potential. *PLoS ONE*, *4*(2), e4338. https://doi.org/10.1371/journal.pone.0004338

Miskovic, V., MacDonald, K. J., Rhodes, L. J., & Cote, K. A. (2019). Changes in EEG multiscale entropy and power-law frequency scaling during the human sleep cycle. *Human Brain Mapping*, *40*(2), 538–551. https://doi.org/10.1002/hbm.24393

Mongrain, V., Carrier, J., & Dumont, M. (2005). Chronotype and sex effects on sleep

architecture and quantitative sleep EEG in healthy young adults. *Sleep*, *28*(7), 819–827. https://doi.org/10.1093/sleep/28.7.819

Moruzzi, G., & Magoun, H. W. (1949). Brain stem reticular formation and activation of the EEG. *Electroencephalography and Clinical Neurophysiology*, *1*(1–4), 455–473. https://doi.org/10.1016/0013-4694(49)90219-9

Moses, J., Lubin, A., Naitoh, P., & Johnson, L. C. (1978). Circadian variation in performance, subjective sleepiness, sleep, and oral temperature during an altered sleep-wake schedule. *Biological Psychology*, *6*(4), 301–308. https://doi.org/10.1016/0301-0511(78)90032-7

Moses, J. M., Johnson, L. C., Naitoh, P., & Lubin, A. (1975). Sleep Stage Deprivation and Total Sleep Loss: Effects On Sleep Behavior. *Psychophysiology*, *12*(2), 141–146. https://doi.org/10.1111/j.1469-8986.1975.tb01264.x

Murakami, S., & Okada, Y. (2006). Contributions of principal neocortical neurons to magnetoencephalography and electroencephalography signals. *Journal of Physiology*, *575*(3), 925–936. https://doi.org/10.1113/jphysiol.2006.105379

Murphy, M., Riedner, B. A., Huber, R., Massimini, M., Ferrarelli, F., & Tononi, G. (2009). Source modeling sleep slow waves. *Proceedings of the National Academy of Sciences of the United States of America*, *106*(5), 1608–1613. https://doi.org/10.1073/pnas.0807933106

Murray, E. J., Williams, H. L., & Lubin, A. (1958). Body temperature and psychological ratings during sleep deprivation. *Journal of Experimental Psychology*, *56*(3), 271–273. https://doi.org/10.1037/h0048421

Muza, R. (2018). Normal Sleep. In *Sleep Disorders in Psychiatric Patients* (pp. 3–25). Springer Berlin Heidelberg. https://doi.org/10.1007/978-3-642-54836-9_1

Nicolas, A., Petit, D., Rompré, S., & Montplaisir, J. (2001). Sleep spindle characteristics in healthy subjects of different age groups. *Clinical Neurophysiology*, *112*(3), 521–527. https://doi.org/10.1016/S1388-2457(00)00556-3

Pani, S. M., Fraschini, M., Figorilli, M., Tamburrino, L., Ferri, R., & Puligheddu, M. (2021). Sleep-related hypermotor epilepsy and non-rapid eye movement parasomnias: Differences in the periodic and aperiodic component of the electroencephalographic power spectra. *Journal of Sleep Research*, *30*(5). https://doi.org/10.1111/jsr.13339

Patrick, G. T. W., & Gilbert, J. A. (1896). Studies from the psychological laboratory of the University of Iowa: On the effects of loss of sleep. *Psychological Review*, *3*(5), 469–483. https://doi.org/10.1037/h0075739

Pereda, E., Gamundi, A., Rial, R., & González, J. (1998). Non-linear behaviour of human EEG: Fractal exponent versus correlation dimension in awake and sleep stages. *Neuroscience Letters*, *250*(2), 91–94. https://doi.org/10.1016/S0304-3940(98)00435-2

Pesonen, A. K., Ujma, P., Halonen, R., Räikkönen, K., & Kuula, L. (2019). The associations between spindle characteristics and cognitive ability in a large adolescent birth cohort. *Intelligence*, *72*, 13–19. https://doi.org/10.1016/j.intell.2018.11.004

Principe, J. C., & Smith, J. R. (1982). Sleep spindle characteristics as a function of age. *Sleep*, *5*(1), 73–84. https://doi.org/10.1093/sleep/5.1.73

Pritchard, W. S. (1992). The brain in fractal time: 1/f-like power spectrum scaling of the human electroencephalogram. *International Journal of Neuroscience*, *66*(1–2), 119–129. https://doi.org/10.3109/00207459208999796

Purcell, S. M., Manoach, D. S., Demanuele, C., Cade, B. E., Mariani, S., Cox, R., Panagiotaropoulou, G., Saxena, R., Pan, J. Q., Smoller, J. W., Redline, S., & Stickgold, R. (2017). Characterizing sleep spindles in 11,630 individuals from the National Sleep Research Resource. *Nature Communications*, *8*. https://doi.org/10.1038/ncomms15930

Rechtschaffen, A., & Kales, A. (1968). *A Manual of Standardized Terminology, Techniques and Scoring System for Sleep Stages of Human Subjects*. Public Health Service, US Government Printing Office.

Riegel, B., Hanlon, A. L., Zhang, X., Fleck, D., Sayers, S. L., Goldberg, L. R., & Weintraub, W. S. (2013). What is the best measure of daytime sleepiness in adults with heart failure? *Journal of the American Association of Nurse Practitioners*, *25*(5), 272–279. https://doi.org/10.1111/j.1745-7599.2012.00784.x

Roenneberg, T., & Foster, R. G. (1997). Twilight Times: Light and the Circadian System. In *Photochemistry and Photobiology* (Vol. 66, Issue 5, pp. 549–561). https://doi.org/10.1111/j.1751-1097.1997.tb03188.x

Roenneberg, T., Pilz, L. K., Zerbini, G., & Winnebeck, E. C. (2019). Chronotype and

social jetlag: A (self-) critical review. In *Biology* (Vol. 8, Issue 3). https://doi.org/10.3390/biology8030054

Rosenblum, Y., Bovy, L., Weber, F. D., Steiger, A., Zeising, M., & Dresler, M. (2022). Increased Aperiodic Neural Activity During Sleep in Major Depressive Disorder. *Biological Psychiatry Global Open Science*. https://doi.org/10.1016/j.bpsgos.2022.10.001

Rosenblum, Y., Esfahani, M. J., Adelhöfer, N., Zerr, P., Furrer, M., Huber, R., Steiger, A., Zeising, M., G. Horváth, C., Schneider, B., Bódizs, R., & Dresler, M. (2023). Fractal cycles of sleep: a new aperiodic activity-based definition of sleep cycles. *BioRxiv*, 2023.07.04.547323. https://doi.org/10.1101/2023.07.04.547323

Rosinvil, T., Lafortune, M., Sekerovic, Z., Bouchard, M., Dubé, J., Latulipe-Loiselle, A., Martin, N., Lina, J. M., & Carrier, J. (2015). Age-related changes in sleep spindles characteristics during daytime recovery following a 25-hour sleep deprivation. *Frontiers in Human Neuroscience*, *9*(JUNE). https://doi.org/10.3389/fnhum.2015.00323

Rüger, B. (1978). Das maximale signifikanzniveau des Tests: "Lehne Ho ab, wenn k unter n gegebenen tests zur ablehnung führen." *Metrika: International Journal for Theoretical and Applied Statistics*, *25*(1), 171–178. https://doi.org/10.1007/BF02204362

Santhi, N., Duffy, J. F., Horowitz, T. S., & Czeisler, C. A. (2005). Scheduling of sleep/darkness affects the circadian phase of night shift workers. *Neuroscience Letters*, *384*(3), 316–320. https://doi.org/10.1016/j.neulet.2005.04.094

Saper, C. B., Chou, T. C., & Scammell, T. E. (2001). The sleep switch: Hypothalamic control of sleep and wakefulness. In *Trends in Neurosciences* (Vol. 24, Issue 12, pp. 726–731). https://doi.org/10.1016/S0166-2236(00)02002-6

Saper, C. B., Fuller, P. M., Pedersen, N. P., Lu, J., & Scammell, T. E. (2010). Sleep State Switching. In *Neuron* (Vol. 68, Issue 6, pp. 1023–1042). https://doi.org/10.1016/j.neuron.2010.11.032

Schabus, M., Hödlmoser, K., Gruber, G., Sauter, C., Anderer, P., Klösch, G., Parapatics, S., Saletu, B., Klimesch, W., & Zeitlhofer, J. (2006). Sleep spindle-related activity in the human EEG and its relation to general cognitive and learning abilities. *European Journal of Neuroscience*, *23*(7), 1738–1746.

https://doi.org/10.1111/j.1460-9568.2006.04694.x

Schneider, B., Szalárdy, O., Ujma, P. P., Simor, P., Gombos, F., Kovács, I., Dresler, M., & Bódizs, R. (2022). Scale-free and oscillatory spectral measures of sleep stages in humans. *Frontiers in Neuroinformatics*, *16*. https://doi.org/10.3389/fninf.2022.989262

Schwarz, J. F. A., Åkerstedt, T., Lindberg, E., Gruber, G., Fischer, H., & Theorell-Haglöw, J. (2017). Age affects sleep microstructure more than sleep macrostructure. *Journal of Sleep Research*, *26*(3), 277–287. https://doi.org/10.1111/jsr.12478

Siegel, J. M., Nienhuis, R., & Tomaszewski, K. S. (1984). REM sleep signs rostral to chronic transections at the pontomedullary junction. *Neuroscience Letters*, *45*(3), 241–246. https://doi.org/10.1016/0304-3940(84)90233-7

Silver, N. C., & Dunlap, W. P. (1987). Averaging Correlation Coefficients: Should Fisher's z Transformation Be Used? *Journal of Applied Psychology*, *72*(1), 146–148. https://doi.org/10.1037/0021-9010.72.1.146

Sprecher, K. E., Riedner, B. A., Smith, R. F., Tononi, G., Davidson, R. J., & Benca, R. M. (2016). High resolution topography of age-related changes in non-rapid eye movement sleep electroencephalography. *PLoS ONE*, *11*(2). https://doi.org/10.1371/journal.pone.0149770

Taillard, J., Gronfier, C., Bioulac, S., Philip, P., & Sagaspe, P. (2021). Sleep in normal aging, homeostatic and circadian regulation and vulnerability to sleep deprivation. In *Brain Sciences* (Vol. 11, Issue 8). https://doi.org/10.3390/brainsci11081003

Takács, J., Bódizs, R., Ujma, P. P., Horváth, K., Rajna, P., & Harmat, L. (2016). Reliability and validity of the Hungarian version of the Pittsburgh Sleep Quality Index (PSQI-HUN): comparing psychiatric patients with control subjects. *Sleep and Breathing*, *20*(3), 1045–1051. https://doi.org/10.1007/s11325-016-1347-7

Tan, X., Campbell, I. G., & Feinberg, I. (2001). Internight reliability and benchmark values for computer analyses of non-rapid eye movement (NREM) and REM EEG in normal young adult and elderly subjects. *Clinical Neurophysiology*, *112*(8), 1540–1552. https://doi.org/10.1016/S1388-2457(01)00570-3

Tucker, A. M., Dinges, D. F., & Van Dongen, H. P. A. (2007). Trait interindividual differences in the sleep physiology of healthy young adults. *Journal of Sleep Research*, *16*(2), 170–180. https://doi.org/10.1111/j.1365-2869.2007.00594.x

Uchida, S., Atsumi, Y., & Kojima, T. (1994). Dynamic relationships between sleep spindles and delta waves during a NREM period. *Brain Research Bulletin*, *33*(3). https://doi.org/10.1016/0361-9230(94)90205-4

Uchida, S., Maloney, T., & Feinberg, I. (1992). Beta (20-28 Hz) and delta (0.3-3 Hz) EEGs oscillate reciprocally across NREM and REM sleep. *Sleep*, *15*(4), 352–358. https://doi.org/10.1093/sleep/15.4.352

Uchida, S., Maloney, T., March, J. D., Azari, R., & Feinberg, I. (1991). Sigma (12-15 Hz) and Delta (0.3-3 Hz) EEG oscillate reciprocally within NREM sleep. *Brain Research Bulletin*, *27*(1). https://doi.org/10.1016/0361-9230(91)90286-S

Ujma, P. P. (2021). Sleep spindles and general cognitive ability – A meta-analysis. *Sleep Spindles & Cortical Up States*, *2*(1), 1–17. https://doi.org/10.1556/2053.2.2018.01

Ujma, P. P., Bódizs, R., & Dresler, M. (2020). Sleep and intelligence: critical review and future directions. In *Current Opinion in Behavioral Sciences* (Vol. 33, pp. 109–117). https://doi.org/10.1016/j.cobeha.2020.01.009

Ujma, P. P., Konrad, B. N., Genzel, L., Bleifuss, A., Simor, P., Pótári, A., Körmendi, J., Gombos, F., Steiger, A., Bódizs, R., & Dresler, M. (2014). Sleep spindles and intelligence: Evidence for a sexual Dimorphism. *Journal of Neuroscience*, *34*(49), 16358–16368. https://doi.org/10.1523/JNEUROSCI.1857-14.2014

Ujma, P. P., Konrad, B. N., Gombos, F., Simor, P., Pótári, A., Genzel, L., Pawlowski, M., Steiger, A., Bódizs, R., & Dresler, M. (2017). The sleep EEG spectrum is a sexually dimorphic marker of general intelligence. *Scientific Reports*, *7*(1). https://doi.org/10.1038/s41598-017-18124-0

Voytek, B., Kramer, M. A., Case, J., Lepage, K. Q., Tempesta, Z. R., Knight, R. T., & Gazzaley, A. (2015). Age-related changes in 1/f neural electrophysiological noise. *Journal of Neuroscience*, *35*(38), 13257–13265. https://doi.org/10.1523/JNEUROSCI.2332-14.2015

Vyazovskiy, V. V., Olcese, U., Hanlon, E. C., Nir, Y., Cirelli, C., & Tononi, G. (2011). Local sleep in awake rats. *Nature*, *472*(7344), 443–447. https://doi.org/10.1038/nature10009

Waschke, L., Donoghue, T., Fiedler, L., Smith, S., Garrett, D. D., Voytek, B., & Obleser, J. (2021). Modality-specific tracking of attention and sensory statistics in the human electrophysiological spectral exponent. *ELife*, *10*.

https://doi.org/10.7554/eLife.70068

Waters, F., Chiu, V., Atkinson, A., & Blom, J. D. (2018). Severe sleep deprivation causes hallucinations and a gradual progression toward psychosis with increasing time awake. In *Frontiers in Psychiatry* (Vol. 9, Issue JUL). https://doi.org/10.3389/fpsyt.2018.00303

Webb, W. B., & Agnew, H. W. (1967). Sleep Cycling Within Twenty-Four Hour Periods. *Journal of Experimental Psychology*, *74*(2 PART 1), 158–160. https://doi.org/10.1037/h0024564

Webb, W. B., & Agnew, H. W. (1971). Stage 4 sleep: Influence of time course variables. *Science*, *174*(4016), 1354–1356. https://doi.org/10.1126/science.174.4016.1354

Wei, H. G., Riel, E., Czeisler, C. A., & Dijk, D. J. (1999). Attenuated amplitude of circadian and sleep-dependent modulation of electroencephalographic sleep spindle characteristics in elderly human subjects. *Neuroscience Letters*, *260*(1), 29–32. https://doi.org/10.1016/S0304-3940(98)00851-9

Wen, H., & Liu, Z. (2016). Separating Fractal and Oscillatory Components in the Power Spectrum of Neurophysiological Signal. *Brain Topography*, *29*(1), 13–26. https://doi.org/10.1007/s10548-015-0448-0

Werth, E., Achermann, P., & Borbély, A. A. (1997). Brain topography of the human sleep EEG: Antero-posterior shifts of spectral power. *NeuroReport*, *8*(1), 123–127. https://doi.org/10.1097/00001756-199612200-00025

Werth, E., Achermann, P., Dijk, D. J., & Borbély, A. A. (1997). Spindle frequency activity in the sleep EEG: Individual differences and topographic distribution. *Electroencephalography and Clinical Neurophysiology*, *103*(5), 535–542. https://doi.org/10.1016/S0013-4694(97)00070-9

Williams, H. L., Hammack, J. T., Daly, R. L., Dement, W. C., & Lubin, A. (1964). Responses to auditory stimulation, sleep loss and the EEG stages of sleep. *Electroencephalography and Clinical Neurophysiology*, *16*(3), 269–279. https://doi.org/10.1016/0013-4694(64)90109-9

Zhang, Y., Wang, Y., Cheng, H., Yan, F., Li, D., Song, D., Wang, Q., & Huang, L. (2023). EEG spectral slope: A reliable indicator for continuous evaluation of consciousness levels during propofol anesthesia. *NeuroImage*, *283*. https://doi.org/10.1016/j.neuroimage.2023.120426

9. Bibliography of the candidate's publications

9.1. Publications constituting the present thesis

Bódizs, R., Szalárdy, O., **Horváth, C.**, Ujma, P. P., Gombos, F., Simor, P., Pótári, A., Zeising, M., Steiger, A., & Dresler, M. (2021). A set of composite, non-redundant EEG measures of NREM sleep based on the power law scaling of the Fourier spectrum. *Scientific Reports*, *11*(1), 2041. https://doi.org/10.1038/s41598-021-81230-7

G. Horváth, C., Szalárdy, O., Ujma, P. P., Simor, P., Gombos, F., Kovács, I., Dresler, M., Bódizs, R., Horváth, C. G., Szalárdy, O., Ujma, P. P., Simor, P., Gombos, F., Kovács, I., Dresler, M., & Bódizs, R. (2022). Overnight dynamics in scale-free and oscillatory spectral parameters of NREM sleep EEG. *Scientific Reports*, *12*(1), 18409. https://doi.org/10.1038/s41598-022-23033-y

G. Horváth, C., & Bódizs, R. (2025). Effect of sleep deprivation on fractal and oscillatory spectral measures of the sleep EEG: A window on basic regulatory processes. *NeuroImage*, *314*. https://doi.org/10.1016/j.neuroimage.2025.121260

9.2. Other publications by the candidate

Bódizs, R., **Horváth, C. G.**, Szalárdy, O., Ujma, P. P., Simor, P., Gombos, F., Kovács, I., Genzel, L., & Dresler, M. (2022). Sleep-spindle frequency: Overnight dynamics, afternoon nap effects, and possible circadian modulation. Journal of Sleep Research, 31(3), 1–13. https://doi.org/10.1111/jsr.13514

Bódizs, R., Schneider, B., Ujma, P. P., **Horváth, C. G.**, Dresler, M., & Rosenblum, Y. (2024). Fundamentals of sleep regulation: Model and benchmark values for fractal and oscillatory neurodynamics. In Progress in Neurobiology (Vol. 234). https://doi.org/10.1016/j.pneurobio.2024.102589

G. Horváth, C., & Bódizs, R. (2024). Association of actigraphy-derived circadian phase indicators with the nadir of spindle frequency. Biological Rhythm Research, 55(1),16–29. https://doi.org/10.1080/09291016.2023.2283656

G. Horváth, C., Schneider, B., Rozner, B., Koczur, M., & Bódizs, R. (2025). Interrelationships between sleep quality, circadian phase and rapid eye movement

sleep: Deriving chronotype from sleep architecture. Behavior Research Methods, 57(5), 150. https://doi.org/10.3758/s13428-025-02671-w

Maczák, B., **Horváth, C. G.,** Bódizs, R., & Vadai, G. (2023). Revealing the Generality of 1/f Noise Based Spectral Characteristics of Human Activity Across Different Datasets. 2023 International Conference on Noise and Fluctuations (ICNF), 1–4. https://doi.org/10.1109/ICNF57520.2023.10472765

Rosenblum, Y., Esfahani, M. J., Adelhöfer, N., Zerr, P., Furrer, M., Huber, R., Steiger, A., Zeising, M., **G. Horváth, C.**, Schneider, B., Bódizs, R., & Dresler, M. (2023). Fractal cycles of sleep: a new aperiodic activity-based definition of sleep cycles. BioRxiv, 2023.07.04.547323. https://doi.org/10.1101/2023.07.04.547323

Ujma, P. P., **Horváth, C. G.**, & Bódizs, R. (2023). Daily rhythms, light exposure and social jetlag correlate with demographic characteristics and health in a nationally representative survey. Scientific Reports, 13(1). https://doi.org/10.1038/s41598-023-39011-x

10. Acknowledgements

First and foremost, I would like to thank my supervisor, *Róbert Bódizs* for his invaluable guidance, expert insights, and continuous support throughout my work.

I would also like to thank the first reviewer, *Péter Simor,* for his valuable comments and constructive suggestions, which greatly contributed to improving the quality of this thesis.

Special thanks go to *Melinda Becske* for assisting with data collection, to *Zoé Vulgarasz* for significantly contributing to the participant recruitment for my study, and to *Bence Schneider* for his collaboration and the exchange of ideas throughout our PhD years.

I also want to thank my PhD colleagues, *Blanka Vojnits* and *Tárek Magyar*, as well as members of the *Psychophysiology and Chronobiology Research Group* for our collaborative work, and to my co-authors for their valuable feedback and contributions.

I also owe sincere thanks to *György Petercsák*, whose timely technical assistance made it possible to recover my work when it appeared to be irretrievably lost.

I would like to thank my *family*, especially my *parents* for showing me the value of hard work, perseverance, and dedication.

Last but not least, I am deeply grateful to my *husband* for everything.

scientific reports

Check for updates

OPEN

A set of composite, non-redundant EEG measures of NREM sleep based on the power law scaling of the Fourier spectrum

Róbert Bódizs[1,2]✉, Orsolya Szalárdy[1,3], Csenge Horváth[1], Péter P. Ujma[1,2], Ferenc Gombos[4,5], Péter Simor[1,6,7], Adrián Pótári[5,8], Marcel Zeising[9,10], Axel Steiger[9] & Martin Dresler[11]

Features of sleep were shown to reflect aging, typical sex differences and cognitive abilities of humans. However, these measures are characterized by redundancy and arbitrariness. Our present approach relies on the assumptions that the spontaneous human brain activity as reflected by the scalp-derived electroencephalogram (EEG) during non-rapid eye movement (NREM) sleep is characterized by arrhythmic, scale-free properties and is based on the power law scaling of the Fourier spectra with the additional consideration of the rhythmic, oscillatory waves at specific frequencies, including sleep spindles. Measures derived are the spectral intercept and slope, as well as the maximal spectral peak amplitude and frequency in the sleep spindle range, effectively reducing 191 spectral measures to 4, which were efficient in characterizing known age-effects, sex-differences and cognitive correlates of sleep EEG. Future clinical and basic studies are supposed to be significantly empowered by the efficient data reduction provided by our approach.

The frequency characteristics of sleep-dependent neuronal oscillations as recorded by scalp EEG are increasingly recognized as potent markers of aging[1–3], health and disease[4], typical and atypical development and maturation[5,6], as well as of neurocognitive features of high practical relevance[7–9]. However, many of these studies are suffering from increased susceptibility to Type I error as a result of an inherently increased level of "researcher degrees of freedom". That is, EEG data can be analysed in almost infinite different ways, by focusing on one or another specific electrophysiological phenomenon[9,10]. Instead of focusing on multiple frequencies or phenomena, our aim is to provide an overall characterization of the broadband NREM sleep EEG. Our data-driven approach is based on the statistical properties of the signal, in order to assess the intercept and the slope, as well as the most prominent/important spectral peak of the Fourier spectrum.

Evidence suggests the linear relationship between the logarithmic amplitude or power of EEG and the logarithm of frequency[11–13]. Such power law scaling is a general, state-independent feature of cortical EEG, suggesting that the Fourier spectrum can be reliably described by an approximation of the parameters of the following function:

$$P(f) = Cf^{\alpha} \quad (1)$$

where P is power ($P \geq 0$) as a function of frequency ($0 \leq f \leq f_{Nyquist}$), C is the constant (or the intercept) expressing the overall, frequency-independent EEG amplitude ($C > 0$), whereas α is the spectral exponent indicating the

[1]Institute of Behavioural Sciences, Semmelweis University, Budapest, Hungary. [2]Epilepsy Center, National Institute of Clinical Neurosciences, Budapest, Hungary. [3]Institute of Cognitive Neuroscience and Psychology, Research Centre for Natural Sciences, Budapest, Hungary. [4]Department of General Psychology, Pázmány Péter Catholic University, Budapest, Hungary. [5]MTA-PPKE Adolescent Development Research Group, Budapest, Hungary. [6]Institute of Psychology, ELTE, Eötvös Loránd University, Budapest, Hungary. [7]UR2NF, Neuropsychology and Functional Neuroimaging Research Unit At CRCN - Center for Research in Cognition and Neurosciences and UNI - ULB Neurosciences Institute, Université Libre de Bruxelles (ULB), Brussels, Belgium. [8]Doctoral School of Psychology (Cognitive Science), Budapest University of Technology and Economics, Budapest, Hungary. [9]Max Planck Institute of Psychiatry, Research Group Sleep Endocrinology, Munich, Germany. [10]Centre of Mental Health, Klinikum Ingolstadt, Ingolstadt, Germany. [11]Donders Institute for Brain, Cognition and Behaviour, Radboud University Medical Center, Nijmegen, The Netherlands. ✉email: bodizs.robert@med.semmelweis-univ.hu

decay rate (slope) of power as a function of frequency. Reported values for the spectral exponent are $-4 < \alpha < -1$, with lower values indicating lower arousal/(deeper) sleep[14,15,18]. That is, instead of providing 191 values for the power spectra of 0.5–48 Hz activity in bins of 0.25 Hz, the background slope of the spectrum of scale-free activity can be characterized just by two parameters (C and α). Most notably, if reliable, this function suggests that classical bandwise or binwise spectral analyses are not considering the frequency-determined nature of power values when applying statistical tests focusing on specific oscillatory phenomena. Similar views were expressed and successfully implemented for the analysis of various time series characterizing the power law scaling of brain activity in humans, some of them emphasizing the conceptual and methodological aspects[12–14,19–23], while others focusing on sleep cycle effects, arousal and consciousness[15,16,24], but none of them specifically targeting the issue of interindividual differences. In addition, available reports do not consider the constant (C) or the intercept as a variable of interest in describing sleep–wake EEG features.

Besides the spectral slope and the constant, there are further specific features of the EEG spectrum, known as spectral peaks[12,19], which are upward deflections in the decreasing power law trend described by function (1) above. Peaks reflect oscillatory activities of specific frequencies[25], which might prevent the reliable estimation of α if they are not considered[24,26]. In order to deliberately describe the power spectrum by taking into account its prominent peaks, we suggest the inclusion of a peak power function in the formula as follows:

$$P(f) = Cf^{\alpha} P_{Peak}(f) \quad (2)$$

Peak power (P_{Peak}) at frequency f equals 1 if there is no peak and is larger than 1 if there is a spectral peak at that frequency. Thus, the number of parameters is increased by considering spectral peaks, but is still lower than the values included in the original spectra, as putative "no peak regions" can be compressed in series of all ones. It has to be noted, that $P_{Peak}(f)$ is a whitened power measure, because it is characterized by roughly equal power along the frequency axis and is thus statistically independent from the spectral slope (α) and intercept (C), which constitute the colored-noise or power-law noise part of the spectrum, characterized by an exponential decrease of power with increasing frequencies (Fig. 1). Although it is known that most subjects might have several peaks in their NREM sleep EEG spectra and the peak that is greatest can vary between individuals and recording locations, in the following we only consider the maximal peak in the 9–18 Hz range, emerging at a specific $f_{maxPeak}$ frequency, with an amplitude exceeding all other potential peak amplitudes ($P_{Peak}(f_{maxPeak}) > P_{Peak}(f)$ for any $9 < f < 18$). No multiple peaks are analysed in this report.

As a proof of concept, we apply these measures on a large sleep EEG dataset with previously demonstrated effects of age, sex, and general intelligence. The issue of individual differences in NREM sleep was not explicitly addressed in former reports on spectral parameters of power law scaled sleep EEG[15,16], with the exception of a report focusing exclusively on whitened spectral peak sizes in the spindle range[27]. Our intention is to fill this gap and broaden the validity of the power law scaling-type of spectral EEG parameters, as well as to provide a set of non-redundant measures of individual differences in NREM sleep EEG.

Age was reported to correlate negatively with NREM sleep EEG slow wave activity, but positively with high frequency activity in healthy adult subjects[28]. In addition, steeper spectral slopes of wakefulness and NREM sleep-derived EEG were found in young as compared to older subjects[11,22].

Thus, we hypothesize (H1) that the slope of the Fast Fourier Transformation (FFT)-based spectrum of NREM sleep EEG is characterized by age-dependent flattening (α closer to 0). In addition, aging was shown to be associated with decreased sleep spindle activity[29,30], thus we hypothesize (H2) a negative correlation between age and spectral peak amplitude as measured by $P_{Peak}(f_{maxPeak})$ value. In addition to decreased spindle activity, the increase in intra-spindle oscillatory frequency (Hz) was shown to be a characteristic feature of aging according to some[29,31], but not all[30] reports. As a consequence, we hypothesize (H3) that maximal spectral peak amplitudes in the spindle range emerge at higher $f_{maxPeak}$ values in aged, as compared to young subjects.

Reported sex differences in NREM and REM sleep EEG indicate higher spectral power in several frequency bands in women, as compared to men[28,32]. Such broad band and state-independent differences suggest a general tendency for a higher EEG amplitude in women, due to a contamination with non-neuronal factors, like skull thickness and bone mineral density[32,33]. As a consequence, we hypothesize (H4) that women are characterized by higher spectral intercepts, than men ($C_{♀} > C_{♂}$). Furthermore, we will reanalyze some of the reported sex differences in sleep spindle density/power, indicating increased sleep spindling in women as compared to men[28,32,34,36], by relying on whitened spectral peak amplitudes of the spindle range ($P_{Peak}(f_{maxPeak})$), the latter being a measure which is independent of overall EEG-amplitude (C).

Based on a largely overlapping dataset, formerly we reported another sex difference in terms of sleep spindle frequency: women were shown to be characterized by higher oscillatory frequencies as compared to men[36]. Thus, our explicit intention is to provide convergent validity of the present method, by testing the following hypothesis (H5): maximal spectral peaks occur at higher frequencies in women as compared to men ($f_{maxPeak♀} > f_{maxPeak♂}$).

Intelligence was shown to correlate positively with NREM sleep EEG sleep spindle activity[7]. Although, a recent metaanalysis casts doubt on the sexual dimorphism of this relationship[9], the dataset we analyse in our current report is characterized by a clear difference among women and men: women were characterized by positive correlation between sleep spindle amplitude/power and IQ, whereas null correlations were reported for men[8,36]. As our current analyses are based on the same dataset, we aim to provide convergent validity of our current method by testing the hypothesis (H6): $P_{Peak}(f_{maxPeak})$ values of the sleep spindle range (9–18 Hz) correlate positively with IQ in women, but not in men. Intelligence was also reported to modulate the relationship between the decrease in NREM sleep EEG slow activity associated with aging: participants showing average IQ (AIQ) scores were characterized by significant negative correlations regarding age vs. slow wave activity, whereas no such correlations were found in individuals with high IQ (HIQ) in an overlapping sample[1]. As the original report provided overwhelming evidence for an age vs relative delta power correlation as being modulated by IQ range, whereas

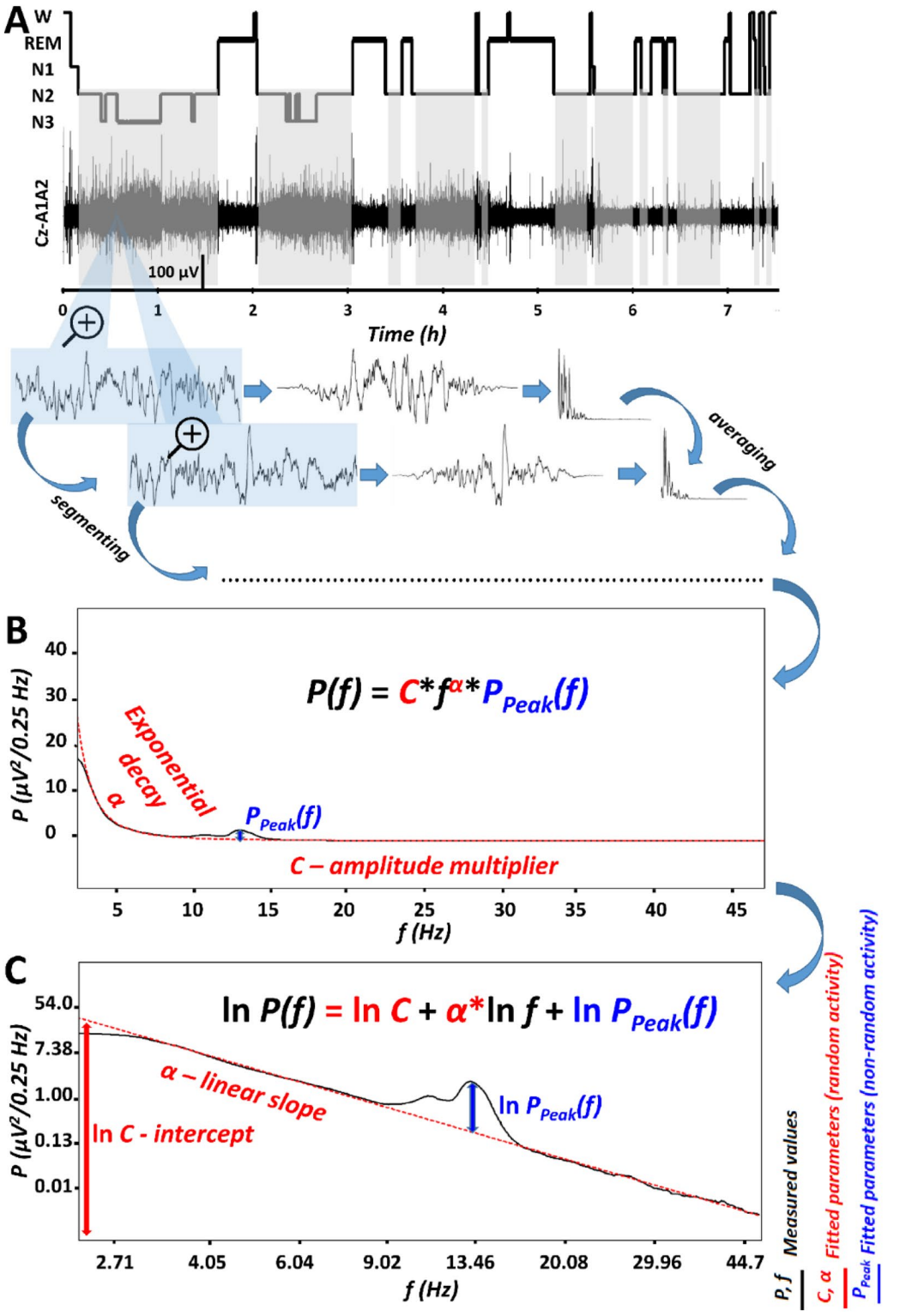

Figure 1. The parametrization of non-rapid eye movement (NREM) sleep electroencephalogram (EEG) spectra. (**A**) Hypnogram and steps of the spectral EEG analyses as exemplified in a representative record of a young male volunteer. Grey shaded areas represent NREM sleep, which is analysed in the present report. Blue-shaded EEG segments are magnified 4 s long epochs, with 2 s overlap and modified with a Hanning window before power spectral analysis via mixed-radix Fast Fourier Transformation (FFT). (**B**) Average spectral power (P) is characterized by a frequency (f)-dependent exponential decay (α), as well as by an overall, frequency-independent amplitude multiplier (C) and a peak power multiplier at critical frequencies [$P_{Peak}(f)$]. (**C**) The natural logarithm of spectral power (P) is a linear function of the natural logarithm of frequency (f), characterized by a linear slope α (which is equal with α in panel **B**) and an intercept (the latter being the natural logarithm of the amplitude multiplier, C in panel **B**). In addition, this linear function has to be summed with the natural logarithm of the peak power multiplier [$P_{Peak}(f)$, equal to the same frequency-dependent function in panel **B**]. Please note that "no peak regions" can be compressed in series of all ones, resulting in reduced number of variables as compared to the bins in the original spectra.

weaker evidence was found for absolute power[1], we do not know if this finding reflects the age-dependency of slow wave activity per se, or the combined age-dependency of slow wave activity and slow/high activity ratio. The former scenario would fit with a null effect for IQ-modulation of age vs spectral slope correlation, whereas the latter would lead to an IQ-dependence of age vs spectral slope relationship (H7).

Results

Goodness of fit: Is the logarithm of spectral power a linear function of the logarithm of frequency? NREM sleep EEG spectra of 175 healthy subjects (81 females, age range 17–60 years), with a maximum of 18 available (artefact-free) common recording locations were included in our analyses. Linears were fitted to the equidistant log–log plots of the EEG power spectra below 48 Hz, excluding the 0–2 and the 6–18 Hz range, both known to be characterized by spectral peaks (slow oscillation and spindles) in NREM sleep (Fig. 1, see details in section "Methods"). The sample mean of fitted slopes ($\overline{\alpha}$) varied between − 2.73 (SD = 0.22) and − 2.33 (SD = 0.22) for the frontocentral (Fz) and left posterior temporal (T5) region, respectively. In turn, the sample mean of the intercepts ($\overline{\ln\ C}$) varied between 3.74 (SD = 0.73) and 5.76 (SD = 0.69) for recording locations T5 and Fz, respectively (Suppl. table 1). Goodness of fit (R^2) of the linear model of the equidistant 2–6 and 18–48 Hz spectral data varied in the range of 0.8955–0.9997 across subjects and EEG recording locatios. The square of the Fisher Z-transformed, averaged and back-transformed Pearson correlations between the fitted linear and the spectral data is $\overline{R}^2 = 0.9952$ (SD = 0.1578).

Here we claim that the spectral slope (α) and the intercept (ln C) carry meaningful information. In order to demonstrate that the present method of determining slope and intercept is comparable with existing methods, we tested these parameters against the respective outputs of a recently published method termed fitting oscillations & one over f (FOOOF)[23]. Our spectral slopes and intercepts correlated significantly with FOOOF slopes and intercepts, respectively. Mean correlation (Fisher-transformed, averaged and back-transformed) over recording locations was r = 0.90 for spectral slopes and r = 0.92 for intercepts (see Suppl. Figure 1).

Spectral peaks in the 9–18 Hz range. Spectral peaks in the alpha/sigma range were determined by a combination of the first and the second derivative tests indicating local maxima in mathematical terms (see details in section "Methods"). Detected peaks were ranked according to their whitened amplitude (coloured noise characterized by the spectral slope (α) and intercept (C) was removed before ranking). At least one peak was detected in 81.16–100% of the subjects, depending on recording location (relatively lower values were found in the temporal locations T3, and T4, whereas above 90% was the rule for other regions, see details in Suppl. Table 2). Spectral peaks with maximal amplitudes in the 9–18 Hz range were found to conform the overall topography vs frequency relationship of sleep spindles. That is, anterior spectral peaks were slower than the posterior ones (Suppl. Figure 2). The total antero-posterior frequency increase of maximal spectral peaks in the 9–18 Hz range ($f_{maxPeak}$) equalled 1.99 Hz (sample mean). However, the above change was largely non-continuous along the antero-posterior cortical axis, as more than 83% (1.67 Hz) of the upward shift in spectral peak frequency emerged in a single, maximal value characterizing the frontal to central (54.77% of the subjects), frontopolar to frontal (36.94%), central to parietal (6.36%) or parietal to occipital (1.91%) shifts. Spectral peak frequencies ($f_{maxPeak}$) which were detected rostral to the maximal antero-posterior upward frequency shift are hypothesized to reflect slow sleep spindles (100% of frontopolar, 63.05% of frontal, 8.28% of central, 1.91% of parietal and 0% of occipital recording sites), whereas the caudal ones are reflections of putative fast sleep spindles (0, 36.95, 91.72, 98.09, and 100% of frontopolar, frontal, central, parietal and occipital regions, respectively) (Fig. 2).

A second spectral peak with roughly half of the amplitude of the first was detected in a subgroup of subjects/EEG recording locations (6.29–50.64%) (Suppl. Table 2). However, in most of the cases the second peaks were roughly 1.5 Hz slower than the reported slow sleep spindle frequencies in an overlapping sample[36], thus it seems that these peaks reflected rather alpha activity (~ 10 Hz) instead of true slow or fast sleep spindles (see also Suppl. Figure 2). That is the method used in the present study was robust enough in terms of the reliable detection of the dominant spectral peak of sleep spindling in the given location, but not sufficiently sensitive in testing the non-dominant sleep spindle peaks (fast spindles in the anterior and slow spindles in the posterior locations, see Suppl. Table 2 for details). A third peak was only detected in a few instances (between 1 and 6 cases, depending on recording locations, data not shown). Given the fact that we only focus on the maximal spectral peak parameters in the following parts of our paper, we can conclude that these parameters reflect the prevailing anterior slow and the posterior fast spindles, depending on recording location. However, the anatomical boundary between prevailing anterior slow and posterior fast sleep spindles varies among subjects, leading to some uncertainty in the frontal leads, which can express both slow and fast sleep spindles (in 63.05% and 36.95% of the cases, respectively).

H1: Age-associated flattening of spectral slope. Positive association between age (years) and NREM sleep EEG spectral exponents (α), indicating age-associated flattening of slopes were found at all recording locations (Suppl. Table 3a). The Rüger's area (consisting of spatially contingent recording locations characterized by uncorrected significances) including all recording locations in this specific case, proved to be significant at both of the new critical probability (p) levels (0.025 and 0.017). Thus, based on the Descriptive Data Analysis (DDA, see details in section "Methods") procedure[37,38], this area can be considered as a significant one (see also Fig. 3A).

H2: Age-dependent decrease in spectral peak amplitude. Maximal whitened spectral peak amplitudes of NREM sleep EEG spindle frequencies ($P_{Peak}(f_{maxPeak})$) and age correlated negatively at 10 recording locations covering the frontocentral, parietal and posterior temporal areas (F3, F4, Fz, C3, Cz, C4, T5, T6, P3,

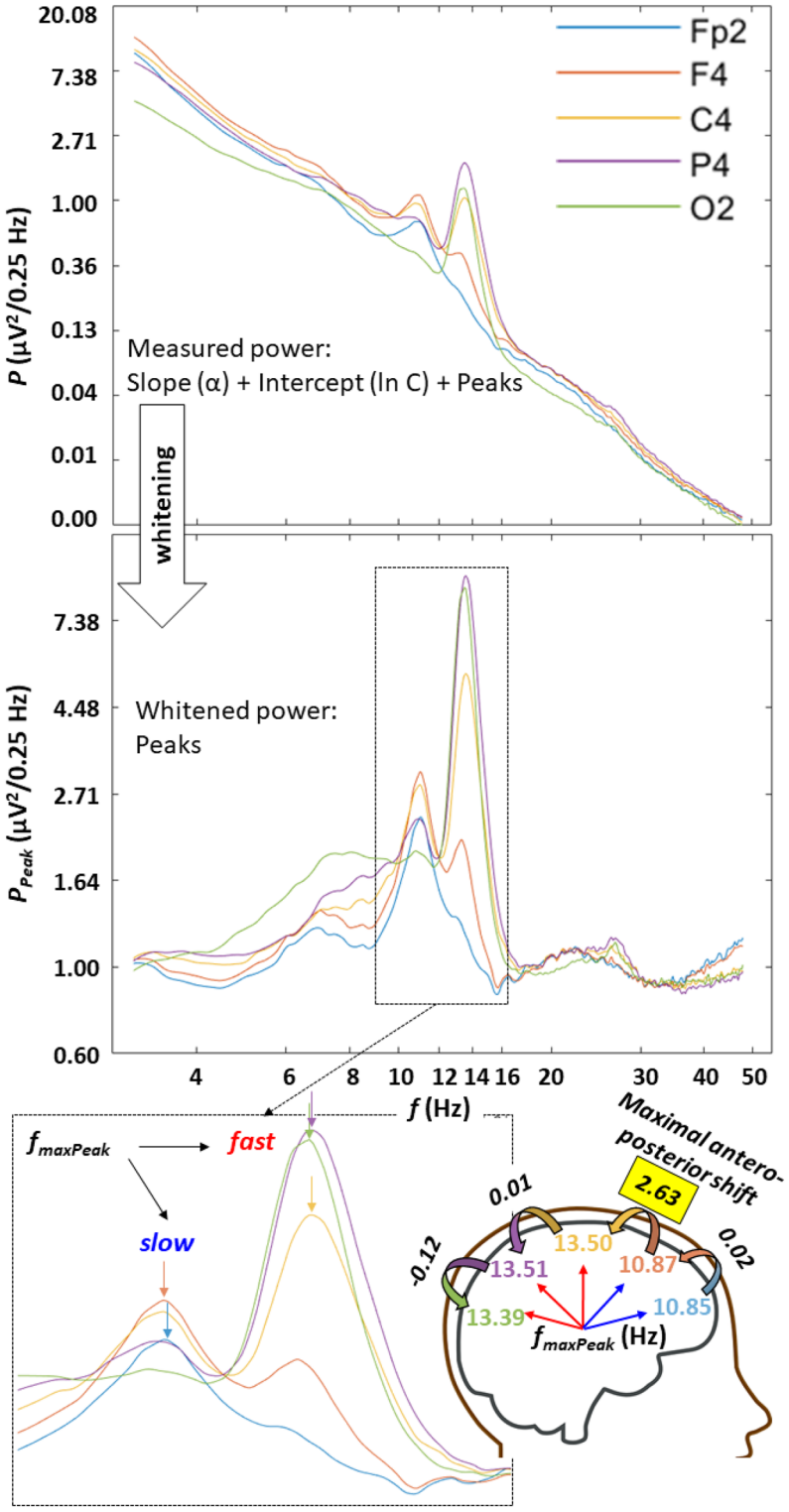

Figure 2. Examples for spectral peaks over the antero-posterior cortical axis in one of the subjects. Upper part: periodograms in the double natural logarithmic plane characterized by a combination of linear trends and spectral peaks. Middle panel: whitened power by subtracting the fitted linears: ln P – (ln C + α ln f); note the uniform baseline power (~ 1) and the spectral peaks. Lower panel: enlarged spectral peaks in the spindle frequency range, characterized by lower frequency maxima in the anterior as compared to the posterior recording locations (see colour-coded arrows); maximal antero-posterior shifts in peak frequency emerged between the frontal and central recording sites, demarcating slow-anterior and fast-posterior sleep spindle-related spectral peaks.

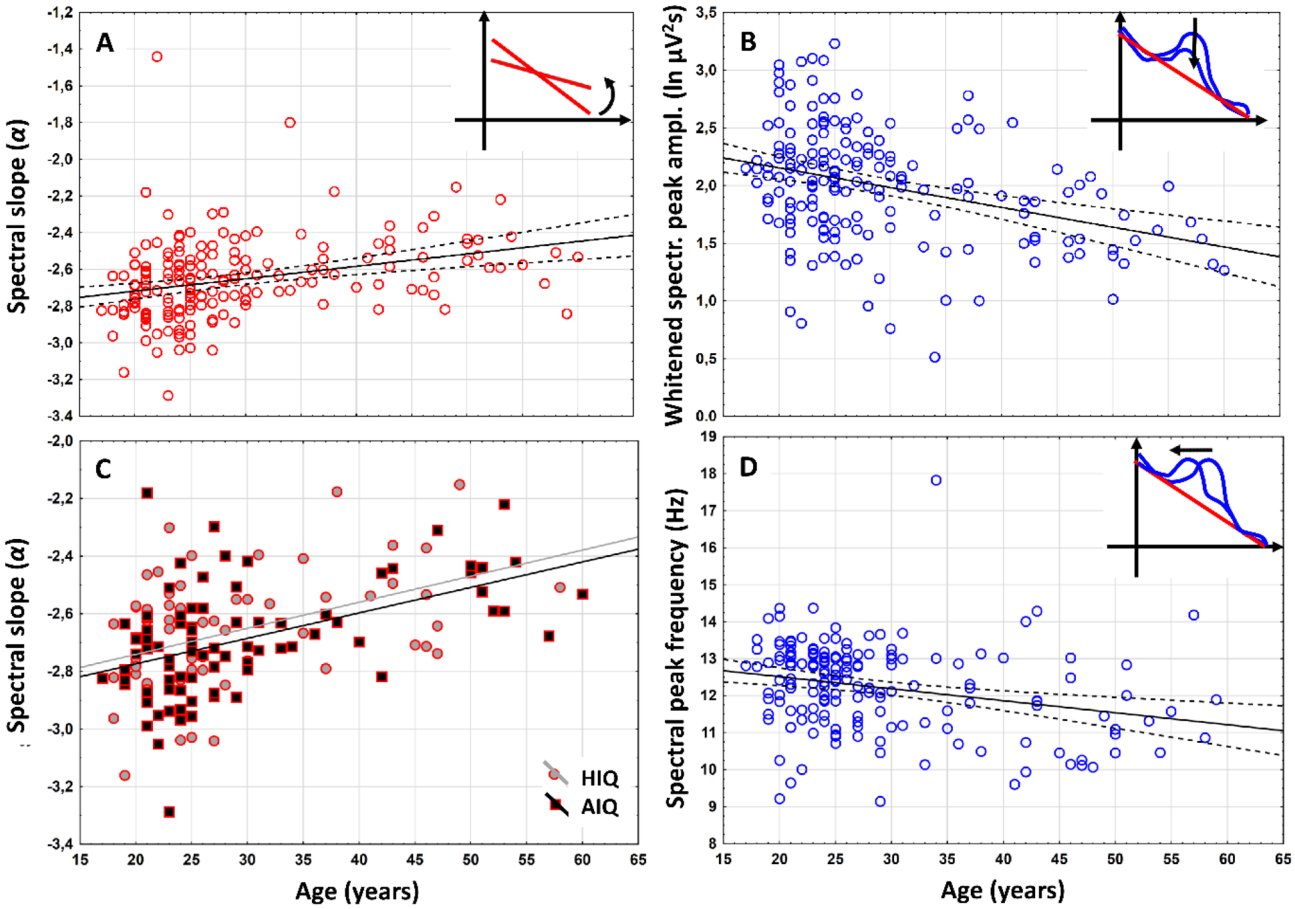

Figure 3. Representative scatterplots of the correlations between age and measures of the NREM sleep EEG spectra at the left prefrontal region (F3). (**A**) Correlation of age with the spectral exponent (α) indicating the flattening of the spectral slope in the aged subjects. (**B**) Correlations of age with the whitened maximal spectral peak amplitude in the sleep spindle frequency range ($P_{Peak}(f_{maxPeak})$. Note the decrease in whitened spectral peak amplitude in the aged. (**C**) Correlation of age with the NREM sleep EEG spectral exponent (α) as categorized by intelligence (*HIQ* high intelligence quotient, *AIQ* average intelligence quotient). Note the lack of an IQ effect. (**D**) Correlation of age with NREM sleep EEG maximal spectral peak frequency ($f_{maxPeak}$) in the spindle range. Note the age-dependent decline in frequency. Color codes are consistent with Fig. 1: red—spectral slopes, blue—spectral peaks.

and P4). The above region remained significant after the control of multiple testing (see a representative example in Fig. 3B).

H3: No age-related increase in spectral peak frequency was found. Maximal sleep spindle spectral peak emerge at lower $f_{maxPeak}$ values in the frontal region of aged, as compared to young subjects. This finding evidently contrasts our prediction. Peak frequency and age correlated negatively at 8 recording locations covering the frontal and the right temporal areas (Fp1, Fp2, F3, F4, Fz, F7, F8 and T4). This Rüger's area was significant, as all correlations conformed to both of the new critical probabilities (Fig. 3D; Suppl. Table 3c).

In order to test if changes in slow/fast spindle peak sizes could underlie these effects, that is if the maximal spindle peak "jumps" from the fast to the slow spindle peak more frequently in frontal recording sites of aged individuals, we compared the age of the following groups of subjects. Group F-Fp was characterized by a maximal antero-posterior frequency increase of $f_{maxPeak}$ between the frontopolar and frontal recording sites, whereas for the C-F group this frequency shift was measured between the frontal and the central region. Mann–Whitney U-test revealed higher age in the C-F, as compared to the F-Fp group ($U = -2.41$; $\eta^2 = 0.713$; $p = 0.015$). That is the age-associated dampening of $f_{maxPeak}$ might indicate a decrease in the emergence of fast sleep spindles in the frontal region in aged subjects.

H4: Spectral intercepts, but not peak amplitudes are higher in women as compared to men. The spectral intercept is the power value at which the spectral slope crosses the y-axis. Women are characterized by significantly higher spectral intercepts [the natural logarithm of *C* values in formula (1) and (2)] compared to men at all recording locations (see an example at location C4 as an example: Fig. 4).

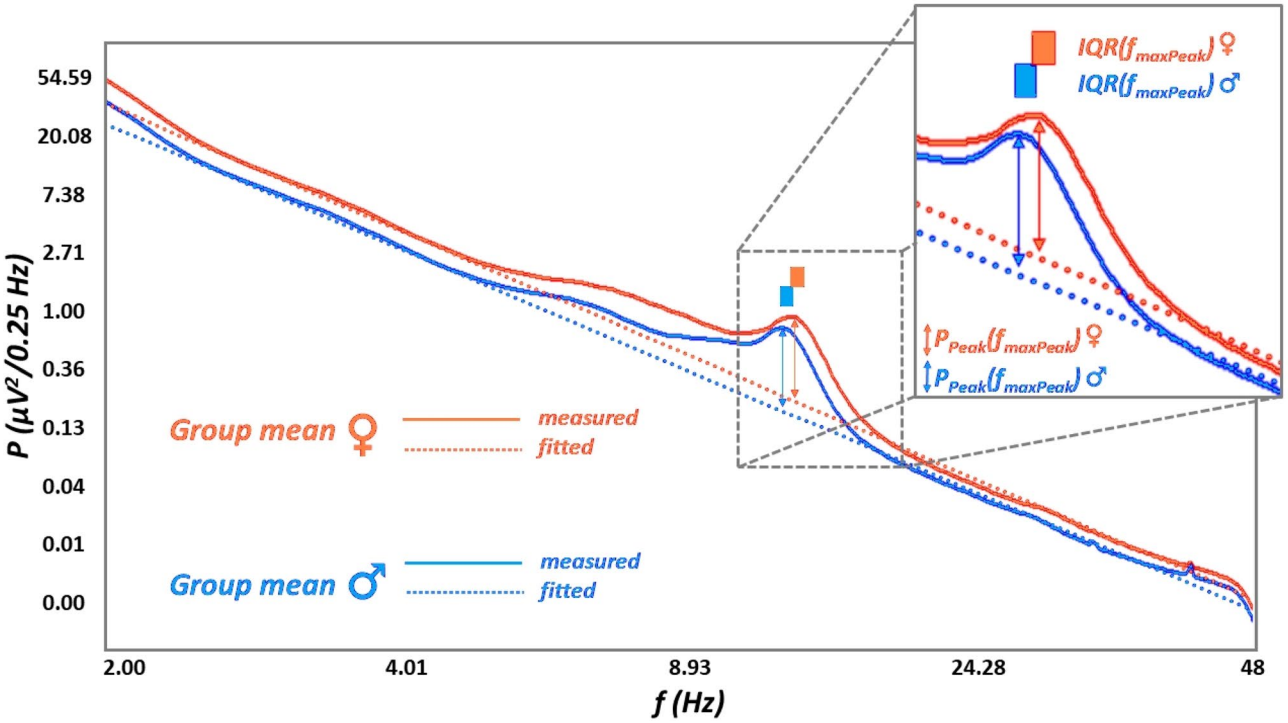

Figure 4. Women vs men differences in measured and parametrized mean NREM sleep EEG spectral power at electrode location C4. The natural logarithm of pectral power was averaged in women and men (continuous lines), as where individual fits (dotted lines) acoording to our current method (see details in section "Methods"). Note the overall amplitude differences (women > men), as well as the higher spectral peak frequencies ($f_{maxPeak}$) in women and the lack of differences in spectral peak amplitudes ($P_{Peak}(f_{maxPeak})$). *IQR* interquartile range.

After correction for multiple testing the Rüger-area remained significant (Suppl. table 4). As predicted women and men did not differ in NREM sleep EEG maximal spectral peak amplitudes of the spindle range ($P_{Peak}(f_{maxPeak})$) at any of the recording locations (Fig. 4; Suppl. table 4b).

H5: Women are characterized by faster sleep spindles. Women were characterized by significantly higher $f_{maxPeak}$ values as compared to men (Fig. 4), except temporal recording locations T3 and T4. The area remained significant after the correction for multiple testing (Table 1).

These findings might be confounded by the factor spindle type in the case if fast spindles are dominant in more anterior leads in females as compared to males. However, the analysis of the localization of the major antero-posterior frequency shift in $f_{maxPeak}$ of women and men did not reveal a significant difference ($\chi^2 = 0.42$; $p = 0.51$).

H6: IQ correlates positively with spectral peak amplitude in women. Pearson correlations revealed significant associations of whitened maximal spectral peak amplitudes ($P_{Peak}(f_{maxPeak})$) pertaining to NREM sleep EEG spindle activity with IQ at recording locations C3 (N = 67, r = 0.33, $p = 0.007$), C4 (N = 66, r = 0.34, $p = 0.005$), Cz (N = 55, r = 0.34, $p = 0.010$), P3 (N = 68, r = 0.26, $p = 0.031$), P4 (N = 68, r = 0.28, $p = 0.020$), and T3 (N = 45, r = 0.32, $p = 0.031$) in women (Fig. 5; Suppl. table 5). The Rüger area at this centroparietal-left temporal region remained significant after the control for multiple testing (4/6 correlations are significant at 0.05/2 and 3/6 correlations at 0.05/3). No significant correlations of whitened spectral peak amplitude and IQ were found in men.

H7: Do age-related flattenings of spectral slopes differ among subjects with average and high IQ? As already presented in the former subheadings (H1) an age-associated flattening of spectral slopes characterizes the NREM sleep EEG of adult volunteers. This effect was separately assessed in subjects with average and high IQ, and results were compared. Age and slopes of the NREM sleep EEG spectra (α) were significantly associated in both subgroups (AIQ and HIQ). We found no significant difference between these correlations, however (Table 2). That is, age-associated flattening of the slopes of the NREM sleep EEG spectra are independent of the subjects' IQ (Fig. 3C).

Overcoming model redundancy by determining the alternative intercept of the spectra. Although our model resulted in good fit with empirical data in terms of background (scale-free) activity and the majority of our hypotheses (including the ones regarding peak power features) were supported by parameters derived from Eq. (2), the spectral slope and the intercept are far from being independent in statistical

Recording location	U (η^2)	*p*	$N_{♀}$	$Md_{♀}$ $(Q1–Q3)_{♀}$	$N_{♂}$	$Md_{♂}$ $(Q1–Q3)_{♂}$	$Md_{♀}–Md_{♂}$
Fp1	1888 (.076)	***.001***	67	11.97 (11.36–12.45)	83	11.32 (10.87–11.93)	0.65
Fp2	1864 (.100)	***<.001***	68	12.00 (11.33–12.44)	87	11.29 (10.83–11.81)	0.71
F3	2191 (.095)	***<.001***	75	12.80 (12.10–13.25)	91	11.86 (11.14–12.86)	0.94
F4	2217 (.088)	***<.001***	76	12.98 (12.06–13.35)	89	11.80 (11.04–12.97)	1.18
Fz	2259 (.028)	*.041*	66	13.06 (11.75–13.41)	85	12.51 (11.10–13.13)	0.55
F7	1492 (.090)	***<.001***	59	12.23 (11.60–12.66)	78	11.59 (11.19–12.04)	0.64
F8	1608 (.088)	***<.000***	63	12.14 (11.53–12.59)	78	11.49 (11.13–12.14)	0.65
C3	2651 (.058)	***.002***	80	13.53 (13.20–13.96)	92	13.26 (12.86–13.59)	0.27
C4	2502 (.075)	***<.001***	79	13.60 (13.33–14.04)	93	13.28 (12.96–13.61)	0.32
Cz	1830 (.107)	***<.001***	68	13.68 (13.39–14.13)	87	13.33 (13.05–13.64)	0.35
P3	2290 (.118)	***<.001***	81	13.71 (13.38–14.12)	94	13.36 (13.03–13.68)	0.35
P4	2368 (.102)	***<.001***	81	13.70 (13.37–14.12)	93	13.38 (13.06–13.68)	0.32
T3	1829 (.002)	.635	55	12.80 (12.19–13.42)	70	12.91 (11.79–13.37)	−0.11
T4	1942 (.005)	.440	57	12.94 (12.14–13.39)	74	12.93 (11.65–13.29)	0.01
T5	1893 (.084)	***<.001***	68	13.62 (13.27–14.06)	84	13.32 (13.00–13.63)	0.27
T6	1730 (.108)	***<.001***	66	13.63 (13.35–14.11)	85	13.33 (12.97–13.62)	0.30
O1	2282 (.111)	***<.001***	80	13.65 (13.34–14.10)	93	13.33 (12.96–13.64)	0.32
O2	2253 (.112)	***<.001***	80	13.65 (13.33–14.12)	92	13.35 (12.99–13.64)	0.30

Table 1. Women vs men differences in NREM sleep EEG spindle spectral peak frequencies. Mann–Whitney U test indicates that women as compared to men are characterized by higher $f_{maxPeak}$ values at which spindle range $P_{Peak}(f)$ maxima emerge. The Rüger area containes 16 nominally significant effects. 15 of these women vs men differences were significant at both of the more stringent criteria ($p < .025$ and $p < .017$), which supports the significance of the area. Italic and bold italic values indicate statistical significance at $p < .05$, and $p < .017$, respectively. *Md* median.

terms. That is, although women vs men differences emerged in our spectral intercepts ($\ln C_{♀} > \ln C_{♂}$) as predicted in H4 (see Suppl. table 4), and no sex differences in NREM sleep EEG spectral slopes (α) were observed (Suppl. table 6a), the intercepts and the slopes are negatively correlated in our database (Suppl. table 6b): subjects with steeper spectral slopes (lower α exponents) are characterized by higher intercepts (apparently higher EEG amplitudes). This might reflect the position of the intercept, which is at $\ln f = 0$ ($f = 1$ Hz). The interpolated 1 Hz power (based on the fitted line in the double logarithmic plots) partially reflects the steepness of the slope of the spectrum.

In order to overcome the above issue of parameter-interdependency, we derived alternative intercepts with the aim of determining parts of the interpolated scale-free spectrum at which our parameter do not reflects the steepness of the slope (α). We based our search for this alternative intercept on two assumptions: (1) the alternative ("slope-free") intercept is situated at the border of low and high frequency activities, delineated by the reported sleep deprivation-induced increases and decreases of spectral power, respectively; (2) intercepts below the border mentioned in point 1. correlate negatively with the spectral slopes, whereas intercepts above this border correlate positively with slopes. Extended wakefulness of human adults is known to increase the NREM sleep EEG spectral power below the sleep spindle frequencies, that is the power of 1–9, 1–12 or 1–13 Hz according to different studies[39–43], whereas power above 10 or 13 Hz was shown to be decreased during recovery sleep[40,42,43]. Thus, we used our fitted model parameters α and $\ln C$, as well as the modified version of formula (3), with the last term ($\ln P_{Peak}(f)$) omitted (see "Methods") to determine the interpolated scale-free natural logarithm power $\ln P(f)$ at frequencies of $f = 7.4$, 10, 12.2, 13.5, 15 and 20 Hz corresponding to natural logarithm values of $\ln f = 2$, 2.3, 2.5, 2.6, 2.7, and 3, respectively. These alternative intercepts representing different scenarios of y-axis crosses (changing the position of the y-axis) were tested for their independence from the slopes (α) by

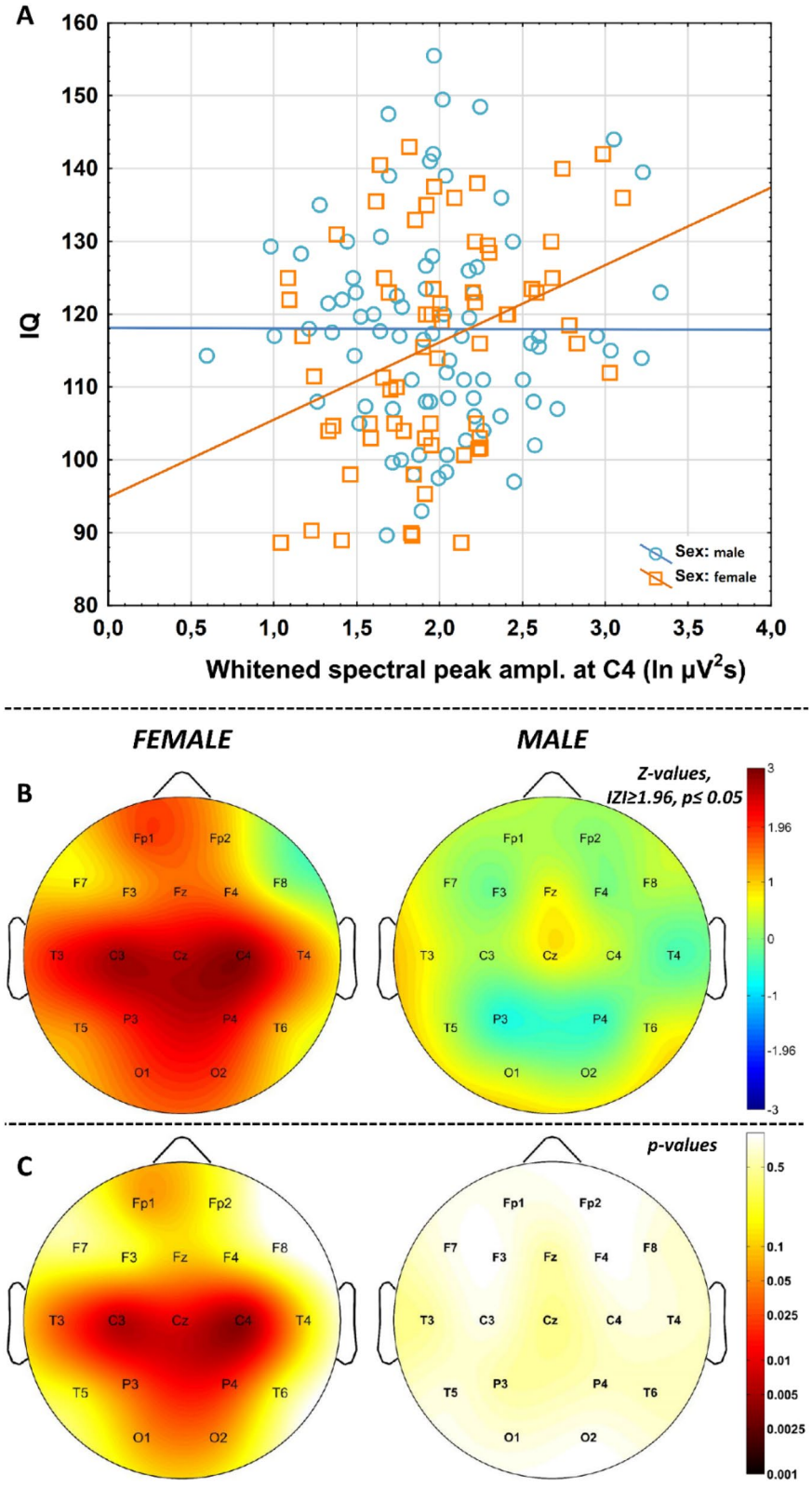

Figure 5. Correlations between NREM sleep EEG spindle frequency whitened spectral peak amplitudes and IQ in females and males. (**A**) Categorized scatterplot representing the correlation between whitened spectral peak amplitude of the NREM sleep EEG spindle frequency range (recording site: F4) and IQ in women and men. (**B** Pearson *r*-values were transformed to *Z*-values and represented on topographical maps. C. Significance probability maps of the correlations presented in B.

Recording location	ρ_{AIQ}	p_{AIQ}	N_{AIQ}	ρ_{HIQ}	p_{HIQ}	N_{HIQ}	$p_{difference}$
Fp1	.44	***<.001***	79	.40	***.001***	60	.787
Fp2	.44	***<.001***	85	.45	**<.001**	63	.901
F3	.48	***<.001***	84	.41	***.001***	64	.622
F4	.52	***<.001***	83	.42	***.001***	64	.476
Fz	.57	***<.001***	70	.45	**<.001**	60	.370
F7	.39	***.001***	70	.45	**<.001**	58	.660
F8	.45	***<.001***	69	.43	***.001***	59	.900
C3	.44	***<.001***	84	.45	**<.001**	64	.956
C4	.45	***<.001***	85	.43	**<.001**	64	.896
Cz	.47	***<.001***	70	.37	***.004***	60	.507
P3	.39	***<.001***	85	.42	***.001***	64	.801
P4	.42	***<.001***	85	.41	***.001***	64	.927
T3	.43	***<.001***	70	.49	**<.001**	59	.640
T4	.51	***<.001***	70	.42	***.001***	60	.507
T5	.32	***.007***	70	.45	***<.001***	58	.412
T6	.40	***.001***	70	.42	***.001***	60	.896
O1	.31	***.004***	85	.40	***.001***	64	.549
O2	.34	***.002***	84	.41	***.001***	64	.610

Table 2. Comparison of the correlations between age and the slope of the NREM sleep EEG spectra in subjects with average and high intelligence (AIQ vs HIQ). Spearman rank correlations (ρ) were significant in both intelligence groups, however, the differences between the higher (HIQ) and average (AIQ) intelligence groups was not significant ($p_{difference}$). Bold italic values indicate statistical significance at $p < .017$.

Pearson correlations (Fig. 6). The pattern of correlations supported our assumptions: alternative intercepts below 12.2 Hz were found to correlate negatively with spectral slopes, whereas above 12.2 or 13.5 Hz (depending on electrode location) positive correlations were found. That is the best "slope-free" intercepts in the scale-free part of the parametrized NREM sleep EEG spectra are emerging at 12.2 Hz and the 13.5 Hz for anterior and posterior recording locations, respectively ($\ln C_{2.5}$ and $\ln C_{2.6}$). The original intercept derived at $\ln f = 0$ could be termed as $\ln C_0$, according to this terminology. We reanalyzed our hypothesis based on the assumption of higher intercepts in women as compared to men, which is the only hypothesis involving term C of the formula (H4). Substituting $\ln C_0$ with $\ln C_{2.5}$ and $\ln C_{2.6}$ resulted in increased mean effects sizes (larger intercepts in women) from $\overline{\eta^2} = 0.084$ to $\overline{\eta^2} = 0.118$ (both averaged over recording locations).

Discussion

When analyzing the Fourier spectra of EEG records performed for long periods of sleep, researchers and clinicians rely on statistics. That is, the periodograms of short modified EEG segments are averaged in order to obtain the averaged spectra[44]. As a consequence, the spectral profiles are inherently statistical in nature. In coherence with former reports focusing on sleep stages and arousal[15,16] our current approach provides a characterization of the NREM sleep EEG Fourier spectra by taking into account their inherent electrophysiological and statistical regularities based on its power law scaling properties. Our focus is on individual differences in NREM sleep and we assume that the approach we follow results in an integrated characterization of NREM sleep EEG, which is superior in terms of construct validity and accuracy. First of all, a frequency-independent amplitude measure potentially reflecting a contamination of neuronal and non-neuronal factors, like brain activity and skull anatomy, can be reliably separated and is not mixed up in power spectral values focusing on specific oscillatory phenomena. Although the natural logarithm of term C derived from formula (1) and (2) ($\ln C_0$) reliably reflects the hypothesized sex differences, the model could be refined by using alternative intercepts, which were independent from the slopes ($\ln C_{2.5}$ and $\ln C_{2.6}$) (Fig. 6). Thus, we were able to determine the slope free intercepts, which—according to our best knowledge – is a first explicit and successful attempt to build a non-redundant, power law scaling-based mathematical model of sleep EEG spectra. The slope free intercept might constitute an ideal normalization value for NREM sleep EEG (spectra) in future basic and clinical studies.

In addition to the spectral intercepts, the power law functions describing the sleep EEG spectra appropriately address the issue of the ratio of EEG power at different frequencies, providing a single measure (α), instead of several ones scattered redundantly in all frequency bins and bands. This approach was found to be effective in deriving measures of consciousness[24], sleep stages[15] and arousal[16] from sleep EEG records, as well as to index aging as a function of scale free wake EEG features[22]. Here we complete these studies with the individual differences approach of NREM sleep EEG, which was suggested to be a seminal perspective of all sleep studies[45].

Last, but not least, spectral peak amplitudes ($P_{Peak}(f)$) are whitened in our approach, that is, the scale-free part of the spectrum is effectively controlled, which might enable researchers to differentiate background and oscillatory activities at specific frequencies.

The findings derived from our approach of parametrizing the NREM sleep EEG spectra clearly supports the robustness and validity of the method presented in this paper, which was inspired by studies aiming to whiten

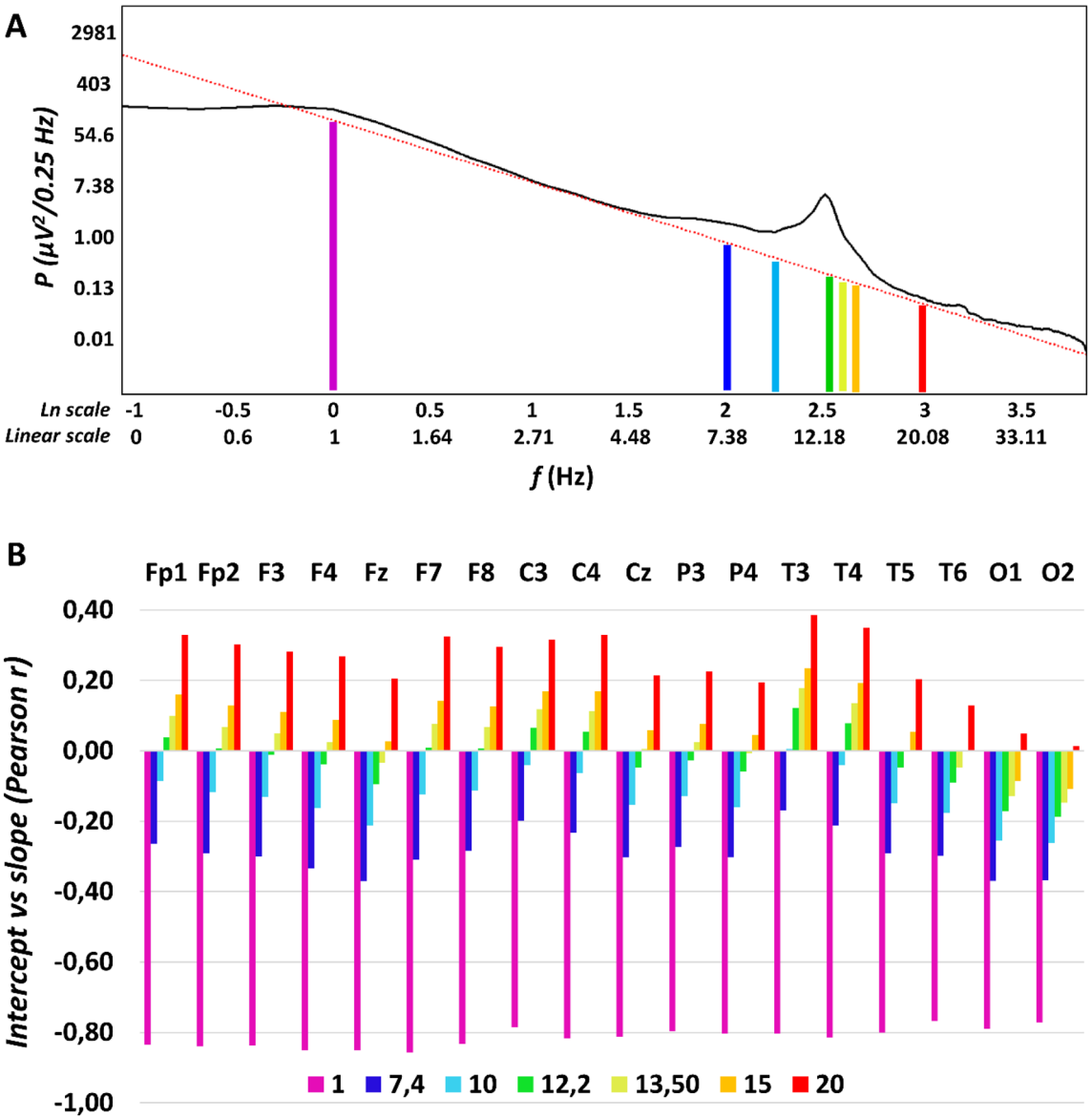

Figure 6. Determining the optimal alternative intercept for the NREM sleep EEG spectra. (**A**) Linear fitted to the double logarithmic plot of an average NREM sleep EEG spectral power (*P*) derived from right frontopolar location (Fp2) in a young female volunteer. Beside the original, violet-coloured intercept at ln $f = 0$ ($f = 1$ Hz), alternative intercepts are depicted at 7.4, 10, 12.2, 13.5, 15 and 20 Hz. (**B**) Between-subject correlations of the potential intercepts (ln *C*) with the slopes of the spectra (α) in a location-dependent manner. Note the negative correlations for low and the positive correlation for high frequencies, respectively. Zero-correlations are seen in the middle of the sleep spindle frequency range (at 12.2 and 13.5 Hz), although occipital recording locations are characterized by a slightly different pattern.

the spectral power in the sleep spindle frequency[27,46]. As predicted (H1), age correlates positively with NREM sleep EEG spectral exponents (Suppl. Table 3a), indicating that aging is associated with flattening of the Fourier spectra (i.e. exponents closer to 0) (Fig. 3). This finding coheres with reports of bandwise power spectral analyses of NREM sleep EEG, indicating decreased low and increased high frequency activity in the NREM sleep EEG of healthy aged subjects[28]. Moreover, the steepness of the slope of the linear describing the relationship between the log-amplitude and the log-frequency of NREM sleep EEG revealed the same age-dependency[11]. Thus, our method is capable of extracting spectral slope information with sufficient precision and is a valid and simple approach to be used in future (translational) studies. The slope of the spectrum is basically a measure of the constant ratio between low and high frequency activities, which was hypothesized to reflect the ratio between inhibition and excitation, the depth of sleep and/or the level of conscious awareness[15,24,47,48]. Findings might indicate that aged subjects have lower sleep depth, but might also open new avenues beyond the exclusive focus on sleep slow waves/oscillation when studying the relationship between aging and sleep. The latter point is supported by our finding on the lack of a difference in the age-dependency of the NREM sleep EEG spectral slopes in subjects with average and high intelligence (Table 2). This finding apparently contrasts the outcomes of our previous report

on the significant differences in age-dependent declines in NREM sleep EEG slow wave/oscillation of average and high IQ subjects. That is in terms of NREM sleep EEG slow waves high IQ subjects tend to age at a slower pace than average IQ subjects[1]. In spite of the fact that the database we used in the two studies are the same, the methods (band-limited spectral analysis focusing on specific frequencies vs. spectral exponent extraction) yield different results. Besides trivial methodological differences (spectral power vs exponent), our current approach of excluding the 0–2 Hz range from slope-fitting might contribute to this difference. That is, our present findings indicate that average and high IQ subjects tend to age at a same pace, at least in terms of their NREM sleep EEG spectral exponents. These contrasting results indicate that our former findings are preferentially reflecting the age- and IQ-dependency of the NREM sleep EEG slow oscillatory mechanism per se, but not the scale-free activity and/or the constant ratio of slow and high frequency activities. The latter could be a subject of aging which is at least partially independent from the well characterized age-dependent decreases in slow oscillations[49] and is equally present in average and high IQ subjects. Recent findings and considerations suggest that the spectral slope derived from an electrophysiological signal indicates the ratio of excitation and inhibition in the underlying neural tissue[47]. Thus, according to our current findings and previously published modeling data[47] aging is characterized by a relative increase in excitation over inhibition during the state of night time NREM sleep, and this effect seems to be relatively independent from the decreased slow oscillation reported in former studies[1,49].

Aging was also shown to be associated with decreased sleep spindle frequency activity and decreased phasic sleep spindles in former studies[30]. These findings cohere with our current report of an age-associated decrease in whitened spectral peak amplitudes of NREM sleep EEG spindle frequency range (Suppl. Table 3b). Reports suggest that the age-dependent decrease in sleep spindles recorded over the prefrontal regions mediates the cognitive decline in later ages[50]. Moreover, it was suggested that this effect reflects the disruption of thalamocortical regulatory mechanisms involved in sleep spindle rhythmogenesis[51]. Thus, our index of whitened NREM sleep EEG spectral peak amplitude in the spindle frequency range could serve as a potential biomarker of the above mentioned[50,51] neurocognitive aspects of aging.

The age-associated increases in the frequency of sleep spindle oscillations (also known as intraspindle frequencies) were reported in several former reports[31], although the largest study did not reveal such changes in adulthood[30]. Our present findings reveal a non-predicted decrease in maximal frontal spectral peak amplitude in the spindle frequency range of NREM sleep EEG. The range of the spindle frequency changes clearly indicate a change from the predominant fast (~ 14 Hz) to predominant slow (~ 12 Hz) sleep spindle spectral peaks during aging. That is, our finding indicates a decrease in relative frontal emergence of fast sleep spindles during aging, rather than a deceleration of sleep spindles at a rate of 0.5 Hz/decade (Fig. 3). This post-hoc assumption is supported by our additional empirical findings indicating the increasing rates of frontal slow sleep spindle dominance in the aged. In addition, the parietal recording locations, which are almost uniformly characterized by fast sleep spindle types of spectral peaks over the whole sample, do not provide any evidence for an age-dependent acceleration of intraspindle oscillatory frequencies. That is, our findings clearly do not support this hypothesis.

Women were shown to be characterized by significantly higher NREM sleep EEG spectral intercepts as compared to men. This difference is not seen in the spectral slopes and is sharpened when using the alternative ("slope-free") intercepts ($\ln C_{2.5}$ and $\ln C_{2.6}$ instead of $\ln C_0$). To the best of our knowledge this is the first report explicitly targeting these issues. We based our hypothesis on findings suggesting that women vs men differences in EEG power are largely frequency-independent[28], thus indicating an overall amplitude effect captured by the term C in formula (1) and (2). That is, previous reports focusing on specific frequency ranges and oscillatory phenomena are confounded by overall amplitude differences in the EEG of women and men. Examples for such potentially confounded findings are reports on women vs men differences in sleep spindle densities/occurrences. Spindles detected by fixed thresholds[34,35] or raw (non-whitened) spectral power values of the spindle frequency range[28,32] indicate sex differences (increased sleep spindle density/activity in women), but are not controlled for overall amplitude differences. It has to be noted however, that one of the early publications cited above hypothesized that women vs men differences in sleep EEG spectral power might reflect sex differences in skull thickness[32], but—at least to our best knowledge—this hypothesis remained largely unexplored from the electrophysiological point of view. Our current approach considers this issue and provides a reliable and potentially useful method for controlling non-specific effects, potentially contaminated with non-neuronal issues in EEG amplitude. The estimation of the spectral intercept provides a simple index which can be included in future biophysical, electrophysiological-modeling studies of the skull-thickness-EEG power issue. Our current findings clearly indicate the lack of sex differences in sleep spindle power when overall amplitude women vs men differences are controlled (Fig. 4; Suppl. table 4).

Women were shown to be characterized by higher frequency sleep spindle oscillations as compared to men according to our former study based on the individual adjustment of sleep spindle frequencies and amplitudes[36]. This finding was strengthened by our current report based on the detection of whitened spectral peak location with 0.0052 Hz resolution (Table 1). That is, our current finding strengthens the validity of our spectral parametrization approach. In addition, the hypotheses suggesting that sleep spindle frequency is accelerated by either progesterone and its neuroactive, indirect GABA-agonist metabolite allopregnanolone[52] or the progesterone-induced hyperthermia[53] during the follicular phase of the menstrual cycle in women are indirectly supported by our present findings. Although our participants were not controlled for menstrual cycle phases and oral contraceptive use, we can assume that at least some of the female subjects were examined during the follicular phase of their menstrual cycle. Furthermore, oral contraceptive use involve the intake of progestagenic compounds, which might induce some of the neural effects of endogenous progesterone in naturally cycling women.

Here we reveal a positive correlation between whitened spectral peak amplitude of sleep spindle frequency activity during NREM sleep and IQ in women, but not in men (Fig. 5; Suppl. table 5). Intelligence was shown to be reflected in the intensity (amplitude and/or density) of phasic sleep spindle events or alternatively in the spectral power of sleep spindle frequency activity during NREM sleep[7–10,36]. In the database we use in our

present study a marked sexual dimorphism of this effect was also revealed: women but not men were shown to be characterized by the sleep spindle amplitude/power vs IQ correlations[8,36]. Although this latter effect was not unequivocally reflected in a significant meta-regression between effect size and % female in the sample in a subsequent metaanalysis[9], here we refer to it because convergent findings obtained by different methods used on the same dataset are an issue of validity of the methods. That is, we reproduced the positive sleep spindle vs. IQ correlation in women by using a linear fitting approach to the log–log spectra of NREM sleep and a concurrent whitening of spectral peaks, without assumptions on time-domain sleep spindle features. Again, this finding might strengthen our views on the reliability of the method of analyzing the constant, the slope and the (whitened) peak attributes of the NREM sleep EEG in human subjects.

Among the shortcomings of our work we would emphasize the lack of slow vs fast sleep spindle differentiation by the current version of our method, as well as the fact that we disregarded low frequency power (< 2 Hz) when fitting the slopes. Fitting of two slightly overlapping spectral peaks instead of just one, would increase considerably the complexity of the approach, whereas our intention was to keep the process as simple and intuitive as possible. Moreover, we intended to follow the already published method of finding the maximal peak in the spindle frequency range and correlating its amplitude/power with neurological-clinical and cognitive data[27,46]. Similarly, the potential and largely unpredictable contamination of low frequency power with sweating artefacts, as well as the high-pass filtering effects of gold-coated electrodes[54] we used in our studies precluded us from a precise measurement of the power law scaling at low frequencies below 2 Hz. Our approach of excluding the alpha and spindle frequencies before fitting a linear to the equidistant double logarithmic NREM sleep EEG power spectra requires a priori knowledge on the position of the spectral peaks and, as a consequence, increases the researchers degrees of freedom. In addition, this approach inherently omits a wide range of frequencies when fitting the linear. Although, there are reported methods for handling the above issues[14], here we focused on the current method because of our the explicit intention of comparability with former reports focusing on NREM sleep EEG power spectra and neurocognition[27,46].

In sum, the parametrization of NREM sleep EEG of healthy adult subjects by relying on the power law scaling behavior of the electrical activity of the brain, as well as by completing this statistical property with the prominent spectral peak at the sleep spindle range, provides an integral method of describing and characterizing individual differences in sleep and cognition. Here we show, that most of the features of NREM sleep EEG can be efficiently compressed in the spectral intercepts, slopes and peaks, at least in terms of demographic (age, sex) and cognitive (IQ) correlates of sleep. It remains to be determined, if known arousal and sleep state-dependent changes[15,16] or overnight sleep dynamics[48] can be efficiently completed with measures of sleep regulatory mechanisms (e.g. homeostatic and circadian factors) derived from our integrative parameters of NREM sleep EEG spectra. In addition, further studies are needed for an adequate handling of multiple spectral peaks and low frequency (< 2 Hz) oscillations in the non-full-band EEG.

Methods

Subjects/databases. Data was combined from multiple databases (Max Planck Institute of Psychiatry, Munich, Germany; Institute of Behavioural Sciences of Semmelweis University, Budapest, Hungary) for this retrospective multicenter study[3,8]. Polysomnography data were recorded from 175 participants 81 females, 94 males, mean age 29.57 years, age range 17–60 years) and IQ scores were measured for 149 participants (68 females, 81 males, mean age 29.23 years, age range 17–60 years). Volunteers were recruited also via Mensa Germany and Mensa Hungary to increase the number of highly intelligent individuals. As some of the participants have missing data of some electrodes and/or IQ scores the data numbers from which the statistical analysis was conducted are always reported in the results.

Based on self-reports, none of the participants had a history of psychiatric or neurological disorders. Alcohol consumption was restricted before recording, but a small amount of caffeine (max. 2 cups of coffee before noon) was allowed to the participants. Based on self reports 8 participants were light or moderate smokers. Data were combined from multiple databases (Max Planck Institute of Psychiatry, Munich, Germany; Institute of Behavioural Sciences of Semmelweis University, Budapest, Hungary). The experiment was conducted in full accordance with the World Medical Association Helsinki Declaration and all applicable national laws and it was approved by the institutional review board, the Ethical Committee of the Semmelweis University, Budapest, or the Ludwig Maximilian University, Munich. Written informed consent was obtained from adults participants and parents/guardians of the children (age: 17 years).

Psychometric intelligence. Standardized nonverbal intelligence tests were recorded from 149 participants: 70 of them completed the Culture Fair Test (CFT)[55,56] and 39 of them completed the Raven Advanced Progressive Matrices (Raven APM)[57] test. 40 participants completed both tests. These tests have been shown to similarly measure abstract pattern completion and are particularly good measures of the general factor of intelligence[58–60]. A composite raw intelligence test score was calculated, expressed as a Raven equivalent score (RES)[1]. RES for Raven APM tests was equal to the actual raw test score, whereas RES of the CFT test raw scores were equal to the Raven APM score corresponding to the IQ percentile derived from CFT performance and the age of the participant. Scores were averaged for participants who completed both tests. Standardization of APM was applied according to 1993 Des Moines (Iowa). Based on their mean IQ score, the sample was split into an average (AIQ: $88 < IQ < 120$; $\overline{IQ} = 106.9$; $N = 85$) and a high intelligence (HIQ: $120 \leq IQ < 156$; $\overline{IQ} = 130.38$; $N = 64$) subgroup[1].

Polysomnography recordings. Detailed data recording procedures and power spectral analysis are also reported in published studies[2,8]. Sleep data were recorded on two consecutive nights by standard polysomnog-

raphy including EEG, electro-occulography (EOG), electrocardiography (ECG) and bipolar submental electromyography (EMG). EEG channels were placed according to the international 10–20 system (Fp1, Fp2, F3, F4, Fz, F7, F8, C3, C4, Cz, P3, P4, T3, T4, T5, T6, O1, O2 and left and right mastoids)[61]. Impedances for the EEG electrodes were kept below 8 kΩ. The sampling frequency was either 249 Hz, 250 Hz or 1024 Hz, depending on recording site (Suppl. table 7). Data were offline re-referenced to the average of the mastoid signals and notch filtered at 50 Hz. Electrodes excluded from the analysis due to artifacts and/or recording failures were treated as missing data. The number missing data for the total 175 participants is reported in Supplementary Table 8, separately for each electrode. Recordings of the first night were used for habituation and therefore were not included in further analyses. Sleep data of the second night in the laboratory were scored for sleep-waking states and stages according to standard AASM criteria on a 20-s basis[62] by an expert. Furthermore, artefactual segments were marked on a 4-s basis and excluded from further analyses.

Power spectral analysis. Power spectral densities were calculated for the NREM (N2 and N3) sleep, in 0.25 Hz bins from 0 Hz to the Nyquist frequency ($f_{Nyquist}$) by relying on 4 s Hanning-tapered, non-artefactual windows. A 50% overlap was used for consecutive windows, whereas mixed-radix FFT for calculating power spectral densities. Power spectral densities from all 4 s windows were then averaged. As data were recorded with different EEG devices producing different analog filter characteristics, average power spectral densities were corrected as follows[1]: An analog waveform generator was connected to the C3 and C4 electrode positions of all EEG devices and sinusoid signals of various frequencies (0.05 Hz, every 0.1 Hz between 0.1–2 Hz, every 1 Hz between 2–20 Hz, every 10 Hz between 10–100 Hz) were generated with 40 and 355 μV amplitudes. The amplitude reduction rate of each recording system at each frequency was determined by calculating the proportion between digital (measured) and analog (generated) amplitudes of sinusoid signals at the corresponding frequency. The amplitude reduction rate was averaged for the 40 and 355 μV at each frequency. The reduction rate at the intermediate frequencies were interpolated by spline interpolation. The measured power spectral density values were corrected with the device-specific amplitude reduction rate by dividing the original value with the squared amplitude reduction rate at the corresponding frequency according to previous suggestions[63,64].

Estimation of the spectral intercepts and slopes. Basically our approach is based on obtaining the power spectrum of the EEG signal (see above), fitting a line to the log–log power and performing a peak detection. In order to manage the second step the power law function (formula (2)) was transformed to one which fits in the double logarithmic plots as follows (Fig. 1C):

$$\mathrm{lnP(f)} = \mathrm{lnC} + \alpha \mathrm{lnf} + \mathrm{lnP_{Peak}(f)} \tag{3}$$

This means that the natural logarithm of spectral power (P) is expressed as a linear function of the natural logarithm of frequency (f). In addition, there are two terms in the equation: the natural logarithm of the constant (C) and the natural logarithm of peak power (P_{Peak}, see Fig. 1). If the latter equals 1 ($P_{Peak} = 1$), that is, there is no peak at a given frequency f, the value is 0 ($\ln 1 = 0$). The logarithmic frequency scale inherently induces increasing data density at higher frequencies. Thus, a linear fit to this data would induce a strong bias against low frequency bins, which would contribute less to the determination of slopes compared to the higher frequency bins. In order to manage this problem and obtain an equal distribution of the data points, power values were interpolated up to the smallest frequency step (0.0052 Hz) by the piecewise cubic Hermite interpolation method. In the next step a linear was fitted to the 2–48 Hz frequency range of this equidistant log–log plot, excluding the 6.0052–17.9948 Hz frequency range corresponding to the alpha and spindle bands (in order to avoid those parts of the NREM sleep EEG spectra which are characterized by oscillatory activities as well). This part of our procedure was inspired by two former studies using a similar approach for whitening of the NREM sleep spindle spectra[27,46]. The slope of the linear is α, whereas its intercept is ln C.

Our intention to determine alternative, slope-free intercepts of the linear function in the double logarithmic plot was performed by using individually fitted α and C values in an alternative version of formula (3). In this case the term expressing spectral peak power $P_{Peak}(f)$ was omitted, and ln $P(f)$ values were calculated for f values equalling 7.4, 10, 12.2, 13.5, 15 or 20 Hz. The goal of this step was the determination of the scale-free part of the spectrum at which the line cross of the y-axis is statistically independent from the slope of the line (α) across subjects.

Estimation of the spectral peak frequencies. Spectral peak frequency was determined in the 9–18 Hz range, separately for each EEG recording location by automatically defining local maxima in mathematical terms. That is, we used the first derivative test in order to find the critical points, followed by the second derivative test to differentiate local maxima and minima. A spectral peak was accepted if the first order derivative was zero and the second order derivative was negative. Calculations were performed as follows: a second-degree polynomial curve fitting was performed using all sets of successive bin triplets (0.75 Hz), with an overlap of 2 bins (0.5 Hz) in the 9–18 Hz range resulting in equations of the following type:

$$P(f) = af^2 + bf + c \tag{4}$$

P: power; f: frequency (9–18 Hz); a, b, and c: fitted parameters.

The first derivative of these functions were calculated for each triplet, resulting in:

$$P'(f) = 2af + b \tag{5}$$

The slope of the function described in formula (5) is $2a$, which was considered as the derivative at the middle of the triplets, resulting in the first derivative function of the spectra. The procedure was repeated for calculating the second derivatives: in this case the first order derivative function served as an input for fitting the quadratic polynomials.

Zero-crossings of the first derivatives were determined by spline interpolation (interpolating the series between the bins of 0.25 Hz). In addition, the second derivative was interpolated by the spline method at each detected zero crossing of the first derivatives. The cases which were characterized by the co-ocurrences of the two criteria below were considered as spectral peak frequencies:

$$P'(f) = 0 \tag{6.1}$$

$$P''(f) < 0 \tag{6.2}$$

Estimation of the spectral peak amplitudes. Spectral power at peak frequencies were estimated by spline interpolation of the double logarithmic plots of the power spectra. The spectral peak amplitude was then whitened by subtracting the estimated power based on the fitted linear function from the peak power containing both arrhythmic and rhythmic activity (Fig. 2):

$$\mathrm{lnP_{Peak}(f)} = \mathrm{lnP(f)} - (\mathrm{lnC} + \alpha \mathrm{lnf}) \tag{7}$$

In order to avoid negative amplitudes due to the logarithmic scale, the power values were shifted for being all positive before this subtraction by adding a constant. This latter step was applied for the calculation of the amplitude measures only. As multiple spectral peaks were detected for some of the participants/EEG recording locations, the one with the largest amplitude was determined and used in this study. If no spectral peak was found in the spindle frequency range, peak values were considered as missing data (see Suppl. table 8). Data analysis was performed by MATLAB 9.5 (Mathworks Inc., https://www.mathworks.com).

Antero-posterior changes in prevailing spectral peak frequency. Frequency measures of spectral peaks with maximal amplitudes ($P_{Peak}(f_{maxPeak})$) were analyzed in terms of antero-posterior changes as follows. First, we formed (para)sagittal regions by averaging $f_{maxPeak}$ values in frontopolar (Fp1, Fp2), frontal (F3, F4, Fz), central (C3, C4, Cz), parietal (P3, P4, Pz), as well as occipital (O1, O2) recording locations. In the following, the regional means of $f_{maxPeak}$ values were serially subtracted in consecutive antero-posterior regions as follows: frontal-frontopolar, central-frontal, parietal-central, occipital-parietal. Outputs express the antero-posterior shifts in $f_{maxPeak}$ (Hz), with positive values indicating antero-posterior increases in frequency (Fig. 2). The successive frequency shifts were summed for each subject, whereas the results of this addition were averaged over the whole sample. In a separate analysis maximal frequency shifts were determined and localized in each subject, resulting a sample mean of maximal antero-posterior frequency shift and a topographical distribution of this shifts.

FOOOF analyses. In order to test the convergent validity of our analyes we run separate analyses with a recently published method[23]. The same frequency range (2–48 Hz) was analyzed and the so-called knee-parameter, unique to the FOOOF-method was omitted, because the latter was specifically designed to describe the lowest frequency end of the spectrum (which we did not include in our analyses).

Statistical analyses. Goodness of fit of the linear to the equidistant log–log spectral data was assessed by Pearson product moment correlations, which were Fisher Z-transformed, averaged and back-transformed according to Silver and Dunlap[65]. Last, but not least the resulting average R-value were squared in order to determine the shared variance. Standard deviation (SD) was assessed from the Fisher-Z-transformed dataset, and the resulting value was back-transformed as well.

We used parametric tests (Pearson correlation, independent sample t-test) on normally distributed data and non-parametric tests (Spearman's rank correlation, Mann–Whitney U test) when the distribution of the data was not Gaussian. The normality of the distributions was analysed by Shapiro–Wilk tests. In order to control Type 1 statistical errors due to multiple electrodes/hypothesis, we used a version of the Descriptive Data Analysis (DDA) protocol[37] adapted for neurophysiological data[38,66]. This procedure tests the global null hypothesis ("all individual null hypotheses in the respective region are true") at level 0.05, against the alternative that at least one of the null hypotheses is wrong. DDA considers the intercorrelations between the different electrodes and is based on defining Rüger's areas[67], which are sets of spatially contingent conventionally (descriptively) significant ($p < 0.05$) results. The global significance of the Rüger area means that at least 1/3 of the descriptive significances are significant at a $p = 0.05/3 = 0.017$ and/or 1/2 of the descriptive significances are significant at $p = 0.05/2 = 0.025$. We used both criteria simultaneously (the "and" operator) in this study. In order to obtain a better localization of regions with significant correlations, associations between NREM sleep EEG spindle frequency whitened spectral peak amplitudes and IQ were represented by significant probability maps[68].

Ethical statements. We confirm that we have read the Journal's position on issues involved in ethical publication and affirm that this report is consistent with those guidelines.

Data availability

All corrected power spectral data, as well as the fitted parameters and the program code used are available at https://osf.io/c487g/.

Received: 25 September 2020; Accepted: 28 December 2020
Published online: 21 January 2021

References

1. Pótári, A. *et al.* Age-related changes in sleep EEG are attenuated in highly intelligent individuals. *Neuroimage* **146**, 554–560. https://doi.org/10.1016/j.neuroimage.2016.09.039 (2017).
2. Ujma, P. P., Simor, P., Steiger, A., Dresler, M. & Bódizs, R. Individual slow-wave morphology is a marker of aging. *Neurobiol. Aging* **80**, 71–82. https://doi.org/10.1016/j.neurobiolaging.2019.04.002 (2019).
3. Ujma, P. P. *et al.* Sleep EEG functional connectivity varies with age and sex, but not general intelligence. *Neurobiol. Aging* **78**, 87–97. https://doi.org/10.1016/j.neurobiolaging.2019.02.007 (2019).
4. Kaskie, R. E. & Ferrarelli, F. Sleep disturbances in schizophrenia: what we know, what still needs to be done. *Curr. Opin. Psychol.* **34**, 68–71. https://doi.org/10.1016/j.copsyc.2019.09.011 (2019).
5. Campbell, I. G., Grimm, K. J., de Bie, E. & Feinberg, I. Sex, puberty, and the timing of sleep EEG measured adolescent brain maturation. *Proc. Natl. Acad. Sci. USA* **109**, 5740–5743. https://doi.org/10.1073/pnas.1120860109 (2012).
6. Bódizs, R., Gombos, F. & Kovács, I. Sleep EEG fingerprints reveal accelerated thalamocortical oscillatory dynamics in Williams syndrome. *Res. Dev. Disabil.* **33**, 153–164. https://doi.org/10.1016/j.ridd.2011.09.004 (2012).
7. Bódizs, R. *et al.* Prediction of general mental ability based on neural oscillation measures of sleep. *J. Sleep Res.* **14**, 285–292. https://doi.org/10.1111/j.1365-2869.2005.00472.x (2005).
8. Ujma, P. P. *et al.* The sleep EEG spectrum is a sexually dimorphic marker of general intelligence. *Sci. Rep.* **7**, 1807. https://doi.org/10.1038/s41598-017-18124-0 (2017).
9. Ujma, P. P. Sleep spindles and general cognitive ability—a meta-analysis. *Sleep Spindles Cortical Up States* https://doi.org/10.1556/2053.2.2018.01 (2018).
10. Ujma, P. P., Bódizs, R. & Dresler, M. Sleep and intelligence: critical review and future directions. *Curr. Opin. Behav. Sci.* **33**, 109–117. https://doi.org/10.1016/j.cobeha.2020.01.009 (2020).
11. Feinberg, I., March, J. D., Fein, G. & Aminoff, M. J. Log amplitude is a linear function of log frequency in NREM sleep EEG of young and elderly normal subjects. *Electroencephalogr. Clin. Neurophysiol.* **58**, 158–160. https://doi.org/10.1016/0013-4694(84)90029-4 (1984).
12. Pritchard, W. S. The brain in fractal time: 1/f-like power spectrum scaling of the human electroecephalogram. *Int. J. Neurosci.* **66**, 119–129. https://doi.org/10.3109/00207459208999796 (1992).
13. Pereda, E., Gamundi, A., Rial, R. & Gonzalez, J. Non-linear behaviour of human EEG: fractal exponent versus correlation dimension in awake and sleep stages. *Neurosci. Lett.* **250**, 91–94. https://doi.org/10.1016/s0304-3940(98)00435-2 (1998).
14. Wen, H. & Liu, Z. Separating fractal and oscillatory components in the power spectrum of neurophysiological signal. *Brain Topogr.* **29**, 13–26. https://doi.org/10.1007/s10548-015-0448-0 (2016).
15. Miskovic, V., MacDonald, K. J., Rhodes, L. J. & Cote, K. A. Changes in EEG multiscale entropy and power-law frequency scaling during the human sleep cycle. *Hum. Brain Mapp.* **40**, 538–551. https://doi.org/10.1002/hbm.24393 (2019).
16. Lendner, J. D. *et al.* An electrophysiological marker of arousal level in humans. *eLife* **9**, e55092. https://doi.org/10.7554/eLife.55092 (2020).
17. Freeman, W. J., Holmes, M. D., West, G. A. & Vanhatalo, S. Fine spatiotemporal structure of phase in human intracranial EEG. *Clin. Neurophysiol.* **117**, 1228–1243. https://doi.org/10.1016/j.clinph.2006.03.012 (2006).
18. Lázár, A. S., Lázár, Z. I. & Bódizs, R. Frequency characteristics of sleep. In *Oxford Handbook of EEG frequency* **(in press)**
19. Dummermuth, G. *et al.* Studies on EEG activities in the beta band. *Eur. Neurol.* **16**, 197–202. https://doi.org/10.1159/000114900 (1977).
20. Miller, K. J., Sorensen, L. B., Ojemann, J. G. & den Nijs, M. Power-law scaling in the brain surface electric potential. *PLoS Comput. Biol.* **5**, e1000609. https://doi.org/10.1371/journal.pcbi.1000609 (2009).
21. He, B. J., Zempel, J. M., Snyder, A. Z. & Raichle, M. The temporal structures and functional significance of scale-free brain activity. *Neuron* **66**, 353–369. https://doi.org/10.1016/j.neuron.2010.04.020 (2010).
22. Voytek, B. *et al.* Age-related changes in 1/f neural electrophysiological noise. *J. Neurosci.* **35**, 13257–13265. https://doi.org/10.1523/JNEUROSCI.2332-14.2015 (2015).
23. Donoghue, T. *et al.* Parameterizing neural power spectra into periodic and aperiodic components. *Nat. Neurosci.* **23**, 1655–1665. https://doi.org/10.1038/s41593-020-00744-x (2020).
24. Colombo, M. A. *et al.* The spectral exponent of the resting EEG indexes the presence of consciousness during unresponsiveness induced by propofol, xenon, and ketamine. *Neuroimage* **189**, 631–644. https://doi.org/10.1016/j.neuroimage.2019.01.024 (2019).
25. Gao, R. Interpreting the electrophysiological power spectrum. *J. Neurophysiol.* **115**, 628–630. https://doi.org/10.1152/jn.00722.2015 (2016).
26. Freeman, W. J. & Zhai, J. Simulated power spectral density (PSD) of background electrocorticogram (ECoG). *Cogn. Neurodyn.* **3**, 97–103. https://doi.org/10.1007/s11571-008-9064-y (2009).
27. Geiger, A. *et al.* The sleep EEG as a marker of intellectual ability in school age children. *Sleep* **34**, 181–189. https://doi.org/10.1093/sleep/34.2.181 (2011).
28. Carrier, J., Land, S., Buysse, D. J., Kupfer, D. J. & Monk, T. H. The effects of age and gender on sleep EEG power spectral density in the middle years of life (ages 20–60 years old). *Psychophysiology* **38**, 232–242. https://doi.org/10.1111/1469-8986.3820232 (2001).
29. Nicolas, A., Petit, D., Rompré, S. & Montplaisir, J. Sleep spindle characteristics in healthy subjects of different age groups. *Clin. Neurophysiol.* **112**, 521–527. https://doi.org/10.1016/s1388-2457(00)00556-3 (2001).
30. Purcell, S. M. *et al.* Characterizing sleep spindles in 11,630 individuals from the national sleep research resource. *Nat. Commun.* **8**, 1593. https://doi.org/10.1038/ncomms1593 (2017).
31. Principe, J. C. & Smith, J. R. Sleep spindle characteristics as a function of age. *Sleep* **5**, 73–84. https://doi.org/10.1093/sleep/5.1.73 (1982).
32. Dijk, D. J., Beersma, D. G. & Bloem, G. M. Sex differences in the sleep EEG of young adults: visual scoring and spectral analysis. *Sleep* **12**, 500–507. https://doi.org/10.1093/sleep/12.6.500 (1989).
33. Looker, A. C. *et al.* Age, gender, and race/ethnic differences in total body and subregional bone density. *Osteoporos. Int.* **20**, 1141–1149. https://doi.org/10.1007/s00198-008-0809-6 (2009).
34. Crowley, K., Trinder, J., Kim, Y., Carrington, M. & Colrain, I. M. The effects of normal aging on sleep spindle and K-complex production. *Clin. Neurophysiol.* **113**, 1615–1622. https://doi.org/10.1016/s1388-2457(02)00237-7 (2002).
35. Huupponen, E. *et al.* A study on gender and age differences in sleep spindles. *Neuropsychobiology* **45**, 99–105. https://doi.org/10.1159/000048684 (2002).

36. Ujma, P. P. *et al.* Sleep spindles and intelligence: evidence for a sexual dimorphism. *J. Neurosci.* **34**, 16358–16368. https://doi.org/10.1523/JNEUROSCI.1857-14.2014 (2014).
37. Abt, K. Descriptive data analysis: a concept between confirmatory and exploratory data analysis. *Methods Inf. Med.* **26**, 77–88. https://doi.org/10.1055/s-0038-1635488 (1987).
38. Abt, K. Statistical aspects of neurophysiologic topography. *J. Clin. Neurophysiol.* **7**, 519–534. https://doi.org/10.1097/00004691-199010000-00007 (1990).
39. Borbély, A. A., Baumann, F., Brandeis, D., Strauch, I. & Lehmann, D. Sleep deprivation: effect on sleep stages and EEG power density in man. *Electroencephalogr. Clin. Neurophysiol.* **51**, 483–495. https://doi.org/10.1016/0013-4694(81)90225-x (1981).
40. Finelli, L. A., Achermann, P. & Borbély, A. A. Individual "fingerprints" in human sleep EEG topography. *Neuropsychopharmacology* **25**, S57–S62. https://doi.org/10.1016/S0893-133X(01)00320-7 (2001).
41. Olbrich, E., Landolt, H. P. & Achermann, P. Effect of prolonged wakefulness on electroencephalographic oscillatory activity during sleep. *J. Sleep Res.* **23**, 253–260. https://doi.org/10.1111/jsr.12123 (2014).
42. Tarokh, L., Rusterholz, T., Achermann, P. & Van Dongen, H. P. The spectrum of the non-rapid eye movement sleep electroencephalogram following total sleep deprivation is trait-like. *J. Sleep Res.* **24**, 360–363. https://doi.org/10.1111/jsr.12279 (2015).
43. Tinguely, G., Finelli, L. A., Landolt, H. P., Borbély, A. A. & Achermann, P. Functional EEG topography in sleep and waking: state-dependent and state-independent features. *Neuroimage* **32**, 283–292. https://doi.org/10.1016/j.neuroimage.2006.03.017 (2006).
44. Welch, P. D. The use of Fast Fourier transform for the estimation of power spectra: a method based on time averaging over short, modified periodograms. *IEEE Trans. Audio Electroacoust.* **15**, 70–73. https://doi.org/10.1109/TAU.1967.1161901 (1967).
45. Tucker, A. M., Dinges, D. F. & Van Dongen, H. P. A. Trait interindividual differences in the sleep physiology of healthy young adults. *J. Sleep Res.* **16**, 170–180. https://doi.org/10.1111/j.1365-2869.2007.00594.x (2007).
46. Gottselig, J. M., Bassetti, C. L. & Achermann, P. Power and coherence of sleep spindle frequency activity following hemispheric stroke. *Brain* **125**, 373–383. https://doi.org/10.1093/brain/awf021 (2002).
47. Gao, R., Peterson, E. J. & Voytek, B. Inferring synaptic excitation/inhibition balance from field potentials. *Neuroimage* **158**, 70–78. https://doi.org/10.1016/j.neuroimage.2017.06.078 (2017).
48. Weiss, B., Clemens, Z., Bódizs, R. & Halász, P. Comparison of fractal and power spectral EEG features: effects of topography and sleep stages. *Brain Res. Bull.* **84**, 359–375. https://doi.org/10.1016/j.brainresbull.2010.12.005 (2011).
49. Mander, B. A. *et al.* Prefrontal atrophy, disrupted NREM slow waves and impaired hippocampal-dependent memory in aging. *Nat. Neurosci.* **16**, 357–364. https://doi.org/10.1038/nn.3324 (2013).
50. Mander, B. A. *et al.* Impaired prefrontal sleep spindle regulation of hippocampal-dependent learning in older adults. *Cereb. Cortex* **24**, 3301–3309. https://doi.org/10.1093/cercor/bht188 (2014).
51. Clawson, B. C., Durkin, J. & Aton, S. J. Form and function of sleep spindles across the lifespan. *Neural Plast.* **2016**, 6936381. https://doi.org/10.1155/2016/6936381 (2016).
52. Driver, H. S., Dijk, D. J., Werth, E., Biedermann, K. & Borbély, A. A. Sleep and the sleep electroencephalogram across the menstrual cycle in young healthy women. *J. Clin. Endocrinol. Metab.* **81**, 728–735. https://doi.org/10.1210/jcem.81.2.8636295 (1996).
53. Deboer, T. Brain temperature dependent changes in the electroencephalogram power spectrum of humans and animals. *J. Sleep Res.* **7**, 254–262. https://doi.org/10.1046/j.1365-2869.1998.00125.x (1998).
54. Vanhatalo, S., Voipio, J. & Kaila, K. Full-band EEG (FbEEG): an emerging standard in electroencephalography. *Clin. Neurophysiol.* **116**, 1–8. https://doi.org/10.1016/j.clinph.2004.09.015 (2005).
55. Cattell, R. *Culture Free Intelligence Test, Scale 1, Handbook* (Institute of Personality and Ability Testing, Champaign, IL, 1949).
56. Cattell, R. B., Krug, S. E. & Barton, K. *Technical Supplement for the Culture Fair Intelligence Tests, Scales 2 and 3* (IPAT, Champaign, IL, 1973).
57. Raven, J., Raven, J. C. & Court, J. H. *Manual for Raven's Progressive Matrices and Vocabulary Scales* (Harcourt Assessment, San Antonio, TX, 2004).
58. Cattell, R. B. & Cattell, A. K. S. *Measuring Intelligence with the Culture Fair Tests* (IPAT, Champaign, IL, 1973).
59. Duncan, J. *et al.* A neural basis for general intelligence. *Science* **289**, 457–460. https://doi.org/10.1126/science.289.5478.457 (2000).
60. Prokosch, M. D., Yeo, R. A. & Miller, G. F. Intelligence tests with higher g-loadings show higher correlations with body symmetry: evidence for a general fitness factor mediated by developmental stability. *Intelligence* **33**, 203–213. https://doi.org/10.1016/j.intell.2004.07.007 (2005).
61. Jasper, H. H. Report of the committee on methods of clinical examination in electroencephalography. *Electroencephalogr. Clin. Neurophysiol.* **10**, 370–375. https://doi.org/10.1016/0013-4694(58)90053-1 (1958).
62. Berry, R. B. *et al. The AASM Manual for the Scoring of Sleep and Associated Events: Rules, Terminology and Technical Specification. Version 2.5* (American Academy of Sleep Medicine, Darien, IL, 2018).
63. Achermann, P. & Borbély, A. A. Low-frequency (< 1 Hz) oscillations in the human sleep electroencephalogram. *Neuroscience* **81**, 213–222. https://doi.org/10.1016/S0306-4522(97)00186-3 (1997).
64. Vasko, R. C. Jr. *et al.* Power spectral analysis of EEG in a multiple-bedroom, multiple-polygraph sleep laboratory. *Int. J. Med. Inform.* **46**, 175–184. https://doi.org/10.1016/s1386-5056(97)00064-6 (1997).
65. Silver, N. C. & Dunlap, W. P. Averaging correlation coefficients: Should Fisher's z transformation be used?. *J. Appl. Psychol.* **72**, 146–148. https://doi.org/10.1037/0021-9010.72.1.146 (1987).
66. Duffy, F. H. *et al.* Quantified neurophysiology with mapping: statistical inference, exploratory and confirmatory data analysis. *Brain Topogr.* **3**, 3–12. https://doi.org/10.1007/bf01128856 (1990).
67. Rüger, B. Das maximale Signifikanziniveau des tests: "Lehne H0 ab, wenn k unter n gegebene Tests zur ablehnung führen". *Metrika* **25**, 171–178. https://doi.org/10.1007/bf02204362 (1978).
68. Hassainia, F., Petit, D. & Montplaisir, J. Significance probability mapping: the final touch in t-statistic mapping. *Brain Topogr.* **7**, 3–8. https://doi.org/10.1007/bf01184832 (1994).

Acknowledgements

We would like to thank Mensa Germany and Mensa Hungary for their help in volunteer recruitment and Bence Schneider for his help in FOOOF analyses. Research supported by the Hungarian Medical Research Council (ETT-162/2003; https://ett.aeek.hu/en/secretariat/), the Hungarian National Research, Development and Innovation Office (K-128117; https://nkfih.gov.hu/about-the-office), the Bial Foundation (https://www.bial.com/com/bial-foundation/) the Higher Education Institutional Excellence Program of the Ministry of Human Capacities in Hungary, within the framework of the Neurology thematic program of the Semmelweis University (http://semmelweis.hu/english/), the Netherlands Organization for Scientific Research (NWO; https://www.nwo.nl/en), the European Cooperation in Science and Technology (COST Action CA18106; https://www.cost.eu/), as well as the general budgets of the Institute of Behavioural Sciences, Semmelweis University (http://semmelweis.hu/magtud/en/) and the Max Planck Institute of Psychiatry (https://www.psych.mpg.de/en). The funders had no role in study design, data collection and analysis, decision to publish, or preparation of the manuscript.

Author contributions

R.B. and O.S. conceived the study. R.B., P.S. M.Z., M.D. acquired data. R.B., O.S., C.H., P.P.U., F.G., A.P. analyzed data. All authors contributed to the interpretation of the findings as well as to the writing and revision of the manuscript.

Competing interests

The authors declare no competing interests.

Additional information

Supplementary Information The online version contains supplementary material available at https://doi.org/10.1038/s41598-021-81230-7.

Correspondence and requests for materials should be addressed to R.B.

Reprints and permissions information is available at www.nature.com/reprints.

Publisher's note Springer Nature remains neutral with regard to jurisdictional claims in published maps and institutional affiliations.

scientific reports

Check for updates

OPEN

Overnight dynamics in scale-free and oscillatory spectral parameters of NREM sleep EEG

Csenge G. Horváth[1]✉, Orsolya Szalárdy[1,2], Péter P. Ujma[1], Péter Simor[3,4], Ferenc Gombos[5,6], Ilona Kovács[6], Martin Dresler[7] & Róbert Bódizs[1]

Unfolding the overnight dynamics in human sleep features plays a pivotal role in understanding sleep regulation. Studies revealed the complex reorganization of the frequency composition of sleep electroencephalogram (EEG) during the course of sleep, however the scale-free and the oscillatory measures remained undistinguished and improperly characterized before. By focusing on the first four non-rapid eye movement (NREM) periods of night sleep records of 251 healthy human subjects (4–69 years), here we reveal the flattening of spectral slopes and decrease in several measures of the spectral intercepts during consecutive sleep cycles. Slopes and intercepts are significant predictors of slow wave activity (SWA), the gold standard measure of sleep intensity. The overnight increase in spectral peak sizes (amplitudes relative to scale-free spectra) in the broad sigma range is paralleled by a U-shaped time course of peak frequencies in frontopolar regions. Although, the set of spectral indices analyzed herein reproduce known age- and sex-effects, the interindividual variability in spectral slope steepness is lower as compared to the variability in SWA. Findings indicate that distinct scale-free and oscillatory measures of sleep EEG could provide composite measures of sleep dynamics with low redundancy, potentially affording new insights into sleep regulatory processes in future studies.

The dynamics of NREM sleep EEG spectral features over consecutive sleep cycles is of crucial importance in understanding the regulation and the function of sleep[1,2], as well as in revealing the physiological bases of insomnia[3] and major depressive disorder[4]. The well-known physiological marker of sleep intensity, the slow wave activity (SWA, power in the 0.75–4.5 Hz range) of sleep EEG was shown to decrease exponentially in consecutive sleep cycles[5,6] reflecting overall sleep–wake history[7]. Furthermore, much less emphasized observations suggest that in contrast to SWA, the power in several spectral bins of the sleep spindle frequency range increases across sleep cycles, whereas beta activity remains nearly stable over consecutive NREM periods[1]. In addition, the time course of gamma EEG activity is characterized by slight overnight increase[8], whereas both beta and gamma frequency EEG activity in NREM sleep are attenuated after periods of extended wakefulness[9]. Last, but not least, both the occurrence rates and the amplitudes of slow and fast sleep spindles were characterized by changing dominance (overnight decreases and increases for slow and fast sleep spindles, respectively), whereas frequencies were shown to follow a U-shaped overnight distribution over consecutive sleep cycles, with decelerations of 0.1 Hz during the middle part of the sleep period for both sleep spindle types[10]. These findings indicate that the overnight dynamics of NREM sleep EEG is a complex and multi-faceted process, involving a broad range of frequencies of the spectrum, but these constituents are not yet fully unraveled at the current stage of knowledge in the field.

Prior research generally confirms that neurophysiological signals comprise a rhythmic oscillatory-, and an arrhythmic (or aperiodic) activity. Thanks to its special statistical property the scalp electroencephalogram (EEG) spectrum follows a power-law distribution[11,12], thus, there is a linear relationship between the logarithm

[1]Institute of Behavioural Sciences, Semmelweis University, Budapest, Hungary. [2]Institute of Cognitive Neuroscience and Psychology, Research Centre for Natural Sciences, Budapest, Hungary. [3]Institute of Psychology, ELTE, Eötvös Loránd University, Budapest, Hungary. [4]UR2NF, Neuropsychology and Functional Neuroimaging Research Unit at CRCN-Center for Research in Cognition and Neurosciences and UNI-ULB Neurosciences Institute, Université Libre de Bruxelles (ULB), Brussels, Belgium. [5]Laboratory for Psychological Research, Pázmány Péter Catholic University, Budapest, Hungary. [6]ELRN-ELTE-PPKE Adolescent Development Research Group, Faculty of Education and Psychology, Eötvös Loránd University, Budapest, Hungary. [7]Donders Institute for Brain, Cognition and Behaviour, Radboud University Medical Center, Nijmegen, The Netherlands. ✉email: horvath.csenge@phd.semmelweis.hu

of amplitude and the logarithm of frequency[13]. This 1/f relationship is the aperiodic component of the signal due to the self-evident scale-free being of the power-law functions. Namely, such a scale-invariant nature suggests that no specific frequency dominates the signal, rather, the spectral slope reflects the overall frequency composition within the time series. The oscillatory part of the power spectrum is shown as upward deflections in specific frequency bands.

Analysing pre-defined oscillatory bands contains several possibilities for biases due to the so-called "researcher degrees of freedom"[14]. That is why the parametrization of neural power spectra has gained much importance in recent years[15]. Former reports on the aperiodic, 1/f-type measures of EEG suggest that depth of sleep or sleep intensity could indeed be reflected by the spectral slope (or exponent) of the signal. Findings which support this assumption were reported in studies revealing the sensitivity of EEG and electrocorticogram (ECoG) spectral slopes in discriminating wakefulness from states of reduced arousal including NREM and REM sleep, as well as general anesthesia or unconsciousness[16,17]. Furthermore, increasingly negatively sloped EEG and ECoG power spectra were reported from wakefulness through REM and N2 to N3 sleep states[11,18,19]. Last, but not least modelling studies indicate that spectral slopes of neural time series data reflect the ratio of inhibition over excitation in the underlying neural tissue, where increased inhibition associates with steeper slopes[20]. However, none of the above studies explicitly focused on across sleep cycle (or overnight) dynamics of spectral slopes, which is of crucial importance in depicting the regulatory aspects of sleep. Moreover, no former study analyzing 1/f-type activity characterized the dynamics of other parameters of the NREM sleep EEG spectra, namely the intercept (or amplitude multiplier) and the parameters of the major spectral peaks (peak power and peak frequency). Here we suggest that an appropriate separation of the rhythmic and aperiodic components of non-rapid eye movement (NREM) sleep EEG activity may provide feasible and non-redundant indicators of known across sleep cycle dynamics hypothetically linked to sleep regulatory processes.

Moreover, it was found that interindividual differences in slow wave sleep (SWS) and in quantitatively evaluated delta power in the NREM sleep are considerable, exceeding the effect sizes attributable to sleep–wake history[21,22]. The striking interindividual variability of healthy subjects lead several researchers to the conclusion that available laboratory measures of sleep are inappropriate for the construction of reference values[23] or for defining "normal" sleep[24], reducing the sensitivity and specificity of clinical tests based on sleep parameters[22]. This means that despite its importance in sleep medicine and research, it is nearly impossible to give an exact metric as a standard for the measurement of overnight sleep dynamics and intensity. In order to provide a more comprehensive picture of across sleep cycle dynamics here we test the spectral slope and peak parameters in terms of overnight changes and associations with SWA. The set of parameters analyzed in our report were found to be composite, non-redundant and efficient in characterizing known age- sex- and cognitive correlates of sleep[14]. Here we test the feasibility of describing overnight sleep dynamics by this set of parameters, assuming that we will encounter a lower interindividual variability, hence, opening the way to define reference values for healthy sleep cycle dynamics. In order to facilitate the reliance on reference values we publish detailed descriptive statistics of our dataset, which might help other researchers in circumscribing the range of healthy sleep in future studies.

We used the method from our earlier publication[14] to obtain the slope and the most prominent peak of the Fourier spectrum, that is, to distinct the periodic and aperiodic part of the NREM sleep EEG activity. In this, we proposed that there is a need to include a peak power function in the power law formula as follows:

$$P(f) = Cf^{\alpha} P_{Peak}(f) \quad (1)$$

where, P is power as a function of frequency, P_{Peak} is the peak power at frequency f (P_{Peak} (f) = 1 if there is no peak and larger if there is), C is the intercept (a constant) which expresses the frequency-independent EEG amplitude, and α is the spectral slope (spectral exponent; negative number). The latter was associated with sleep depth and arousal level[17,18]. As in our previous work, we define $f_{maxPeak}$ as the frequency at which P_{Peak} reaches its maximum level.

Based on previously published and above cited findings, our main hypotheses are the following:

- The spectral slope (α) and peak amplitude (the maxima of P_{Peak}) increase during successive NREM periods (indicating flattening spectra and increasing oscillatory spindle activities, respectively).
- Spectral slope correlates negatively with SWA, the gold-standard measure of sleep intensity.
- The $f_{maxPeak}$ values (i.e. the frequency of the largest peak in the spindle range) in the frontopolar and parieto-occipital regions are characterized by a U-shaped distribution across consecutive sleep cycles (reflecting the overnight dynamics of slow and fast sleep spindle frequencies, respectively).
- $f_{maxPeak}$ values in the central regions are characterized by a linear increase over the night (reflecting the changing dominance of fast over slow sleep spindles which are mixed in this region).

Results

The number of full sleep cycles were between 2 and 5 among participants (mean: 4.25). All subjects (N = 251) had at least two, 249 had at least three, 240 had four or more, and 75 had five complete sleep cycles. The last (5th) cycles were not included in the models because they would have reduced the sample size considerably. The main effect of hemisphere (left vs. right) was not significant in either of the models, so it was not investigated further ($p > 0.05$).

Goodness-of-fit in the separate sleep cycles. As in our earlier publication[14], the equidistant log–log plots of the NREM EEG power spectra were fitted with linear functions below 48 Hz, furthermore, these fittings was performed with the exclusion of the 0–2 and the 6–18 Hz range to avoid spectral peaks such as slow

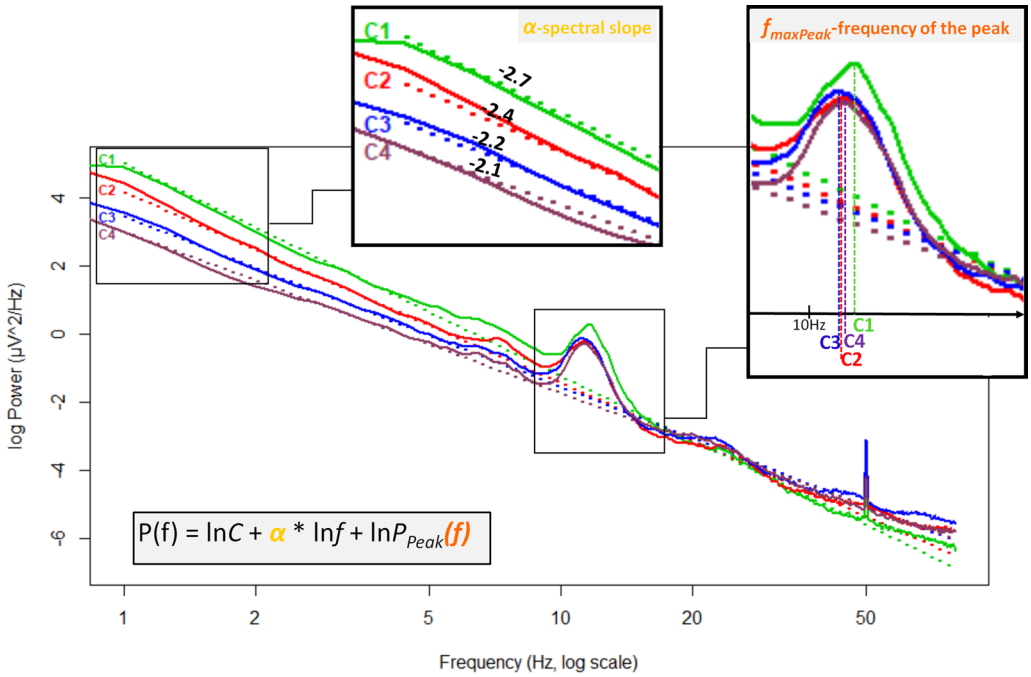

Figure 1. Example for cycle dynamics of spectral slopes and peak frequencies in a 20-year-old male subject in the right frontopolar EEG location (Fp2). C1, C2, C3, C4 reflects cycles 1–4, respectively. Note that slope values show a non-linear increase. Furthermore, the frequencies of the largest peak form a U-shape curve throughout the night, that is, in the middle of the night the peak frequencies are lower than in cycle 1 and 4.

oscillation and sleep spindles. The sample mean of slope and intercept values were − 2.71 (SD = 0.28) and 5.53 (SD = 1.11) in cycle 1, − 2.61 (SD = 0.38) and 5.03 (SD = 1.01) in cycle 2, − 2.46 (SD = 0.68) and 4.65 (SD = 0.93) in cycle 3, − 2.398 (SD = 0.65) and 4.46 (SD = 0.88) in cycle 4, respectively. Goodness of fit of the linear model of the equidistant 2–6 and 18–48 Hz spectral data varied in the range of 0.9195–0.9998 in cycle 1, 0.9002–0.9998 in cycle 2, 0.8938–0.9998 in cycle 3, 0.7686–0.9997 in cycle 4 across subjects and EEG recording locations. The square of the Fisher Z-transformed, averaged and back-transformed Pearson correlations between the fitted linear and the spectral data is $\overline{R}^2 = 0.9844$ (SD = 0.42).

Dynamics of slope and maximal peak amplitude throughout the night. Sleep cycles ($F(3,696) = 210.78$, $p < 0.001$, $N = 240$), age groups ($F(3,232) = 17.05$, $p < 0.001$, $N_{child} = 30$, $N_{teenager} = 36$, $N_{y.adult} = 142$, $N_{m.a.adult} = 32$; here, and throughout the text, the marks y.adult and m.a.adult refers to young adults and middle-aged adults, respectively) and region ($F(4,928) = 211.14$, $p < 0.001$, $N = 240$) had significant main effects on the slope of the spectrum: later cycles, older ages and more posterior regions predicted smaller absolute values of the spectral slope parameters. In addition these main effects interacted as follows: cycle × age groups ($F(9,696) = 15$, $p < 0.0001$), region × age groups ($F(12,928) = 3.66$, $p < 0.0001$), cycle × region ($F(12,2784) = 51.92$, $p < 0.0001$), indicating accelerated overnight slope changes in children as compared to adults, lack of striking regional differences in children, and regional differences in overnight dynamics, respectively. Post hoc test (see results in Table 2) revealed that slope values were significantly higher (smaller absolute value i.e., flatter slope) in each sleep cycle compared to the preceding ones in the young adult group (see an example in Fig. 1). However, in the children and teenager groups this significantly increasing effect throughout the night was evident just for the first three cycles. Only a trend appeared in the fourth cycles for this effect. Finally, in the middle-aged group, the increment of the spectral slope values was smaller during sleep which resulted in the lack of a significant difference between successive cycles (Fig. 2a). The differences between regions were significant in all cycles (Fig. 2b).

Amplitudes of the largest peaks were significantly affected by age group ($F(3) = 11.93$, $p < 0.001$, $N_{child} = 9$, $N_{teenager} = 33$, $N_{y.adult} = 125$, $N_{m.a.adult} = 22$), cycle ($F(3) = 78.45$, $p < 0.001$, $N = 189$), and region ($F(4) = 56.94$, $p < 0.001$, $N = 189$). Effect of sex was not significant. Cycle × age group ($F(9) = 3.65$, $p < 0.001$), region × age group ($F(12) = 8.67$, $p < 0.001$), cycle × region ($F(12) = 16.64$, $p < 0.001$), indicating attenuated overnight spectral peak amplitude increase in middle-aged adult subjects, decreased peak amplitude in centro-posterior regions of children, faster overnight amplitude increase in posterior regions, respectively. Post hoc test of cycle × age group interaction revealed a significant increase in peak amplitudes throughout the 4 sleep cycles in the young adult group (Table 2).

Overnight dynamics of SWA and its correlation with the slope. The same models were used to assess SWA at derivation F3. As SWA values are squared numbers, these data evidently do not meet the criteria of parametric statistical tests. Consequently, before running the statistical tests a logarithmic transformation was performed. Nonetheless, the original parameter is the one which is often used in the literature. That is why the

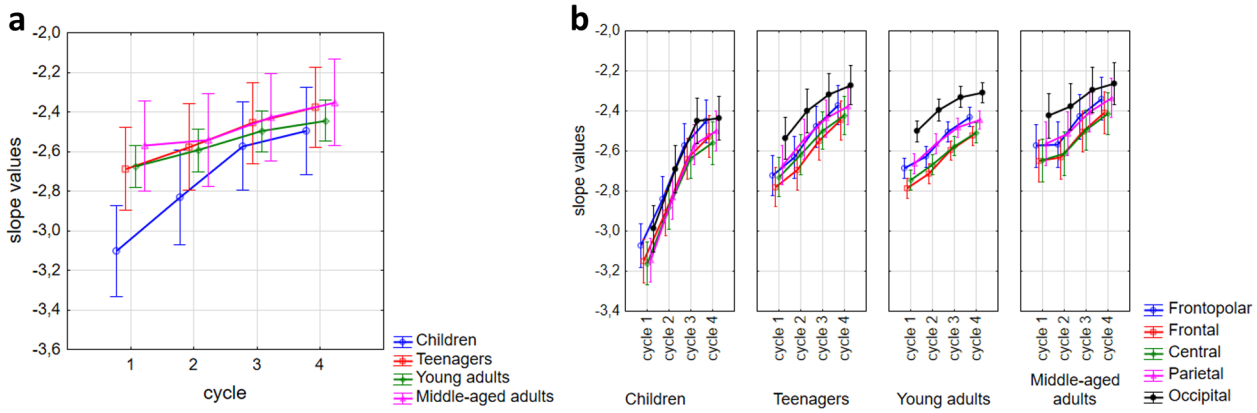

Figure 2. NREM sleep EEG spectral slopes as functions of sleep cycles, age and recording sites. (**a**) Representation of cycle × age group interaction in spectral slope values. (**b**) Depiction of cycle × region × age group interaction in spectral slope values. Dots are group mean values, whereas vertical bars denote 95% confidence intervals.

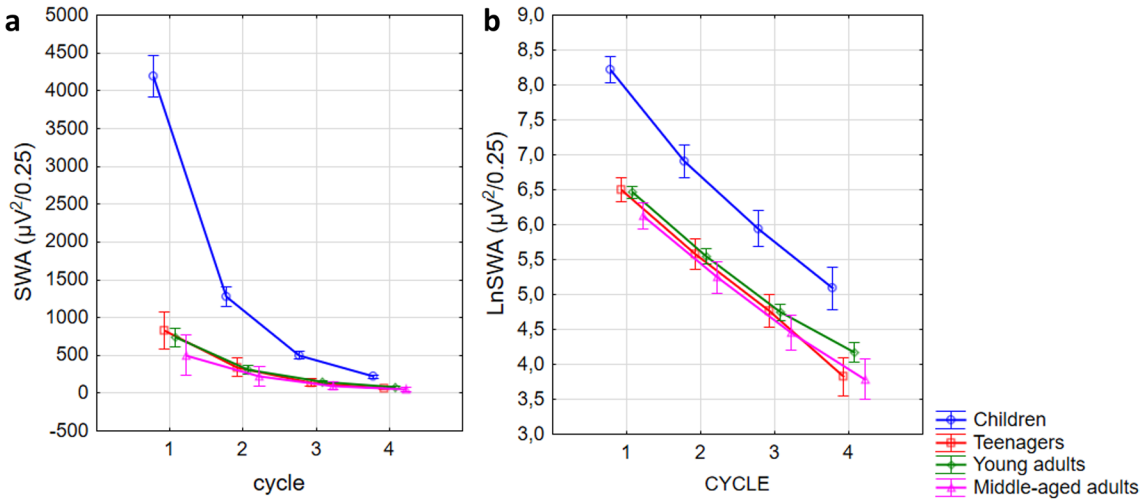

Figure 3. Cycle-by-cycle dynamics of slow wave activity. The left panel shows the common measure of slow wave activity in different age groups and sleep cycles. The natural logarithm of SWA is depicted in the right panel. Note that the decrement of lnSWA is nearly linear.

general linear model is reported here for both the classical SWA and for the logarithm of SWA (*lnSWA*). However, in the comparative estimations between the slope and SWA the log-transformed metric will be reported.

Cycle ($N = 240$; SWA: $F(3,696) = 524.88$, $p < 0.001$; lnSWA: $F(3,696) = 858.84$, $p < 0.001$), and age effect ($N_{child} = 30$, $N_{teenager} = 36$, $N_{y.adult} = 142$, $N_{m.a.adult} = 32$; SWA: $F(232,3) = 707.98$, $p < 0.001$; lnSWA: $F(232,3) = 58.68$, $p < 0.001$), in addition, the interaction between them (SWA: $F(9,696) = 153.85$, $p < 0.001$; lnSWA: $F(9,696) = 5.42$, $p < 0.001$) was evident. Although a significant decrease in logarithmized SWA was evident in all age groups in all cycles according to the post hoc tests ($p < 0.001$), in case of the classical SWA this effect was only significant in the children and young adult group for the first three ($p < 0.01$), and in the teenager group for the first two cycles ($p < 0.001$). In the other cycles and in the middle-aged group the decreasing trend was not significant ($p > 0.05$) (Fig. 3).

In order to test whether spectral slope values and the natural logarithm of SWA index are overlapping concepts Pearson correlation analyses were applied. Analyses were focused on the left frontal recording location (F3). Significant, negative, moderate to strong correlations were found in all cycles between the two metrics (Fig. 4) (Cycle 1: $N = 251$ $r = -0.73$, $p < 0.001$; Cycle 2: $N = 251$ $r = -0.61$, $p < 0.001$; Cycle 3: $N = 249$ $r = -0.56$, $p < 0.001$; Cycle 4: $N = 240$ $r = -0.56$, $p < 0.001$).

Interindividual differences in slope and SWA (/lnSWA) values. Our main goal was to propose a sleep intensity index which varies less among people than the slow wave activity. Thus, we checked the amount of outliers as well as the coefficients of variation in these two metrics (slope values and SWA) at derivation F3 (Fig. 5).

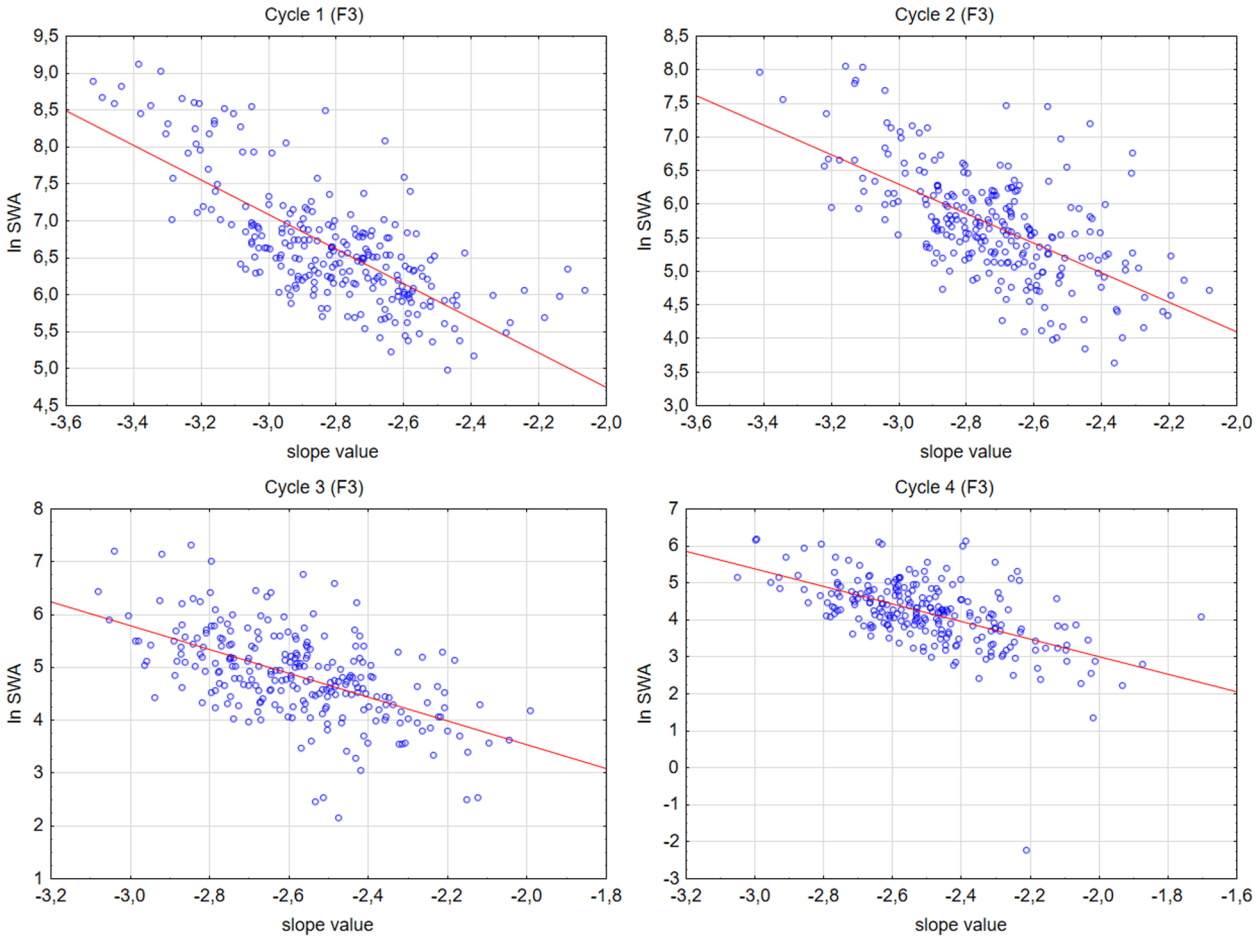

Figure 4. Scatterplots of the correlations between spectral slope value and lnSWA at the left frontal EEG location (F3).

In order to make the two measures (spectral slopes and lnSWA) comparable there was a need to rescale them according to a common absolute null point, which is a pre-requisite of assessing a relative standard deviation (coefficient of variation). As neither lnSWA nor the slope values were lower than − 4 we add 4 to both variables in all individual datapoints. Based on this rescaling we could calculate the coefficients of variation in both metrics which proved to be more than twice higher in the lnSWA as compared to the spectral slopes (Table 1).

Is there a cycle dynamic of the alternative intercepts? Here we did not analyse the original intercept considering its interdependency with the slope. The square of the Fisher Z-transformed, averaged and back-transformed Pearson correlations between the original intercept (lnC_0 at ln f = 0, f = 1 Hz) and the spectral slope is: cycle 1: $\overline{R}^2 = 0.69$ (SD = 0.11), cycle 2: $\overline{R}^2 = 0.61$ (SD = 0.11), cycle 3: $\overline{R}^2 = 0.54$ (SD = 0.09), cycle 4: $\overline{R}^2 = 0.50$ (SD = 0.06). However, cycle significantly affected both alternative intercepts: $lnC_{2.5}$ ($F(3,696) = 339.9$, $p < 0.0001$) and $lnC_{2.6}$ ($F(3,696) = 274.8$, $p < 0.0001$). Post hoc test of cycle effect revealed a significant difference between all cycles with respect to $lnC_{2.5}$ ($N = 240$, $p < 0.001$, $M_{C1} = -1.08$, $SE = 0.03$; $M_{C2} = -1.32$, $SE = 0.03$; $M_{C3} = -1.4$, $SE = 0.03$; $M_{C4} = -1.43$, $SE = 0.03$) as well with regard $lnC_{2.6}$ ($N = 240$, $p < 0.001$, $M_{C1} = -1.35$, $SE = 0.03$; $M_{C2} = -1.58$, $SE = 0.03$; $M_{C3} = -1.65$, $SE = 0.03$; $M_{C4} = -1.67$, $SE = 0.03$). Due to the similar cycle dynamics of the two alternative intercepts we hypothesized that the two metrics are highly correlated. The square of the Fisher Z-transformed, averaged and back-transformed Pearson correlations between the two alternative intercepts in the 4 sleep cycles are: cycle 1: $\overline{R}^2 = 0.99$ (SD = 0.072), cycle 2: $\overline{R}^2 = 0.99$ (SD = 0.075), cycle 3: $\overline{R}^2 = 0.99$ (SD = 0.083), cycle 4: $\overline{R}^2 = 0.99$ (SD = 0.077). Thus we used just $lnC_{2.5}$ for further analyses. In addition to cycle, age groups ($F(3,232) = 100.9$, $p < 0.0001$), sex ($F(1,232) = 9.6$, $p < 0.0001$) and region ($F(4,928) = 110.7$, $p < 0.0001$) had significant main effects on $lnC_{2.5}$. These effects reflect decreasing $lnC_{2.5}$ across successive NREM periods, and age groups, as well as higher $lnC_{2.5}$ in women as compared to men and in anterior as compared to posterior regions. Furthermore, significant interactions were evident for cycle × age groups ($F(9,696) = 2.98$, $p = 0.002$), region × age groups ($F(12,928) = 4.96$, $p < 0.0001$), region × sex ($F(4,928) = 5.51$, $p = 0.0002$), and cycle × region($F(12,2784) = 6.97$, $p < 0.0001$, indicating increased $lnC_{2.5}$ values in first cycle of children, increased $lnC_{2.5}$ in the fronto-central regions of children, decreased $lnC_{2.5}$ in posterior regions of men, lack of decreasing from cycle 3 to 4 in central and parietal regions compared to other regions, respectively.

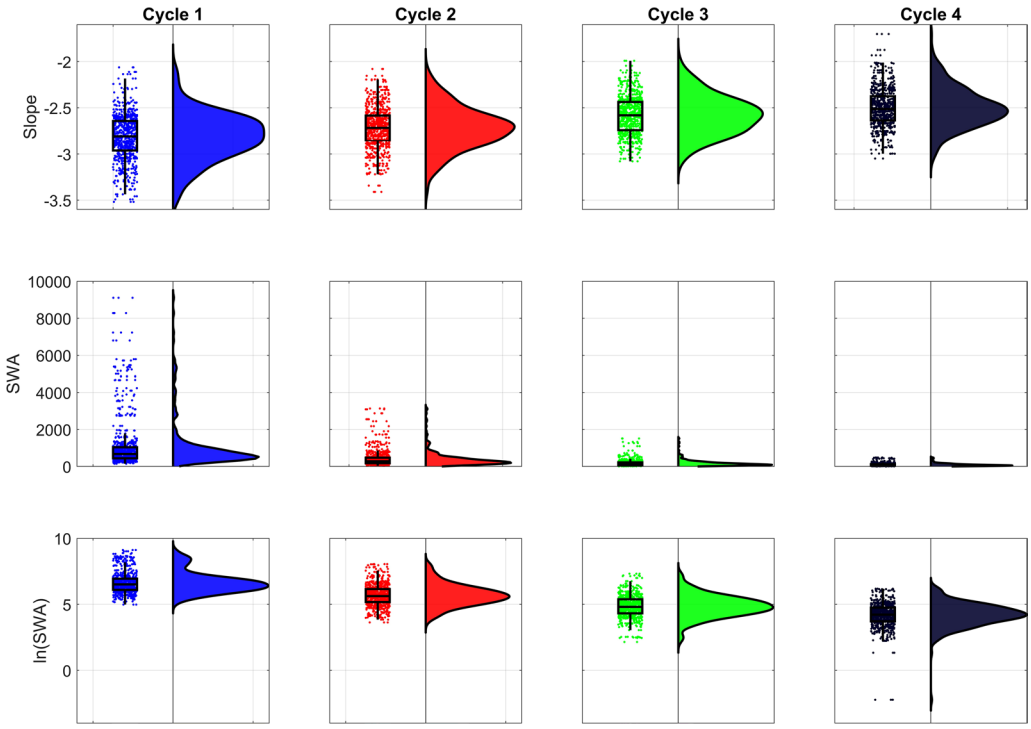

Figure 5. Raincloud plot of NREM sleep EEG spectral slopes, SWA, and lnSWA in the first four sleep cycles. Note the skewness and/or bimodality of the distributions, as well as the increased number of outliers of SWA and lnSWA compared to slope values.

	Cycle	Valid N	Mean	Minimum	Maximum	Std.Dev.	Coef.Var.
ln SWA+4	1	251	10.65	8.98	13.12	0.81	7.64
	2	251	9.68	7.63	12.05	0.81	8.38
	3	249	8.85	6.15	11.32	0.84	9.46
	4	240	8.18	1.77	10.18	0.91	11.11
slope+4	1	251	6.82	6.06	7.52	0.25	3.72
	2	251	6.72	6.08	7.41	0.23	3.38
	3	249	6.58	5.99	7.08	0.21	3.16
	4	240	6.50	5.70	7.05	0.21	3.30

Table 1. Descriptive statistics and coefficients of variation of NREM sleep EEG lnSWA and spectral slopes (left frontal recording location: F3).

Can the classical measure of sleep intensity (SWA) be predicted by the spectral slope and alternative intercept? As the alternative intercepts have shown a cyclic change, we were curious about how much the slope and the $lnC_{2.5}$ contribute to the nature of SWA in different cycles.

A linear regression model was built to predict SWA from slope of the spectrum and $lnC_{2.5}$ in all cycles (fitted regression model in cycle 1: SWA = − 4293.8–0.44*(slope) + 0.59*($lnC_{2.5}$); cycle 2: SWA = − 1165.1–0.39*(slope) + 0.59*($lnC_{2.5}$); cycle 3: SWA = − 378.3–0.36*(slope) + 0.63*($lnC_{2.5}$); cycle 4: SWA = − 230.6–0.45*(slope) + 0.57*(ln $C_{2.5}$)). The model gave significant result in each case with both of the predictors having a significant contribution (cycle 1: $R^2 = 0.73$, $F(2,248) = 334.8$, $p < 0.0001$; cycle 2: $R^2 = 0.60$, $F(2,248) = 187.7$, $p < 0,0001$; cycle 3: $R^2 = 0.58$, $F(2,246) = 172.9$, $p < 0,0001$; cycle 4: $R^2 = 0.51$, $F(2,237) = 123.3$, $p < 0.0001$). The contribution of slope was lower than of $lnC_{2.5}$ and it has a negative sign (decrease in lnSWA; cycle 1: $\beta = -0.44$, $p < 0.0001$; cycle 2: $\beta = -0.39$, $p < 0.0001$; cycle 3: $\beta = -0.36$, $p < 0.0001$; cycle 4: $\beta = -0.45$, $p < 0.0001$) while the alternative intercept contributed to the model with a positive sign (increase in lnSWA; cycle 1: $\beta = 0.59$, $p < 0.0001$; cycle 2: $\beta = 0.59$, $p < 0.0001$; cycle 3: $\beta = 0.63$, $p < 0.0001$; cycle 4: $\beta = 0.57$, $p < 0.0001$). Thus, the two predictors together explained about the 73%, 60%, 58%, 51% of the variance in the 1st, 2nd, 3rd, 4th sleep cycles respectively.

Overnight change in the frequencies of the maximal peaks ($f_{maxPeak}$) in the spindle frequency range (9–18 Hz). Frequencies of the maximal peaks were significantly affected by age ($F(3,181) = 10.34$,

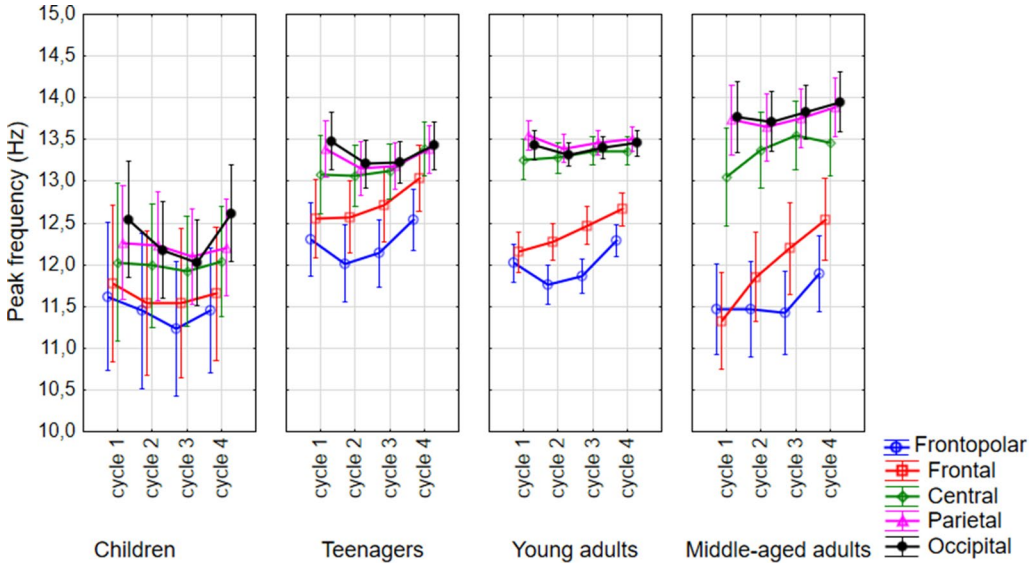

Figure 6. Cycle dynamics of the frequencies of the maximal peaks in the spindle range. Dots are group mean values, whereas vertical bars denote 95% confidence intervals.

		C1 vs. C2 p-value	C2 vs. C3 p-value	C3 vs. C4 p-value	M_{c1}	SE_{c1}	M_{c2}	SE_{c2}	M_{c3}	SE_{c3}	M_{c4}	SE_{c4}
Slope	Children	< 0.0001	< 0.0001	0.644	− 3.10	0.037	− 2.83	0.038	− 2.57	0.036	− 2.50	0.036
	Teenagers	0.034	0.012	0.452	− 2.69	0.034	− 2.58	0.035	− 2.46	0.033	− 2.38	0.032
	Young adults	< 0.0001	< 0.0001	0.048	− 2.68	0.017	− 2.59	0.018	− 2.50	0.017	− 2.44	0.016
	Middle-aged	1.000	0.052	0.591	− 2.57	0.036	− 2.54	0.038	− 2.43	0.035	− 2.35	0.035
	Frontopolar	< 0.0001	< 0.0001	< 0.0001	− 2.76	0.017	− 2.67	0.018	− 2.50	0.017	− 2.40	0.017
	Frontal	< 0.0001	< 0.0001	< 0.0001	− 2.84	0.017	− 2.74	0.017	− 2.57	0.016	− 2.48	0.016
	Central	< 0.0001	< 0.0001	< 0.0001	− 2.82	0.017	− 2.70	0.017	− 2.55	0.016	− 2.48	0.017
	Parietal	< 0.0001	< 0.0001	< 0.0001	− 2.76	0.017	− 2.61	0.017	− 2.47	0.016	− 2.41	0.016
	Occipital	< 0.0001	< 0.0001	< 0.0001	− 2.61	0.018	− 2.47	0.018	− 2.35	0.018	− 2.32	0.017
Max peak frequency	Children	1.000	1.000	0.972	12.05	0.213	11.88	0.202	11.77	0.183	11.99	0.190
	Teenagers	0.724	1.000	0.011	12.96	0.106	12.81	0.100	12.88	0.090	13.15	0.094
	Young adults	0.834	0.303	0.010	12.88	0.054	12.81	0.051	12.91	0.046	13.05	0.048
	Middle-aged	0.999	0.981	0.578	12.67	0.131	12.81	0.124	12.95	0.112	13.15	0.116
	Frontopolar	< 0.0001	0.980	< 0.0001	11.85	0.100	11.67	0.110	11.66	0.090	12.04	0.090
	Frontal	0.167	0.001	< 0.0001	11.95	0.110	12.06	0.100	12.23	0.100	12.48	0.090
	Central	1.000	0.940	1.000	12.85	0.110	12.93	0.090	12.99	0.080	13.06	0.080
	Parietal	0.043	1.000	0.930	13.23	0.080	13.11	0.080	13.12	0.070	13.24	0.070
	Occipital	0.109	0.999	0.507	13.30	0.080	13.11	0.070	13.12	0.060	13.36	0.070
Max peak amplitude	Children	0.031	0.137	1.000	0.94	0.15	1.28	0.16	1.49	0.16	1.63	0.16
	Teenagers	< 0.0001	0.073	0.999	1.67	0.07	1.92	0.08	2.07	0.08	2.13	0.08
	Young adults	< 0.0001	< 0.0001	0.001	1.85	0.040	2.04	0.040	2.15	0.040	2.26	0.040
	Middle-aged	1.000	0.973	1.000	1.60	0.090	1.67	0.100	1.76	0.100	1.77	0.100
	Frontopolar	0.991	< 0.0001	< 0.0001	1.37	0.063	1.43	0.065	1.54	0.066	1.66	0.068
	Frontal	< 0.0001	< 0.0001	< 0.0001	1.61	0.056	1.75	0.061	1.88	0.059	1.96	0.060
	Central	< 0.0001	< 0.0001	< 0.0001	1.59	0.053	1.88	0.060	2.06	0.057	2.15	0.057
	Parietal	< 0.0001	< 0.0001	< 0.0001	1.72	0.054	2.04	0.060	2.21	0.060	2.28	0.058
	Occipital	< 0.0001	< 0.0001	< 0.0001	1.29	0.053	1.53	0.060	1.66	0.061	1.69	0.059

Table 2. Descriptive statistics and post-hoc test (unequal N HSD) results on the cycle dynamics of the 3 spectral parameters. The table displays the difference between sleep cycles (C1, C2, C3, C4) in particular age groups and regions. M, mean; SE, standard error.

$p < 0.001$, $N_{child} = 9$, $N_{teenager} = 33$, $N_{y.adult} = 125$, $N_{m.a.adult} = 22$) sex ($F(1,181) = 4.10$, $p = 0.044$, $N_{male} = 104$, $N_{female} = 85$), sleep cycles ($F(3,543) = 11.65$, $p < 0.001$, $N = 189$), and region ($F(4,724) = 150.10$, $p < 0.001$, $N = 189$). These effects indicate the already reported lower sleep spindle frequencies in children, adult males, earlier sleep cycles, and more anterior regions, respectively. Although $f_{maxPeak}$ values formed a U-shape-like curve throughout the first 4 sleep cycles (Fig. 6), post hoc test revealed that the first 3 cycles were not significantly different from each other, whereas the $f_{maxPeak}$ values in the 4th cycle were significantly higher than in the others. During the night, the overall frequency increase along the anterior–posterior axis was 1.53 Hz in the 1st, 1.59 Hz in the 2nd, 1.5 Hz in the 3rd, and 1.14 Hz was in the 4th sleep cycle. The maximal value and location of the frequency shifts were also estimated in the different sleep cycles. Antero-posterior frequency shifts in adjacent (para)sagittal regions were tested by an adaptation of the Kullback–Leibler distance type measure involving surrogate control analyses[25]. Tests revealed striking divergences of empirically measured antero-posterior frequency shifts from the uniform distribution indicating largely non-continuous rostro-caudal changes in the frequencies of maximal spectral peaks (Z-values of the Kullback–Leibler distances were 64.69, 84.26, 80.97, and 61.77 for cycles 1, 2, 3, and 4, respectively, $p < 0.00001$ for each cycle). In terms of descriptive statistics, we found that the maximal frequency shift has a dominant location in every cycle. In the first, second and fourth sleep cycles the central to frontal region was the location of the maximal frequency shift for most of the sample (54.2%, 50.6%, and 40.6%, respectively), whereas in the third cycle, the 45% of the subjects had their maximal frequency shift in the frontal to frontopolar region (Suppl. Table 1).

Significant interaction between sleep cycles × age groups was observed ($F(9,543) = 2.38$, $p = 0.012$). Post hoc test of cycle and age groups interaction revealed that $f_{maxPeak}$ values in the fourth cycles of teenagers and young adults are higher than in the previous ones (Table 2). There was a trend for a U-shaped curve (higher first and fourth cycle, lower middle cycles) for all but the middle-aged adult group (Fig. 6). Effects of sleep cycles on maximal peak frequencies depended on electrode location (cycle × region: $F(12,2172) = 5.34$, $p < 0.001$). In the frontopolar regions the maximal peak frequencies in the second and third cycles were significantly lower than in the first and fourth (see also Fig. 1). In the parietal and occipital regions there was a trend for this effect, however, the peak frequencies in the frontal and central area did not show a U-shaped curve throughout the night (Table 2). Region and age groups significantly interacted in predicting spectral peak frequencies ($F(12,724) = 9.51$, $p < 0.0001$). That is, children had significantly lower peak frequencies in central, parietal and occipital regions than the other groups, whereas teenagers had higher frontopolar and frontal peak frequency values than middle aged adults in the same regions (Fig. 6; Suppl. Table 2, Suppl. Table 3).

Discussion

A precise description of the overnight dynamics of sleep EEG is essential for a better recognition of sleep characteristics and for understanding the underlying processes. In this proof-of-concept study we focused on overnight dynamics of the parameters that describe the power law scaling of the NREM EEG spectrum based on the analysis of successive sleep cycles. Overall, we found that both aperiodic and periodic components of the Fourier spectra undergo remarkable overnight changes. Namely, the slope values increased (absolute values decreased) and the alternative intercepts decreased during the night, besides, the largest peak of the spectrum was characterized by continuously increasing amplitudes in consecutive NREM episodes, and decreased frequencies in the middle of the night in the frontopolar region (U-shape curve in consecutive sleep cycles). Our findings suggest that sleep intensity can be approached by the scale-free measure of frequency dependent decay rate of EEG power, that is by the spectral slope (in the log–log plane) or spectral exponent (in the linear coordinate system). However, the absolute value of the spectral slope (exponent) is not the only measure characterized by overnight decreasing dynamics, nor in predicting SWA, the gold standard measure of sleep intensity. The alternative intercept measure termed $lnC_{2.5}$ is characterized by similar features. Furthermore, the maximal peak frequencies of the Fourier spectra decelerate in the 2. and 3. sleep cycles in the frontopolar, but not in the frontal and central regions. The latter regions might be characterized by the reorganization of the fast and slow spindles during the night.

The number of studies indicating that the power-law exponent of EEG spectra is a correlate of sleep depth, consciousness, and arousal increases steadily. Reduced conscious awareness (or arousal) was related to steeper spectral slopes in these studies[16–18]. Besides, in our former study[14], we found that aging was associated with decreased steepness of the whole night NREM sleep EEG Fourier spectra. This finding coheres with the literature indicating decreased SWA[26] and at the same time increased high frequency EEG activity[27] in the aged. In the present study, we analyzed the cycle-to-cycle dynamics of spectral exponents, as well as SWA at derivation F3. In coherence with the above-mentioned reports, we found an overall age effect in spectral slopes (exponents), SWA and lnSWA. That is with aging, the absolute values of the NREM sleep EEG spectral slopes got smaller at all derivations and in all sleep cycles, whereas the well-known SWA reduction with the progression of age was also evident. A decrement in stage 3 or slow wave sleep, and in slow wave activity (for an overview see[26]) was often associated with the reduction of sleep depth in the elderly. Further similarities between the spectral slopes and SWA was seen in the cycle dynamics of the metrics. Regarding slope values an increasing trend (absolute values declining) can be seen in all age groups throughout the cycles and the opposite trends (because of the opposite sign) were seen in the cycle dynamics of SWA and lnSWA. Thus, increasing and decreasing spectral exponents and SWA in successive sleep cycle were significant in the whole sample, respectively. However, this cycle effect was not significant neither with respect to slopes nor in terms of SWA in the middle-aged group (Fig. 3, Table 2). That is, the increase of the slope values and decrease of SWA throughout the night was smaller in middle-aged as compared to younger subjects. This finding parallels earlier reports on the reduced decay rate of SWA in aged subjects and can be modelled by the assumed attenuation of sleep efficiency in the elderly[28,29]. Nevertheless, it seems that the slope of the Fourier spectrum behaves similar to the classical SWA. Not only with respect to their non-linear decay as sleep progresses, but also regarding age and their regional differences

along the fronto-posterior gradient. In the frontal and central regions, the slope was steeper than in the occipital region. It is known that delta waves have higher values over the frontal areas[30]. Furthermore, the two metrics highly correlated which fact alone suggest a convergent validity of the slope. In the light of former studies on sleep depth and spectral exponents and our findings on the spectral slopes in relation with age, cycle dynamics and regional differences, we can suggest that α can be a promising alternative indicator of sleep intensity. Although the reliability and trait-like nature of SWA is indisputable, the slope also has its own advantages. Firstly, this metric is normally distributed, which makes it "usable" in standard statistical models. Secondly, its variability between individuals is much smaller than the interindividual variability of the SWA, even if the log-normalized value of the SWA is considered. That is, the spectral slope is a less individual specific metric. One of the largest criticism in the literature with regard to SWA is its large interindividual variability which make impossible to set up a given reference point for healthy sleep[22–24]. Although slope values smooth down the individual trait effects of specific to the particular subjects as compared to SWA, yet it does not completely blur the fundamental individual differences (such as age or regional), thus it could provide a road toward setting up reference values of sleep intensity in later studies. If this assumption holds true, in the future, we could make difference between healthy and unhealthy sleep with the help of this metric, but less between two individuals with healthy sleep (which latter is one of the main advantage of the classical power values in general and SWA in particular). Hints for the reliability of this assumption were already published in a report indicating flattened spectral slopes in insomnia and sleep misperception subjects[31]. Of course, this idea needs further investigations including even larger datasets, protocols involving the experimental challenge of the sleep homeostat, and /or, measurements of the same subjects across time to reveal inter- and intraindividual differences more widely.

The overnight dynamics of the "slope-free" alternative intercepts were also tested. Results were similar to the ones reported for the spectral slopes in terms of cycle, age, and region effects. However, we found that these alternative intercepts are not independent from the slope if we parametrize the spectra in separate sleep cycles. Indeed, the regression models revealed that these intercepts and the spectral slopes are reliable predictors of SWA. A social isolation EEG study found reduction in broadband power as a result of isolation[32], suggesting the neural origin and homeostatic relevance of the spectral intercept. However, for a better understanding of the role of broadband power/spectral intercept, as well as the dynamical change of the assumed slope-free intercept during the successive sleep cycles, future studies should explicitly focus on this phenomenon.

Maximal peak frequency values in the spindle frequency range (9–18 Hz) were hypothesized to show a U-shaped distribution over consecutive sleep cycles in the frontopolar and parieto-occipital regions. In a recent report[10] we revealed that slow and fast sleep spindle frequencies display a U-shaped overnight dynamic, dampening with age and during daytime-sleep sleep spindles are faster than during the night. While our former study revealing the U-shaped overnight dynamics of sleep spindle frequencies was based on the Individual Adjustment Method (IAM)[10], here we relied on the peak frequency of the whitened power spectra of NREM sleep EEG. Whitening means the removal of the power law trend of the spectra, a step implemented before peak detection in the current, but not in our former study based on the inflection points of the amplitude spectra of NREM sleep EEG. Further differences between our current spectral parametrization and former IAM-based study find its roots in the robust, overall mean frequencies used in the IAM, which contrast the EEG recording location-specific approach in the present report. Last, but not least, IAM sleep spindle frequencies are categorized into slow and fast instances based on both frequency and topography, whereas this distinction is not inherent to the current approach during which we only focused on the EEG recording-specific maxima of the whitened power. Anyhow, the known sex[33,34], age[35,36], and region[37] effects on sleep spindle frequencies were reproduced by this measure. Namely, women had higher, children had lower maximal peak frequencies than men and other age groups, respectively. Furthermore, maximal peak frequencies were lower in anterior as compared to posterior regions. That is, the frequency of the largest peak is roughly corresponding to the sleep spindle frequency. In the present report we found a significant U-shaped curve dynamic of maximal oscillatory peak frequency in the frontopolar region. However, in the frontal and central regions the maximal peak frequencies did not show U-shaped curve during the night. This phenomenon can be due to the changing predominance of slow and fast spindles in consecutive sleep cycles. Fast spindle frequency activity was found to increase during the night, but at the same time a decrease in slow frequency spindling activity was also reported[37,38]. Indeed, in the present study we found that the amplitude of the largest peaks increased in consecutive sleep cycles. As the regional differences between the fast and slow spindle frequencies are powerful and there is a well-known spindle activity growing during the night, it is possible that we see the blurring of the two types of spindles moving towards the central regions. Indeed, in the first two cycles, the dominant location of the maximal frequency shift was the central-to-frontal area in the sample. For the third cycle, this maximal frequency shift moved forward to the frontal-to frontopolar region. This phenomenon can be due to the increase of the fast spindle dominance. However, although in the 4th cycle the maximal frequency shift was occurred again in the central-to-frontal area in most of the subjects (~ 40% of the sample), the difference between the percentage distribution regarding the most and second most dominant location of the maximal frequency shifts getting smaller as the cycles progressed (see Suppl. Table 1). That is, there is an obvious central-to-frontal predominance of the maximal frequency shift in the first cycle but nearly-equal dominances in the 4th cycle regarding central-to-frontal and frontal-to-frontopolar areas. Thus, we suggest that the cycle dynamic of the maximal peak frequencies is contaminated by nocturnal reorganization of the fast and slow spindles in these regions.

There is a lack of and a desperate need for a set of reliable, standardisable polysomnography markers suitable for the assessment of sleep regulation and quality. Such EEG indicators would reduce the complicatedness and arbitrariness of measuring healthy sleep in the related fields of research and medicine. With the present report, we aimed to describe the overnight dynamics of both periodic and aperiodic components of the NREM EEG power spectra. We would like to draw attention to the possibility that these nocturnal patterns may reveal important information on assumed sleep regulatory processes, thus, the description of them is an essential initial step in

this field of research. However, there are some shortcomings of this study which need to be handled in the future. Firstly, the parametrization of the power spectra was only adapted to NREM sleep. It would be interesting to test the development of the spectral slope during the whole sleep in all states. Secondly, the frequency range of the linear fitting (2–48 Hz, excluding the 6–18 Hz frequency range) was chosen arbitrarily which can influence the results. In addition, it is known, that the amount and size of spectral peaks can be variable among people, thus considering only the most prominent spectral peaks (in the spindle range) could bias our results. There is a need for more precise extraction of the spindle frequency values from the parametrized power spectra and the comparison our results with other parametrization methods such as Fitting Oscillations & One-Over-F[15] or Irregular Resampling Auto-Spectral Analysis[39]. Finally, we think that future studies could reveal the role of these parameters in sleep regulatory mechanisms, for example by comparing them with gold standard sleep regulatory indicators (SWA, melatonin, core body temperature) in specific conditions (such as sleep deprivation, sleep displacement).

Methods

Subjects. For this retrospective study, second night records of the already published night-time polysomnography data were used from the Budapest-Munich database[40] to avoid first night effect. Age ranges of the 251 participants (122 females) were between 4 and 69 years with a mean of 25.13. Maximum of two cups of coffee were allowed before noon but alcohol consumption was restricted. Eight participants were light smokers, for them, smoking was not prohibited. All subjects were free of psychiatric or neurological disorders based on self-reports. Ethics Committee of the Semmelweis University (Budapest, Hungary) or the Medical Faculty of the Ludwig Maximilians University (Munich, Germany) approved the research protocols, and the experiment was implemented in accordance with the Declaration of Helsinki. Every participant (or in case of underage, their parents/guardians) signed an informed consent about their attendance in the study.

Polysomnography. The polysomnography included EEG derivations at Fp1, Fp2, F3, F4, C3, C4, P3, P4, O1, O2 and re-referenced to mathematically linked mastoids, (all of which were placed according to international 10–20 system), furthermore, electromyography (EMG), electro-oculography (EOG) and electrocardiography (ECG) were also used. The sampling frequency for the EEG was either 249 Hz, 250 Hz or 1024 Hz and the impedances for the electrodes were kept below 8 kΩ. After the scoring of the EEG records a 4-s based artefact removal was happened. Determination of sleep cycles was based on the criteria proposed by Aeschbach and Borbély[1].

Power spectral analysis. Artefact-free, 4 s epochs with 2 s overlap were Hanning-tapered, mixed-radix fast Fourier transformed, power spectra derived in $\mu V^2/0.25$ Hz. Furthermore, EEG location-specific average power spectral density of the NREM (N2 and N3) periods of sleep cycles was calculated.

Definition of SWA. Slow-wave activity was defined as the power spectral density of 0.75–4.5 Hz EEG activity (sum of the bin power values). Analysis was performed on the left frontal EEG recording location (F3) and averaged in chunks of NREM (N2 and N3) periods of complete sleep cycles.

Spectrum parametrization. The comprehensive description of the parametrization of the power spectra can be seen in our earlier publication[14], here, the basic steps are summarized. The log–log scale of NREM (N2 and N3) sleep EEG spectra was interpolated to equidistant bins of the smallest frequency step (piecewise cubic Hermite interpolation, 0.0052 Hz). To estimate the slope of the spectrum a linear function was fitted to the data but the frequency ranges below 2 and between 6 and 18 were excluded to avoid the non-random oscillatory parts. The peak detection was conducted in the 9–18 Hz frequency range, known as broad sigma range, searching for local maxima and minima in mathematical terms. Thus, we used the first and second derivative to define critical points and differentiate maxima and minima, respectively. A spectral peak was detected and accepted if the first derivative was equal 0 and the second derivative was smaller than 0.

Statistical analysis. The 251 subjects were organized in groups along age as in our earlier report[40]. The age ranges in the resulting four groups were the following: 4 years ≤ children < 10 years, N = 31, 15 females; 10 years ≤ teenagers < 20 years, N = 36, 18 females; 20 years ≤ young adults < 40 years, N = 150, 75 females; and 40 years ≤ middle-aged adults ≤ 69 years, N = 34, 14 females. All statistical analyses were carried out with Statistica 13 software. We used general linear models to test our hypotheses. Age groups and sex were between-subject factors whereas sleep cycle, region (frontopolar, frontal, central, parietal, occipital) and hemisphere (left, right) serve as within-subject factors in the models. Second level interactions of the variables with significant main effects are considered herein. With respect to SWA, a logarithmic transformation was also applied. The values of SWA are squared numbers which do not meet the criteria of parametric statistical tests. Thus, in the comparison with the spectral slope we used the logarithm of the SWA values (lnSWA). Furthermore, as SWA was calculated only on the left frontal EEG location we did not include region and hemisphere as factors in the statistical models where we analysed SWA or lnSWA. In case of significant effects or interactions we used the Unequal N HSD post hoc test for further examinations.

The antero-posterior distributions of spectral peak frequencies were tested by the following procedure. First, we formed parasagittal regions by averaging peak frequency values in frontopolar (Fp1, Fp2), frontal (F3, F4), central (C3, C4), parietal (P3, P4), as well as occipital (O1, O2) recording locations. In the following, the regional means of spectral peak frequencies were serially subtracted in adjacent antero-posterior regions

as follows: frontal-frontopolar, central-frontal, parietal-central, occipital-parietal[14]. These successive frequency shifts were subjected to an analysis based on an adaptation of the Kullback–Leibler distance (KL distance)[25] which is widely used in statistics for estimating the difference between two distributions. The mean frequency shifts were calculated for adjacent locations as 4 bins (frontal-frontopolar, central-frontal, parietal-central, occipital-parietal) and normalized dividing each bin value by the sum over the bins, which defines the distribution P(x). The uniform distribution Q(x) was defined as the equal distribution over the four bins, 0.25. The KL distance were then calculated using the following formula: KL = sum(P(x)*log(P(x)/Q(x))). Specifically, we compared the empirical frequency shifts with the outcomes of a randomization based on 1000 iterations in each of the 4 sleep cycles separately. The observed KL values were then z-standardized to the shuffled values, where normalized z-values directly reflect p-values, Z-values of the Kullback–Leibler distances equal to 1.645 corresponds to the 5% p-value, and larger values reflect $p < 0.05$. We aimed to test if region-specific differences in peak frequencies form a uniform antero-posterior distribution with an equal probability of antero-posterior changes over all adjacent parasagittal regions (null hypothesis assuming continuous antero-posterior changes in peak frequencies) or the changes are non-continuous (assuming a differentiation between slow and fast types of sleep spindles based on non-continuous antero-posterior shifts). Furthermore, we provided a descriptive analysis on the dominant (maximal) frequency shift in each sleep cycle based on our former approach[14].

Ethical statement. We confirm that we have read the Journal's position on issues involved in ethical publication and affirm that this report is consistent with those guidelines.

Data availability

All data generated or analysed during this study are included in this published article (and its Supplementary Information files). The datasets generated during and/or analysed during the current study are available in the OSF repository, https://osf.io/q37w4/.

Received: 1 June 2022; Accepted: 25 October 2022
Published online: 01 November 2022

References

1. Aeschbach, D. & Borbély, A. A. All-night dynamics of the human sleep EEG. *J. Sleep Res.* **2**, 70–81 (1993).
2. Dijk, D. J., Hayes, B. & Czeisler, C. A. Dynamics of electroencephalographic sleep spindles and slow wave activity in men: Effect of sleep deprivation. *Brain Res.* **626**, 190–199 (1993).
3. Lunsford-Avery, J. R., Edinger, J. D. & Krystal, A. D. Optimizing computation of overnight decline in delta power: Evidence for slower rate of decline in delta power in insomnia patients. *Clin. Neurophysiol.* **132**, 545–553 (2021).
4. Nissen, C. *et al.* Delta sleep ratio as a predictor of sleep deprivation response in major depression. *J. Psychiatr. Res.* **35**, 155–163 (2001).
5. Dijk, D. J. Regulation and functional correlates of slow wave sleep. *J. Clin. Sleep Med.* **5**, 2 (2009).
6. Achermann, P., Dijk, D. J., Brunner, D. P. & Borbély, A. A. A model of human sleep homeostasis based on EEG slow-wave activity: Quantitative comparison of data and simulations. *Brain Res. Bull.* **31**, 97–113 (1993).
7. Dijk, D. J., Brunner, D. P., Beersma, D. G. M. & Borbely, A. A. Electroencephalogram power density and slow wave sleep as a function of prior waking and circadian phase. *Sleep* **13**, 430–440 (1990).
8. Ferri, R., Elia, M., Musumeci, S. A. & Pettinato, S. The time course of high-frequency bands (15–45 Hz) in all-night spectral analysis of sleep EEG. *Clin. Neurophysiol.* **111**, 1258–1265 (2000).
9. Finelli, L. A., Ackermann, P. & Borbély, A. A. Individual 'fingerprints' in human sleep EEG topography. *Neuropsychopharmacology* **25**, S57–S62 (2001).
10. Bódizs, R. *et al.* Sleep-spindle frequency: Overnight dynamics, afternoon nap effects, and possible circadian modulation. *J. Sleep Res.* **31**, 1–13. https://doi.org/10.1111/jsr.13514 (2021).
11. Pereda, E., Gamundi, A., Rial, R. & González, J. Non-linear behaviour of human EEG: Fractal exponent versus correlation dimension in awake and sleep stages. *Neurosci. Lett.* **250**, 91–94 (1998).
12. Pritchard, W. S. The brain in fractal time: 1/f-like power spectrum scaling of the human electroencephalogram. *Int. J. Neurosci.* **66**, 119–129 (1992).
13. Feinberg, I., March, J. D., Floyd, T. C., Fein, G. & Aminoff, M. J. Log amplitude is a linear function of log frequency in NREM sleep EEG of young and elderly normal subjects. *Electroencephalogr. Clin. Neurophysiol.* **58**, 158–160 (1984).
14. Bódizs, R. *et al.* A set of composite, non-redundant EEG measures of NREM sleep based on the power law scaling of the Fourier spectrum. *Sci. Rep.* **11**, 2041 (2021).
15. Donoghue, T. *et al.* Parameterizing neural power spectra into periodic and aperiodic components. *Nat. Neurosci.* **23**, 1655–1665 (2020).
16. Colombo, M. A. *et al.* The spectral exponent of the resting EEG indexes the presence of consciousness during unresponsiveness induced by propofol, xenon, and ketamine. *Neuroimage* **189**, 631–644 (2019).
17. Lendner, J. D. *et al.* An electrophysiological marker of arousal level in humans. *Elife* **9**, 1–29 (2020).
18. Miskovic, V., MacDonald, K. J., Rhodes, L. J. & Cote, K. A. Changes in EEG multiscale entropy and power-law frequency scaling during the human sleep cycle. *Hum. Brain Mapp.* **40**, 538–551 (2019).
19. Freeman, W. J., Holmes, M. D., West, G. A. & Vanhatalo, S. Fine spatiotemporal structure of phase in human intracranial EEG. *Clin. Neurophysiol.* **117**, 1228–1243 (2006).
20. Gao, R., Peterson, E. J. & Voytek, B. Inferring synaptic excitation/inhibition balance from field potentials. *Neuroimage* **158**, 70–78 (2017).
21. Webb, W. B. & Agnew, H. W. Stage 4 sleep: Influence of time course variables. *Science* **174**, 1354–1356 (1971).
22. Tucker, A. M., Dinges, D. F. & Van Dongen, H. P. A. Trait interindividual differences in the sleep physiology of healthy young adults. *J. Sleep Res.* **16**, 170–180 (2007).
23. Hertenstein, E. *et al.* Reference data for polysomnography-measured and subjective sleep in healthy adults. *J. Clin. Sleep Med.* **14**, 523–532 (2018).
24. Gander, P., Signal, L., Van Dongen, H. P. A., Muller, D. & Van Den Berg, M. Stable inter-individual differences in slow-wave sleep during nocturnal sleep and naps. *Sleep Biol. Rhythms* **8**, 239–244 (2010).
25. Kullback, S. & Leibler, R. A. On Information and Sufficiency. *Ann. Math. Stat.* **22**, 79–86 (1951).

26. Taillard, J., Gronfier, C., Bioulac, S., Philip, P. & Sagaspe, P. Sleep in normal aging, homeostatic and circadian regulation and vulnerability to sleep deprivation. *Brain Sci.* **11**, 1003 (2021).
27. Carrier, J., Land, S., Buysse, D. J., Kupfer, D. J. & Monk, T. H. The effects of age and gender on sleep EEG power spectral density in the middle years of life (ages 20–60 years old). *Psychophysiology* **38**, 232–242 (2001).
28. Landolt, H. P., Dijk, D. J., Achermann, P. & Borbély, A. A. Effect of age on the sleep EEG: Slow-wave activity and spindle frequency activity in young and middle-aged men. *Brain Res.* **738**, 205–212 (1996).
29. Dijk, D. J., Beersma, D. G. M. & van den Hoofdakker, R. H. All night spectral analysis of EEG sleep in young adult and middle-aged male subjects. *Neurobiol. Aging* **10**, 677–682 (1989).
30. Werth, E., Achermann, P. & Borbély, A. A. Brain topography of the human sleep EEG: Antero-posterior shifts of spectral power. *NeuroReport* **8**, 123–127 (1997).
31. Andrillon, T. *et al.* Revisiting the value of polysomnographic data in insomnia: More than meets the eye. *Sleep Med.* **66**, 184–200 (2020).
32. Weber, J., Klein, T. & Abeln, V. Shifts in broadband power and alpha peak frequency observed during long-term isolation. *Sci. Rep.* **10**, 1 (2020).
33. Markovic, A., Kaess, M. & Tarokh, L. Gender differences in adolescent sleep neurophysiology: A high-density sleep EEG study. *Sci. Rep.* **10**, 5 (2020).
34. Ujma, P. P. *et al.* Sleep spindles and intelligence: Evidence for a sexual Dimorphism. *J. Neurosci.* **34**, 16358–16368 (2014).
35. Campbell, I. G. & Feinberg, I. Maturational patterns of sigma frequency power across childhood and adolescence: A longitudinal study. *Sleep* **39**, 193–201 (2016).
36. Ujma, P. P., Sándor, P., Szakadát, S., Gombos, F. & Bódizs, R. Sleep spindles and intelligence in early childhood-developmental and trait-dependent aspects. *Dev. Psychol.* **52**, 2118–2129 (2016).
37. Werth, E., Achermann, P., Dijk, D. J. & Borbély, A. A. Spindle frequency activity in the sleep EEG: Individual differences and topographic distribution. *Electroencephalogr. Clin. Neurophysiol.* **103**, 535–542 (1997).
38. Bódizs, R., Körmendi, J., Rigó, P. & Lázár, A. S. The individual adjustment method of sleep spindle analysis: Methodological improvements and roots in the fingerprint paradigm. *J. Neurosci. Methods* **178**, 205–213 (2009).
39. Wen, H. & Liu, Z. Separating fractal and oscillatory components in the power spectrum of neurophysiological signal. *Brain Topogr.* **29**, 13–26 (2016).
40. Bódizs, R. *et al.* The hemispheric lateralization of sleep spindles in humans. *Sleep Spindl. Cortical Up States* **1**, 42–54 (2017).

Acknowledgements

Research supported by the Hungarian National Research, Development and Innovation Office (K-128117; https://nkfih.gov.hu/about-the-office), the Ministry of Innovation and Technology of Hungary from the National Research, Development and Innovation Fund, financed under the TKP2021-EGA-25 funding scheme, the Netherlands Organization for Scientific Research (NWO; https://www.nwo.nl/en), the European Cooperation in Science and Technology (COST Action CA18106; https://www.cost.eu/), as well as the general budgets of the Institute of Behavioural Sciences, Semmelweis University (http://semmelweis.hu/magtud/en/) and the Max Planck Institute of Psychiatry (https://www.psych.mpg.de/en). The funders had no role in study design, data collection and analysis, decision to publish, or preparation of the manuscript.

Author contributions

C.G.H. and R.B. conceived the study; R.B., P.S., I.K., and M.D. contributed to data collection; O.S., R.B., C.G.H., P.P.U., P.S., and F.G. contributed to data analysis; all authors drafted the manuscript, critically revised the major intellectual content and approved the final version of the paper.

Funding

Open access funding provided by Semmelweis University.

Competing interests

The authors declare no competing interests.

Additional information

Supplementary Information The online version contains supplementary material available at https://doi.org/10.1038/s41598-022-23033-y.

Correspondence and requests for materials should be addressed to C.G.H.

NeuroImage 314 (2025) 121260

Contents lists available at ScienceDirect

NeuroImage

journal homepage: www.elsevier.com/locate/ynimg

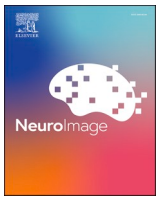

Effect of sleep deprivation on fractal and oscillatory spectral measures of the sleep EEG: A window on basic regulatory processes

Csenge G. Horváth *, Róbert Bódizs

Institute of Behavioural Sciences, Semmelweis University, Nagyvárad tér 4. 20th floor, Budapest H-1089, Hungary

ARTICLE INFO

Keywords:
Sleep deprivation
Homeostasis
NREM phase
Circadian rhythm
Sleep spindles
Aperiodic activity
sleep EEG

ABSTRACT

Sleep is vital for sustaining life; therefore, reliable measurement of its regulatory processes is of significant importance in research and medicine. Here we examine the effect of extended wakefulness on the putative indicators of fundamental sleep regulatory processes (spectral slope and spindle frequency) proposed by the Fractal and Oscillatory Adjustment model of sleep regulation by involving a healthy young adult sample in a 35-hour long sleep deprivation protocol. Wearable headband EEG-derived results revealed that NREM sleep electroencephalogram (EEG) spectral slope estimated in the 2–48 Hz range is an accurate indicator of the predicted changes in sleep depth induced by sleep deprivation (steepened slopes in recovery sleep) or by the overnight dissipation of sleep pressure (flattening slopes during successive sleep cycles). While the baseline overnight dynamics of the center frequency of the sleep spindle oscillations followed a U-shaped curve, and the timing of its minimum (the presumed phase indicator) correlated with questionnaire-based chronotype metrics as predicted, a different picture emerged during recovery sleep. Advanced recovery sleep advanced the timing of the minima of the oscillatory spindle frequency, reduced considerably its relationship with chronotype, but retained partially its U-shaped overnight evolution. Overall, our study supports the use of the spectral slope of the sleep EEG as a homeostatic marker of wake-sleep regulation, in addition, encourages further research on the EEG-derived measure of the circadian rhythm, primarily focusing on its interaction with the homeostatic process.

1. Introduction

In the past few years, the characterization and appropriate parametrization of the EEG Fourier power spectrum has gained increasing interest, as it became clear that besides the undeniable importance of neural oscillations, the aperiodic brain activity also carries substantial information on neural functioning. The same holds true for the field of sleep research, where nowadays -after the proper distinction of the periodic and aperiodic part of the spectrum-, analyses of the aperiodic component came to the forefront.

The so-called spectral slope (or spectral exponent) describes the linear relationship between the logarithm of power and the logarithm of frequency which is due to the power-law distribution of the EEG spectrum (Bódizs et al., 2021; Feinberg et al., 1984; Pritchard, 1992). In a recent paper of ours, we thoroughly reviewed the literature and came to the conclusion that results regarding the spatio-temporal and age-related variation of the sleep EEG spectrum are highly consistent with the assumption of the pivotal role of aperiodic activity in wake-sleep regulation (Bódizs et al., 2024). The EEG metrics of aperiodic activity were found to be a suitable indicators of consciousness and arousal (Colombo et al., 2019; Lendner et al., 2020; Waschke et al., 2021; Zhang et al., 2023), as well as reliable measures in distinguishing between different brain states like resting and active wakefulness or between stages of sleep (Favaro et al., 2023; Höhn et al., 2024; Miskovic et al., 2019; Schneider et al., 2022). Additionally, we found that the temporal evolution of the spectral slope throughout the night depends on the preliminary amount of sleep, that is slope flattens as sleep progresses (Horváth, et al., 2022), based on which it is a putative indicator of sleep-wake history. Hence, results of the literature support the assumption that EEG spectral slope could be a reliable marker of sleep homeostasis. To put it simply, sleep homeostasis refers somehow to the constancy of the sleep-wake dynamics. When one state overloads, the other has to recover so that the system can be stable again.

However, to maintain a balanced functioning within the context of ecologically definitive day-night cycles, the timing of sleep and wake is also an important factor. Formerly we proposed a putative sleep timing-related EEG measure derived from the oscillatory (periodic) activity emerging in the spindle frequency range (Bódizs et al., 2024). Sleep

* Corresponding author.
E-mail address: horvath.csenge@phd.semmelweis.hu (C. G. Horváth).

https://doi.org/10.1016/j.neuroimage.2025.121260
Received 26 November 2024; Received in revised form 13 April 2025; Accepted 8 May 2025
Available online 9 May 2025

spindles are major EEG graphoelements of the NREM sleep EEG composed by 0.5–3 s long trains of waves of 11–16 Hz frequency and characteristic biphasic amplitude evolution: progressive increase followed by gradual decrease. This type of oscillations is hypothesized to critically depend on the inhibitory projections of the thalamic reticular nucleus and reflect the hyperpolarization-rebound sequences of thalamocortical cells. The spectral EEG signature of sleep spindle oscillations is known to contribute to the periodic component of the Fourier spectra in the form of spectral peaks at distinct frequencies (Bódizs et al., 2009; Fernandez and Lüthi, 2020). Former research indicate that sleep spindle frequency can convey information on sleep timing (Bódizs et al., 2022). Accordingly, spindle frequency was found to covariate with reliable circadian indicators, like core body temperature (correlation) and melatonin (anticorrelation) (Knoblauch et al., 2005; Wei et al., 1999), furthermore, the timing of the nadir of the spindle frequency (NSSF) associated with actigraphy-derived circadian phase index (Horváth and Bódizs, 2024). Time-of-day dependence of spindle frequency activity was proved directly with specific study designs targeting the separated analysis of circadian phase and sleep-wake history (Aeschbach et al., 1997; Dijk, 1999). These studies found larger spindle activity at lower spindle frequencies during the night-time and this activity dominance transferred to higher frequencies towards daytime. Further indirect proofs of time-of-day-dependency are the results showing spindle frequency is higher during daytime as compared to night-time sleep (Bódizs et al., 2022; Rosinvil et al., 2015), and follows a U-shape curve during the night with the minimum around the middle of the sleep period potentially reflecting night time temperature drop-related oscillatory deceleration and/or direct melatoninergic effects (Bódizs et al., 2022; Csernai et al., 2019; Horváth, et al., 2022; Horváth and Bódizs, 2024).

The ground-breaking framework which considers the interaction of timing and sleep homeostasis as the foundations of sleep regulatory mechanisms is the two-process model of sleep regulation proposed by Alexander Borbély (1982). However, the original model relies only on the oscillatory activity of the brain, and no EEG indicator for the circadian process (that is for the timing) was suggested. In our recent work, we recommended a new, so-called Fractal and Oscillatory Adjustment Model by revising the two-process model (Bódizs et al., 2024). In this work, we took into account the discovery that periodic and aperiodic components are two types of coexisting brain activity with equally important information content. Besides this model proposition, our aim was to support the assumptions that sleep homeostasis is reliably reflected by the spectral slope while circadian regulatory process can be indexed by the oscillatory frequency in the spindle band.

To validate the above assumptions, we implemented the recordings and analyses of baseline- and recovery sleep (BS and RS, respectively) of healthy young adults with the use of a sleep deprivation (and displacement) study design adapted from Dijk et al. (1990). Here we applied a 35-hour long home sleep deprivation protocol relying on wearable headband EEG devices, with chronotype-dependent BS bedtimes. To our best knowledge this is the first report in which spectral slope and oscillatory spindle frequency were examined by experimental challenge of the homeostatic process (35-hours of sleep deprivation) and with a slight rescheduling of sleep with the aim of unravelling the circadian clock (RS period advanced by ~4.5 h). We parametrized the NREM EEG power spectra for every sleep cycle (NREM-REM periods), furthermore, we defined spindle frequency as the center frequency of the most prominent peak in the 9–16 Hz frequency range (CF) as indicated by the parametrization procedure. Both the effect of sleep deprivation and the overnight dynamics of spectral slope and CF were thoroughly analysed, and the following hypotheses were tested:

A) The NREM sleep EEG spectral slope:

hyp 1. will be flatter in BS than in RS in the first 4 cycles of sleep (experimental challenge of the sleep homeostat results in increased sleep EEG spectral slope steepness)

hyp 2. will flatten during the night in both sleep condition (BS and RS) in parallel with the decrease of sleep pressure

hyp 3. values of the BS and RS conditions will differ to a greater extent in the first cycles, as compared to the last cycles of sleep due to the increased sleep pressure caused by the deprivation at the beginning of the night, as well as because of the concept of homeostasis assumes that a near-equilibrium state should return at the end of recovery sleep.

hyp 4. will be the steepest at the beginning of the night and this steepest slope will be flatter in BS than in RS. However, there will be no difference regarding minimal values (same explanation as for hyp 3) which are hypothesized to occur at the end of the night in both conditions.

B) Spindle center frequency (CF):

hyp 1. will develop differently during the first 4 cycles of sleep in BS compared to RS. CF will evolve according to a U-shaped curve (decelerate in 2nd or 3rd cycle) in the first 4 cycles of sleep in BS, but not in RS. We hypothesized this latter is caused by the advanced sleep schedule (sleeping period starts approximately 4.5 hours earlier than the habitual bedtime of the participants), as well as because of the heightened number of sleep cycles in RS (the 4th cycle should fall around the middle of the night).

hyp 2. will follow a U-shape-like evolution (deceleration followed by acceleration) in both BS and RS, when the whole sleep period is considered.

hyp 3. values will not differ in the last and first cycles of the two nights

hyp 4. minima will appear around the same time in both nights, that is NSSF will not differ between conditions as it depends more on time-of-day. Furthermore, NSSF in BS (when the sleep schedule is regular) will occur around the middle of the sleep period.

Finally, for validation purposes we intended to replicate the SWA results of Dijk et al. (1990), (Dijk et al., 1990). Namely, elevated SWA in RS, SWA decrease in the first 3–4 sleep cycles and nearly uniform SWA levels in the later sleep cycles.

2. Methods

2.1. Sample

In this experimental study $N = 46$ healthy young adults participated in a 7-day long protocol involving actigraphy, headband-wearable recorded sleep EEG, and a 35 hour-long sleep deprivation followed by ad libitum recovery sleep. Due to poor quality EEG recordings or complete data loss the final sample consisted of $N = 38$ subjects (age range: 18–39 years, mean age= 24.9, 19 females).

Participants were enrolled by a combination of convenience and snowball sampling procedures involving personal contacts and social media calls. All subjects were free of psychiatric or neurological disorders based on self-reports. In addition, the exclusion criteria of the study included the Hungarian version of Pittsburgh Sleep Quality Index (Takács et al., 2016) score over 5, Beck Depression Inventory (Beck et al., 1961) score over 12 (moderate and severe depression symptoms (Rózsa et al., 2001), alarm clock usage on free days, extreme circadian preference (MCTQ chronotype scores outside of the ±2 SD of reported values in young Hungarian subjects according to Haraszti et al. (2014) and shift work, as well as reported acute and/or chronic medical diagnoses or ongoing pharmacological treatments.

2.2. Study protocol

After the questionnaire-based testing of inclusion/exclusion criteria, enrolled participants had to wear a GENEActiv triaxial accelerometer (Activinsights, Cambridge, United Kingdom) for 7 days on their non-

dominant wrist. No instructions were given for the first 4 days except not to take off the actigraphy device for any activity. On the 5th day, participants had to go to the laboratory to learn how to use the mobile EEG device and to perform Mnemonic Similarity Test (Stark et al., 2013), N-back (Layden, 2018) and a perceptual inference paradigm (Pálffy et al., 2021). On this same evening (5th night of the experiment), subjects slept with the wearable EEG headband in their own home. During this BS EEG measurement, the bedtime was freely chosen by the participants thus, they could go to bed according to their own preferences. The use of an alarm clock was prohibited in both the mornings of headband-EEG-recorded sleep (BS and RS). After waking up from BS, the sleep deprivation part of the study began. Participants had to stay awake for 35 hours during which alcohol and any kind of stimulant consumption was prohibited with the exception of caffeine. Participants were allowed to consume as much coffee as they typically would in an average 24-hour day; however, caffeine intake was restricted to no more than the equivalent of 3 espresso shots during the entire sleep deprivation period. As it was an at-home examination, participants could freely choose their activities throughout the 35 hours of wakefulness, however, they had to have continuous contact with the experimenter (at least one report on their well-being and actual activity per hour via mobile phone messages) and complete questionnaires (sleepiness scales) at specified time points (in the 0th, 12th, 24th, and 35th hour of the sleep deprivation). Moreover, in the 24th and 34th hour of sleep deprivation, experimenters went to the participants' homes to record the cognitive tasks and check their well-being and their adherence to the study protocol in person. Overall, compliance with the study protocol was checked by verifying whether all hourly text messages were sent, and the questionnaires were completed at every given time points by the participants. Finally, compliance was confirmed through offline post-participation evaluation of actigraphy data if there were no indications of sleep during the 35-hour period. At the end of the sleep deprivation, the experimenter helped the subjects to put on the EEG headband and instructed them to turn off the lights and go to bed. This was the recovery night sleep EEG measurement. After waking up, participants' last task was to fill out the sleepiness scales one more time, then the experiment ended. In the present study some of the questionnaires (MCTQ, sleepiness scales) and the sleep EEG data were analysed.

National Public Health Centre Institutional Committee of Science and Research Ethics approved the research protocols, and the experiment was implemented in accordance with the Declaration of Helsinki. Every participant signed an informed consent about their attendance in the study.

2.3. Sleep EEG

Electroencephalography of sleep was recorded by Hypnodyne corp. Zmax EEG headband with sampling rate of 256 Hz at derivations F7-Fpz and F8-Fpz re-referenced to their common average. Manual sleep scoring and artefact removal was performed in 20 and 4 s epochs, respectively. Sleep recordings were divided into sleep cycles (successive NREM+REM episodes) and only NREM sleep was analysed in each cycle. Determination of sleep cycles was based on the modified Feinberg and Floyd criteria (Feinberg and Floyd, 1979) proposed by Jenni and Carskadon (2004) with the consideration of skipped REMs in the first cycle of sleep. Manual artefact removal was followed by a power spectral density (PSD) analysis using the Welch method. The EEG signal was divided into 4-second epochs with 50 % overlap. A Hann window was applied to each epoch, and the Fast Fourier Transform (FFT) was computed for all NREM (N2 + N3) periods within each sleep cycle. Finally, the resulting spectral estimates were averaged across all 4-second epochs within each sleep cycle. For spectral calculations, the number of analysable epochs across individuals and sleep cycles ranged from 158 to 1442 epochs in BS (C1–C6), and 154 to 1448 epochs in RS (C1–C9). The mean number of artefact-free epochs during BS was 752.8 in C1, 741.2, in C2, 786.3 in C3, 671.6 in C4, 547 in C5, 552.8 in C6. During RS, the mean was 759.8 in C1, 706.9 in C2, 793.6 in C3, 783.3 in C4, 814.7 in C5, 798 in C6, 682.8 in C7, 625 in C8, and 550 in C9.

2.3.1. Definition of SWA

SWA was calculated as the sum of the bin power values in the 0.75–4.5 Hz EEG activity range of the averaged N2 & N3 episodes of complete sleep cycles.

2.3.2. Parametrization of the sleep EEG spectrum

The fitting oscillations and 1-over-f (FOOOF) method, developed by Donoghue et al. (2020), aims to parametrize the power spectrum into aperiodic and periodic components. The method can be described briefly with the following steps. First, it estimates and removes an approximated aperiodic component from the spectrum, thus creating a flattened version of the spectrum that highlights the spectral peaks. Then, Gaussians are iteratively fitted and subtracted to isolate the periodic components. Periodic components are removed from the spectrum, and the aperiodic part is re-fitted, then the combined version of the periodic and refitted aperiodic component can be used for further analyses.

To avoid over- or under fitting, the settings recommended by Schneider et al. (2022) was used in the present study. Fitting range was set to the 2–48 Hz frequency interval, the bandwidth of accepted peaks (peak width limit) was set to 0.7–3 Hz, the peak threshold was set to 1, aperiodic mode was set to 'fixed'. No minimum peak height or maximum number of peaks was specified; in this case, the default settings were applied.

2.3.3. Definition of CF in the spindle frequency range

To define spindle frequency, we ranked the three largest peaks (obtained using the FOOOF method) based on amplitude. In the next step, among these three peaks, we identified the one with the highest amplitude that fell within the 9–16 Hz frequency range (representing the broad spindle frequency range). This method was applied to all spectra in all sleep cycles, and the resulting frequency was analysed as spindle frequency, referred to as (spindle) CF throughout the remainder of the present study. If none of the top three peaks fell within the spindle frequency range, the corresponding spectrum was considered to lack a spindle peak, and therefore no CF value was assigned.

2.4. Questionnaires

2.4.1. Munich chronotype questionnaire

MCTQ collects information on usual bed- and wake times, sleep latency and inertia, separately for working and free days. From these time points, the middle of the sleep periods is calculated. Finally, chronotype is given as the oversleeping adjusted sleep midpoint on the free days (MSFsc) (Roenneberg et al., 2003). In most cases, this variable was used as a continuous predictor. However, groups of the different chronotypes (early-, intermediate-, and evening types) were also calculated. A person was classified either early or evening types if their values fell outside the $\pm$ 1 SD range (but within $\pm$2 SD) and as intermediate if their MSFsc fell inside the $\pm$ 1 SD range of the mean of young Hungarian subjects reported by Haraszti et al. (2014).

2.4.2. Sleepiness scales

Sleepiness was measured by two scales at the above-mentioned timepoints. Firstly, by using a simple likert-scale from 1 to 10 which was reported more sensitive to daytime dysfunction than other subjective rating scales (Riegel et al., 2013): participants were asked to rate their sleepiness level where 1 meant 'not sleepy at all' while 10 referred to 'very sleepy'. Secondly, with the widely-used Stanford Sleepiness Scale (Hoddes et al., 1973). The instrument consists of 7 phrases describing sleepiness, and participants are asked to choose the one which best indicates their current sleepiness level.

2.5. Statistics

All statistical analyses were carried out using TIBCO Statistica software. Data examination was performed in multiple settings.

We were interested in the overnight dynamics of specific spectral EEG parameters during the two nights (BS and RS) separately, as well as in the comparison of BS vs. RS. Both research questions were analysed in two ways. Firstly, in a simplified manner where we strived for keeping the sample size as high as possible, thus, the number of analysable sleep cycles were limited (the first 4 cycles were examined). Furthermore, we grouped participants according to their number of sleep cycles, and evaluated the overnight dynamics in these groups separately. In this case the sample sizes were low in the groups, but we could assess the overnight dynamics for the total night of each participant who had complete recordings. As the cycle effect was hypothesized to be substantial, we considered a group analysable if its sample size was at least $N = 7$, consequently the BS groups with 3 and 7, furthermore, RS groups with 6 and 10 sleep cycles had to be excluded as these consisted of a maximum of 3 participants. Finally, specific sleep cycles (at the beginning, the middle, and the end of the night sleep periods), as well as the sleep cycle numbers corresponding to the minimum and maximum values of the parameters were compared between the two nights.

Differences between variables and conditions were tested with the appropriate parametric statistical tests on normally distributed data: dependent sample *t*-test for two variable/condition comparison, Repeated Measures ANOVA where more than two variables/time-points were involved, General Linear models in case of multiple factors included. If the sample size was <10 (cycle group-wise analyses) or one of the variables included in the analysis had non-Gaussian distribution, non-parametric statistical version of the above-mentioned tests were used: Wilcoxon Matched pairs test, Friedman ANOVA. Except regarding SWA analyses, where logarithmic transformation of the data was performed in order to avoid statistical biases caused by the use of squared values in parametric statistical tests. In the descriptive statistics mean (m) and standard deviation (SD) are reported for data with normal distribution, and median (Mdn) with interquartile range (IQR=[lower border, upper border]) for non-normally distributed data. Test of normality was performed by Shapiro-Wilk W test for all variables. According to its results, the following variables significantly deviated from a normal distribution: the number of sleep cycles in both BS and RS, the sleep cycle in which participants had their CF minimum in BS, slope in BS cycle 4 and RS cycle 7, both sleepiness scales at all time-points, the cycles which contain the BS and RS slope value minimum and maximum.

The threshold of significance was defined as $p < 0.05$ in all analyses, in addition, Bonferroni correction was applied with the appropriate significance level, where multiple comparisons were conducted.

3. Results

Out of the recordings of the 38 participants 3 in the baseline and 7 in the recovery nights were incomplete due to device failure (e.g. poor quality data, electrode contact problems, unexpected shutdown of the device). These recordings were not involved in the analyses which assume the total length of the nights (e.g. whole night dynamics, minimum/maximum values during the night, circadian analyses), but included in the cycle-based (sample mean) comparisons between BS and RS.

Participants stayed awake for Mdn=35.79 hours (~35 h. and 47 min; min-max range: 34.9–37.3) during the extended wakefulness period. This was estimated from the scored recordings of BS and RS (length of the period between the end of BS last sleep epoch and RS sleep initiation for participants whose BS recording was complete). The average sleep duration during the BS and RS conditions was m_{BS}=7.9 (min-max: 5.8–10.7) hours and m_{RS}=12.2 (min-max: 9.7–14.74) hours, respectively, whereas the sample median of the number of sleep cycles increased from Mdn_{BS}=5 (min-max:3–7) to Mdn_{RS}=8 (min-max: 6–10) due to the experimental intervention involving sleep deprivation and RS phase advancement (analyses based on complete recordings).

The sample mean of MSFsc (MCTQ-based chronotype metric) was at 04:34 (SD=1:16 hh:mm). In total, 7 early-, 15 intermediate-, and 16 evening type (5, 6, 8 females respectively) subjects' data were analysed. Participants slept according to their circadian timing in BS as the time of day at BS start (derived from the EEG recordings) strongly positively correlated with the MCTQ-based chronotype results ($r = 0.61$, $p < 0.0001$). However, the correlation between the questionnaire-derived chronotype and RS start times was weaker and non-significant ($r = 0.3$, $p = 0.07$; Fig. 1/A). Sleepiness level increased the most from 12th to the 24th hour of the sleep deprivation period according to both scales and reduced again after waking up from RS (Fig 1./B). The difference in sleepiness levels between successive time points is significant from the 12th to the 24th hour ($t_{likert}(37)=-9.78$, $t_{SSS}(37)=-9.82$, $p < 0.0001$) and from the 35th hour to RS wake ($t_{likert}(37)=6.81$, $t_{SSS}(37)=6.2$, $p < 0.0001$).

3.1. EEG spectral slope

Effect of sleep deprivation was tested on the whole sample with General linear model using cycle and sleep condition (RS vs. BS) as within subject factors. Spectral slope was significantly steeper after sleep deprivation ($F = 65.94$, $p < 0.0001$) and flattened in the first 4 cycles of sleep ($F = 98.25$, $p < 0.0001$; Table 1), furthermore the condition × cycle interaction was also significant ($F = 2.95$, $p = 0.037$, Fig. 2.). Unequal N HSD posthoc test was conducted to examine whether successive sleep cycles differed from each other in terms of the EEG spectral slope values. Sample-level slope difference (Fig. 2.) was significant between C2 vs. C3 (BS & RS: $p < 0.001$,) and C3 vs. C4 (BS: $p = 0.02$, RS: $p < 0.001$) in both conditions, but not between C1 vs. C2 (BS: $p = 1.0$, RS: $p = 0.83$).

In order to further analyse the overnight dynamics of the whole sleep period and the differences of BS and RS, group-level and cycle-specific analyses were conducted.

Cycle count-based group analyses showed that the cycle effect remained significant even if the whole sleep period was considered (Table 2; Fig.5.). To check whether successive sleep cycles differed from each other Wilcoxon matched-pairs test was carried out, followed by Bonferroni correction for multiple comparisons resulting in a significance levels set at $p < 0.0125$, $p < 0.01$, $p < 0.008$, $p < 0.007$, $p < 0.00625$, $p < 0.00555$ for 4, 5, 6, 7, 8, 9 comparisons, respectively. After the correction, no significant difference in BS spectral slopes of successive cycles (e.g. cycle 1 vs. cycle 2, cycle 2 vs. cycle 3, …, cycle 6 vs. cycle 7) was revealed (in none of the cycle count based groups). However, RS spectral slope differences remained significant in the 9-cycle group between C2 and C3 ($Z = 2.8$, $p = 0.0051$).

Furthermore, we compared the parameter in the first and last cycle of the sleep periods (BS C1 vs. RS C1, BS C_{last} vs. RS C_{last}) as we hypothesized that the main difference will be at the beginning of the night. Indeed, in the first cycle of BS the slope was flatter than in RS (BS: $m = 2.4$, SD=0.1; RS: $m = 2.63$, SD=0.2, $t(35)=-6.6$, $p < 0.0001$), whereas, slope values of the last cycles were not significantly different in the two conditions (BS: $m = 2.06$, SD=0.15; RS: $m = 2.08$, SD=0.14; $t(29)=-0.5$, $p = 0.62$). As a next step, we defined the maximum and minimum slope values along with their corresponding sleep cycle numbers to support the assumption that the steepest and flattest values are at the beginning and at the end of the sleep period, respectively. Besides, we compared them between sleep conditions in order to test the hypothesis stating that the BS vs RS difference in slope maxima will be larger than the divergence in the minima. In BS, slope was the steepest in the first cycle of sleep for 16, in the 2nd cycle for 17, and in the 3rd for 2 subjects; in RS, 18 subjects had their steepest slope in the 1st sleep cycle, and 13 in the 2nd (remaining participants did not have complete recordings). Slope maximum was significantly steeper in RS ($t(29)=-9.5$, $p <$

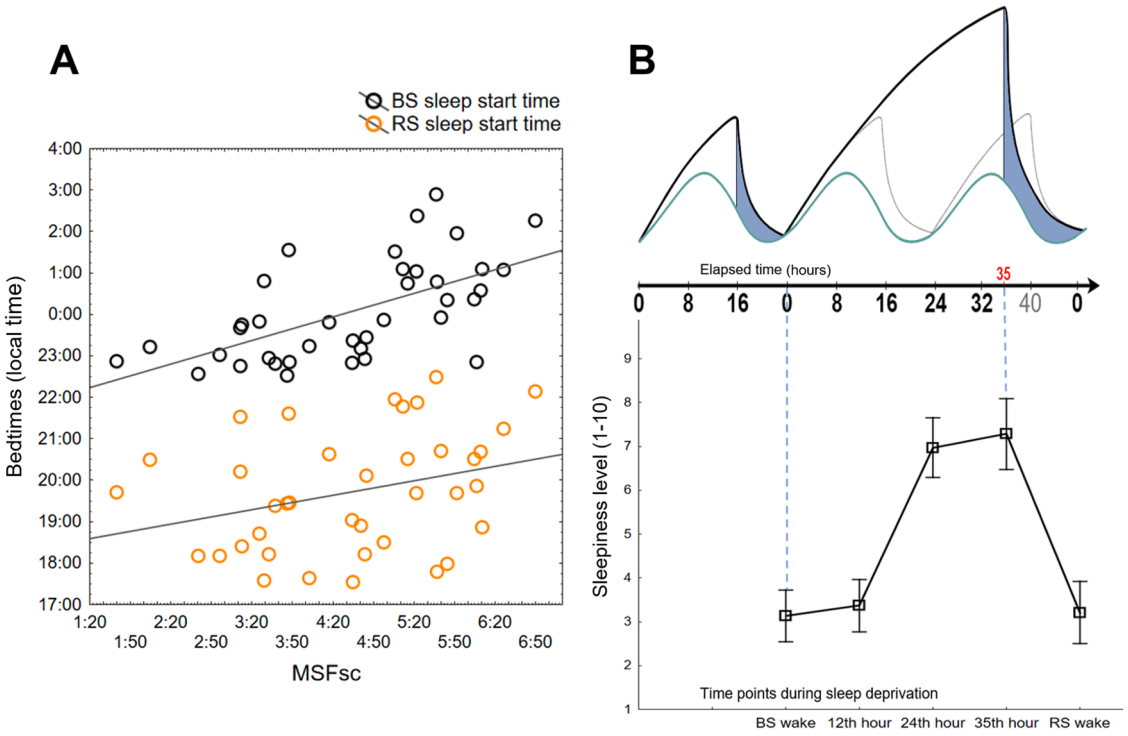

Fig. 1. Subjective chronotype and sleepiness along with the expected sleep pressure and circadian time according to the two-process model of sleep regulation. A) Correlation between the MCTQ chronotype indicator (MSFsc) and actual bedtimes of BS and RS. B) Schematic representation of the expected behaviour of the two sleep regulatory processes (top) and the actual development of sleepiness according to the Likert scale (bottom) during the experiment. On the top, blue area indicates the approximate time duration of the sleep periods, while the black and light-grey lines demonstrate the homeostatic sleep pressure due to the intervention, and under normal circumstances without sleep deprivation, respectively (note the heightened sleep pressure due to the extended wakefulness). On the bottom, the graph displays the sample means with 95 % confidence intervals of sleepiness levels at different time points during the wakefulness.

Table 1
Sample means and standard deviation of slope values in the first four sleep cycles.

	baseline			recovery		
cycle	N	Mean	SD	N	Mean	SD
1	36	2.402602	0.126357	38	2.625733	0.214957
2	36	2.388576	0.170833	36	2.615997	0.199933
3	37	2.218177	0.205926	34	2.410661	0.189354
4	36	2.100263	0.179556	33	2.247819	0.129501

0.0001), furthermore, BS and RS did not differ significantly in terms of which sleep cycle contained the steepest slope value ($Z = 0.2$, $p = 0.23$, BS: Mdn=2 (2nd cycle), IQR=[1,2]; RS: Mdn=1(1st cycle), IQR=[1,2]). Minimum slope values did not differ between BS and RS (t(29)=−1.2, $p = 0.24$), moreover, the cycle number of the last cycles significantly differed from the cycle number in which the minimum values (flattest slopes) occurred, that is flattest slope did not always fall in the last sleep cycle of the night (**BS**: $Z = 4.2$, $p < 0.0001$, *cycle index of* C_{last}: Mdn=5, IQR=[5, 6], *cycle index of* C_{min}: Mdn=4.5, IQR=[3, 5]; **RS**: $Z = 3.9$, $p < 0.0001$, *cycle index of* C_{last}: Mdn=8, IQR=[7, 9], *cycle index of* C_{min}: Mdn=7, IQR=[6, 8]).

3.2. Slow wave activity

Both the effect of sleep deprivation and sleep cycles were significant on lnSWA according to the General Linear Model applied to the first 4 cycles of the two sleep conditions (BS/RS: F(1,32)=22.23, $p < 0.001$, cycle: F(3,96)=80.1, $p < 0.001$; Fig. 2.). Condition × cycle interaction was not significant (F(3,96)=2.17, $p = 0.096$). Similar to the spectral slope results, sample-level lnSWA difference was significant between C2 vs. C3 (BS & RS: $p < 0.001$,) and C3 vs. C4 (BS: $p = 0.05$, RS: $p = 0.002$) in both conditions, but not between C1 vs. C2 (BS & RS: $p = 0.99$). Cycle count-based group analyses revealed significant cycle effects even if the whole sleep period was considered (Table 2). However, there were no significant difference between successive sleep cycles according to the Bonferroni corrected Wilcoxon matched-pairs test results in none of the cycle-count based groups, except in RS 9-cycle group where C3 vs. C4 ($Z = 2.8$, $p = 0.0051$), and in BS 6-cycle group where C2 vs. C3 ($Z = 2.67$, $p = 0.0076$) differences remained significant after the correction. Finally, as hypothesized, lnSWA was significantly higher in the first cycle of RS ($m = 4.8$, SD=0.51) than in BS C1 ($m = 4.5$, SD=0.5) (t(37)=−3.6, $p < 0.001$), but returned to similar levels for the last cycle of sleep in both nights (Fig. 3. BS C_{last}:$m = 3.1$, SD=0.6, vs. RS C_{last}: $m = 2.9$, SD=0.5; t(29)=1.13, $p = 0.27$, $m = 2.9$, SD=0.5).

3.3. Spindle frequency

General Linear Model applied to the first 4 cycle of the whole sample with condition (BS/RS) and cycle as within subject factors, revealed that, only cycle affected significantly CF (BS/RS: F(1,27)=3.13, $p = 0.1$, cycle: F(3,81)=3.27, $p = 0.025$). The interaction was not significant.

Similar to the approach used for spectral slope analyses, further details on the overnight dynamics of the total night in the separate cycle count-based groups, as well as CF similarities/differences of the two sleep conditions were analysed.

Cycle effect in CF was significant in all groups except the 4-cycle group in BS and 7-cycle group in RS (Fig. 5., see descriptive statistics in Table 3). However, as we hypothesized that CF will decelerate around the middle of the night sleep period, we conducted sample-level comparisons between the middle- and first-, as well as between the middle- and last sleep cycles' CF values using dependent sample *t*-test with Bonferroni correction for multiple comparisons, resulting in a significance level set at $p < 0.025$ for the 2 comparisons. Where the maximum

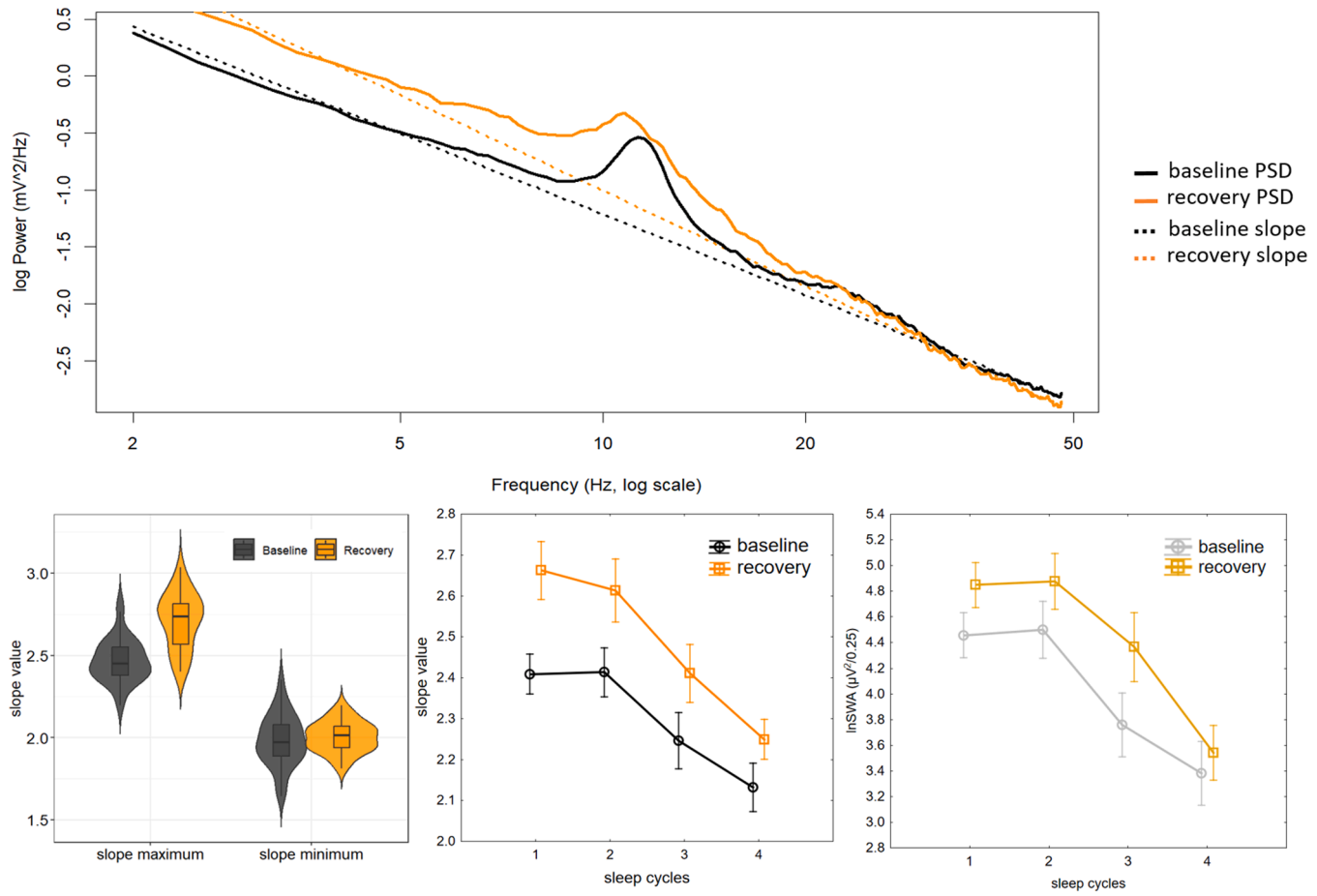

Fig. 2. Spectral slopes of the NREM sleep EEG during the first four sleep cycles of the baseline and the recovery nights. Upper panel shows the spectrum of the first cycle of sleep for BS (black) and RS (orange), as well as the fitted aperiodic components with dashed lines in a 24-year-old male participant. Violin plots (left side of the lower panel) depict the distribution of the maximal and minimal slope values, whereas inner boxplots show the difference between sleep conditions: while maximum slope values got larger due to the sleep deprivation, slope minima returned to approximately the same level in the two conditions. Middle and right panels show the sample means and 95 % confidence interval of slope values and lnSWA, respectively, in the first 4 cycle of sleep in BS and RS. At the beginning of the sleep RS as compared to BS Spectral slopes and lnSWA are steeper and larger, respectively.

Table 2
Overnight cycle effect of slope, CF and lnSWA in the separate cycle count-based groups. Friedman ANOVA revealed significant or marginally significant cycle effect in all groups except with regards CF in the BSC4 group.

Groups defined by maximum cycle count	Sample size	Slope		CF		lnSWA	
	N (N for CF)	χ2	p	χ2	p	χ2	p
BSC4	7 (6)	7.3	0.06	1.8	0.61	14.7	0.002
BSC5	12 (10)	33.33	<0.0001	13.5	0.009	24.87	<0.001
BSC6	11	37.13	<0.0001	23.94	0.0002	37.96	<0.0001
ReSC7	8 (7)	41.3	<0.0001	11.51	0.07	42.5	<0.0001
ReSC8	8 (7)	47.54	<0.0001	22.86	0.002	42.5	<0.0001
ReSC9	10	60.27	<0.0001	34.24	<0.0001	61.1	<0.0001

cycle count was an even number, average of the two middle cycles was considered as the middle of sleep. In the middle of the sleep period CF was significantly slower than in the last sleep cycle in both conditions (**BS**: C_{middle} [$m = 11.85$, SD=0.7] vs. C_{last} [$m = 12.25$, SD=0.7]: t(34)=−3.8, $p < 0.001$; **RS**: C_{middle} [$m = 11.8$, SD=0.66] vs. C_{last} [$m = 12.31$, SD=0.6]: t(30)=−5.3, $p < 0.0001$), however, sleep middle CFs did not differ significantly from CFs of the first sleep cycles (**BS**: C_{first} [$m = 12.03$, SD=0.6] vs. $C_{middle:}$ t(32)=1.86, $p = 0.07$; **RS**: C_{first} [$m = 11.93$, SD=0.7] vs. $C_{middle:}$ t(28)=1.04, $p = 0.31$). Furthermore, we compared last and first CF values in the sample to test whether the beginning and the end of sleep is similar regarding spindle CF. Last cycle CFs were significantly faster than first cycle CFs in both condition (**BS**: t(33)=−3.8, $p < 0.001$; **RS**: t(28)=−4.2, $p < 0.001$).

In line with our hypothesis we found no significant CF difference in the last and first cycles of sleep between BS and RS (C_{last}: t(29)=0.12, $p = 0.91$, C_{first}: t(32)=0.89, $p = 0.38$). Additionally, we calculated the middle time of the sleep cycle which contains the slowest CF value (NSSF). First, we tested whether NSSF reflects the subjectively measured chronotype (MCTQ MSFsc and the created chronotype groups). According to the results of One-Way ANOVA, there is a difference in BS NSSF among the different chronotype groups (F(2)=3.81, $p = 0.03$, m_{early}=2:18, SD=2:34, m_{interm}=3:04, SD=2:15, m_{late}=4:45, SD=1:44 hh:mm), but no difference can be captured when the RS NSSF is tested (F(2)=1.08, $p = 0.4$, m_{early}=23:07, SD=1:14, m_{interm}=00:59, SD=2:08, m_{late}=0:56, SD=3:17 hh:mm; Fig.4.), which latter result was supported by the correlational findings showing a strong positive correlation between BS

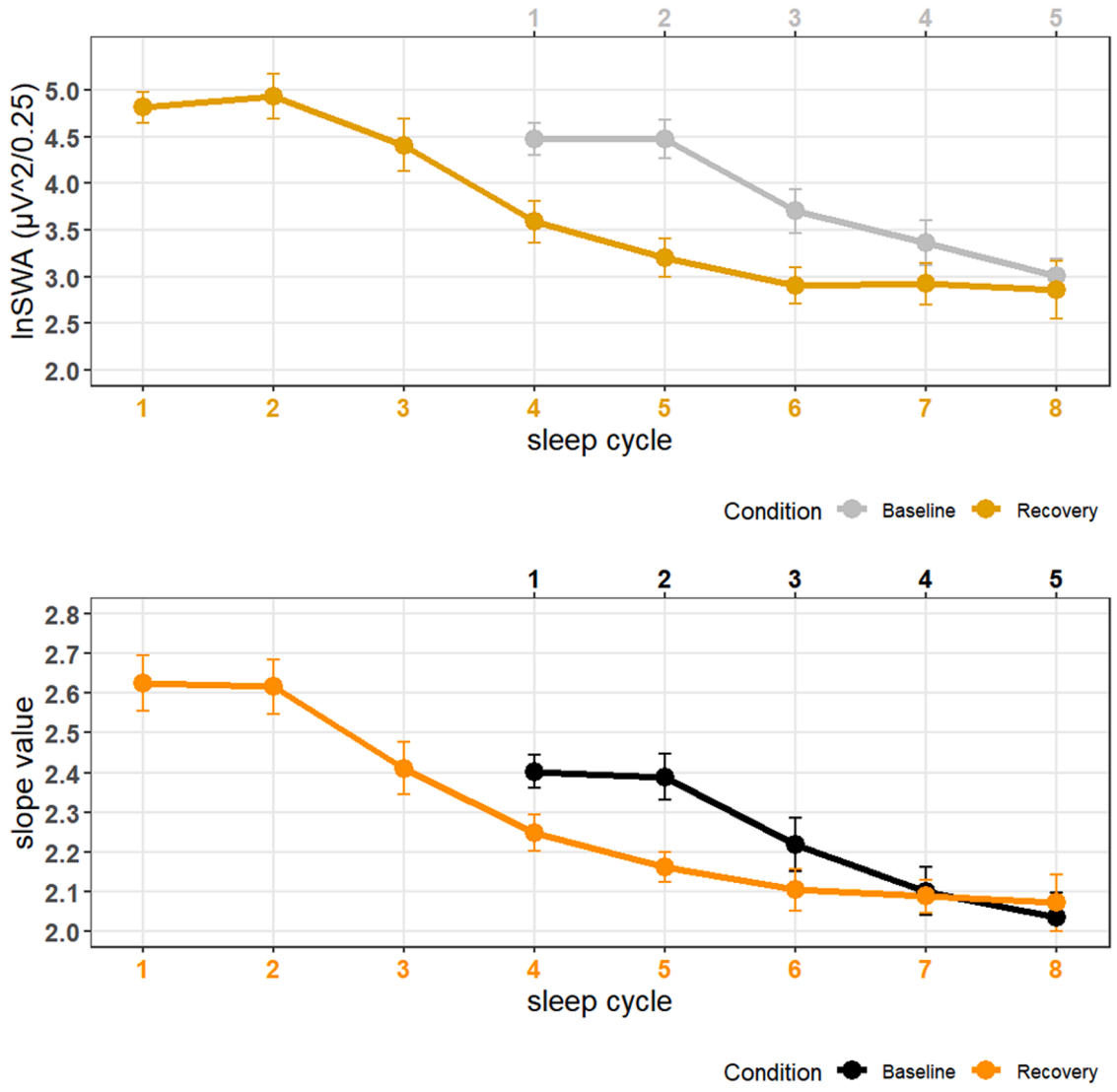

Fig. 3. *NREM sleep EEG SWA and spectral slope values in successive sleep cycles.* Sample means and 95 % confidence intervals are displayed in accordance with the phase advanced RS as compared to regularly timed BS (phase shift: approximately 3 sleep cycles).

Table 3
Sample sizes, medians and interquartile ranges of CF values in the different cycle count-based groups.

Cycle	N	Mdn	IQR:25 %	IQR:75 %	N	Mdn	IQR:25 %	IQR:75 %	N	Mdn	IQR:25 %	IQR:75 %
	BSC4				***BSC5***				***BSC6***			
1	7	12.20	11.26	12.47	11	12.01	11.74	12.39	11	11.76	11.57	12.31
2	6	11.92	10.98	12.28	10	11.93	11.68	12.32	11	11.78	11.33	12.25
3	6	11.99	11.15	12.24	12	11.95	11.38	12.35	11	11.74	11.41	12.24
4	7	12.29	10.96	12.53	12	12.27	11.79	12.61	11	11.84	11.53	12.29
5					12	12.47	11.89	12.87	11	11.94	11.59	12.52
6									11	12.11	11.74	12.67
7												
	RSC7				***RSC8***				***RSC9***			
1	8	11.69	11.33	12.08	7	12.22	11.64	12.46	10	11.95	11.62	12.38
2	7	11.53	11.37	12.19	7	11.93	11.89	12.22	10	11.60	11.34	12.29
3	7	11.50	11.29	12.03	7	11.78	11.60	12.17	10	11.88	11.62	12.14
4	8	11.89	11.06	12.34	8	11.72	11.25	12.09	10	12.06	11.49	12.11
5	8	11.65	11.10	12.18	8	11.87	11.65	12.62	10	11.85	11.23	12.22
6	8	11.92	11.28	12.38	8	12.08	11.80	12.64	10	12.05	11.11	12.73
7	8	12.06	11.57	12.52	8	12.44	11.88	12.99	10	12.00	11.59	12.38
8					8	12.57	11.92	12.82	10	12.04	12.01	12.43
9									10	12.31	11.87	12.60

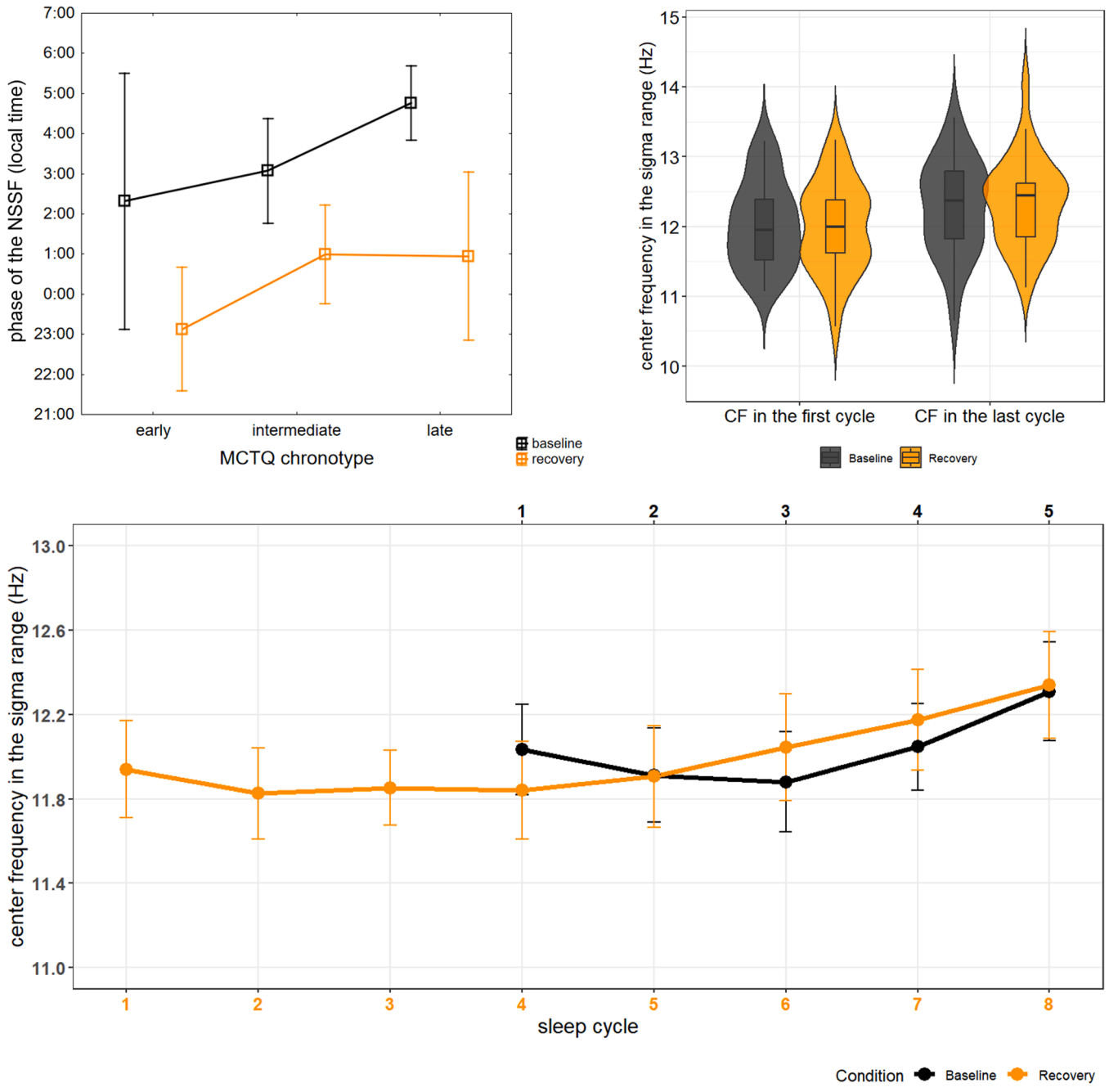

Fig. 4. Difference in the phase of the CF minima (NSSF) in RS and BS between MCTQ chronotype groups, and in CF values between sleep conditions. Subjectively measured chronotype is well reflected in the time of BS NSSF, but not in RS NSSF, additionally, NSSF times differ between sleep conditions (upper left panel). Distribution, and medians of CF in the first and last cycles of the sleep episodes are not different (violin/boxplot on the right). Lower panel represents the sample means and 95 % confidence intervals of CF in successive sleep cycles in both conditions and displays the shifted sleep period which was advanced by approximately 3 sleep cycles.

NSSF and MSFsc ($r = 0.56$, $p < 0.0001$), but no significant correlation between RS NSSF and MSFsc ($r = 0.2$, $p = 0.28$). In the next step, NSSF was compared between sleep conditions to prove hypothesis 8 stating that CF minima will appear around the same time on both nights. However, in contrast to our assumptions, NSSF developed significantly earlier in RS as compared to BS (t(28)=5.7, $p < 0.0001$, BS: m = 03:44, SD=2:14 hh:mm; RS: m = 00:40, SD=2:34 hh:mm). To examine this difference in more detail, we calculated the time of the middle of the sleep periods in BS and RS for every participant (with complete recordings) and compared it with NSSF values, following the intuition that as the minimum occurs around the middle of the sleep under normal circumstances, the cause of earlier RS NSSF could be attributed to its stronger association with the sleep midpoint, rather than with the time of day. Results indicated similar NSSF and sleep period middle times in BS (as reflected by the statistically similar means and the strong positive correlation between the two metrics: *NSSF* vs. *Midsleep:* $Z = 0.97$, $p = 0.33$, Mdn_{NSSF}=04:07, $Mdn_{Midsleep}$=03:47 hh:mm; Spearman $R = 0.64$, $p < 0.0001$), but not in RS (significant difference: *NSSF* vs. *Midsleep*: t(30)=3.2, $p = 0.003$, Mdn_{NSSF}=00:11, $Mdn_{Midsleep}$=01:46 hh:mm; nominally lower, but still significant correlation: $r = 0.41$, $p = 0.02$).

4. Discussion

The aim of the present study was to provide further evidence for the

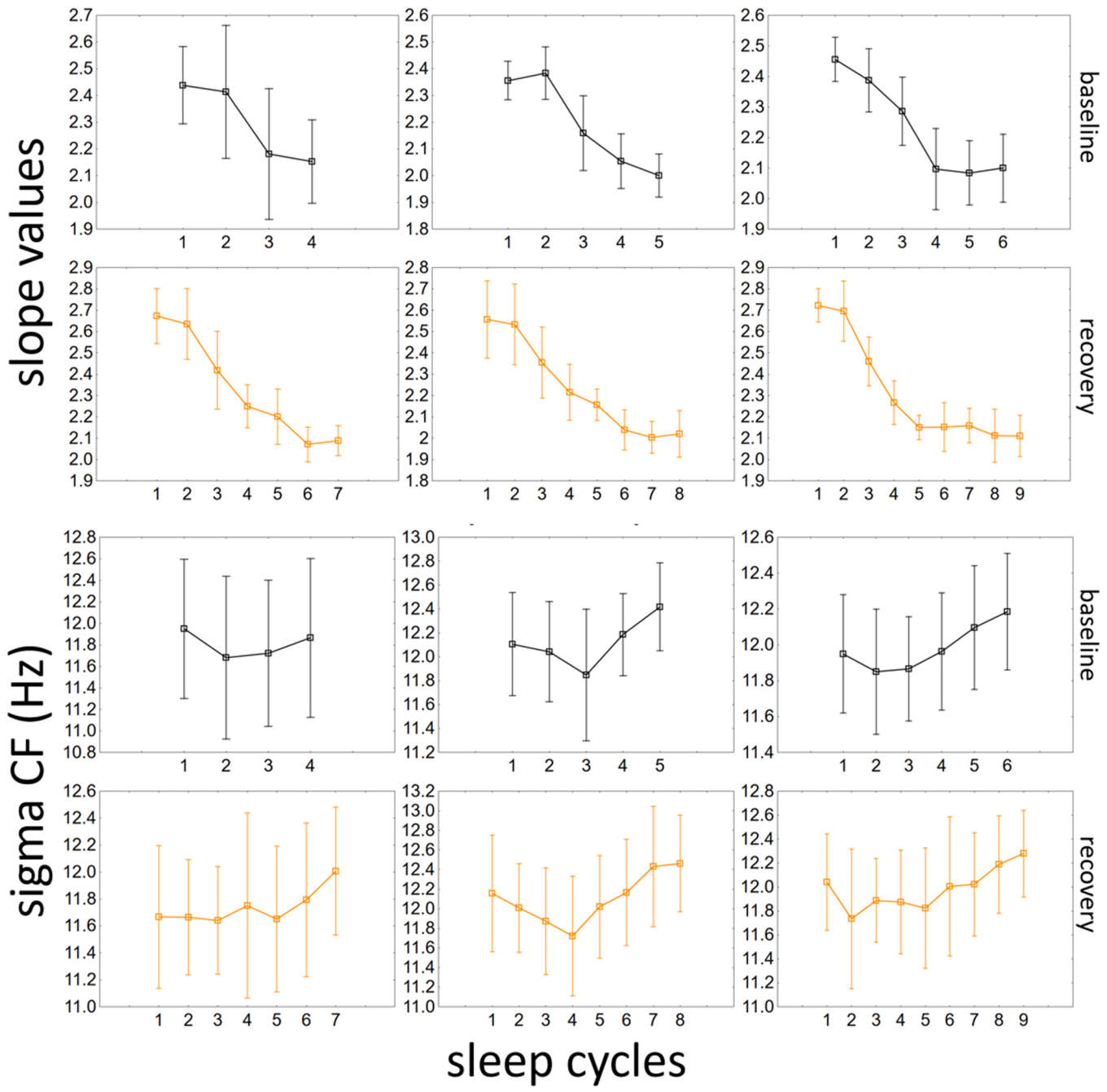

Fig. 5. *Overnight dynamics of slope values and CFs in the different cycle count-based groups.* Means (open squares) and 95 % confidence intervals (vertical lines) can be seen in successive sleep cycles. NREM sleep EEG spectral slopes get flatter during the night, while CF follows a decreasing trend then starts to increase toward the end of the night.

significance of NREM sleep EEG spectral parameters in estimating the fundamental processes of sleep regulation. In addition, we aimed to provide further advancement of the idea of home sleep recordings (Korkalainen et al., 2021) by setting up an experimental intervention (sleep deprivation) taking place in the subjects' home and not in the laboratory. Firstly, NREM sleep EEG spectral slope changed along with changes in sleep pressure and evolved similar to lnSWA (homeostatic process): it got flatter in both sleep conditions in parallel with the diminishing sleep need during the night (while lnSWA decreased); moreover, it got steeper in RS just as sleep pressure is increased after sleep deprivation (while lnSWA was increased). These findings suggest that sleep homeostasis can indeed be studied by measuring the spectral slope of the wearable headband-recorded EEG in ecologically valid, home settings. Secondly, spindle CF deceleration in the middle of the sleep period was captured in BS (with minimal CF in the middle of the night) which resulted in a U-shaped curve-like overnight dynamics of this parameter. Nonetheless, although the evolution of CF in RS was the same (CF deceleration followed by an acceleration to or above the initial CF level), the timing of minimal CF (NSSF) was neither in the middle of the sleep period, nor at the same time as that in BS.

4.1. *Aperiodic brain activity: an index of sleep homeostasis*

Results of previous research works unanimously imply the brain state indexing role of spectral slope. Some of them emphasize its distinguishing function between outwardly clearly distinct brain states

such as wakefulness and unconsciousness (Lendner et al., 2020). Others found proof on its fine-tuned discriminating ability within a specific brain state, like the distinction between "resting" and "working" awake brain (Höhn et al., 2024), as well as between sleep cycles (Rosenblum et al., 2022) or sleep stages (Schneider et al., 2022) in nocturnal EEG records. Our approach takes into account both these finer and larger scale findings and hypothesize that spectral slope can give an insight into the homeostatic process of sleep-wake regulation. Results of the present-, and our former study support this claim indirectly, as we found that spectral slope is behaving similar to the gold-standard measure of sleep homeostasis the slow wave activity (SWA) during the course of regular sleep periods. Both SWA reduction and slope flattening were revealed to correlate with age, with the progression of sleep during the night, and along the fronto-posterior gradient (Horváth, et al., 2022). In our previous reports we also discussed the advantages of slope over SWA (Bódizs et al., 2024; Horváth, et al., 2022), which is however not the scope of the present study.

Here we provide direct evidence for slope as a homeostatic marker using a total, 35-hour long sleep deprivation protocol. In line with the prior findings, spectral slope flattened during the night in the first 4 cycles of sleep, and this cycle effect remained significant even when the whole sleep period was considered in the small-sample sized groups divided along the number of sleep cycles' participants had.

Cycle-to-cycle decrease in slope steepness proved to be significant between C2 and C3, C3 and C4 in both BS and RS, when the first 4 cycles of the sample were analysed, furthermore, between C2 and C3 in the 9-cycle group in RS. These findings are analogous to the SWA-related results of Dijk et al. (1990) reporting a similar study design with extended sleep after 36 hours of wakefulness. They found reduced SWA in consecutive sleep cycles over the first 3 cycles in BS, and over the first 5 cycles in RS after which this canonical measure of sleep intensity reached a nearly constant level. Later cycles were not found to be significantly different in terms of SWA. We could replicate those findings as the tendency was the same regarding both spectral slope and lnSWA in all the cycle count based groups. It should be noted that no logarithmic-, neither Bonferroni correction was applied in the earlier report.

Comparing RS and BS, a significant condition effect and increased SWA in the first 2 cycles of RS was captured in the study of Dijk et al. (1990). When we compared slope values among conditions, we also found an overall effect of sleep deprivation. Slope was steeper after deprivation in the first 4 cycles of sleep, the maximum slope value indicated steeper slope in RS than in BS, however, slope minimum did not differ in the two conditions. This parallels earlier finding reporting a steady level to which SWA returns, and that early RS SWA exceeds that in BS (Aeschbach et al., 1997; Dijk et al., 1990). The maximum slope values occurred at the beginning of the sleep periods while the minima were found around the end of nights, however, in contrast to our assumptions, the steepest values were not exclusively present in the first cycle. In BS the distribution of first and second sleep cycle containing the steepest slope was almost 50–50 % in the sample, however, in RS this "balance" shifted towards the first cycle. A possible explanation for the lack of a significant difference between the first and the second NREM period in terms of EEG spectral slopes is the "first use effect" of the headband EEG device in BS, which could disturb the very beginning of sleep resulting in slightly flatter slopes in the first compared to the second sleep cycle.

Our finding on the increase of NREM sleep EEG spectral slope steepness following the challenge of the sleep homeostat induced by extended wakefulness is the first experimental evidence supporting the reliability of fractal spectra in indicating sleep intensity.

4.2. Oscillatory frequency in the spindle range

Oscillatory frequency of sleep spindles was suggested recently as an EEG-biomarker for circadian rhythm by the Fractal and Oscillatory Adjustment Model (Bódizs et al., 2024) of sleep regulation. This suggestion was based on several findings supporting time-of-day modulation of spindles (Dijk et al., 1997), its association with validated circadian markers (Knoblauch et al., 2005; Wei et al., 1999), and its change during the lifespan (Bódizs et al., 2022; Purcell et al., 2017; Wei et al., 1999) in parallel with the age-related changes in circadian biology (Duffy et al., 2015; Roenneberg et al., 2004).

When the overnight dynamics in CF of the two nights were tested separately for complete recordings, the cycle effect was significant in most groups, but not when the first 4 cycle of the entire sample were analysed. This is logical considering the expected behaviour of CF mid-sleep deceleration and that more than half of the participants had >4 sleep cycles already in BS (Mdn_{BS}=5 cycle). To capture mid-sleep deceleration of CF, a comparison of the first and last cycle with the middle cycle was conducted. CF was found to be significantly faster in the last cycles of sleep than in the middle, but there was only a tendency regarding first-to-middle cycle deceleration in both sleep conditions. Furthermore, when we compared first with last cycles separately in the two conditions, we found that last CF values were significantly faster than first ones. The pattern of CF development throughout the night indeed followed a U-shape, and the deceleration in the first half of the night is a consequent finding in earlier reports (Bódizs et al., 2022; Horváth, et al., 2022, also see the development in dominant frequency changes during the night in Aeschbach et al., 1997), but not always a statistically significant change. It is possible that spindle frequency peaks somewhere in the first half of the biological day, which is supported by findings showing that spindle frequency is higher in daytime sleep compared to that occurring during night time (Knoblauch et al., 2003, 2005; Rosinvil et al., 2015; Wei et al., 1999). On the other hand, it is also possible that the differences in the methods of spindle frequency definition resulted in discrepancies between former and current results. Although in our previous studies, we found that the largest peak of the spectrum in the 9 – 18 Hz range reliably reflects spindle activity as it shows the similar sex-, age-, topographical- and cognitive ability-related features as the ones formerly reported for sleep spindles (Bódizs et al., 2021; Horváth, et al., 2022), the definition of CF was slightly different here than in our earlier studies as here we did not directly search for the largest peak across the broad sigma range. Instead, we ranked the first three peaks with the largest amplitudes and "chose" the (largest) one which fell within the 9–16 Hz frequency range. Furthermore, no direct sleep spindle detection procedure was implemented in our current study, whereas this was the case in our first study on spindle frequency dynamic during the night (Bódizs et al., 2022).

However, the long-term sleep deprivation might also have an impact on the partially inconsistent findings regarding RS in the present study. Although CF correspondence in the last and first cycles of the different sleep conditions was fulfilled, CF development in the first 4 cycles was not different between the sleep conditions. Furthermore, there were large discrepancies regarding the assumed phase-indicator, NSSF. On the one hand, we hypothesized that overnight CF trajectory will differ between conditions, as the bedtime was earlier, and as sleep period was longer for all participants in RS. Besides, we assumed that NSSF will be around the same time in the two nights suggesting a time-of-day dependency of this variable. However, the tendency of CF deceleration started already in the second cycle of sleep in RS (such as in BS), and NSSF occurred significantly earlier in RS than in BS. Furthermore, although BS NSSF was reflected in subjective chronotype, and occurred around the middle of the night, this was not true for NSSF in RS. One possible explanation can be the severity of the intervention. 35 hours of wakefulness challenges the homeostatic process to such extent that the regulation of circadian pacemaker may be overshadowed. Indeed, in their recent literature review, Franken and Dijk (2024) concluded that the two processes are much more entangled as compared to the basic assumption expressed in the original two process model. Furthermore, data on biomarkers of the circadian rhythm seems to support the above entanglement. The phase-advancing effect of morning bright light measured in terms of Dim Light Melatonin Onset (DLMO) indices was

found to be reduced after acute, short-time sleep deprivation (Burgess, 2010), whereas a delayed acrophase of melatonin and suppressed BMAL1 gene expression after one night sleep deprivation was found (Ackermann et al., 2013). The circadian phase shifting effect of darkness was also reported (Buxton et al., 2000; Santhi et al., 2005). As in the present study a lights-off instruction was given to the participants at bedtime, early darkness in RS could advance the circadian phase of the participants, which could result in earlier NSSF. Besides, a study reporting electrical activity of the suprachiasmatic nucleus (SCN; the pacemaker of the circadian timing system) along with EEG revealed that neuronal activity of SCN depends on the vigilance state of the animal, for instance, NREM sleep is lowering it (Deboer et al., 2003). This finding supports the idea that earlier sleep window can modulate CF development even if it is primarily related to the circadian process (like SCN-activity). Given that CF-related variables in BS mostly behaved as expected, such as U-shape dynamics (mid-sleep deceleration), or the associations between subjectively measured chronotype and BS NSSF, we think that after all the advanced sleep protocol was rather a limitation of the time-of-day analyses in this study. Thus, further studies with the direct modulation of the circadian cycle, with the follow up of spindle frequency development in the whole 24-hour period are needed.

4.3. Limitations and overall conclusions

Overall, our findings corroborate the idea of Fractal and Oscillatory Adjustment Model, thus support the use of spectral slope as a homeostatic marker, and highly recommend further research on spindle frequency as a circadian phase indicator. Among the limitations we can mention the lack of adaptation night, and the advanced sleep protocol which latter contradicted our expectations regarding the time-of-day analyses as outlined above. However, despite further constraints such as the availability of frontolateral EEG recordings only, small group sizes, or limited age-range, results are clear regarding spectral slope as an indicator of sleep homeostasis, and promising about CF.

Data availability

The datasets generated during and/or analysed during the current study are available in the OSF repository, https://osf.io/wjsxz/.

CRediT authorship contribution statement

Csenge G. Horváth: Writing – review & editing, Writing – original draft, Visualization, Validation, Resources, Project administration, Methodology, Investigation, Formal analysis, Data curation, Conceptualization. **Róbert Bódizs:** Writing – review & editing, Writing – original draft, Supervision, Resources, Project administration, Funding acquisition, Conceptualization.

Declaration of competing interest

The authors declare that they have no known competing financial interests or personal relationships that could have appeared to influence the work reported in this paper.

Acknowledgments

We thank Melinda Becske's help in data collection, the significant contribution of Zoé Vulgarasz in the process of recruiting participants and Bence Schneider for his involvement in FOOOF analyses.

This research has been implemented with the support provided by the Ministry of Innovation and Technology (TKP2021-EGA-25 and TKP2021-NKTA-47). The funders had no role in study design, data collection and analysis, decision to publish, or preparation of the manuscript.

References

Ackermann, K., Plomp, R., Lao, O., Middleton, B., Revell, V.L., Skene, D.J., Kayser, M., 2013. Effect of sleep deprivation on rhythms of clock gene expression and melatonin in humans. Chronobiol. Int. 30 (7), 901–909. https://doi.org/10.3109/07420528.2013.784773.

Aeschbach, D., Dijk, D.J., Borbély, A.A., 1997. Dynamics of EEG spindle frequency activity during extended sleep in humans: relationship to slow-wave activity and time of day. Brain Res. 748 (1–2), 131–136. https://doi.org/10.1016/S0006-8993(96)01275-9.

Beck, A.T., Ward, C.H., Mendelson, M., Mock, J., Erbaugh, J., 1961. An inventory for measuring depression. Arch. Gen. Psychiatry 4 (6), 561–571. https://doi.org/10.1001/archpsyc.1961.01710120031004.

Bódizs, R., Horváth, C.G., Szalárdy, O., Ujma, P.P., Simor, P., Gombos, F., Kovács, I., Genzel, L., Dresler, M., 2022. Sleep-spindle frequency: overnight dynamics, afternoon nap effects, and possible circadian modulation. J. Sleep Res. 31 (3), 1–13. https://doi.org/10.1111/jsr.13514.

Bódizs, R., Körmendi, J., Rigó, P., Lázár, A.S., 2009. The individual adjustment method of sleep spindle analysis: methodological improvements and roots in the fingerprint paradigm. J. Neurosci. Methods 178 (1), 205–213. https://doi.org/10.1016/j.jneumeth.2008.11.006.

Bódizs, R., Schneider, B., Ujma, P.P., Horváth, C.G., Dresler, M., Rosenblum, Y., 2024. Fundamentals of sleep regulation: model and benchmark values for fractal and oscillatory neurodynamics. In: Progress in Neurobiology, 234. https://doi.org/10.1016/j.pneurobio.2024.102589.

Bódizs, R., Szalárdy, O., Horváth, C., Ujma, P.P., Gombos, F., Simor, P., Pótári, A., Zeising, M., Steiger, A., Dresler, M., 2021. A set of composite, non-redundant EEG measures of NREM sleep based on the power law scaling of the fourier spectrum. Sci. Rep. 11 (1), 2041. https://doi.org/10.1038/s41598-021-81230-7.

Borbély, A.A., 1982. A two process model of sleep regulation. Hum. Neurobiol. 1 (3), 195–204.

Burgess, H.J., 2010. Partial sleep deprivation reduces phase advances to light in humans. J. Biol. Rhythms 25 (6), 460–468. https://doi.org/10.1177/0748730410385544.

Buxton, O.M., L'Hermite-Balériaux, M., Turek, F.W., Van Cauter, E., 2000. Daytime naps in darkness phase shift the human circadian rhythms of melatonin and thyrotropin secretion. Am. J. Physiol. Regul. Integrat. Comparat. Physiol. 278 (2 47–2). https://doi.org/10.1152/ajpregu.2000.278.2.r373.

Colombo, M.A., Napolitani, M., Boly, M., Gosseries, O., Casarotto, S., Rosanova, M., Brichant, J.F., Boveroux, P., Rex, S., Laureys, S., Massimini, M., Chieregato, A., Sarasso, S., 2019. The spectral exponent of the resting EEG indexes the presence of consciousness during unresponsiveness induced by propofol, xenon, and ketamine. NeuroImage 189, 631–644. https://doi.org/10.1016/j.neuroimage.2019.01.024.

Csernai, M., Borbély, S., Kocsis, K., Burka, D., Fekete, Z., Balogh, V., Káli, S., Emri, Z., Barthó, P., 2019. Dynamics of sleep oscillations is coupled to brain temperature on multiple scales. J. Physiol. 597 (15), 4069–4086. https://doi.org/10.1113/JP277664.

Deboer, T., Vansteensel, M.J., Détári, L., Meijer, J.H., 2003. Sleep states alter activity of suprachiasmatic nucleus neurons. Nat. Neurosci. 6 (10), 1086–1090. https://doi.org/10.1038/nn1122.

Dijk, D.J., 1999. Circadian variation of EEG power spectra in NREM and REM sleep in humans: dissociation from body temperature. J. Sleep Res. 8 (3), 189–195. https://doi.org/10.1046/j.1365-2869.1999.00159.x.

Dijk, D.J., Brunner, D.P., Borbély, A.A., 1990. Time course of EEG power density during long sleep in humans. Am. J. Physiol. Regul. Integrat. Comparat. Physiol. 258 (3), R650–R661. https://doi.org/10.1152/ajpregu.1990.258.3.r650.

Dijk, D.J., Shanahan, T.L., Duffy, J.F., Ronda, J.M., Czeisler, C.A., 1997. Variation of electroencephalographic activity during non-rapid eye movement and rapid eye movement sleep with phase of circadian melatonin rhythm in humans. J. Physiol. 505 (3), 851–858. https://doi.org/10.1111/j.1469-7793.1997.851ba.x.

Donoghue, T., Haller, M., Peterson, E.J., Varma, P., Sebastian, P., Gao, R., Noto, T., Lara, A.H., Wallis, J.D., Knight, R.T., Shestyuk, A., Voytek, B., 2020. Parameterizing neural power spectra into periodic and aperiodic components. Nat. Neurosci. 23 (12), 1655–1665. https://doi.org/10.1038/s41593-020-00744-x.

Duffy, J.F., Zitting, K.M., Chinoy, E.D., 2015. Aging and circadian rhythms. Sleep Med. Clin. 10 (4), 423–434. https://doi.org/10.1016/j.jsmc.2015.08.002.

Favaro, J., Colombo, M.A., Mikulan, E., Sartori, S., Nosadini, M., Pelizza, M.F., Rosanova, M., Sarasso, S., Massimini, M., Toldo, I., 2023. The maturation of aperiodic EEG activity across development reveals a progressive differentiation of wakefulness from sleep. NeuroImage 277, 120264. https://doi.org/10.1016/j.neuroimage.2023.120264.

Feinberg, I., Floyd, T.C., 1979. Systematic trends across the night in Human sleep cycles. Psychophysiology 16 (3), 283–291. https://doi.org/10.1111/j.1469-8986.1979.tb02991.x.

Feinberg, I., March, J.D., Floyd, T.C., Fein, G., Aminoff, M.J., 1984. Log amplitude is a linear function of log frequency in NREM sleep EEG of young and elderly normal subjects. Electroencephalogr. Clin. Neurophysiol. 58 (2), 158–160. https://doi.org/10.1016/0013-4694(84)90029-4.

Fernandez, L.M.J., Lüthi, A., 2020. Sleep spindles: mechanisms and functions. Physiol. Rev. 100 (2), 805–868. https://doi.org/10.1152/physrev.00042.2018.

Franken, P., Dijk, D.J., 2024. Sleep and circadian rhythmicity as entangled processes serving homeostasis. Nature Rev. Neurosci. 25 (1), 43–59. https://doi.org/10.1038/s41583-023-00764-z.

Haraszti, R.Á., Ella, K., Gyöngyösi, N., Roenneberg, T., Káldi, K., 2014. Social jetlag negatively correlates with academic performance in undergraduates. Chronobiol. Int. (5), 31. https://doi.org/10.3109/07420528.2013.879164.

Hoddes, E., Zarcone, V., Smythe, H., Phillips, R., Dement, W.C., 1973. Quantification of sleepiness: a new approach. Psychophysiology 10 (4), 431–436. https://doi.org/10.1111/j.1469-8986.1973.tb00801.x.

Höhn, C., Hahn, M.A., Lendner, J.D., Hoedlmoser, K., 2024. Spectral Slope and lempel-ziv complexity as robust markers of brain states during sleep and wakefulness. Eneuro. https://doi.org/10.1523/eneuro.0259-23.2024. ENEURO.0259-23.2024.

Horváth, C.G., Bódizs, R., 2024. Association of actigraphy-derived circadian phase indicators with the nadir of spindle frequency. Biol. Rhythm Res. 55 (1), 16–29. https://doi.org/10.1080/09291016.2023.2283656.

Horváth, C.G., Szalárdy, O., Ujma, P.P., Simor, P., Gombos, F., Kovács, I., Dresler, M., Bódizs, R., 2022. Overnight dynamics in scale-free and oscillatory spectral parameters of NREM sleep EEG. Sci. Rep. 12 (1), 18409. https://doi.org/10.1038/s41598-022-23033-y.

Jenni, O.G., Carskadon, M.A., 2004. Spectral analysis of the sleep electroencephalogram during adolescence. Sleep 27 (4), 774–783. https://doi.org/10.1093/sleep/27.4.774.

Knoblauch, V., Martens, W., Wirz-Justice, A., Kräuchi, K., Cajochen, C., 2003. Regional differences in the circadian modulation of human sleep spindle characteristics. Eur. J. Neurosci. 18 (1), 155–163. https://doi.org/10.1046/j.1460-9568.2003.02729.x.

Knoblauch, V., Münch, M., Blatter, K., Martens, W.L.J., Schröder, C., Schnitzler, C., Wirz-Justice, A., Cajochen, C., 2005. Age-related changes in the circadian modulation of sleep-spindle frequency during nap sleep. Sleep 28 (9). https://doi.org/10.1093/sleep/28.9.1093.

Korkalainen, H., Nikkonen, S., Kainulainen, S., Dwivedi, A.K., Myllymaa, S., Leppänen, T., Töyräs, J., 2021. Self-applied home sleep recordings: the future of sleep medicine. Sleep Med. Clin. 16 (4), 545–556. https://doi.org/10.1016/j.jsmc.2021.07.003.

Layden, E. (2018). N-back for Matlab.

Lendner, J.D., Helfrich, R.F., Mander, B.A., Romundstad, L., Lin, J.J., Walker, M.P., Larsson, P.G., Knight, R.T., 2020. An electrophysiological marker of arousal level in humans. ELife 9, 1–29. https://doi.org/10.7554/eLife.55092.

Miskovic, V., MacDonald, K.J., Rhodes, L.J., Cote, K.A., 2019. Changes in EEG multiscale entropy and power-law frequency scaling during the human sleep cycle. Hum Brain Mapp. 40 (2), 538–551. https://doi.org/10.1002/hbm.24393.

Pálffy, Z., Farkas, K., Csukly, G., Kéri, S., Polner, B., 2021. Cross-modal auditory priors drive the perception of bistable visual stimuli with reliable differences between individuals. Sci. Rep. 11 (1). https://doi.org/10.1038/s41598-021-96198-7.

Pritchard, W.S., 1992. The brain in fractal time: 1/f-like power spectrum scaling of the human electroencephalogram. Int. J. Neurosci. 66 (1–2), 119–129. https://doi.org/10.3109/00207459208999796.

Purcell, S.M., Manoach, D.S., Demanuele, C., Cade, B.E., Mariani, S., Cox, R., Panagiotaropoulou, G., Saxena, R., Pan, J.Q., Smoller, J.W., Redline, S., Stickgold, R., 2017. Characterizing sleep spindles in 11,630 individuals from the national sleep research resource. Nat. Commun. 8. https://doi.org/10.1038/ncomms15930.

Riegel, B., Hanlon, A.L., Zhang, X., Fleck, D., Sayers, S.L., Goldberg, L.R., Weintraub, W. S., 2013. What is the best measure of daytime sleepiness in adults with heart failure? J. Am. Assoc. Nurse Pract. 25 (5), 272–279. https://doi.org/10.1111/j.1745-7599.2012.00784.x.

Roenneberg, T., Kuehnle, T., Pramstaller, P.P., Ricken, J., Havel, M., Guth, A., Merrow, M., 2004. A marker for the end of adolescence. Curr. Biol. 14 (24). https://doi.org/10.1016/j.cub.2004.11.039.

Roenneberg, T., Wirz-Justice, A., Merrow, M., 2003. Life between clocks: daily temporal patterns of human chronotypes. J. Biol. Rhythms 18 (1), 80–90. https://doi.org/10.1177/0748730402239679.

Rosenblum, Y., Bovy, L., Weber, F.D., Steiger, A., Zeising, M., Dresler, M., 2022. Increased aperiodic neural activity during sleep in major depressive disorder. Biol. Psych. Global Open Sci. https://doi.org/10.1016/j.bpsgos.2022.10.001.

Rosinvil, T., Lafortune, M., Sekerovic, Z., Bouchard, M., Dubé, J., Latulipe-Loiselle, A., Martin, N., Lina, J.M., Carrier, J., 2015. Age-related changes in sleep spindles characteristics during daytime recovery following a 25-hour sleep deprivation. Front. Hum. Neurosci. 9 (JUNE). https://doi.org/10.3389/fnhum.2015.00323.

Rózsa, S., Szádóczky, E., Füredi, J., 2001. A Beck depresszió kérdőív rövidített változatának jellemzői hazai mintán. Psychiatria Hungar. 16 (4).

Santhi, N., Duffy, J.F., Horowitz, T.S., Czeisler, C.A., 2005. Scheduling of sleep/darkness affects the circadian phase of night shift workers. Neurosci. Lett. 384 (3), 316–320. https://doi.org/10.1016/j.neulet.2005.04.094.

Schneider, B., Szalárdy, O., Ujma, P.P., Simor, P., Gombos, F., Kovács, I., Dresler, M., Bódizs, R., 2022. Scale-free and oscillatory spectral measures of sleep stages in humans. In: Frontiers in Neuroinformatics, 16. https://doi.org/10.3389/fninf.2022.989262.

Stark, S.M., Yassa, M.A., Lacy, J.W., Stark, C.E.L., 2013. A task to assess behavioral pattern separation (BPS) in humans: data from healthy aging and mild cognitive impairment. Neuropsychologia (12), 51. https://doi.org/10.1016/j.neuropsychologia.2012.12.014.

Takács, J., Bódizs, R., Ujma, P.P., Horváth, K., Rajna, P., Harmat, L., 2016. Reliability and validity of the Hungarian version of the Pittsburgh sleep quality index (PSQI-HUN): comparing psychiatric patients with control subjects. Sleep Breath. 20 (3), 1045–1051. https://doi.org/10.1007/s11325-016-1347-7.

Waschke, L., Donoghue, T., Fiedler, L., Smith, S., Garrett, D.D., Voytek, B., Obleser, J., 2021. Modality-specific tracking of attention and sensory statistics in the human electrophysiological spectral exponent. ELife 10. https://doi.org/10.7554/eLife.70068.

Wei, H.G., Riel, E., Czeisler, C.A., Dijk, D.J., 1999. Attenuated amplitude of circadian and sleep-dependent modulation of electroencephalographic sleep spindle characteristics in elderly human subjects. Neurosci. Lett. 260 (1), 29–32. https://doi.org/10.1016/S0304-3940(98)00851-9.

Zhang, Y., Wang, Y., Cheng, H., Yan, F., Li, D., Song, D., Wang, Q., Huang, L., 2023. EEG spectral slope: a reliable indicator for continuous evaluation of consciousness levels during propofol anesthesia. NeuroImage 283. https://doi.org/10.1016/j.neuroimage.2023.120426.